

Production of Plant-Expressed Virus-Like Particle Vaccines against Infectious Bronchitis Coronavirus and Vaccine Efficacy in Chickens

By

Kamogelo Mmapitso Sepotokele

Submitted in fulfilment in accordance with the requirements for the degree Doctor of
Philosophy (PhD)

Department of Production Animal Studies

Faculty of Veterinary Sciences

University of Pretoria

November 2022

Supervisor: Prof. Celia Abolnik

Co-Supervisor: Dr Martha. M. O’Kennedy

DECLARATION

Full Name of Student: Kamogelo Mmapitso Sepotokele

Student Number: 10389629

Thesis Topic: Production of Plant-Expressed Virus-Like Particle Vaccines against Infectious Bronchitis Coronavirus and Vaccine Efficacy in Chickens

- a) I understand what plagiarism is and am aware of the University's policy in this regard.
- b) I declare that this thesis is my own original work. Where other people's work has been used (either from a printed source, Internet or any other source), this has been properly acknowledged and referenced in accordance with departmental requirements.
- c) I have not used work previously produced by another student or any other person to hand in as my own.
- d) I have not allowed, and will not allow, anyone to copy my work with the intention of passing it off as his or her own work.

Signature:



KM Sepotokele

ACKNOWLEDGEMENTS

There are so many people without whom none of this could have been possible.

My two amazing supervisors, Dr Martha M. O’Kennedy and Prof. Celia Abolnik, primarily for providing me with this amazing opportunity to further my studies, but even more so for your immeasurable support, advice, mentorship, and guidance. You both pushed me to produce work that I can truly say I am incredibly proud of. Thank you so much.

My parents and siblings for supporting me and pushing me to keep going throughout this journey. A special thanks to my sister, who forced me to get out of my own head and start believing in myself. To all the friends that regularly reminded me that they believed in me and that I am capable of anything I put my mind to.

I am particularly grateful to the following people whose contribution formed much of the backbone of this thesis:

- Dr DBR Wandrag, Dr P. Smith, Michaela Hayes, Thlasila Aphane, and Thandeka Phiri for their support, input, and assistance during my animal trials at UP (Department of Production Animal Studies).
- Albert Mabetha, Sharon Kgasago, Sipho Mamputha, and Alma Truys for technical assistance at the CSIR. Special thanks to Dr Tanja Smith for providing invaluable resources, support and guidance.
- Antoinette Lensink and Danielle Henn at for TEM imaging UP (Electron Microscopy Unit).
- The team at the Department of Veterinary Tropical Diseases (UP) for serology testing, with a special thanks to Ms Karen Ebersohn.
- The Department of Science and Innovation/ National Research Foundation (DSI/NRF), University of Pretoria, and the HWSETA for financial support.
- *Nicotiana Benthamiana* mutant Δ XT/FT plants were used under a licence agreement (Research purposes only) with Professor Herta Steinkellner from the University of Natural Resources and Life Sciences, Vienna, Austria (BOKU)

And to the author of this thesis, for perservering, in order to achieve your lifelong dream. I am immensely proud of you.

TABLE OF CONTENTS

	Page
SUMMARY	x
PUBLISHED OR SUBMITTED RESULTS	xi
LIST OF ABBREVIATIONS AND ACRONYMS	xii
LIST OF FIGURES	xvi
LIST OF TABLES	xxi
CHAPTER 1: LITERATURE REVIEW	1
1.1. Introduction	1
1.2. Classification and Structure of IBV	4
1.3. Genome Organisation	5
1.4. Structural Proteins of IBV	5
1.4.1. Membrane Protein	6
1.4.2. Envelope Protein	6
1.4.3. Nucleocapsid Protein	7
1.4.4. Spike Protein	7
1.5. Classification of IBV Strains	8
1.5.1. Serotypes	9
1.5.2. Genotypes	10
1.5.3. Protectotypes	12
1.6. IBV Pathogenesis	12
1.7. Clinical Signs of IBV	14
1.8. Diagnosing IBV	15
1.9. Control of IBV	17

1.10. Types of IBV Vaccines	20
1.10.1. Live-attenuated Vaccines	20
1.10.2. Inactivated Variant Vaccines	21
1.10.3. Recombinant Vaccines	21
1.10.4. Peptide, Subunit, and DNA Vaccines	23
1.10.5. VLP Vaccines	25
1.11. Transient Protein Expression in Plants	26
1.12. Plant Expression Vector Systems	28
1.13. Vaccines Developed for other Coronaviruses	29
1.14. MSc Findings	31
1.15. Aims and Objectives	33
CHAPTER 2: DESIGN, OPTIMISATION, AND EXPRESSION OF THE FULL-LENGTH IBV SPIKE PROTEIN	34
2.1. Introduction	34
2.2. Materials and Methods	38
2.2.1. Design and Synthesis of Synthetic Gene Constructs	38
2.2.2. Cloning into pEAQ-HT Plant Expression Vector Plasmid	40
2.2.3. Transformation into Electrocompetent DH10B Cells	40
2.2.4. Transformation into Electrocompetent <i>Agrobacterium tumefaciens</i> AGL-1 Cells	41
2.2.5. Infiltration of <i>Nicotiana benthamiana</i> Plants	41
2.2.6. Harvest of Leaf Material and Protein Extraction	42
2.2.7. Protein Confirmation	43
2.2.7.1. SDS-PAGE and Immunoblotting	43
2.2.7.2. LC-MS/MS Based Peptide Sequencing	43
2.2.7.3. Transmission Electron Microscopy (TEM) Analysis	44

2.3. Results	45
2.3.1. Cloning and Expression of Synthetic Gene Constructs	45
2.3.2. Protein Detection and Confirmation of Construct mIBV-S2P	45
2.4. Discussion	49
CHAPTER 3: DESIGN, OPTIMISATION, AND EXPRESSION OF IBV SPIKE CONSTRUCTS MODIFIED WITH THE IAV HA2 PROTEIN	51
3.1. Introduction	51
3.2. Materials and Methods	54
3.2.1. Design and Synthesis of Synthetic Gene Constructs	54
3.2.2. Cloning into pEAQ-HT Plant Expression Vector Plasmid	56
3.3. Results	57
3.3.1. Cloning and Expression of Synthetic Gene Constructs	57
3.3.2. Protein Detection and Confirmation of Constructs rIBV-S1-IAV-H6 and rIBV-S1-IAV-H6 ^{TM/CT}	58
3.3.3. Protein Detection and Confirmation of Construct mIBV-S2P-IAV-H6 ^{TM/CT}	62
3.3.4. Protein Detection and Confirmation of Construct mIBV-S2P-IAV-H6 ^{CTonly}	66
3.3.5. Effect of Ratio on Protein Expression and VLP Assembly	71
3.4. Discussion	74
CHAPTER 4: DESIGN, OPTIMISATION, AND EXPRESSION OF NDV-F MODIFIED IBV SPIKE CONSTRUCTS AND PILOT IMMUNOGENICITY STUDY	77
4.1. Introduction	77
4.2. Materials and Methods	80
4.2.1. Development, Optimisation, and Expression of Modified IBV Spike Constructs	80
4.2.1.1. Design and Synthesis of Synthetic Gene Constructs	80
4.2.1.2. Cloning into pEAQ-HT Plant Expression Vector Plasmid	82

4.2.2.	Preparation of VLP Batch for Pilot Immunogenicity Study	82
4.2.2.1.	Agroinfiltration	82
4.2.2.2.	Harvest of Leaf Material, Protein Extraction, and Purification	83
4.2.2.3.	Protein Quantitation	83
4.2.2.3.1.	Total Protein Quantitation	83
4.2.2.3.2.	Spike Protein Quantitation	83
4.2.2.4.	Pilot Immunogenicity Study	84
4.2.2.4.1.	Animals	84
4.2.2.4.2.	Feed	84
4.2.2.4.3.	Vaccine Preparation	85
4.2.2.4.4.	Experimental Design	85
4.2.2.4.5.	Serology and HI Testing	86
4.2.2.4.6.	Statistical Analysis	87
4.3.	Results	88
4.3.1.	Cloning and Expression of Synthetic Gene Constructs	88
4.3.2.	Protein Detection and Confirmation of Construct rIBV-S1-NDV-F ^{TM/CT}	88
4.3.3.	Protein Detection and Confirmation of Construct mIBV-S2P-NDV-F ^{TM/CT}	91
4.3.4.	Protein Detection and Confirmation of Construct mIBV-S2P-NDV-F ^{CTonly}	95
4.3.5.	Effect of Ratio on Protein Expression and VLP Assembly	102
4.3.6.	Pilot Immunogenicity Study Results	105
4.3.6.1.	Protein Detection and Confirmation of mIBV-S2P-NDV-F ^{TM/CT}	105
4.3.6.2.	HI Testing	107
4.4.	Discussion	109

CHAPTER 5: EFFICACY OF PLANT-PRODUCED IB VLPS IN SPF CHICKENS AGAINST HOMOLOGOUS CHALLENGE WITH A LIVE VIRUS	113
5.1. Introduction	113
5.2. Materials and Methods	118
5.2.1. Production of IB VLPs	118
5.2.2. Efficacy Study	118
5.2.2.1. Animals	118
5.2.2.2. Housing, Feed, and Water	118
5.2.2.3. Preparation of Live-attenuated Vaccines	119
5.2.2.4. Preparation of VLP Vaccine	120
5.2.2.5. Challenge Virus	120
5.2.2.6. Experimental Design	120
5.2.2.7. Serology and HI Testing	122
5.2.2.8. Quantitative Real-time Reverse Transcription PCR	122
5.2.2.9. Ciliary Motility Scoring	123
5.2.2.10. Statistical Analysis	124
5.3. Results	125
5.3.1. Production of IB VLPs	125
5.3.2. Serology Testing	127
5.3.2.1. Pre-prime Bleed (Day 0)	130
5.3.2.2. Pre-boost Bleed (Day 21)	130
5.3.2.3. Pre-challenge Bleed (Day 42)	130
5.3.2.4. Post Bleed (Day 49)	130
5.3.3. HI Testing	131
5.3.4. qRT-PCR Results	133

5.3.4.1.	Oropharyngeal Viral Shedding	134
5.3.4.2.	Cloacal Viral Shedding	139
5.3.5.	Ciliary Motility Scoring	144
5.3.6.	Clinical Signs	146
5.4.	Discussion	147
FINAL CONCLUSIONS AND FUTURE PERSPECTIVES		151
REFERENCES		158
APPENDIX		183

SUMMARY

Infectious Bronchitis Virus (or IBV) is the root cause of extremely infectious respiratory disease that occurs in chickens. It has a high mutation rate that causes the emergence of multiple variants that are difficult to control, leading to major worldwide economic losses to the poultry industry. In this study, virus-like particles (VLPs) were produced using *Agrobacterium*-mediated transient protein expression in *Nicotiana benthamiana* plants as potential vaccines against IBV. Modifying the full-length IBV Spike (S) protein resulted in high levels of VLPs resembling native IBV particles visualised under transmission electron microscopy. The highest VLP expression levels were obtained when the native IBV S protein transmembrane (TM) domain and cytosolic tail (CT) sequences were substituted with the equivalent sequences of the Fusion (F) protein of Newcastle Disease Virus (NDV), and co-infiltrated with the NDV matrix protein. The second highest VLP expression levels were obtained when the TM and CT were substituted with the equivalent sequences of the Influenza A Virus (IAV) Haemagglutinin (HA) protein, and co-infiltrated with the IAV M2 protein. The lowest VLP expression levels were obtained when the chimeric modified S protein with its native TM and CT was co-infiltrated with the IBV Membrane, Envelope, and Nucleocapsid proteins. There was seroconversion in SPF chickens that received a single intramuscular immunisation of 5 µg or 20 µg (S protein content) adjuvanted IBV VLPs, with geometric mean S protein specific haemagglutination inhibition (HI) titres of 9.1 log₂ and 10.5 log₂ respectively after two weeks. In a challenge study with the live virus, the VLP vaccinated chickens elicited S protein specific antibodies at a level comparable to those elicited by those vaccinated with a live-attenuated vaccine mix (IBV Ma-5 and 4-91 vaccines) with geometric mean HI titres of 6.8 and 7.2 log₂ respectively. The VLP vaccine was able to reduce both oropharyngeal and cloacal viral shedding between 3 and 7 days post challenge, which was similar to the reduction seen in the birds vaccinated with the live-attenuated vaccine mix. The birds vaccinated with the plant-produced VLP vaccine showed higher tracheal ciliary motility than those vaccinated with the live vaccines, with no adverse vaccine effects observed. These plant-produced IB VLPs have great potential for the global poultry industry as they are highly immunogenic, safe, and they can easily be updated to antigenically match any circulating IBV variant both speedily and cost-effectively.

The results of Chapters, 2, 3, and 4 were submitted to the *Frontiers in Plant Science (Plant Biotechnology)* journal:

“Optimization of Infectious Bronchitis virus-like particle expression in *Nicotiana benthamiana* as potential poultry vaccines”

Sepotokele, KM., O’Kennedy, MM., Wandrag, DBR., and Abolnik, C.

The results of Chapter 5 are currently being prepared for submission to the *Veterinary Microbiology* journal:

“Efficacy of a plant-produced Infectious Bronchitis Coronavirus virus-like particle vaccine in SPF chickens”

Sepotokele, KM., O’Kennedy, MM., Hayes, MC., Wandrag, DBR., Smith, P., and Abolnik, C.

LIST OF ABBREVIATIONS AND ACRONYMS

IBV	Infectious Bronchitis Virus
%	Percentage
°C	Degrees Celsius
μF	Microfarads
μg	Microgram
2P	2 proline substitutions
4-91	Infectious Bronchitis Virus serotype 4-91
<i>A. tumefaciens</i>	<i>Agrobacterium tumefaciens</i>
AGP	Agar gel precipitation
AHSV	African horse sickness virus
ANOVA	Analysis of variance
BCA	Bicinchoninic acid assay
BSA	Bovine serum albumin
BSL	Biosafety level
BTV	Bluetongue virus
CCT	Chaperonin containing TCP-1
cDNA	Complementary deoxyribonucleic acid
ck/ZA/3665/11	QX-like IBV strain
COVID-19	Coronavirus disease caused by Severe Acute Respiratory Syndrome Coronavirus 2
CPMV	Cowpea Mosaic Virus
CRBC	Chicken red blood cells
Cryo-EM	Cryogenic Electron Microscopy
CT	Cytosolic tail
DIVA	Differentiating infected from vaccinated animals
DNA	Deoxyribonucleic acid
dNTP	Deoxyribonucleotide triphosphate
dpc	Days post challenge
dpi	Days post infiltration
E	Infectious Bronchitis Virus Envelope protein
<i>E. coli</i>	<i>Escherichia coli</i>
EDIII	Envelope protein domain III

EID₅₀	Egg infectious dose
ELISA	Enzyme-linked immunosorbent assay
ER	Endoplasmic reticulum
F	Newcastle Disease Virus Fusion protein
Fw	Forward primer
FP	Fusion Peptide
g	Gram
GMT	Geometric mean titre
HA	Influenza A Virus Haemagglutinin protein
HEPA	High efficiency particulate air
HI	Haemagglutination inhibition
HN	Haemagglutinin-neuraminidase
HPAI	Highly Pathogenic Avian Influenza
HR	Heptad repeat region
HRP	Horseradish peroxidase
HSP	Heat-shock protein
HT	Hypertranslational
HVR	Hypervariable region
IAV	Influenza A Virus
IAV M1	Influenza A Virus Matrix 1 protein
IAV M2	Influenza A Virus Matrix 2 protein
IBDV	Infectious bursal disease virus
IFNAR	Interferon- α/β receptor
IgA	Immunoglobulin A
IgG	Immunoglobulin G antibody
ILTV	Infectious laryngotracheitis virus
kb	Kilobase
kDa	KiloDaltons
kg	Kilogram
kV	KiloVolts
LB	Luria Bertani
LC-MS/MS	Liquid chromatography mass spectrometry
M	Infectious Bronchitis Virus Membrane protein

Ma5	Infectious Bronchitis Virus serotype Massachusetts
MERS-CoV	Middle East respiratory syndrome Coronavirus
MES	N-morpholinoethanesulfonic acid
mg	Milligram
MG	<i>Mycoplasma gallisepticum</i>
MHV	Murine hepatitis virus
ml	Millilitre
mM	MilliMolar
mRNA	Messenger ribonucleic acid
mW	Molecular weight
N	Infectious Bronchitis Virus Nucleocapsid protein
<i>N. benthamiana</i>	<i>Nicotiana benthamiana</i>
NDV	Newcastle Disease Virus
ng	Nanogram
Ni	Nickel
nm	Nanometre
Ns	Not significant
OD	Optical Density
Pa	Pascals
PBS	Phosphate-buffered saline
PCR	Polymerase chain reaction
PEDV	Porcine epidemic diarrhea virus
PVDF	Polyvinylidene difluoride
qRT-PCR	Real-time or quantitative real-time RT-PCR
R	South African Rand
Rv	Reverse primer
RBD	Receptor-binding domain
RNA	Ribonucleic acid
rpm	Revolutions per minute
RT-PCR	Reverse transcriptase polymerase chain reaction
S	Infectious Bronchitis Virus Spike protein
S/P	Sample to positive ratio
S1	Spike protein subunit 1

S2	Spike protein subunit 2
SARS-CoV-2	Severe Acute Respiratory Syndrome Coronavirus 2
SDS-PAGE	Sodium dodecyl sulphate-polyacrylamide gel electrophoresis
Sf9	Spodoptera frugiperda insect cells
SPF	Specific pathogen-free
T-DNA	Transfer deoxyribonucleic acid
TEM	Transmission electron microscopy
Ti	Tumour-inducing
TM	Transmembrane domain
USA	United States of America
UTR	Untranslated region
V	Volts
Vir	Virulence genes
VLP	Virus-like particle
VN	Virus Neutralisation
VP2	Viral protein 2
VTM	Viral Transport Media
w/v	Weight/volume
WNV	West Nile virus
WOAH	World Organisation of Animal Health
x g	Times gravity
α	Alpha
β	Beta
γ	Gamma
Δ	Delta
Ω	Ohm

LIST OF FIGURES

	Page
Figure 1.1. Negative-stained transmission electron microscopy image of a purified live QX-like IBV strain ck/ZA/3665/11	4
Figure 1.2. Infectious Bronchitis Virus genome organisation coding for the structural and non-structural proteins (Not drawn to scale)	5
Figure 1.3. Schematic diagram of the structure of Infectious Bronchitis Virus indicating the structural proteins	6
Figure 1.4. Schematic diagram of the S1 and S2 subunits of the IBV spike protein	8
Figure 1.5. Schematic representation of the process of transient protein expression using agrobacterium-mediated gene transfer	27
Figure 2.1. Protein sequence of the synthetic gene sequence mIBV-S2P, highlighting the stabilising proline mutations in the S2 subunit of the sequence	39
Figure 2.2. Schematic diagram illustrating the full-length IBV target protein with stabilising mutations (mIBV-S2P)	39
Figure 2.3. SDS-PAGE (a) and Western blot (b) of plant-produced IBV S protein (mIBV-S2P) purified in PBS or bicine buffer	46
Figure 2.4. Protein confirmation using LC-MS/MS-based peptide sequencing of the modified IBV spike protein construct, mIBV-S2P	47
Figure 2.5. Negative-stained transmission electron microscopy images of plant-produced IBV virus-like particles expressed with the synthetic gene construct, mIBV-S2P in <i>N. benthamiana</i> .	48
Figure 3.1. SDS-PAGE (a) and Western blot (b) of plant-produced rIBV-S1-IAV-H6 protein purified in PBS or bicine buffer	59

Figure 3.2. SDS-PAGE (a) and Western blot (b) of plant-produced rIBV-S1-IAV-H6 ^{TM/CT} protein purified in PBS or bicine buffer	60
Figure 3.3. Negative-stained transmission electron microscopy images of plant-produced IBV virus-like particles expressed with the synthetic gene constructs rIBV-S1-IAV-H6 and rIBV-S1-IAV-H6 ^{TM/CT} in <i>N. benthamiana</i>	61
Figure 3.4. SDS-PAGE (a) and Western blot (b) of plant-produced IBV S protein (mIBV-S2P-IAV-H6 ^{TM/CT}) purified in PBS or bicine buffer	63
Figure 3.5. Protein confirmation using LC-MS/MS-based peptide sequencing of the modified IBV spike protein construct, mIBV-S2P-IAV-H6 ^{TM/CT}	64
Figure 3.6. Negative-stained transmission electron microscopy images of plant-produced IBV virus-like particles expressed with the synthetic gene construct, mIBV-S2P-IAV-H6 ^{TM/CT} in <i>N. benthamiana</i>	65
Figure 3.7. SDS-PAGE (a) and Western blot (b) of plant-produced mIBV-S2P-IAV-H6 ^{CTonly} protein co-infiltrated at different ratios with the IAV M2 protein	67
Figure 3.8. Protein confirmation using LC-MS/MS-based peptide sequencing of the modified IBV spike protein construct, mIBV-S2P-IAV-H6 ^{CTonly} co-expressed at different ratios with the IAV M2 protein	68
Figure 3.9. Negative-stained transmission electron microscopy images of plant-produced IBV virus-like particles expressed with the synthetic gene constructs mIBV-S2P-IAV-H6 ^{CTonly} in <i>N. benthamiana</i> in different ratios with IAV M2	70
Figure 3.10. SDS-PAGE (a) and Western blot (b) of plant-produced IBV S protein (mIBV-S2P-IAV-H6 ^{TM/CT}) co-infiltrated at different ratios with the IAV M2 protein	72
Figure 3.11. Negative-stained transmission electron microscopy images of plant-produced IBV virus-like particles expressed with the synthetic gene construct mIBV-S2P-IAV-H6 ^{TM/CT} in <i>N. benthamiana</i> at different ratios with its complementary protein IAV M2	73
Figure 4.1. SDS-PAGE (a) and Western blot (b) of plant-produced rIBV-S1-NDV-F ^{TM/CT} protein purified in PBS or bicine buffer	89

Figure 4.2. Negative-stained transmission electron microscopy images of plant-produced IBV virus-like particles expressed with the synthetic gene construct rIBV-S1-NDV-F ^{TM/CT} in <i>N. benthamiana</i>	90
Figure 4.3. SDS-PAGE (a) and Western blot (b) of plant-produced IBV S protein (mIBV-S2P-NDV-F ^{TM/CT}) purified in PBS or bicine buffer	92
Figure 4.4. Protein confirmation using LC-MS/MS-based peptide sequencing of the modified IBV spike protein construct, mIBV-S2P-NDV-F ^{TM/CT}	93
Figure 4.5. Negative-stained transmission electron microscopy images of plant-produced IBV virus-like particles expressed with the synthetic gene construct mIBV-S2P-NDV-F ^{TM/CT} in <i>N. benthamiana</i>	94
Figure 4.6. SDS-PAGE (a) and Western blot (b) of plant-produced mIBV-S2P-NDV-F ^{CTonly} protein co-infiltrated at different ratios with the NDV matrix protein	97
Figure 4.7. Protein confirmation using LC-MS/MS-based peptide sequencing of the modified IBV spike protein construct, mIBV-S2P-NDV-F ^{CTonly} co-expressed at different ratios with the NDV matrix protein	99
Figure 4.8. Negative-stained transmission electron microscopy images of plant-produced IBV virus-like particles expressed with the synthetic gene construct mIBV-S2P-NDV-F ^{CTonly} in <i>N. benthamiana</i> in different ratios with NDV matrix	102
Figure 4.9. SDS-PAGE (a) and Western blot (b) of plant-produced IBV S protein (mIBV-S2P-NDV-F ^{TM/CT}) co-infiltrated at different ratios with the NDV matrix protein	103
Figure 4.10. Negative-stained transmission electron microscopy images of plant-produced IBV virus-like particles expressed with the synthetic gene construct mIBV-S2P-NDV-F ^{TM/CT} in <i>N. benthamiana</i> in different ratios with its complementary protein, NDV matrix	105
Figure 4.11. SDS-PAGE (a) and Western blot (b) of plant-produced mIBV-S2P-NDV-F ^{TM/CT} protein co-infiltrated at a 4:1 ratio with the NDV matrix protein harvested in PBS and bicine buffers	106

Figure 4.12. Haemagglutination inhibition (HI) titres for the chicken sera two weeks after a single immunisation with 5 µg and 20 µg doses of the mIBV-S2P-NDV-F ^{TM/CT} :matrix VLPs	108
Figure 5.1. Experimental design of the efficacy study (49 days)	122
Figure 5.2. SDS-PAGE (a) and Western blot (b) of plant-produced mIBV-S2P-NDV-F ^{TM/CT} protein co-infiltrated at a 4:1 ratio with the NDV matrix protein harvested in PBS, Bicine, or Tris Buffers	126
Figure 5.3. Negative-stained transmission electron microscopy images of plant-produced IBV virus-like particles expressed with the synthetic gene constructs mIBV-S2P-NDV-F ^{TM/CT} in <i>N. benthamiana</i> in different ratios with NDV matrix	127
Figure 5.4. Antibody titres ± standard deviation for the chicken sera taken at 4 different time points during the trial	131
Figure 5.5. Haemagglutination inhibition (HI) log ₂ titres for the chicken sera in Groups A and B taken on day 42 (pre-challenge)	133
Figure 5.6. Viral RNA log ₁₀ EID ₅₀ /ml equivalents ± standard deviation for the oropharyngeal swabs taken at 3, 5, and 7 days post challenge	137
Figure 5.7. Viral RNA log ₁₀ EID ₅₀ /ml equivalents ± standard deviation for the cloacal swabs taken at 3, 5, and 7 days post challenge	142
Figure S1. SDS-PAGE (a) and Western blot (b) of plant-produced IBV S protein (mIBV-S2P, mIBV-S2P-IAV-H6 ^{TM/CT} , and mIBV-S2P-NDV-F ^{TM/CT}) purified in PBS or bicine buffer	189
Figure S2. SDS-PAGE (a) and Western blot (b) of plant-produced rIBV-S1-IAV-H6 ^{TM/CT} and rIBV-S1-NDV-F ^{TM/CT} proteins purified in PBS or bicine buffer	190
Figure S3. SDS-PAGE (a) and Western blot (b) of plant-produced IBV S protein (mIBV-S2P-IAV-H6 ^{TM/CT} and mIBV-S2P-NDV-F ^{TM/CT}) co-infiltrated at different ratios with their complementary proteins	191
Figure S4. Densitometric analysis by SDS-PAGE of partially-purified mIBV-S2P-NDV-F ^{TM/CT} VLPs	193

Figure S5. Densitometric analysis by SDS-PAGE of partially-purified mIBV-S2P-NDV-F^{TM/CT} VLPs

194

LIST OF TABLES

	Page
Table 1.1. Summary of characteristics of live-attenuated and inactivated IBV vaccines	19
Table 2.1. Primers used for Colony PCR verification	40
Table 2.2. Gene construct co-infiltration ratios (Chapter 2)	45
Table 3.1. Schematic diagrams of modified constructs designed in Chapter 3	55
Table 3.2. Primers used for synthetic IAV construct design	55
Table 3.3. Gene construct co-infiltration ratios (Chapter 3)	57
Table 4.1. Schematic diagrams of modified constructs designed in Chapter 4	81
Table 4.2. Primers used for synthetic NDV construct design	81
Table 4.3. Gene construct co-infiltration ratios (Chapter 4)	88
Table 4.4. Log ₂ HI titres at 14 days post vaccination	107
Table 5.1. Treatment Groups for the Efficacy Study	119
Table 5.2. Serology test results	128 - 129
Table 5.3. Log ₂ HI titres for the blood samples taken prior to viral challenge	132
Table 5.4. Individual qRT-PCR results for the oropharyngeal swabs	134 - 135
Table 5.5. Fold differences between the mean titres of each group on the different days post challenge for the oropharyngeal swabs	138
Table 5.6. Individual qRT-PCR results for the cloacal swabs	139 - 140
Table 5.7. Fold differences between the mean titres of each group on the different days post challenge for the cloacal swabs	143
Table 5.8. Ciliary motility scores	144 - 145

Table S1. Schematic diagrams of all designed modified constructs and expression levels

192

CHAPTER 1

LITERATURE REVIEW

1.1. Introduction

Avian Infectious Bronchitis Virus (IBV) is a World Organisation of Animal Health (WOAH)-listed disease with substantial economic implications within the poultry industry across the globe. IBV results in severe respiratory infection that occurs in chicken species (Liu *et al.*, 2013a). The largest sub-sector of South Africa's agricultural sector is the poultry industry, with the poultry and egg industries producing a turnover of over R47 billion annually. The total losses caused by IBV infections for every flock have been estimated to be between 10 - 20 % of market value. Although the virus has no known effects on human health, controlling it is becoming increasingly important due to concerns surrounding the use of antibiotics to treat secondary infections, resulting in incidents of antibiotic resistance (de Wit and Cook, 2019).

IBV was first described in the United States in the 1930s (Schalk and Hawn, 1931). It has since been reported in areas of Asia, Europe, Australia, Africa, as well as America (Jackwood, 2012; Cavanagh, 2007). There are more than 20 different serotypes of IBV globally which are found in both commercial and backyard chickens (Zhou *et al.*, 2004; Cook *et al.*, 2012; Jackwood, 2012). Many of the identified serotypes of IBV have either completely died out, or become endemic to particular regions (Bochkov *et al.*, 2006). Various serotypes co-circulate in particular regions, while others exist on multiple continents, negatively impacting the poultry industry over time (Jackwood and de Wit, 2013; Terregino *et al.*, 2008). The WOAH has classified IBV as a notifiable disease (https://www.woah.org/en/what-we-do/standards/codes-and-manuals/terrestrial-code-online-access/?id=169&L=1&htmfile=chapitre_oie_listed_disease.htm), and its economic impact globally ranks it second only to avian influenza (WorldBank and TAFS-Forum, 2011).

IBV's rapid mutation ability leads to the continual emergence of new antigenically and genetically distinct IBV strains, which complicates control of the virus using conventional vaccination programs (de Wit *et al.*, 2011; Cavanagh and Gelb, 2008). There are more than 50 variants of IBV circulating globally, with each variant offering little to no cross-protection against other variants (Bande *et al.*, 2015). The emergence of new variants renders existing

vaccines redundant, and requires new vaccines to be developed to provide the antigenic matching required for optimal protection against disease (Meeusen *et al.*, 2007).

Within Africa, Infectious Bronchitis Virus is enzootic, and is among the list of viral respiratory diseases which most commonly affect chickens, causing disease in poultry farms regardless of their vaccination status (Liu *et al.*, 2003; Casais *et al.*, 2003). The virus was first described in North Africa in the 1950s (Ahmed, 1954), and later confirmed by Eissa *et al.*, in 1963 and then El Houadfi & Jones (1985) in 1983. IBV in the Southern parts of Africa was first isolated in 1984 by Morley and Thomson. This isolated variant was not well protected by the Massachusetts vaccine (Cook *et al.*, 1999). The QX-like variant of IBV was initially reported in 2011 in Zimbabwe (Toffan *et al.*, 2011). IBV's genetic variation in South Africa is not well studied, or at least, not made public knowledge by commercial companies that sell vaccines for its control. A serological incidence of 43 % was reported in South Africa for IBV, in QwaQwa (Thekiso *et al.*, 2003) after which two distinct strains of IBV were revealed to circulate in South Africa which included a QX-like variant as well as a Massachusetts variant (Knoetze *et al.*, 2014).

Controlling IBV generally involves using either live-attenuated or inactivated vaccines (Shirvani *et al.*, 2018). However, these vaccine types come with disadvantages. For example, there are concerns regarding the safety of attenuated viruses as they have been found to be a source of IBV outbreaks (de Wit and Cook, 2014; Nix *et al.*, 2000). Vaccine strains that are used for live attenuation are not considered genetically stable and are known for reverting back to virulence (Meeusen *et al.*, 2007; Bande *et al.*, 2015). On the other hand, inactivated vaccines are less able to elicit strong immune responses against IBV (Ladman *et al.*, 2002; Collisson *et al.*, 2000). Their production and method of administration (intra-muscular injection) is highly costly and time-consuming (Meeusen *et al.*, 2007; Bande *et al.*, 2015) and their effectiveness is dependent on prior priming with an attenuated vaccine (de Wit and Cook, 2019). Neither attenuated nor inactivated virus vaccines are able to provide broad and effective protection against IBV because of a lack of antigenic matching between serotypes of the vaccine and the variant strain that is circulating in the field (Casais *et al.*, 2003; Seyfi Abad Shapouri *et al.*, 2004).

For this reason, safe, cost-effective, efficacious, antigen-matched vaccines are required to control IBV and prevent further economic losses caused by the disease. The development of such vaccines has been researched but these tend to be costly, and the method of application,

which is normally by intramuscular injection, remains unsuitable for large-scale applications (Jackwood and de Wit, 2013).

Biopharming is defined as the manufacture of recombinant pharmaceutical proteins with plants being used as bioreactors. Plants offer useful alternatives in terms of producing pharmaceuticals such as antigens for diagnostics and vaccines due to their ability to cost-effectively produce large amounts of target proteins. Transient expression using plants is one of the most rapid and cost-effective recombinant platforms available (D'Aoust *et al.*, 2008). Virus-like particle (VLP) vaccines can efficiently be assembled using plant-based transient expression and, compared to other expression systems, plants do not support the production of endotoxins or the growth of infectious prions and viruses that infect humans, making them safer to use (Moustafa *et al.*, 2016). They also assist with necessary post-translational modifications (Tschofen *et al.*, 2016) and allow for the expression of multiple proteins (Castilho and Steinkellner, 2012; Castilho *et al.*, 2010).

The method of plant-based transient expression has been utilised to produce VLPs for several animal viruses (Liu *et al.*, 2013b), most notably, the development of VLPs against Influenza A Virus (IAV) for human vaccines (D'Aoust *et al.*, 2008). Fraunhofer Society (Germany) and Medicago, Inc. (Canada) have developed VLPs for seasonal as well as pandemic influenza that are in the later stages of clinical trials. In the veterinary sector, superior efficacy of a plant-produced antigen-matched IAV (H6 subtype) VLP subunit vaccine has been demonstrated in SPF chickens to have great potential for the health of poultry (Smith *et al.*, 2019). Chimeric bluetongue virus (BTV) VLPs were also produced by expressing the BTV capsid proteins from multiple serotypes in *Nicotiana benthamiana* plants, and these VLPs were shown to induce high levels of serotype-specific neutralizing antibodies similar to those induced by a live-attenuated vaccine and that were long-lasting (Mokoena *et al.*, 2019). Similarly, chimeric VLPs and soluble viral protein 2 (VP2) against African horse sickness virus (AHSV) were formed in *Nicotiana benthamiana* plants that were shown to elicit high titres of serum antibody demonstrating protective efficacy in IFNAR^{-/-} mice (O'Kennedy *et al.*, 2022). Plant-produced AHS VLPs were shown to stimulate high titres of serotype-specific neutralizing antibodies in guinea pigs, and then in horses demonstrating both safety and high immunogenicity (Dennis *et al.*, 2018a; Dennis *et al.*, 2018b; Rutkowska *et al.*, 2019). Stander and co-workers generated a West Nile virus (WNV) VLP-display based vaccine candidate by fusing to and displaying the WNV envelope protein domain III (EDIII) on AP205 phage VLPs after each was separately

produced in *N. benthamiana* plants (Stander *et al.*, 2021). The result was conjugated VLPs displaying the EDIII that were able to elicit potent IgG responses to WNV EDIII (Stander *et al.*, 2021). Porcine epidemic diarrhea virus (PEDV) VLPs were expressed in *N. benthamiana* plants but with low yields and difficulty with purification (Peyret *et al.*, 2021). Most recently, Abolnik and co-workers produced a recombinant VLP which displayed the haemagglutinin protein of the H5N8 highly pathogenic strain of IAV in *N. benthamiana* plants (Abolnik *et al.*, 2022). Two immunisations with the H5 VLPs exhibited high HI titres in hens and vaccinated birds were fully protected from homologous challenge with the H5N8 HPAI virus with reduced oropharyngeal and cloacal viral shedding (Abolnik *et al.*, 2022). Plant-produced VLPs for IBV have up until the results of this thesis not yet been reported.

1.2. Classification and Structure of IBV

IBV belongs to the family *Coronaviridae* (*Coronavirinae* subfamily) within the *Nidovirales* order (de Groot *et al.*, 2011; de Groot *et al.*, 2012; Wickramasinghe *et al.*, 2014; Ujike and Taguchi, 2015). It is a *Gammacoronavirus* (Jackwood and de Wit, 2013) that primarily causes disease in the domestic chicken (*Gallus gallus*) (Wickramasinghe *et al.*, 2014; Eterradossi and Britton, 2013). This enveloped RNA virus is rounded or pleomorphic in morphology. The virus particles range from 80 to 120 nm in diameter and are surrounded by club or petal-shaped surface protrusions that are approximately 16 to 21 nm in length (Fig. 1.1) (Jackwood and de Wit, 2013; Liu *et al.*, 2013a; Cavanagh and Gelb, 2008). These protrusions are referred to as spikes, which give the virus particle its crown-like form, hence its name – Corona (crown) (Jackwood and de Wit, 2013).

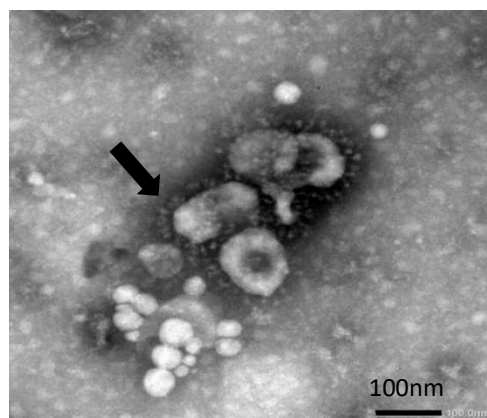


Figure 1.1. Negative-stained transmission electron microscopy image of a purified live QX-like IBV strain ck/ZA/3665/11 (clarified allantoic fluid containing the challenge strain used in Chapter 5). The arrow indicates the IBV spikes. The bar represents 100 nm.

1.3. Genome Organisation

IBV contains a single-stranded linear positive-sense RNA genome of between 27.5 and 28 kb in length (Jackwood and de Wit, 2013; Zhang *et al.*, 2010; Masters and Perlman, 2013). The viral genome is organised as follows: 5' untranslated region (UTR)-leader-replicase(1a-1b)-S-3a-3b-E-M-5a-5b-N-3'UTR (Fig. 1.2) (Jackwood and de Wit, 2013). The untranslated regions play a role in the transcription as well as replication of viral RNA and there is a 5' cap and a polyA tail on the 3' end of the genome (Zhang *et al.*, 2010; Jackwood and de Wit, 2013).

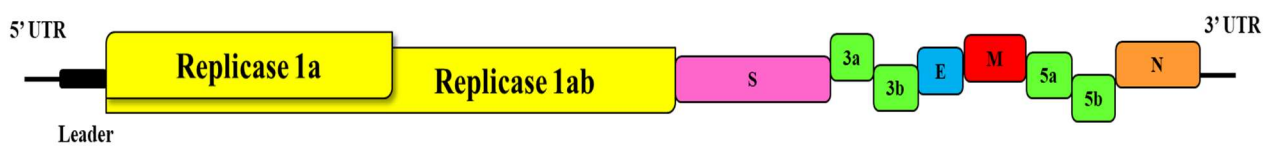


Figure 1.2. Infectious Bronchitis Virus genome organisation coding for the structural and non-structural proteins (Not drawn to scale) (adapted from Jackwood and de Wit, 2013)

On its 5' end, the genome codes for the overlapping polyproteins 1a and 1b, that are processed into 15 non-structural proteins which are involved in viral replication and translation of the viral RNA-dependent RNA polymerase (Perlman *et al.*, 2008; Liu *et al.*, 2014; Ziebuhr *et al.*, 2000). On its 3' end, the genome encodes the virus' four structural proteins which are the envelope (E), nucleocapsid (N), spike (S), and membrane (M) proteins. The non-structural proteins on the 3' end, namely 3a, 3b, 5a, and 5b, have unknown functions (Bournnell *et al.*, 1987; Jackwood and de Wit, 2013).

1.4. Structural Proteins of IBV

The IBV particle is comprised of four core structural proteins; the Membrane (M), Envelope (E), Nucleocapsid (N), and Spike (S) proteins.

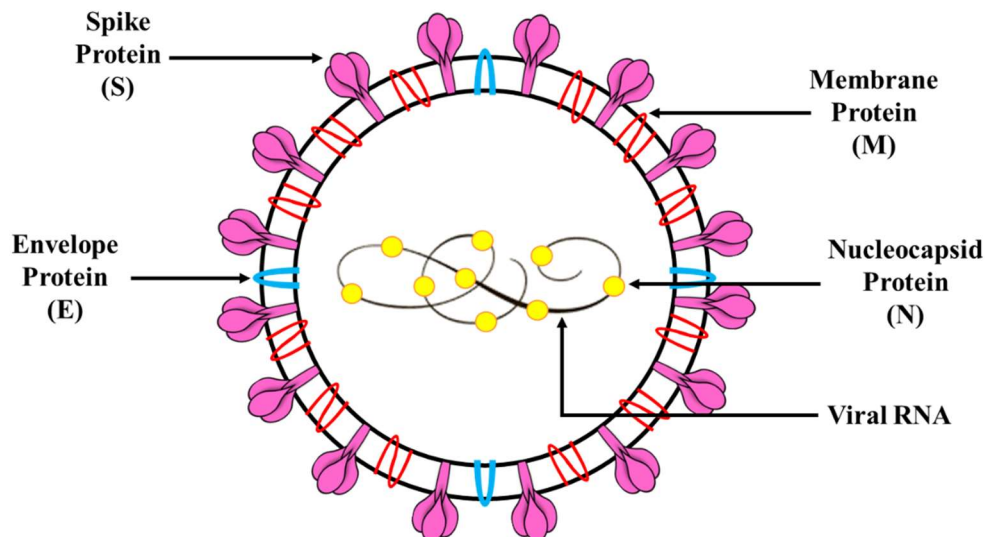


Figure 1.3. Schematic diagram of the structure of Infectious Bronchitis Virus indicating the structural proteins (adapted from Abdel-Moneim, 2017).

1.4.1. Membrane Protein

The membrane protein (M) is the most abundant of the structural proteins and interacts with the S protein as well as the viral ribonucleocapsid to aid in viral particle formation (de Haan *et al.*, 2000; Bande *et al.*, 2016). Its interaction with the RNA packaging signal of the virus may also make the M protein vital for RNA packaging into the viral nucleocapsid (Narayanan *et al.*, 2003). This protein ranges from 25 to 33 kDa in size and has its smaller domain facing the outer edge of the virus envelope (Fig. 1.3) (Abdel-Moneim, 2017). Its larger carboxyl-terminal domain is located on the interior of the virus envelope along with a triple membrane (Lai and Cavanagh, 1997). The entire protein spans the viral envelope three times (Jackwood and de Wit, 2013; Ruch and Machamer, 2011). This glycoprotein gets sent to the pre-Golgi region and it undergoes glycosylation via N linkage (Lai and Cavanagh, 1997; Abdel-Moneim, 2017).

1.4.2. Envelope Protein

The envelope protein (E) is the least abundant structural protein found in the virions. It is part of the viral envelope with a size that falls between 9 and 12 kDa (Godet *et al.*, 1992). It comprises the cytoplasmic C-terminal and extremely hydrophobic transmembrane N terminal domains, both of which are found in the lumen of the virus. It extends twice over the lipid bilayer (Fig. 1.3) (Maeda *et al.*, 2001). In cells infected with IBV, the E protein localises to the

Golgi complex and contributes to viral envelope formation, viral particle assembly, ion channel activity, budding of the virus, and cell apoptosis (Wilson *et al.*, 2006; Corse and Machamer, 2003). The expression of the E protein on its own is enough to ensure the release of vesicles from cells that have been transfected with the virus (Maeda *et al.*, 1999).

1.4.3. Nucleocapsid Protein

The nucleocapsid protein (N) is greatly conserved among coronaviruses (Williams *et al.*, 1992). This phosphoprotein ranges from 50 to 60 kDa in size and plays a role in cytotoxic T lymphocyte induction (Collisson *et al.*, 2000; Seo *et al.*, 1997). Genome packaging is mediated by the N protein, which encapsulates the viral RNA, binding with it, and forming a helical ribonucleoprotein complex within the virion (Fig. 1.3) (Cavanagh, 2007; Jayaram *et al.*, 2005). This assists with the transcription, replication, and translation of the viral RNA, as well as its packaging into the virus particle (Jayaram *et al.*, 2005). The N protein may offer support in assembling the virus particle through E and M protein interactions (Jayaram *et al.*, 2006). The N-terminal domain of the N protein was also found to contain peptides from the epitopes of novel linear B-cells (Yu *et al.*, 2010).

1.4.4. Spike Protein

The spike glycoprotein (S) is a trimer protruding from the viral surface (Fig. 1.3) which comprises subunits S1 and S2 that form when the Spike glycoprotein is cleaved post-translationally (Fig. 1.4) and correspond to about 520 and 625 amino acids long (Cavanagh, 2007; Jackwood and de Wit, 2013). This is mediated by the host cell's furin-like protease (Cavanagh *et al.*, 1986; Liu *et al.*, 2013a). The S2 subunit (84 kDa) at the C-terminal end of the protein anchors the protein to the membrane by non-covalently associating with the N-terminal S1 subunit (90 kDa) (Lai and Cavanagh, 1997). The larger part of the ectodomain is formed by the S1 subunit which forms the bulb of the S protein. This subunit is the portion of the S protein that is able to induce neutralising antibodies (Koch *et al.*, 1990; Kant *et al.*, 1992, and includes the receptor-binding domain (RBD) which aids in host cell viral attachment (Promkuntod *et al.*, 2014). The S2 subunit makes up the smaller part of the ectodomain which forms the narrow S protein stalk along with the short transmembrane (TM) domain and endodomain (Wickramasinghe *et al.*, 2014). This smaller stalk subunit assists with viral host cell attachment and has antigenic viral epitopes (Toro *et al.*, 2014b). The molecular mass of

the S protein monomer is close to 128 kDa preceding glycosylation (Masters and Perlman, 2013). The N-terminal signal peptide, after being cleaved, directs the S protein to undergo glycosylation at the ER, increasing its molecular mass to around 200 kDa in size (Wickramasinghe *et al.*, 2014; Binns *et al.*, 1985). The monomers thereafter form either dimers or trimers by means of oligomerisation (Lewicki and Gallagher, 2002).

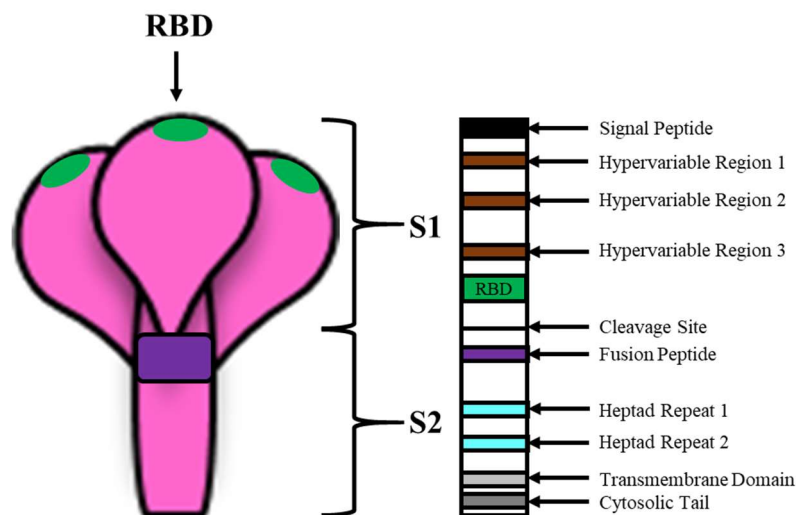


Figure 1.4. Schematic diagram of the S1 and S2 subunits of the IBV spike protein (adapted from Kung *et al.*, 2022).

The Spike glycoprotein is classified as a viral fusion peptide (class 1) which has a part in viral host cell attachment (which is facilitated by the variable S1 domain), fusion and entry (which is facilitated by the S2 subunit, which is highly conserved) (Wickramasinghe *et al.*, 2011; Masters and Perlman, 2013; Casais *et al.*, 2003). It is a type 1 membrane protein that comprises a fusion peptide (FP), two heptad repeat regions (HR1 and HR2), a precoil domain, a receptor-binding domain (RBD), an interhelical domain, a cleavage site, a transmembrane domain, and a cytoplasmic tail (CT) (Fig. 1.4) (Perlman *et al.*, 2008; Koch *et al.*, 1990).

1.5. Classification of IBV Strains

There are various methods that have been established for differentiating between different IBV strains (Valastro *et al.*, 2016). The methods that focus on investigating either the antigenic or genetic properties of an IBV strain describe serotype or genotype designation, respectively, while the methods that evaluate immune responses resulting from chickens that have been

challenged with an IBV strain describe protectotype designation (Lohr, 1988). These three different designations however, do not always group the IBV strains in the same manner, which means there is currently no definitive classification system that is agreed upon (Valastro *et al.*, 2016).

1.5.1. Serotypes

IBV serotypes are determined by the S protein. To be specific, the emergence of different serotypes as well as genotypes of IBV are a result of mutations that arise in the S1 subunit of the S protein (Liu *et al.*, 2003). New IBV serotypes emerge when natural selection acts on molecular changes such as genetic shift resulting from recombination events or natural errors that the RNA-dependent RNA polymerase makes which result in genetic mutations (Kusters *et al.*, 1990; Hanada *et al.*, 2004). This virus uses its ability to replicate rapidly, as well as large population sizes to generate genetic diversity (Jackwood *et al.*, 2012). Selection pressures may also arise from the use of various vaccines in the poultry industry (Jackwood *et al.*, 2012). Evidence of this is found in the number of variant viruses that have genetic sequences which are incredibly similar to that of the vaccines that were used to vaccinate the flocks (Nix *et al.*, 2000). It is said that the use of vaccines not only causes new IBV variants to arise through recombination, but they can also impose selection pressure on the evolution of circulating field strains (Fan *et al.*, 2019). McKinley and coworkers (2008) presented data that showed that the selection of a subpopulation of intra-vaccine quasispecies is a result of the infection and replication of the IBV vaccine viruses in chickens and that there is an occurrence of genetic mutation among different IB vaccines. (McKinley *et al.*, 2008). Zhao *et al.*, (2016) did a study with results that indicated that selected IBV isolates from China were evolving at a fast rate due to the immune selection pressure caused by vaccine use. There are also some cases where new variants have been shown to arise as a result of recombination between attenuated vaccines and IBV strains that are circulating in the field (Jia *et al.*, 1995). The nephropathogenic strains of IBV that have an affinity for kidney tissues have been thought to be derived from mutations caused by the widespread use of modified live-attenuated IBV vaccines (Butcher *et al.*, 2022). Using these vaccines to protect respiratory tissues against infections essentially forced the virus to mutate to allow it to affect the less protected tissues, i.e. the kidney tissues (Butcher *et al.*, 2018).

There is a lot of antigenic variation amongst different strains of IBV (Jackwood and de Wit, 2013) meaning that a vaccine that has been developed based on a certain IBV serotype might offer poor levels of protection against an antigenically-distinct strain of IBV (WOAH, 2019). Classifying IBV types by serotypes involves treating the virus with neutralizing antibodies and performing 2-way cross-virus neutralisation (VN) tests using embryonating chicken eggs. The unknown virus is treated with antisera of known strains of IBV, followed by the preparation of serotype-specific antibody against the unknown virus which is then treated with known IBV strains (Jackwood and de Wit, 2013). The Archetti and Horsfall formula is then used to calculate a relatedness value (Archetti and Horsfall, 1950). Serotype-specific monoclonal antibodies have been used in indirect immunofluorescence assays, virus-neutralisation assays (VN), or enzyme-linked immunosorbent assays (ELISA), however, these are only available for very few IBV serotypes (Karaca *et al.*, 1992; Kant *et al.*, 1992).

Serotypes can also be determined using haemagglutination inhibition (HI) assays, however, most strains of IBV are not able to haemagglutinate chicken red blood cells (CRBC) without prior treatment with neuraminidase to induce haemagglutination activity (Ruano *et al.*, 2000; Gelb and Jackwood, 2008). HI antibody responses that result from a single exposure to the virus may have a high specificity to the IBV strain, which, along with the limited cross-reactivity of the primary immune response, allow isolates to be serotyped using this method (Jackwood and de Wit, 2013). However, after multiple exposure to the virus, particularly in birds that have been vaccinated, there are varying levels of cross-reactions that make differentiating strains using HI tests difficult (Cook *et al.*, 1987; Gelb and Jackwood, 2008).

Of the many different serotypes that exist, hundreds of variations may exist globally, which makes it imperative to study the molecular evolution of this virus (Jordan, 2016). Because so many serotypes exist, identifying regional serotypes is important for the purpose of developing effective vaccination strategies (Zhou *et al.*, 2004).

1.5.2. Genotypes

IBV has a rapid ability to mutate itself, leading to the constant emergence of new genotypes and serotypes (Cavanagh and Gelb, 2008). This continuous emergence of new variants makes this virus incredibly difficult to control using conventional vaccination programs with commercial vaccines (de Wit *et al.*, 2011). RNA viruses are known to be prone to a high

genomic mutation rate because they have a low reproduction fidelity, and the RNA polymerase has low processivity. This allows the virus to evade host defences, resulting in further evolution. Coronaviruses in particular are RNA viruses with the largest genome, which means that it has a higher likelihood of mutation under environmental and vaccination pressures (Compton *et al.*, 1993). Because it is a coronavirus, and therefore a single-stranded RNA virus, IBV is able to vastly change its genome through genetic recombination and spontaneous mutation events (Cavanagh and Gelb, 2008). If these events take place in the hypervariable regions (HVRs) of the spike gene, these events are likely to cause new variants to emerge (de Wit *et al.*, 2011). IBV isolates are classified into genotypes by examining the sequence of the S protein (Jackwood and de Wit, 2013). Although it may not always be the case, an amino acid similarity of 90 % or higher in the HVRs of the S1 subunit (genotype), generally puts strains into the same serotype classification (Cavanagh, 2001; Jackwood and de Wit, 2013; Gallardo, 2021). The sequence of the S1 gene or its HVR is amplified using reverse transcriptase polymerase chain reaction (RT-PCR), after which either restriction fragment length polymorphism or more commonly, nucleic acid sequencing is performed which groups different IBV strains by genotype (Lin *et al.*, 1991; Lee *et al.*, 2003; Kwon *et al.*, 1993; Jackwood *et al.*, 1997; Keeler *et al.*, 1998).

Variant strains of IBV are strains that although not fully genetically different, are phenotypically different from conventional strains, and are able to escape the immunity derived from the conventional serotype-specific vaccine types (Gallardo, 2021). Although many of these new variants lack the ability to replicate making them unable to survive long term, some emerge and can become economically important either in a specific region, or globally (de Wit *et al.*, 2011). de Wit and co-workers (2011) described the widespread distribution of IBV variants worldwide with some remaining endemic to certain geographical regions while others proliferate readily throughout other parts of the globe. Some variants including the QX variant and the 4-91 variant are of major importance due to their spreading over parts of Africa, Asia, and Europe in a short period of time (de Wit *et al.*, 2011). There are over 32 genotypes of IBV circulating and these offer little to no cross-protection against other variants (Bande *et al.*, 2015; Jara *et al.*, 2021). To be specific, there have been seven genotypes of IBV defined based on S1 subunit gene nucleotide sequences and these encompass at least 35 different IBV lineages (Xu *et al.*, 2019; Valastro *et al.*, 2016).

1.5.3. Protectotypes

While serotyping and genotyping are useful methods of characterising IBV variants, they may not always group them similarly (de Wit and Cook, 2014). The complex relationship between genotype and serotype makes it difficult to find the best method for determining which IBV vaccines are able to protect against certain IBV variants (de Wit and Cook, 2014). Therefore, IBV variants are sometimes grouped into protectotypes rather than genotypes or phenotypes, where the clinical effects of IBV within the field are considered (de Wit and Cook, 2014). The term “protectotype” is used to define the level of cross-protection that is provided by existing vaccines against IBV genotypes and serotypes (Lohr, 1988). It has previously been shown that higher levels of variation between the S1 sequences of various strains of IBV result in lower levels of cross-protection between strains (Ladman *et al.*, 2006; Cavanagh *et al.*, 1997).

In vivo protection studies are used to help group the variants into protectotypes, but the best method required for optimal results is more difficult to determine (Hofstad, 1975). This difficulty is largely due to the type of disease IBV causes. The virus primarily infects the upper respiratory tract cells, making respiratory infections the most significant indicator of an IBV infection (de Wit and Cook, 2014). It is therefore most crucial to confirm that a vaccine against IBV is able to protect against the respiratory infection caused by the virus. However, due to the difficulty in quantifying clinical signs in experimental circumstances, it is not easy to achieve such confirmation (de Wit and Cook, 2014).

1.6. IBV Pathogenesis

IBV is primarily a disease of the respiratory system but several field isolates and variants of IBV are also capable of infecting the renal, digestive, and reproductive systems of chickens. The progression of disease varies, depending on the strain of IBV, as well as on which system was infected (Bande *et al.*, 2016). The disease is transmitted to the upper-respiratory tract via direct contact with infected birds from the same flock where infectious particles are either inhaled or ingested (Matthijs *et al.*, 2008; Jackwood and de Wit, 2013). It can also be transmitted indirectly by exposure to contaminated objects that may carry and transfer the disease, as well as through aerosol droplets and faecal matter (Jackwood and de Wit, 2013).

The main replication site of the virus is the upper respiratory tract (Khataby *et al.*, 2020) and viremia then follows resulting in the virus disseminating to other host cell tissues (McMartin,

1993; Khataby *et al.*, 2020). The virus has been shown to multiply in ciliated epithelial cells as well as in mucus secretory cells (Khataby *et al.*, 2020; Lee *et al.*, 2003).

Although the cell receptor for IBV is yet to be elucidated, the attachment of the spike protein to the target cell requires an α -2,3-linked sialic acid (Wickramasinghe *et al.*, 2011; Promkuntod *et al.*, 2014). Once the spike protein receptor binding site has attached the virus to a specific host cell receptor, viral fusion and cell entry occurs. The viral receptor binding causes the S protein to undergo a conformational change that activates membrane fusion. Following membrane fusion, is the release of the nucleocapsid into the host cytoplasm where the viral RNA is uncoated in order for it to be transcribed and translated (Abdel-Moneim, 2017).

IBV replicates in the cytoplasm of the host cell, and produces a co-terminal set at the 3' end consisting of five subgenomic mRNAs (messenger RNA) synthesised through discontinuous transcription (Masters, 2006; Tan *et al.*, 2012). Each of these mRNAs contains a 5' leader sequence linked to the mRNA when viral transcription occurs (Jackwood and de Wit, 2013). While a variety of the mRNAs are polycistronic, coding for more than one polypeptide, the majority of them encode the protein found at the outermost 5' end. The mRNA1, the full IBV genome, codes for the viral polymerase polyproteins, while the 5 subgenomic mRNAs encode the Spike (mRNA2); 3a/b, and Envelope (mRNA3); Membrane (mRNA4); 5a/b (mRNA5); lastly the Nucleocapsid (mRNA6) proteins (Jackwood and de Wit, 2013). Replication of the full IBV genome takes place through continuous transcription (Masters, 2006; Tan *et al.*, 2012). As the virus enters the host cell, its genome mimics mRNA which codes for the non-structural proteins (2-16). The mRNA forms to create the viral polymerase encased in vesicles with a double membrane located within the Golgi apparatus (Hagemeijer *et al.*, 2010). Transcription of subgenomic mRNAs, as well as viral protein translation happens in the host cell cytoplasm (Jackwood and de Wit, 2013). Virus particles assemble and get transported to the plasma membrane of the host cell in vesicles from a vesicular compartment found between the Golgi apparatus and the rough endoplasmic reticulum (ER) (Klumperman *et al.*, 1994). The IBV E protein provides a strong temporary anchor for the IBV M protein to relocate in the pre-Golgi compartments, preparing the membrane for budding (Raamsman *et al.*, 2000). A canonical dilysine ER retrieval signal (KKXX-COOH) located on the CT of the spike protein plays a vital role in the accumulation of proteins near the budding sites (Ujike and Taguchi, 2015). Interactions between the M, N, and E proteins are what allow virus particle budding from the endoplasmic reticulum (Klumperman *et al.*, 1994). The virions are then transported to the

plasma membrane through the Golgi via the exocytic pathway; following fusion and budding from the host cell (Jackwood and de Wit, 2013).

1.7. Clinical Signs of IBV

Infectious Bronchitis Virus has a short incubation time with its clinical signs developing between 24 - 48 hours of being infected (Jackwood and de Wit, 2013). The clinical manifestations and severity of the disease will depend largely on the IBV strain as well as which system it infects (Bande *et al.*, 2016). When the upper-respiratory tract is infected, the clinical signs of an IBV infection include sneezing, nasal discharge, coughing, gasping, as well as tracheal rales (Cavanagh and Gelb, 2008; Jackwood and de Wit, 2013). Some chickens experience watery eyes and swollen sinuses. The birds appear to lack energy, consume less feed and lose weight (Jackwood and de Wit, 2013). They begin to group together around common sources of heat and their feathers begin to appear ruffled (Cavanagh and Gelb, 2008). Other clinical signs of infection include oedema, periorbital cellulitis, or conjunctivitis with frothy discharge from the eyes (Bande *et al.*, 2016).

Nephropathogenic IBV strains cause inflammation in the kidneys as well as decreased kidney function (Jackwood and de Wit, 2013). The clinical signs of these strains are inflamed, pale kidneys, in addition to swollen tubules and ureters due to urates (Jackwood and de Wit, 2013; Cumming, 1963). Although several strains of IBV are somewhat linked to nephritis, birds that are older than 2 weeks of age tend to demonstrate a higher resistance to these nephropathogenic effects (Jackwood and de Wit, 2013). In broilers, some additional clinical signs are the excessive intake of water, wet droppings, depression, and death (Cumming, 1969).

The infection of the reproductive tract results in oviduct lesions which leads to a clear reduction in egg production and quality. The results of this being soft or rough-shelled eggs, thin shells with diminished pigmentation, and malformed eggs. The eggs may also contain a thin and watery albumin, or they may not successfully hatch (Jackwood and de Wit, 2013). Depending on the IBV strain, the bird's immunity, and other factors, the level of egg production may even drop by 70 % of what is expected from healthy chickens (Box and Ellis, 1985; van Eck, 1983; Broadfoot *et al.*, 1954). Older birds are more resistant to oviduct lesions and have a decreased chance of mortality than younger chicks (Chong and Apostolov, 1982; Butcher *et al.*, 1990).

1.8. Diagnosing IBV

In order to accurately diagnose IBV, the clinical signs and the clinical history of the infected bird need to be analysed. The virus needs to be isolated, the serotype or genotype identified, and viral RNA detected. Diagnosis also involves using antibody-based antigen capture tests, sero-conversion, and lesion scoring (Jackwood and de Wit, 2013; Gelb and Jackwood, 2008). The virus serotype has often been determined using virus neutralisation (VN) and haemagglutination inhibition (HI) tests, which have been replaced with molecular-based tests due to their disadvantages. HI tests are prone to non-specific cross-reactivity, while VN tests are both labour-intensive and time-consuming (Jackwood and de Wit, 2013).

Important factors to consider when diagnosing IBV include the immune status of the infected bird, how much time has passed between infection and sample taking, as well as the pathogenesis of the virus (Dhinaker and Jones, 1997; de Wit, 2000). The preferred sample to be taken in the first week after being infected is fresh tracheal tissue and should be analysed within the first 3-5 days of being infected. During viral spread, the titre of the virus decreases quickly. Cecal tonsil and kidney samples may be collected *post mortem* (Jackwood and de Wit, 2013). Both unhealthy and healthy chickens within a large flock should be sampled, with the samples being inoculated into specific pathogen-free (SPF) eggs, and passaged 3-4 times before they can be considered negative. A sample is considered negative once it is unable to cause lesions or embryo death, as well as ciliostasis of tracheal organ cultures (Gelb and Jackwood, 2008). HI, immunofluorescence, immunochemistry, VN, detection of viral nucleic acid, or electron microscope detection is then used to detect viral presence (Jackwood and de Wit, 2013). In embryonated chicken eggs, IBV can be detected using IBV-specific monoclonal antibodies or polyclonal sera with either immunofluorescence, immunohistochemistry, or immunoperoxidase assays (de Wit, 2000; Jackwood and de Wit, 2013). These, however, are difficult to interpret due to non-specific reactions. The agar gel precipitation (AGP) test can be used for allantoic fluid, tracheal material or inoculated eggs (Gelb *et al.*, 1981). Its sensitivity on organs is higher than that of more modern assays (de Wit, 2000).

When IBV is grown in allantoic fluid or tracheal organ cultures, it can be detected and classified using antigen-capture or indirect enzyme-linked immunosorbent assays (ELISA) making use of monoclonal antibodies (Ignjatovic and Ashton, 1996). These assays are also useful for serological tests for IBV antibodies because many samples can be tested rapidly and inexpensively (Jackwood and de Wit, 2013). Monoclonal antibodies however, are only

available for a very small number of IBV serotypes (Kant *et al.*, 1992; Karaca *et al.*, 1992). The disadvantage of ELISA, AGP, and immunofluorescence tests is that they all bind antibodies to antigens that are group-specific, so they cannot be used for the differentiation of IBV serotypes (Jackwood and de Wit, 2013).

Conventional RT-PCR can also be used for the detection of IBV RNA, however, it may need initial serial passage in embryonating SPF chicken eggs in order to obtain a positive result (Jackwood and de Wit, 2013). Nested RT-PCR can detect low levels of viral RNA, however, it can lead to false positives due to its high sensitivity as well as false positives resulting from the high probability of cross-contamination. A positive RT-PCR test is only able to confirm the presence of the viral RNA and is still not able to determine the IBV serotype (Jackwood and de Wit, 2013).

Real-time or quantitative real-time RT-PCR (qRT-PCR) is gaining popularity as a way to directly detect IBV from clinical samples (i.e., tracheal swabs) after challenge (Callison *et al.*, 2006). With qRT-PCR, it is possible to examine numerous clinical samples in a small amount of time, it provides indication of the amount of viral RNA present in the sample, and it is a cost-effective test (Jackwood and de Wit, 2013). The advantages of qRT-PCR include high sensitivity, extensive dynamic range, short run times, its functional simplicity, as well as a high sequence specificity (Wong and Medrano, 2005). qRT-PCR allows for the examination of the samples in real-time, measured using a fluorescent probe, which allows the PCR product to be quantified. Because qRT-PCR is performed in real-time, unlike standard RT-PCR assays, an agarose gel is not required (Adams, 2020). It is commonly used for determining the copy number by referencing a standard curve of known concentrations more accurately than other PCR tests (Adams, 2020).

qRT-PCR assays are used either for detecting all types of IBV generally, or for specifically detecting a single IBV serotype (Callison *et al.*, 2006; Roh *et al.*, 2014). Generic IBV qRT-PCR assays target a part of the virus genome which is greatly conserved amongst the IBV serotypes, which allows it to detect IBV in general, though not the genotype (Jordan, 2017). Genotype-specific qRT-PCR tests are able to target sequences of the more highly diverse hypervariable regions (HVRs) which correlate to specific serotypes (Jordan, 2017). To identify the IBV strain, the S1 gene amplicons must be analysed with genotyping techniques including sequence analysis of the S1 gene hypervariable regions, restriction fragment length

polymorphism and genotype-specific RT-PCR (Jackwood and de Wit, 2013; Kwon *et al.*, 1993).

1.9. Control of IBV

For IBV control, it is important to ensure high biosecurity, including isolating birds that are infected, repopulating the flock with day old birds, as well as disinfecting any surfaces or equipment that has been exposed to the virus. The chickens need to be vaccinated to avoid the virus spreading further (Jackwood and de Wit, 2013).

Although strict biosecurity is essential for controlling IBV, vaccination is usually required to increase the chickens' ability to resist IBV challenge (de Wit *et al.*, 2011). However, because the virus exists as many different serotypes and variants, successful vaccination can be difficult to achieve (de Wit *et al.*, 2011). Many vaccination strategies involve using live-attenuated as well as inactivated oil-adjuvanted vaccines. Live-attenuated vaccines are typically used in younger birds to establish early protection against future IBV challenge. They are used to prime future breeders and layers prior to boosting with an inactivated vaccine (de Wit *et al.*, 2011).

The first reported vaccine, isolated in 1941 at the University of Massachusetts, was the strain, van Roeckel M-41, which was a Massachusetts IBV serotype (van Roeckel *et al.*, 1942). It was the first vaccine to be developed in the United States and the Mass 41 vaccines currently used globally were derived from it (Jackwood and de Wit, 2013). Live-attenuated Mass/Mass41/41 and Mass/H120/55 vaccines that are of the Massachusetts serotype are the most commonly used vaccine strains around the world (Jackwood and de Wit, 2013). Most IBV vaccines have been based on live-attenuated or inactivated vaccines that are derived from either classical or variant strains of IBV (Bande *et al.*, 2015). These vaccines were developed from strains such as Ma5, M41, Conn, and Ark that originated from the USA, strains such as H120 and H52 originating from the Netherlands, or strains such as 793/B, D274, and CR88 originating from Europe (Bande *et al.*, 2015). These strains however, demonstrated poor immune responses, particularly against the IBV strains local to those areas (Bande *et al.*, 2015).

The vaccination of broilers against IBV involves using modified live-attenuated vaccines, while the vaccination of layers against IBV typically consisted of the administration of a range of live-attenuated vaccines and gradually progressing from a mild to an aggressive vaccination

route. For example, beginning with water administration and progressing to a fine particle spray vaccination (Butcher *et al.*, 2022). The vaccination of breeders against IBV follows a similar program with the difference being the administration of an inactivated vaccine in order to stimulate the production of antibodies (Butcher *et al.*, 2022). Inactivated vaccines are known to induce greater levels of circulating antibodies than those induced by live-attenuated vaccines, making them valuable in breeder programs requiring the protection of maternal antibodies (Butcher *et al.*, 2022). Modified live-attenuated vaccines are better at stimulating higher local antibody (IgA) responses resulting from local mucosal infection and cell mediation involving the T cell system (Butcher *et al.*, 2022). This makes them more valuable in the protection of commercial layers.

No combination of strains of IBV vaccines is able to offer full protection against all heterologous IBV challenges, however, some combinations may be able to offer broad-spectrum coverage (Butcher *et al.*, 2022). Cook *et al.*, (1999) showed that using more than one live-attenuated IBV vaccine type was able to offer broader protection in broilers than using just one. The use of live-attenuated Massachusetts (Mass) and 4-91 (793B) IBV strains together demonstrated increased protection in young chicks after challenge with different variants of IBV (Valastro *et al.*, 2016). Multiple vaccines of varying serotypes are commonly used simultaneously to increase flock protection (inducing homologous protection) which requires knowledge of the evolution of IBV serotypes (Jordan, 2017). Usually, vaccines belonging to a particular genotype or serotype, can protect the bird against homologous challenge. Sometimes, there is a varying degree of partial protection offered against strains of other genotypes, serotypes, or protectotypes (de Wit *et al.*, 2011). Homologous protection refers to the protection afforded by recent infection or recent vaccination against a particular strain, whereas heterologous protection refers to the variation in the level of protection afforded by one IBV strain against other strains (Jackwood and de Wit, 2013).

In some cases, only two vaccine serotypes are applied that are able to provide broad-spectrum heterologous cross-protection. This is referred to as protectotype vaccination which, in contrast to vaccination strategies that are centred on specific neutralising antibodies providing sterilising immunity, focuses on decreasing IBV infection sufficiently in order to protect against tracheal ciliostasis (Jordan, 2017). Protecting the tracheal cilia lowers the probability of being infected by a secondary bacterial infection and thus reduces losses caused by IBV infections (Jackwood *et al.*, 2015). The ideal way to protect chickens from IBV challenge, would be to identify the serotypes that are most dominant in the particular region, and

determine whether available vaccines have the potential to cross-protect against these serotypes (Butcher *et al.*, 2022). Once the dominant circulating strain in a region is identified, a combination of carefully selected strains of vaccines can be used to immunize layers, breeders, and broilers. Classically used strains of IBV have been demonstrated to be useful as partial primers for administering an inactivated IBV vaccine which contains variant and standard strains (Butcher *et al.*, 2022). While inactivated IBV vaccines are not as effective at stimulating local and cell-mediated immunity as well as modified live-attenuated IBV vaccines, they can offer some protection against variant strains without risking introducing new IBV strains into the population (Butcher *et al.*, 2022). The irresponsible use of live-attenuated IBV vaccines can lead to new strains emerging causing vaccines to be a problem as opposed to a solution (Bande *et al.*, 2015, Butcher *et al.*, 2022). Nephropathogenic strains of IBV have an affinity for the tissues of the kidney, potentially causing severe renal damage (Jackwood and de Wit, 2013). The nephropathogenic strains may have emerged from a mutation resulting from selection pressure caused by extensive use of modified live-attenuated IBV vaccines (Butcher *et al.*, 2022). Over the years, these strains have become more widespread.

Table 1.1. Summary of characteristics of live-attenuated and inactivated IBV vaccines

Live-attenuated IBV Vaccines	Inactivated IBV Vaccines
Typically used in younger birds to establish early protection, modified live-attenuated vaccines used in broilers	Valuable in breeder programs requiring protection of maternal antibodies
Better at stimulating higher local antibody (IgA) responses	Induce more circulating antibodies, less effective at stimulating local and cell-mediated immunity
Useful to prime future breeders and layers before boosting with inactivated vaccines	Used as a booster, requiring prior priming with a live-attenuated vaccine
Irresponsible/extensive use of modified live-attenuated vaccines can introduce new IBV strains due to selection pressure	Can offer protection against variant strains without risk of introducing new IBV strains into population
Derived from strains originating from the USA, Netherlands, or Europe	Derived from strains originating from the USA, Netherlands, or Europe
Cumbersome method of production requiring specific pathogen-free (SPF) chicken eggs	Costly, time-consuming production, requiring SPF chicken eggs, and unsuitable method of administration
Cannot offer broad and effective protection due to lack of antigenic matching between serotypes	Cannot offer broad and effective protection due to lack of antigenic matching between serotypes

1.10. Types of IBV Vaccines

1.10.1. Live-attenuated Vaccines

Live-attenuated vaccine types are produced by the serial passage of a live or wild virus in embryonated eggs (Bijlenga *et al.*, 2004). They are most commonly employed for vaccinating broiler chickens as well as for the first stage of vaccinating breeder and layer type chickens (Jackwood and de Wit, 2013). Deltamune (Pty) Ltd in South Africa uses this method for the development of tailored autogenous vaccines, which are vaccines developed from either a pathogen or an antigen that has been isolated from an animal, with the intention of using it for treating that particular animal (Saléry, 2017).

A downside of this vaccine type is that extensive serial passage can cause a decrease in the vaccine's immunogenicity resulting in inadequate protection against IBV. The stability and degree of live-attenuation among vaccine types varies (Jackwood and de Wit, 2013). It has also been shown that back-passage in a flock of chickens can lead to increased vaccine virulence (Hopkins and Yoder, 1986). Constantly circulating the virus vaccine increases its virulence and results in some of the flock being improperly vaccinated. Cyclic infections in flocks are also enhanced when fractional doses are used (Jackwood and de Wit, 2013). The widespread use of modified live-attenuated vaccines has been associated with the emergence of new IBV variants that are derived from mutations resulting from selection pressure (Butcher *et al.*, 2022).

Vaccinating with a single vaccine serotype is not always able to offer adequate protection against circulating strains of IBV, therefore, in order to achieve more broad-spectrum protection, vaccines of other serotypes are added to the vaccination program which are homologous with some of the circulating IBV strains (Jackwood *et al.*, 2003; Jackwood *et al.*, 2010). Alternatively, suitable combinations of vaccines are used which have been shown to induce broad cross-protection against multiple IBV strains (de Wit *et al.*, 2011; Terregino *et al.*, 2008).

Recombinant IBV vaccines can be generated using reverse genetics much faster than by attenuation, however, there is a risk of the vaccine reverting back to virulence (McGinnes and Morrison, 2014; Jordan, 2017).

1.10.2. Inactivated Variant Vaccines

The seed strains used to make inactivated variant vaccines are grown in embryonated chicken eggs and the vaccine is then developed by inactivating the seed virus through the use of chemicals such as formalin or beta-propiolactone (WOAH, 2018a; Jackwood and de Wit, 2013). Adapting field viruses to the high titre growth properties required to produce inactivated variant vaccines, and having access to a supply of specific pathogen free eggs are one of the main disadvantages of this traditional method of preparing inactivated vaccines (Vaughn *et al.*, 2009). The vaccines are typically formulated using mineral oil adjuvants before they are used on breeders and layers prior to egg production (Jackwood and de Wit, 2013; Jansen *et al.*, 2006). They induce high titres of serum antibody, and protect the internal tissues, kidney, and reproductive tracts (Jackwood and de Wit, 2013; de Wit *et al.*, 2011; Ladman *et al.*, 2002; Box *et al.*, 1980). When compared to live-attenuated vaccines however, they are less effective at protecting the respiratory tract from infection after challenging with a homologous IBV (Cook *et al.*, 1986). They can only induce humoral immunity and require individual administration by subcutaneous or intramuscular injection which is not practical when vaccinating larger flocks (Bande *et al.*, 2016). As with all egg-based methods, live embryos are sacrificed during the vaccine production process, which touches on animal ethics issues. Lastly, the efficacy of these inactivated IBV vaccines is heavily dependent upon prior priming with live-attenuated IBV vaccines (Jackwood and de Wit, 2013).

New variant IBV strains have been used to make inactivated autogenous vaccines that can be used to control IBV in laying birds as an alternative to the use of live variants that can potentially spread and affect neighbouring poultry flocks (Jackwood and de Wit, 2013). These inactivated variant vaccines have the potential to offer better protection against challenge with the live virulent variant strain of IBV than the traditional inactivated vaccines made using the classical strains of IBV such as the Mass type or the Conn types that are commonly used (Ladman *et al.*, 2002; Jackwood and de Wit, 2013).

1.10.3. Recombinant Vaccine Types

Recombinant IBV vaccine types express IBV antigen either alone or along with antigen from other pathogens (Jordan, 2017; Li *et al.*, 2016). The issues with RNA mutation are lowered (Song *et al.*, 1998). Their production generally involves using turkey herpesvirus or fowlpox virus viral backbones (Jordan, 2017). While genes that encode antigenic proteins from various

viruses including infectious laryngotracheitis virus (ILTV) (Vagnozzi *et al.*, 2012), Newcastle disease virus (NDV) (Morgan *et al.*, 1992), and infectious bursal disease virus (IBDV) (Darteil *et al.*, 1995) have been successfully inserted into these viral backbones, effectively inducing suitable immune responses in chickens, attempts to develop a recombinant IBV vaccine using the same viral backbones expressing the S1 subunit of the IBV spike gene have resulted in varied protection levels after challenge with a homologous virus (Toro *et al.*, 2014a; Jordan, 2017; Johnson *et al.*, 2003).

Recombinant IBV vaccine types are challenging to administer, requiring individual intramuscular injection or oculo-nasal administration and offer less protection against IBV than inactivated or live-attenuated vaccines (Yang *et al.*, 2016; Jordan, 2017; Li *et al.*, 2016). Multiple vaccinations tend to be needed and maternal and intrinsic immunity may hinder the live vector, decrease antigen uptake which affects the transgene's expression, thus interfering with the immune response (Jordan, 2017; Faulkner *et al.*, 2013).

Recombinant systems incorporating the S1 or S2 subunit of the IBV spike gene sequence into other viral backbones, for example, duck enteritis virus, avian metapneumovirus, or NDV, have shown promise due to their respiratory tropism (particularly with avian metapneumovirus and NDV) (Li *et al.*, 2016; Toro *et al.*, 2014b; Falchieri *et al.*, 2013). They had the potential to induce more robust immune responses in the head-associated lymphatic tissues and initial studies demonstrated some protection from homologous IBV challenge (Jordan, 2017).

Recombinant IBV that are generated using reverse genetics are promising vaccine candidates as they can be engineered in a laboratory, fulfilling the needs of the poultry industry (Jordan, 2017). The process behind this vaccine type involves cloning an IBV vaccine virus genome in a lab which can be manipulated using PCR, direct gene cloning, or homologous recombination (Casais *et al.*, 2001; Britton *et al.*, 2005). The reverse-engineered genome is then transfected into a cell-culture system which can replicate it, produce the proteins required for viral assembly, and produce fully-functional IBV particles (Jordan, 2017). Replacement of the IBV spike sequence used for a recombinant IBV vaccine with that of a different serotype has been shown to change the recombinant to the new serotype capable of inducing a protective immune response against challenge with the live virus of the new serotype (Jordan, 2017; Hodgeson *et al.*, 2004). This gives this system the advantage of being able to create an attenuated live vaccine against new emerging IBV variants by recombinant techniques far quicker than by traditional attenuation by serially passaging in embryonating chicken eggs (Jordan, 2017).

Because recombinant IBV vaccines are live viruses capable of infection and replication, the immune responses generated by recombinant IBV vaccines is similar to that of a live-attenuated vaccine. Their application would be similar to that used for live-attenuated viruses, however, the initial cost for producing the recombinant virus is substantially higher than that of the traditional serial passaging method. The disadvantage of these vaccines are that currently, each new recombinant would need to be licenced as a new virus, which would take too long considering how rapidly IBV mutates (Jordan, 2017).

Yang *et al.*, (2016) generated a recombinant IBV vaccine against the H120 strain which expressed the NDV haemagglutinin-neuraminidase (HN) protein using reverse genetics, which exhibited pathogenicity, viral titres, and growth dynamics similar to those exhibited by the parental H120 strain, but with added haemagglutination activity acquired from NDV. SPF chickens vaccinated with this recombinant virus induced humoral immune responses similar to those induced by a commercial LaSota/H120 bivalent vaccine, and offered significant protection against both NDV and IBV challenge (Yang *et al.*, 2016).

There are no commercially available recombinant IBV vaccines at present (Jordan, 2017).

1.10.4. Peptide, Subunit, and DNA Vaccines

Peptide, subunit, and DNA vaccines are all based on presenting the immune system of the host with an antigen to stimulate it to produce antibodies against that particular disease agent (Jordan, 2017). Although they do partially protect against challenge from IBV, they are costly to produce and impractical to apply at a large-scale in the poultry industry, requiring individual intramuscular injection multiple times (Yang *et al.*, 2009).

Subunit vaccine types are normally an antigenic protein derived from particular pathogens which can be considered safe as they make use of an antigenic protein from a pathogen rather than infectious virus particles (Jordan, 2017). They are also very stable and suitable for mass production (Yang *et al.*, 2009; Bande *et al.*, 2016). Several IBV recombinant subunit vaccines have been attempted making use of the recombinant S1 protein or other proteins (Andoh *et al.*, 2015). A recombinant S1 protein that was expressed in a baculovirus insect cell expression system was shown to provide effective levels of protection against IBV infection in chickens (Song *et al.*, 1998). Andoh and co-workers (2015) expressed a recombinant IBV S1 protein in mammalian cells as a secreted protein that was fused to a trimerization motif peptide and

purified via Ni Sepharose (Andoh *et al.*, 2015). This recombinant IBV S1 protein was highly glycosylated and induced anti-S1 antibodies although the neutralising antigenicity was much lower than that of an inactivated IBV virus vaccine suggesting that while it retained non-neutralising epitopes, its unnatural glycosylation pattern may have resulted in a conformation that lacked neutralising epitopes (Andoh *et al.*, 2015).

Peptide vaccines use small amino acid fragments from the pathogen's antigenic protein (Jordan, 2017). Multiple IBV S1 and N protein gene derived epitopes have been used for developing this type of vaccine against IBV and were shown to offer high protection against it (Yang *et al.*, 2009). Immunising chickens with recombinant S1 epitope peptides that were expressed using *Escherichia coli* (*E. coli*) was able to protect the chickens from IBV infection (Yang *et al.*, 2009a; Yang *et al.*, 2009b). To offer this level of protection, they require the use of either a delivery system, or an adjuvant to induce a more robust immune response (Skwarczynski and Toth, 2016; Li *et al.*, 2014). This is because their small size makes them weak immunogens on their own (Li *et al.*, 2014). Unlike folded proteins, they are susceptible to being degraded by enzymes (Skwarczynski and Toth, 2016).

Plasmid-based DNA vaccines as well as non-plasmid-based nucleic acids encode an antigenic protein expressed in the the host cells (Jordan, 2017). Immunising chickens with genes coding for multiple IBV structural proteins has been shown to increase both cellular and humoral immune responses when compared to using single genes. DNA vaccines have displayed instances of protective immunity (Yu *et al.*, 2001; Guo *et al.*, 2010; Song *et al.*, 1998). They also decrease interference caused by underdeveloped immune systems as well as from maternal antibodies (Jazayeri and Poh, 2019; Siegrist, 2001; Oshop *et al.*, 2002). The S1 sequence of the IBV spike protein must be considered when cloning into a DNA plasmid as a single amino acid mutation can severely reduce the protection conferred against vial challenge (Toro *et al.*, 2014a; Toro *et al.*, 2014b). Although most studies express only the S1 subunit, it has been shown that the S2 subunit also infers protection against heterologous IBV challenge (Toro *et al.*, 2014a; Toro *et al.*, 2014b). A nanoparticle multi-epitope DNA vaccine was produced using chitosan nanoparticles as a gene carrier (Qin *et al.*, 2022). This vaccine harboured a previously designed multi-epitope gene expression box (Qin *et al.*, 2021) that was shown to offer significant protection against both heterologous and homologous challenge with IBV. This nanoparticle multi-epitope DNA vaccine was able to induce strong IBV-specific immune responses and offer partial protection against homologous IBV challenge in chickens (Qin *et al.*, 2022).

1.10.5. VLP Vaccines

Virus-like particles are formed by expressing the structural proteins of a virus which self-assemble to form multiprotein nanostructures that are replicas of genuine virus particles (Ong *et al.*, 2017; McGinnes and Morrison, 2014; Jennings and Bachmann, 2008). They are considered safe as they contain no genetic material with which to replicate and cause infection (McGinnes and Morrison, 2014; Noad and Roy, 2003). They allow for differentiation between infected and vaccinated animals (DIVA compliant) (Liu *et al.*, 2013b). They are modifiable, can be rapidly produced, and induce both humoral and cellular immunity (Ukrami *et al.*, 2017; Blokhina *et al.*, 2013; Zdanowicz and Chroboczek, 2016).

IB VLPs made up of only the full-length S and M proteins have been assembled in Sf9 insect cells using a baculovirus expression system (Liu *et al.*, 2013a). They effectively induced humoral immune responses in both mice and chickens and cellular responses in mice comparable to or higher than the H120 IBV vaccine, respectively. Xu *et al.*, (2016) co-infected Sf9 cells with S, E, or M genes coded for by recombinant baculoviruses to assemble IB VLPs. A recombinant S protein was created which had the IBV S1 sequence fused to the IBV S2 TM and CT sequence linked by a flexible peptide. Resultant VLPs elicited antibodies against IBV as efficiently as the inactivated M41 IBV vaccine did, and induced robust humoral immune responses in chickens (Xu *et al.*, 2016).

Influenza VLPs have been investigated as a platform for expressing the IBV S1 protein to produce a chimeric VLP vaccine (Lv *et al.*, 2014). This was done through the fusion of the IBV S1 protein to the IAV H5N1 neuraminidase protein TM and CT sequences. The created fusion protein was expressed in a baculovirus expression system and the resultant chimeric VLPs induced higher humoral and cellular immune responses in both mice and chickens than the H120 IBV vaccine did (Lv *et al.*, 2014). Wu *et al.*, (2019a) separately fused the TM and CT domains of the IBV S protein to its S1 subunit as well as to the Newcastle disease (NDV) Fusion protein. A chimeric vaccine was produced in a baculovirus expression system using both resultant fusion proteins and the IBV M protein. The vaccine elicited efficient humoral and cellular immune responses in chickens and fully protect against death when challenged with either IBV or NDV (Wu *et al.*, 2019a).

1.11. Transient Protein Expression in Plants

The use of plants for protein expression is cost-effective, robust, and scalable (Theunemann *et al.*, 2013; Chen *et al.*, 2006). They are safe to use as they do not contain contaminating animal pathogens, the growth of infectious prions and viruses that infect humans is unsupported and no contaminating endotoxins can be produced (Moustafa *et al.*, 2016; Theunemann *et al.*, 2013). All of the required post-translational modifications can be mediated by the plant and more than one protein can be co-expressed (Faye *et al.*, 2005; Castilho *et al.*, 2010). This makes them attractive for the production of virus-like particles where more than one protein needs to be expressed and assembled in the same cell. The process of transient protein expression does not allow foreign genes to be genetically passed down and horizontal transmission also does not occur. Proteins and constructs can be speedily produced (Pogue *et al.*, 2010; Rybicki, 2010).

Transient protein expression using plants involves using *Agrobacterium tumefaciens* to transfer T-DNA to a plant host cell nucleus through agroinfiltration using plant-based protein expression vector systems (Fig. 1.5) (D'Aoust *et al.*, 2008). *Agrobacterium tumefaciens* is a gram-negative soil bacterium that has the ability to cause crown gall tumours in infected dicotyledonous plants at their wound sites (Christie, 2009; Su *et al.*, 2012). During infection, the *A. tumefaciens* is able to transfer a defined sequence of its tumour-inducing (Ti) plasmid to the plant cells (Chilton *et al.*, 1977). A set of virulence (*vir*) genes located on the Ti plasmid can be used to induce the Ti plasmid (or T-DNA) to integrate randomly into the nuclear genome of the plant. This Ti plasmid is used extensively to transfer the genes of *A. tumefaciens* into plants (Su *et al.*, 2012). The T-DNA of *A. tumefaciens* encodes genes that disrupt the growth of plant cells as well as division events (Christie, 2009). The oncogenic DNA may be excised and replaced with any gene of interest in order to mediate gene transfer using the *A. tumefaciens*. This discovery that *A. tumefaciens* is a natural as well as efficient delivery vector for DNA has made a huge contribution to the plant genetic engineering industry which has utilised this ability to improve crops, and to use plants to produce high levels of bio-medically important pharmaceutical proteins (Christie, 2009). The process of agroinfiltration can either be performed using a syringe for bench scale infiltration, or using a vacuum chamber for more large-scale infiltration (Leuzinger *et al.*, 2013). Virus-derived vectors (described in the next section) which contain the gene of interest are delivered to fully developed plants via agroinfiltration using the *A. tumefaciens* (Leuzinger *et al.*, 2013). After delivery, the gene construct directs the transient production of the desired protein of interest, which will then be

harvested and isolated after the incubation period (1-2 weeks). For the syringe-infiltration method, a small nick is created on the leaf epidermis, and the *Agrobacterium* suspensions containing the gene of interest cloned into the plant expression vector, is gently injected into the intercellular space of the leaf through the nick or through the stomata with a needle-less syringe (Fig. 1.5) (Leuzinger *et al.*, 2013).

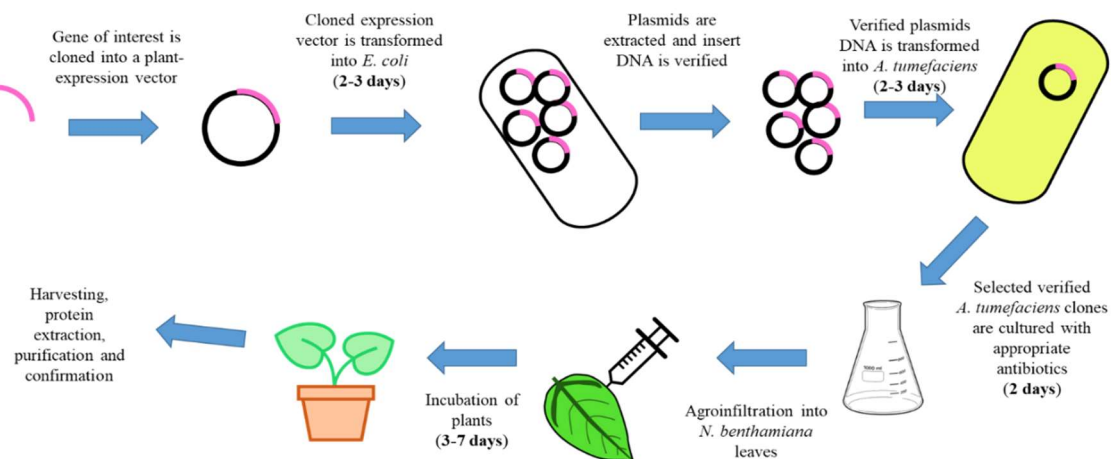


Figure 1.5. Schematic representation of the process of transient protein expression using agrobacterium-mediated gene transfer. Adapted from Pawar and Waghmare, 2016 (<https://www.biotecharticles.com/Biotech-Research-Article/Agroinfiltration-Effective-Method-of-Gene-Transfer-3735.html>).

Transient protein expression is limited to only leaf tissues that have been agroinfiltrated with *Agrobacterium* cultures of interest (Sainsbury *et al.*, 2009). Because the tissue of the leaves is then inevitably limited, it becomes imperative to maximising the levels of protein expression. While this can be done using replicating virus-based vectors, the disadvantages include the complexity and size of the proteins that are able to be expressed, the genetic stability of the constructs during viral genome replication, and biocontainment concerns (Sainsbury *et al.*, 2009). The leaf tissue of *Nicotiana benthamiana* is amenable to transformation and allows for the expression of high levels of protein making it a desirable host (Sheludko *et al.*, 2007). It is susceptible to a variety of plant viruses, facilitating replication of the gene in the plant expression vector that is delivered by the *A. tumefaciens* (Goodin *et al.*, 2008). A stable *N. benthamiana* line which facilitates mammalian-like glycosylation (Δ XT/FT), has been developed. The absence of plant-specific glycans may eliminate any potential negative side effects they can cause making it important for developing recombinant proteins for animal and

human health (Strasser *et al.*, 2008). The high production speed of plant protein expression systems makes it an appealing alternative to live-attenuated vaccines which can take up to a year to produce (Jordan, 2017).

1.12. Plant-based Protein Expression Vector Systems

Cowpea Mosaic Virus (CPMV) is a Comovirus from the family *Comoviridae* that infects legume species such as cowpea (*Vigna unguiculata*) as well as *Nicotiana benthamiana* as its experimental host (Sainsbury *et al.*, 2010; Sainsbury *et al.*, 2012). It is bipartite by nature, consisting of two positive-strand RNA molecules that are encapsidated separately. This allows proteins from multiple RNA-2 molecules to be expressed and synthesised in co-inoculated tissue and assembled in a single cell, making it an attractive viral vector for the development of VLPs (Giritch *et al.*, 2006; Sainsbury *et al.*, 2012).

The hypertranslational "CPMV-HT" expression system or pEAQ-HT expression vector series were developed from a modified version of the Cowpea Mosaic Virus (CPMV) RNA-2 (Sainsbury *et al.*, 2009; 2012). The complete open reading frame of the RNA-2 that was found downstream of the second AUG in frame at the 512th position was deleted and replaced with any sequence containing compatible ends, resulting in a replication-competent deleted vector. This provided the vectors with the benefit of biocontainment as opposed to the vectors centred on the unmodified RNA-2 (Sainsbury *et al.*, 2010; 2012). Modifying the RNA-2 amplified protein expression levels and removed the need for replication (Sainsbury and Lomonosoff, 2008; Sainsbury *et al.*, 2010).

The pEAQ-HT expression system allows large quantities of foreign proteins to be transiently expressed in plants (Sainsbury and Lomonosoff, 2008; Sainsbury *et al.*, 2012). The plasmids are small, binary, modular vectors which make it possible to insert several coding sequences on one T-DNA fragment (Sainsbury *et al.*, 2012). A P19 silencing suppressor was positioned on that T-DNA (Sainsbury *et al.*, 2010). The vector contains several restriction sites for insertion of a sequence or expression cassette via recombination-based or restriction enzyme-based cloning (Sainsbury *et al.*, 2010; 2012). It can be used for co-expression of multiple proteins and protein purification is made easier by equipping the vectors with sequences needed for His-tagging the target proteins on either the C- or N- terminal (Sainsbury *et al.*, 2012).

1.13. Vaccines Developed for other Coronaviruses

Several vaccines have been developed against other coronaviruses including vector-based, DNA, subunit, and VLP vaccines. Viruses such as adenovirus, togavirus, measles, poxvirus, and others have been used as vectors. A modified vaccinia virus Ankara is a promising viral vector which has been shown not to replicate in mammalian cells (Song *et al.*, 2013; Volz *et al.*, 2015; Haagmans *et al.*, 2016). Varying lengths of Middle East respiratory syndrome Coronavirus (MERS-CoV) S protein fragments were expressed using this vector. The S1 subunit, the receptor-binding domain, and the full-length S protein were expressed which resulted in the induction of T-cell responses and neutralising antibodies against MERS-CoV (Enjuanes *et al.*, 2016).

DNA vaccines that express either the full S protein or smaller fragments have been shown to effectively protect against a MERS-CoV infection. These vaccines were able to bring about the production of antigen-specific neutralising antibodies in monkeys, camels, and in mice (Muthumani *et al.*, 2015). In the vaccinated monkeys, very strong antigen-specific cellular immune reactions were recorded. Wang *et al.*, (2015) found that priming mice and non-human primates with the full-length S DNA followed by boosting with just the S1 subunit was able to induce potent neutralising antibody reactions against numerous strains of MERS-CoV and protect non-human primates from challenge with MERS-CoV (Enjuanes *et al.*, 2016).

Subunit vaccines based on the receptor binding domain of a recombinant S protein from MERS-CoV offered partial protection against MERS-CoV infection in immunised monkeys (Lan *et al.*, 2015). They reduced pneumonia as well as viral titres in the monkeys. Several of the S protein fragments from MERS-CoV were able to induce neutralising antibody responses in rabbits and in mice (Ma *et al.*, 2014b; Jiang *et al.*, 2014; Mou *et al.*, 2013). Linking the amino acid residues 377-588 of the S protein to human Fc as well as using an adjuvant resulted in improved cellular and humoral immune responses in mice (Zhang *et al.*, 2016; Tang *et al.*, 2015).

A plant-produced subunit vaccine candidate that is based on Severe Acute Respiratory Syndrome Coronavirus 2 (SARS-CoV-2) Spike glycoprotein fragments fused to LickM, which is a carrier protein that was derived from *Clostridium thermocellum* b-1,1-1,4-glucanase was produced by iBio (USA). This carrier protein has been used with IAV HA (Mett *et al.*, 2008). Another plant-produced subunit vaccine candidate has been developed by Kentucky

BioProcessing and is currently in phase 1-2 clinical trials (NCT04473690) although scientific data is yet to be published for either. Pre-published reports from another group described the transient co-expression of the S1 subunit of the S glycoprotein and the nucleocapsid protein as plant-produced subunit vaccine candidates (Mamedov *et al.*, 2020).

A chimeric SARS-CoV S protein was constructed by replacing the TM and CT sequences of the SARS-CoV spike protein with the equivalent sequences of influenza A HA protein. The S sequence was then ligated together with the influenza A matrix 1 (M1) protein to enhance the formation of VLPs. Bacmids were produced and transfected into insect cells to generate recombinant baculoviruses. This chimeric VLP was shown to protect mice against SARS-CoV challenge and its polymeric nature allowed it to effectively induce potent immune reactions (Liu *et al.*, 2011).

For the human COVID-19 pandemic, VLPs that expressed the full-length S protein of the *Betacoronavirus*, SARS-CoV-2 were expressed in tobacco plants. In order to successfully express these VLPs, two consecutive proline mutations were introduced into the loop between the first heptad repeat and the central helix of the S2 subunit which would help stabilise the S protein's prefusion state (Pallesen *et al.*, 2017; Ward *et al.*, 2021). Additionally, the native signal sequence was substituted with a plant signal sequence, and the TM and CT domains were replaced with those of an IAV H5 subtype HA protein (Ward *et al.*, 2021). The native unmodified full-length Spike protein was successfully expressed via transient protein expression in *Nicotiana benthamiana* plants either on its own, or when co-expressed with the IBV E and M structural proteins (Jung *et al.*, 2022). Covifenz, a candidate recombinant plant-produced VLP vaccine displaying the prefusion state spike protein of the original COVID-19 SARS-CoV-2 strain was developed by Medicago Inc (Canada) and underwent Phase 3 clinical trials, the results of which showed that the adjuvanted vaccine was able to effectively prevent COVID-19 from several SARS-CoV-2 variants with varied efficacy (Hager *et al.*, 2022).

Peyret *et al.*, (2021) analysed incorporating the envelope, membrane, and spike proteins of Porcine epidemic diarrhea virus (PEDV) into VLPs that are expressed in *N. benthamiana* plants. VLPs successfully formed, but low yield and purification difficulties complicate protein and VLP quantification (Peyret *et al.*, 2021).

While several of these types of vaccines have also been described for IBV, including VLPs in other expression systems, VLPs for IBV have yet to be reported in transient plant-based protein

expression systems, most likely due to the challenge experienced with getting them to express in high levels in the plants. However, IBV proteins and fusion proteins have been described in transgenic plants. Gong *et al.*, (1996) created a fusion protein which combined the IBV M protein with the β -glucuronidase bacterial enzyme. The resultant fusion protein was then expressed in transgenic tobacco cells. When this fusion protein was overexpressed, it was found that the oligomerization action of the β -glucuronidase enzyme resulted in the formation of a domain in the ER membrane where membranes that are adjacent are zippered together (Gong *et al.*, 1996). These were called Z-membranes, which lacked ER markers and accumulated to form multilayered structures in the cells. These Z-membranes allowed chimeric proteins to be isolated from other ER components, resulting in their stable and active accumulation in the cells. Isolating the proteins limits their exposure to degrading enzymes, may preserve protein activity, and limits interference with host functions (Gong *et al.*, 1996).

A cDNA construct that codes for the S1 protein of IBV was genetically transformed into transgenic potato plants by agroinfiltration using *Agrobacterium*. The expressed S1 protein was then used to vaccinate chickens and mice which were shown to produce antibodies that could protect against IBV infection (Zhou *et al.*, 2003). Chickens that had been vaccinated showed complete protection against IBV challenge after three sets of immunizations (Zhou *et al.*, 2003).

1.14. MSc Findings

My previous research undertaken for a Master's degree at the University of Pretoria (Sepotokele, 2020) investigated transiently co-expressing and assembling structural proteins (S, M, E, and N) of IBV in *Nicotiana benthamiana* plants in order to produce VLPs. Native and recombinant versions of a QX-like IBV spike protein derived from the ck/ZA/3665/11 strain (Abolnik, 2015) were designed aiming to improve plant protein expression and VLP assembly by using the C-terminal sequences of the Influenza A Virus haemagglutinin gene (H6 Sublineage 1). These were chicken codon-optimised and synthesised with a stop codon added downstream of the gene. Primers were used to create and modify recombinant genes 4) and 5).

The original and recombinant constructs created were:

- 1) The native Spike gene (IBV S)
- 2) A recombinant Spike, native TM replaced by the equivalent sequence of IAV HA (rIBV S-IAV-TM)
- 3) A recombinant Spike, native TM and CT replaced by the equivalent sequences of IAV HA (rIBV S-IAV-TM+CT)
- 4) A recombinant Spike, native signal peptide replaced by a murine signal peptide, a KOZAK sequence inserted upstream of the S1 gene, and the ER retention signal removed (mIBV S^{-KKSV})
- 5) A recombinant Spike with the native signal peptide replaced by a murine signal peptide, a KOZAK sequence added upstream of the S1 gene, the ER retention signal removed, and the native TM substituted with the equivalent sequence of IAV HA (mIBV S-IAV-TM^{-KKSV})

These were independently cloned into pEAQ-HT along with the envelope, membrane, and nucleocapsid proteins. The IAV matrix 2 protein in the pEAQ-HT vector was available for co-expression with recombinant 3). Several strains of *Agrobacterium* as well as different ratios of each construct were compared for suitability in mediating VLP production in plants.

VLPs were not detected with TEM, which indicated that VLPs may not have successfully assembled or that they were too low in abundance to be detected. Immunogold labelling also indicated no particles resembling IBV particles. However, the IBV proteins were co-expressed successfully in *N. benthamiana* ΔXT/FT (facilitating mammalian-like glycosylation) leaf material as S, M and E were confirmed by Liquid chromatography mass spectrometry (LC-MS/MS) in density gradient ultracentrifugation fractions and confirmed by immunological detection, but in low yields. LC-MS/MS confirmed the presence of the structural proteins of IBV indicating that they had assembled into high molecular weight structures. LC-MS/MS also showed that the number of peptides that were detected for the IBV S protein were higher for the recombinant versions of the proteins. This indicated that the attempts to improve overall expression may succeed. Low expression of the S protein may explain why no VLPs were detected, but it is also possible that the S protein was not integrated into the VLPs. The number of peptides detected for the other three structural proteins were low by comparison, which suggests a reason why VLPs may not have successfully assembled.

1.15. Aims and Objectives

AIM:

The aim of this project, building on the knowledge gained during my MSc study, was to improve the design and successfully transiently produce Spike-protein displaying IBV virus-like particles (VLPs) in *N. benthamiana*, and demonstrate their potential as variant vaccines in conferring clinical protection against challenge with homologous live virus in chickens.

OBJECTIVES:

- a) To produce IB VLPs in *N. benthamiana* Δ X_T/F_T plants through the transient expression and assembly of the major surface antigen, the Spike (S) protein, using stabilising mutations. These were complemented by the Membrane, Envelope, and Nucleocapsid proteins to potentially enhance the expression and assembly of VLPs (Chapter 2).
- b) To design hybrids of the IBV S protein S1 subunit fused to either the Influenza A Virus (IAV) haemagglutinin protein HA2 subunit, or just the transmembrane domain (TM) and cytosolic tail (CT) of the IAV haemagglutinin protein. Alternatively, the full-length IBV S protein with stabilising mutations as described in a) were further modified to substitute the native IBV spike TM and/or CT with that/those of the IAV HA2 subunit. These hybrids were then transiently expressed in *N. benthamiana* complemented by the M1 and/or M2 proteins of IAV to potentially enhance the expression and assembly of VLPs (Chapter 3).
- c) To design a hybrid of the IBV S protein S1 subunit fused to the TM and CT of the Newcastle Disease Virus (NDV) Fusion Protein (F). Alternatively, the full-length IBV S protein with stabilising mutations as described in a) was further modified to substitute the native IBV spike TM and/or CT with that/those of the NDV F subunit. These hybrids were then transiently expressed in *N. benthamiana* plants complemented by the NDV matrix protein to potentially enhance the expression and assembly of VLPs (Chapter 4).
- d) To assess the immunogenicity of the IB VLP of the best expressing construct in a pilot study in SPF chickens (Chapter 4).
- e) To assess the efficacy of the IB VLP in a challenge study with live homologous virus in animal trials using SPF chickens (Chapter 5).

CHAPTER 2

DESIGN, OPTIMISATION, AND EXPRESSION OF THE FULL-LENGTH IBV SPIKE PROTEIN

2.1. Introduction

The main target for this chapter was the full-length Infectious Bronchitis Virus (IBV) Spike (S) protein, which has previously been described for the formation of virus-like particles (VLPs) expressed in insect cell expression system using recombinant baculovirus vectors (Liu *et al.*, 2013a). Plant-based virus-like particles (VLPs) for IBV have not yet been described in the scientific literature.

My previous research involved expressing the native IBV S protein with the membrane (M), envelope (E), and nucleocapsid (N) proteins in *Nicotiana benthamiana* plants to produce VLPs against IBV (previously described in section 1.14) (Sepotokele, 2020). The results showed that the proteins were expressed and may have assembled into higher molecular weight structures even though no VLPs were visualised. Low expression levels are rarely a surprising result with regards to many viral glycoproteins. One of the speculated reasons for this is a lack of necessary viral chaperone proteins required to ensure proper folding of the proteins (Margolin *et al.*, 2018). Several modifications were made in order to enhance protein expression and enhance VLP assembly including substituting the native IBV transmembrane (TM) domain and/or cytosolic tail (CT) with the equivalent sequences of the Influenza A virus (IAV) haemagglutinin (HA) protein. In two of the additional modified constructs, a KOZAK sequence was added upstream of the S1 gene, the native signal peptide was replaced by a murine signal peptide, and lastly the endoplasmic reticulum (ER) retention signal was taken out in order to keep the S protein from being retained in the ER and to enhance VLP assembly. Signal peptides have been shown to affect the efficiency and capability of translocation. The use of signal peptides has been demonstrated to significantly increase protein production (Ohmuro-Matsuyama and Yamaji, 2017). Using signal peptides from alternative species may increase translocation efficiency (Mousavi *et al.*, 2017). This is commonly practised for the purpose of recombinant protein expression and has been used for the development of plant-produced Influenza A Virus (IAV) virus-like particles (VLPs) (D'Aoust *et al.*, 2008). In previous projects that involved the plant-based expression of various recombinant proteins at the CSIR, the substitution of the native signal peptide with a murine signal peptide yielded great results. For

this reason, the murine signal peptide was used for this study. While results showed that the modifications did slightly elevate glycoprotein expression as detected in the density gradient ultracentrifugation fractions, the number of peptides detected by liquid chromatography mass spectrometry (LC-MS/MS) for the S protein were very few with less than 20 % coverage for all the constructs, and there were still no VLPs visualised under a transmission electron microscope (TEM) (Sepotokele, 2020). The original hypothesis was that only assembled VLPs would be detected in the density gradient ultracentrifugation fractions. Nevertheless, sodium dodecyl sulphate-polyacrylamide gel electrophoresis (SDS-PAGE) and immunoblotting results showed that protein expression levels were still low for the S protein (as well as various modifications thereof). The modifications, however, showed a slight increase in expression levels, based on the LC-MS/MS results. The peptides identified were higher for the modified S protein constructs. The peptides identified for the other structural proteins (E, N, and M) were either few, or absent, which could also explain why VLPs may not have successfully assembled (Sepotokele, 2020).

The conclusion was that while the structural proteins may have been expressed, they may have failed to form VLPs. Harvesting at 6dpi was optimal, and the AGL-1 *Agrobacterium* strain yielded better results than when GV3103::pMP90 or LBA4404 strains were used. SDS-PAGE results showed that the proteins were most abundant in the 20 - 30 % iodixanol density gradient fractions (Fractions 10 and 11). The ratios of infiltrated protein only showed improvement in some of the experiments. Experimenting with the ratios further would likely assist in optimising protein expression and VLP assembly (Sepotokele, 2020).

In the present study, the stabilising mutations were incorporated to elevate the expression of the IBV structural proteins and drive VLP formation. In recent years, various researchers observed cryo-EM (cryogenic electron microscopy) structures of the trimeric prefusion spike protein ectodomains of murine hepatitis virus (MHV), HCoV-HKU1, and HCoV-NL63 (Walls *et al.*, 2016a; Kirchdoerfer *et al.*, 2016; Walls *et al.*, 2016b). These cryo-EM structures showed that the spike proteins formed a mushroom-like structure with three identical spike S1 subunits forming an interwoven cap on top of the S2 subunit stem. It was found that when the trimer was in this conformation, the receptor binding domains (RBDs) found on the C-terminal of each S1 subunit were not accessible for receptor binding. A conformational change of the trimer would be required to make the RBDs accessible (Walls *et al.*, 2016a; Kirchdoerfer *et al.*, 2016; Walls *et al.*, 2016b).

The coronavirus S protein is a class 1 trimeric fusion protein which is found in a metastable fusion conformation. In order for its viral membrane to fuse with a host cell membrane, it structurally rearranges into a more highly stable postfusion state (Li, 2016; Bosch *et al.*, 2003). This process takes place when the S1 subunit binds to the host cell receptor which triggers destabilisation of the prefusion trimer. This, in turn, leads to the S2 subunit being shed, and the S1 subunit transitioning into the highly stable postfusion conformation (Walls *et al.*, 2017).

In order for the RBD of the S1 subunit to engage the host cell receptor, it undergoes a hinge-like conformational change that will either expose or hide the receptor binding elements (Kirchdoerfer *et al.*, 2018). The receptor-inaccessible state is considered the “down” conformation whereby the receptor is hidden, while the receptor-accessible state, with the receptor being exposed, is referred to as the “up” conformation. The latter state is thought to be less stable than the first (Gui *et al.*, 2017; Pallesen *et al.*, 2017; Walls *et al.*, 2019).

Stabilising mutations have been developed for coronavirus spike proteins that are able to prevent the protein transitioning from its prefusion to its post fusion state. Antibody epitopes that are present in the protein’s prefusion state are likely to be what cause neutralising antibody responses (Kirchdoerfer *et al.*, 2018). Because the prefusion state is so unstable, it poses a challenge for the production of protein antigens for antigenic presentation of these epitopes (Kirchdoerfer *et al.*, 2018). To stabilise the S protein prefusion state, two proline mutations were incorporated (Pallesen *et al.*, 2017) which allowed a stabilised Middle East respiratory syndrome coronavirus (MERS-CoV) Spike 2P (2 proline substitutions) ectodomain to maintain a stable prefusion conformation. The S protein in this stable prefusion state had a much higher immunogenicity and also showed a similar antibody recognition as the wild-type S protein. Pallesen *et al.*, (2017) found four arrangements of the S trimer’s apex representing one receptor-inaccessible state, and three different receptor-accessible states whereby either one, two, or all three RBDs were exposed.

A general strategy for retaining the S protein of betacoronaviruses in its prefusion conformation is therefore to introduce two consecutive proline residues at the start of the central helix (Pallesen *et al.*, 2017). Pallesen *et al.*, (2017) found that when single proline substitutions were introduced into the loop between the first heptad repeat (HR1) and the central helix of MERS-CoV S2, the expression levels of the prefusion ectodomains were highly elevated. This approach was therefore considered for improving the low protein expression that was experienced for the IBV S protein as well as improving the probability of IB VLP formation.

Co-expression with the other structural proteins of IBV may also enhance VLP assembly by acting as chaperones or necessary proteins in the formation of VLPs similar to native IBV particles.

The aim of this chapter was to produce IB VLPs in *N. benthamiana* plants through the transient expression and assembly of the complete major surface antigen, the Spike (S) protein incorporating the stabilizing proline mutations described by Pallesen *et al.*, (2017) with the membrane-associated structural proteins of IBV (M, E, and N).

2.2. Materials and Methods

2.2.1. Design and Synthesis of Synthetic Gene Constructs

A synthetic gene sequence coding for the full-length IBV spike (S) protein (ck/ZA/3665/11, QX-like strain) (Abolnik, 2015) (Protein ID AKC34133) was designed (Fig. 2.1). *AgeI* and *XhoI* restriction sites were added to the 5' and 3' ends, in turn, with a stop codon added downstream of the sequence to facilitate cloning into pEAQ-HT. Any other *AgeI* and *XhoI* sites in the gene were mutated. The native signal peptide was replaced by a murine signal peptide (m), a KOZAK sequence was included upstream of the S1 subunit, and the S1 subunit was fused to the S2 subunit through the use of a linker (SSGGGGGS) (Fig. 2.2). Two proline residues (2P) were introduced into the predicted loop between the first IBV heptad repeat region (HR1) and the central helix of the S2 subunit to increase expression of the prefusion S protein, stabilise this prefusion state, as well as to expose the receptor binding domain (RBD) of the S protein, increasing immunogenicity (Fig. 2.1 and 2.2) (Pallesen *et al.*, 2017). These were identified based on the predicted 2P mutations in other coronaviruses (Pallesen *et al.*, 2017).

To potentially improve VLP assembly in plants, gene sequences coding for the IBV membrane (M) (Protein ID AKC34136), envelope (E) (Protein ID AKC34135), and nucleocapsid (N) (Protein ID AKC34140) proteins were used. These were synthesised previously to contain *AgeI* and *XhoI* restriction sites on the 5' and 3' ends, and a stop codon downstream of each sequence. Any additional *AgeI* and *XhoI* sites in the sequence were mutated.

The genes were chicken codon-optimised for optimal expression in domestic chickens (*Gallus gallus*) and synthesised by BioBasic Canada Inc.

MGWSWIFLFLLSGAAGVHCNLFDSDNNYVYYYQSAFRPPNGWHLQGGAYAVVNSTNHTSNA
 GSAQGCTVGVIKDVYNQSVASIAMTAPLQGMAWFCTAYCNFSDTTVFVTHCYHIRISAMKNGS
 LFYNLTVSVSKYPNFKSFQCVNNFTSVYLNGLVFTSNKTTDVTSAGVYFKAGGPVNYSIMKEF
 KVLAYFVNGTAQDVILCDNSPKGLLACQYNTGNFSDGFYPFTNSTLVREKFIVYRESSFNNTLAL
 TNFTFTNVSNAQPNSGGVNTFHLYQTQTAQSGYYNFNLSFLSQFVYKASDFMYGSYHPSCSFRP
 ETINSGLWFNSLSVSLTYGPLQGGCKQSVFSGKATCCYAYSYKGPMAACKGVYSGELRTNFECG
 LLVYVTKSDGSRIQTRTEPLVLTQYNYNNITLDKCVAYNIYGRVGQGFITNVTDSAANFSYLAD
 GGLAILDTSGAIDVFVVQGIYGLNYYKVNPCEDVNQQFVVSGGNIVGILTSRNETGSEQVENQF
 YVKLTN**SSGGGGGS**IGQNVTS CPYVSYGRFCIEPDGSLKMIVPEELKQFVAPLLNITESVLIPNSF
 NLTVTDEYIQTRMDKVQINCLQYVCGNSLECRKLFQQYGPVCDNILSVVNSVSQKEDMELLSF
 YSSTKPKGYDTPVLSNVSTGEFNISLLLKTPISSGRSFIEDLLFTSVETVGLPTDAEYKKCTAGPL
 GTLKDLICAREYNGLLVLPPIITADMQTMYTASLVGAMAFGGITSAAAIPFATQIQARINHLGITQ
 SLLMKNQEKIAASFNKAIGHMQEGFR**STSLALQQIQD**VVNKQSAILTETMNSLNKNFNGAITSVIQ
DIYAQLDPPQADAQVDRLITGR**LSSLSVLASAKQSEYIRVSQQRELATKKINECVKSQSNRYGFC**
GSGRHVLSIPQNAPNGIVFIHFTYTPESFVNVTAVGFCVNPANASQYAIVPANGRGVFIQVNGSY
 YITARDMYMPRDITAGDIVTLTSCQANYVNVNKTVINTEFVEDDDFNFNDELKWWNDTKHELP
 DFDEFNYTVPVLNISNEIDRIQEVIQGLNDSLIDLETLSILKTYIKWPWYVWLAIFFAIIFILILGW
 VFFMTGCCGCCCGCFGIPLMSKCGKKSSYYTTFDNDVVTEQYRPKKS**V**

Figure 2.1. Protein sequence of the synthetic gene sequence mIBV-S2P, highlighting the stabilising proline mutations in the S2 subunit of the sequence. Murine signal peptide (highlighted in blue), linker (highlighted in black), S2 subunit (highlighted in grey), heptad repeat 1 (highlighted in yellow), central helix (highlighted in green), and the 2 proline substitutions (highlighted in red).

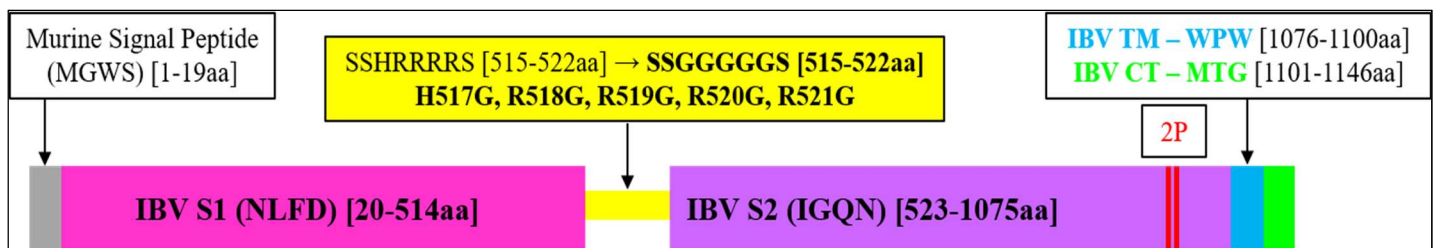


Figure 2.2. Schematic diagram illustrating the full-length IBV target protein with stabilising mutations (mIBV-S2P). (Murine signal peptide (m), full length Spike protein (S), SSGGGGGS linker between IBV S1 and S2 subunits, 2P mutation, WPW – start of IBV TM sequence, MTG – start of IBV CT sequence).

2.2.2. Cloning into pEAQ-HT Plant Expression Vector Plasmid

Using sticky-end directional *AgeI*/*XhoI* restriction enzyme-based cloning, the sequence of the synthesised S gene was cloned into pEAQ-HT. The sequence was digested with *AgeI* and *XhoI* to cut out the gene of interest and generate compatible sticky ends. The same was done with the pEAQ-HT vector. The digested gene and vector were separated on a 1 % [w/v] agarose gel in 1 x TAE buffer (40 mM Tris (Tris(hydroxymethyl)aminomethane), 20 mM acetic acid, and 1 mM EDTA, pH 8) and the Zymoclean™ Gel DNA Recovery Kit was used for purification. The purified target gene was then ligated into the linearised pEAQ-HT plasmid using the FastLink DNA Ligase kit (Epicentre, United States of America) following manufacturer's instructions.

Both UP and CSIR have licence agreements until 2023 with Plant Bioscience Ltd., (PBL, Norwich) for research using the pEAQ-HT CMPV technology.

2.2.3. Transformation into Electrocompetent DH10B Cells

The ligated constructs were transformed into electrocompetent DH10B *Escherichia coli* (*E.coli*) cells by using a Gene Pulser™ (BioRad, United States of America) at 1.8 kV, 25 μ F, and 200 Ω . The cells were allowed to recover in SOC media (super optimal broth with catabolite repression) (0.5 % (w/v) yeast extract, 2 % (w/v) Tryptone, 10 mM NaCl, 2.5 mM KCl, 2.5 mM MgCl₂, 20 mM MgSO₄, 20 mM Glucose) after transformation at 37 °C for an hour at 175 rpm. Recovered cells were spread-plated onto Luria Bertani (LB) agar plates (5 g/L yeast extract, 10 g/L Tryptone, 10 g/L NaCl, and 15 g/L agar) which contained 50 μ g/ml Kanamycin in order to select for pEAQ-HT and left to incubate overnight at 37 °C. Successfully ligated clones were verified by colony PCR using pEAQ-HT specific primers (Table 2.1).

Table 2.1. Primers used for Colony PCR verification

Primer	Sequence (5' – 3')
pEAQ-HT - F	ACT TGT TAC GAT TCT GCT GAC TTT CGG CGG
pEAQ-HT - R	CGA CCT GCT AAA CAG GAG CTC ACA AAG A

Colony PCR reactions were prepared using the Ampliqon DNA PCR kit (Ampliqon A/S, Denmark). The PCR mix contained 0.2 μ M forward/ reverse primer (Table 2.1), Ampliqon DNA polymerase master mix red containing Taq DNA polymerase which contained 1.5 mM $MgCl_2$ as well as dNTPs. Colonies were picked from the overnight Luria Bertani (LB) agar plate and resuspended into the prepared PCR mix. PCR reactions were prepared as directed by the manufacturer and were performed in the GeneAmp 2720 Thermocycler (Applied Biosystems). The PCR cycling conditions were set up as follows: 1 cycle of 95 °C for 2 min, followed by 35 cycles of 95 °C for 30 sec, 55 °C for 30 sec and 72 °C for 2 min, followed by 1 cycle of 72 °C for 5 min. Resultant PCR products were then separated on a 1 % agarose gel with GeneRuler DNA ladder mix (SM0331, Thermo Fisher Scientific) as the molecular weight marker. Insert-containing colonies were propagated in Luria bertani broth (10 g/L Tryptone, 10 g/L NaCl, and 5 g/L yeast extract) and the plasmids extracted using the Zyppy Plasmid Miniprep kit. The sequences encoding the structural proteins were confirmed by dideoxy Sanger DNA sequencing (Inqaba Biotechnical Industries (Pty) Ltd).

2.2.4. Transformation into Electrocompetent *Agrobacterium tumefaciens* AGL-1 Cells

Previously, three different strains of *Agrobacterium tumefaciens* were compared (AGL-1, LBA4404, and GV3103::pMP90) (Sepotokele, 2020). The AGL-1 strain yielded better expression than the GV3103::pMP90 and LBA4404 strains and was therefore chosen for use in this study. Once positive clones were confirmed, each of the verified plasmids were transformed into electrocompetent AGL-1 cells (ATCC_ BAA-101TM) using a GenePulserTM (BioRad, USA) at 1.44 kV, 25 μ F, and 200 Ω . The transformed cells were thereafter recovered in SOC media at 28 °C for 3 hours at 175 rpm. Recovered cells were plated onto LB agar plates containing 50 μ g/ml Kanamycin for selection of pEAQ-HT constructs, as well as Rifampicin (30 μ g/ml) and Carbenicillin (100 μ g/ml) for selection of AGL-1 colonies. These were incubated for 2 – 5 days at 28 °C. Colonies were picked and positive clones verified by colony PCR as before.

2.2.5. Infiltration of *Nicotiana benthamiana* Plants

Verified positive AGL-1 clones were streaked out onto LB agar plates containing suitable selective antibiotics and incubated at 28 °C for 2 – 5 days. The overnight plate cultures were

inoculated into LB containing the same antibiotics and incubated at 28 °C overnight at 175 rpm. The overnight cultures were centrifuged at 7000 x g for 7 minutes at room temperature. The resultant pellet was resuspended thoroughly in MES (2-(N-morpholino)ethanesulfonic acid) infiltration buffer (10 mM MES, 10 mM MgCl₂, and 200 μM 3,5- Dimethoxy-4-hydroxy-acetophenone; pH 5.6) to a final optical density of between 1 and 1.5 at 600 nm (OD₆₀₀). The *A. tumefaciens* suspensions were combined to a final ratio of 2:1:1:1 (S:M:E:N) and left to incubate for an hour at room temperature. The combined *A. tumefaciens* suspensions were syringe-infiltrated into the leaves of 3 – 4 week old *N. benthamiana* ΔXT/FT plants (Strasser *et al.*, 2008) and watered daily in the growth room until harvest. *N. benthamiana* ΔXT/FT is a glycosylation mutant with a targeted downregulation of xylose and fucose expression that facilitates mammalian-like glycosylation (Strasser *et al.*, 2008).

2.2.6. Harvest of Leaf Material and Protein Extraction

The infiltrated leaves were harvested at 6 days post infiltration, which was previously determined to be the optimal harvest time (Sepotokele, 2020). The harvested leaves were homogenised in two volumes of either 1 x PBS (10X PBS pH 7.4, 27 mM KCl, 18 mM KH₂PO₄, 140 mM NaCl, 100 mM Na₂HPO₄), 1 x Bicine (50 mM Bicine, pH 8.4; 20 mM NaCl), or 1 x Tris (50 mM Tris, pH 8.0; 150 mM NaCl) extraction buffers supplemented with 0.04 % sodium metabisulfite. Protease inhibitor cocktail (Sigma-Aldrich, P2714) was added just prior to protein extraction. The juice was filtered through two layers of mira cloth and centrifuged at 7000 x g at 4 °C for 4 minutes. The resultant supernatant was purified via sucrose density ultracentrifugation. The sucrose density gradient was prepared by dissolving sterile sucrose in sterile 1 x PBS buffer to make up 20 % and 70 % sucrose solutions. The clarified leaf supernatant was gently loaded on top of the sucrose gradient (3 ml of 20 % sucrose on top of 2 ml of 70 % sucrose) in 38.5 ml ultra-clear™ Beckman tubes (Beckman coulter). The tubes were ultra-centrifuged at 10 °C for 2 hours at 32 000 x g after which the gradients were collected in fractions of 500 μl each from the bottom of the tubes using a Minipuls2 peristaltic pump (Gilson). A total of 8 fractions were collected.

2.2.7. Protein Confirmation

2.2.7.1. SDS-PAGE and Immunoblotting

Partially purified sucrose gradient fractions 2, 3, and 4 (which were previously determined to contain the highest S protein content (Sepotokele, 2020)), were prepared and examined by sodium dodecyl sulphate-polyacrylamide gel electrophoresis (SDS-PAGE) as well as immunoblotting. The samples were separated on a 12 % SDS PAGE gel that was prepared as described by the manufacturer (BioRad TGX™ and TGX stain-free™ FastCast™ Acrylamide Kit) under reducing conditions prior to staining in Coomassie Brilliant Blue G-250. For immunoblotting, the samples were separated on a prepared 12 % SDS polyacrylamide gel under reducing conditions and then transferred to a Polyvinylidene difluoride (PVDF) membrane found in the Trans-blot® Turbo™ Transfer pack (BioRad) using the mixed molecular weight application (25 V, 1.3 A, for 7 minutes) on the Trans-blot® Turbo™ Transfer system (BioRad) following manufacturer's instructions. The membrane was blocked overnight in a solution of 1 x PBS containing 3 % [w/v] Bovine serum albumin (BSA) and 0.1 % [w/v] TWEEN20. Immunoblotting was performed with 1:1000 of antisera that had been collected from a commercial flock that was vaccinated with a combination of commercial Mass-type vaccines (University of Pretoria) followed by 1:2000 of Goat- α -chicken HRP secondary antibody (Abcam, Novex) and Precision Protein™ StrepTactin-HRP conjugate (BioRad). Clarity™ Western ECL chemilluminescence substrate (BioRad) was added to the membrane and proteins were visualised with the ChemiDoc™ MP Imager (BioRad) as per manufacturer's instructions.

2.2.7.2. LC-MS/MS Based Peptide Sequencing

SDS-PAGE protein bands corresponding to the expected target protein size were excised from the stained SDS-PAGE gel and analysed by LC-MS/MS at CSIR Biosciences using the method in Shevchenko *et al.*, (2007). The MS/MS spectra that were obtained were compared with sequences from the Uniprot Swissprot protein database by using the Paragon search engine (AB Sciex) on the Protein pilot v5. Only the proteins that had a confidence level ≥ 99.9 % were reported.

2.2.7.3. Transmission Electron Microscopy (TEM) Analysis

Fraction 3 of the partially purified sucrose gradient (which showed the strongest bands on the SDS-PAGE gels, immunoblots, as well as the highest number of peptides for LC-MS/MS) was adsorbed onto a carbon-coated holey copper grid prior to staining. The grid was floated onto 12.5 μ l of the sucrose fraction for 5 minutes and then washed in 5 μ l of sterile milliQ water 5 times, with excessive water blotted off in between. The grids were stained for 30 seconds in 2 % uranyl acetate (pH 4.2) with the excess blotted off. The grids were air dried prior to imaging for VLPs using the JEOL JEM-1400 Flash Transmission Electron Microscope (JEOL) at the Laboratory for Microscopy and Microanalysis (University of Pretoria, Onderstepoort). A 1 ml sample of SPF chicken egg allantoic fluid which contained the live ck/ZA/3665/11 QX-like strain was also clarified by centrifugation and analysed by TEM.

2.3. Results

2.3.1. Cloning and Expression of Synthetic Gene Constructs

The synthetic gene construct designed in Chapter 2 was successfully cloned into pEAQ-HT expression vector and successfully transformed into AGL-1 agrobacterium and transiently co-expressed in *N. benthamiana* plants as in Table 2.2 with complementary structural or chaperone proteins. This was confirmed by colony PCR and Sanger sequencing. Table 2.2 shows the ratios of constructs to complementary protein/s. Glycerol stocks of sequence validated constructs were stored at -80°C until required for infiltrations, and six biological repeats were performed for construct mIBV-S2P with different ratios, accessory proteins, and extraction buffers attempted.

Table 2.2. Gene construct co-infiltration ratios (Chapter 2)

Construct	Approximate mW (kDa)	Co-infiltrated with:	Ratio
mIBV-S2P	127	M + E and/or N	2:1:1 S:M:E
			2:1:1:1 S:M:E:N

2.3.2. Protein Detection and Confirmation of Construct mIBV-S2P

The gene construct, mIBV-S2P showed high levels of protein expression in the plants. There were bands on the SDS-PAGE gel correlating to the expected size of the constructs (Fig. 2.3 (a)). The bands were noticeably higher than the band around the same size in the negative control as was the band in the positive control. This suggests that this was not a plant protein and was likely to be the S protein. Liquid chromatography mass spectrometry (LC-MS/MS) based peptide sequencing further confirmed it to be the IBV S protein (Fig. 2.4) with 24 unique peptides being detected at 23 % coverage. The IBV antisera was not able to strongly detect IBV S protein specific bands correlating to the expected size of the construct, with very faint bands being seen in lanes 6 and 7 (Fig. 2.3 (b)). The S protein was not detected in the QX-like positive control. This was most likely because the spike protein quantity in the in the purified virus used for the control was very low and also because the flock that the virus was purified from was immunized with Mass-type IBV vaccines, and the level of cross-protection between the S protein of different serotypes is known to be low (Cavanagh, 2003). The IBV N protein

was strongly detected by the QX-like IBV antisera in the purified mIBV-S2P:M:E:N VLP protein extract as well as in the positive control. This was not surprising as the nucleocapsid protein is strongly conserved between serotypes (Williams *et al.*, 1992). Visualisation under the TEM showed particles that closely resembled native IBV particles, and ranged from 65 nm to 172 nm in diameter, with most of the particles falling between 80 nm and 120 nm in diameter (Fig. 2.5). The spikes surrounding them ranged from 11 nm to 24 nm in length, typical of IBV particles (Jackwood and de Wit, 2013).

There was no noticeable difference observed between the VLPs purified using PBS buffer and the VLPs purified using bicine buffer. Results were consistently similar for PBS and Bicine buffer when repeated, so PBS was chosen as it is the most commonly used biological buffer for research (Perchetti *et al.*, 2020).

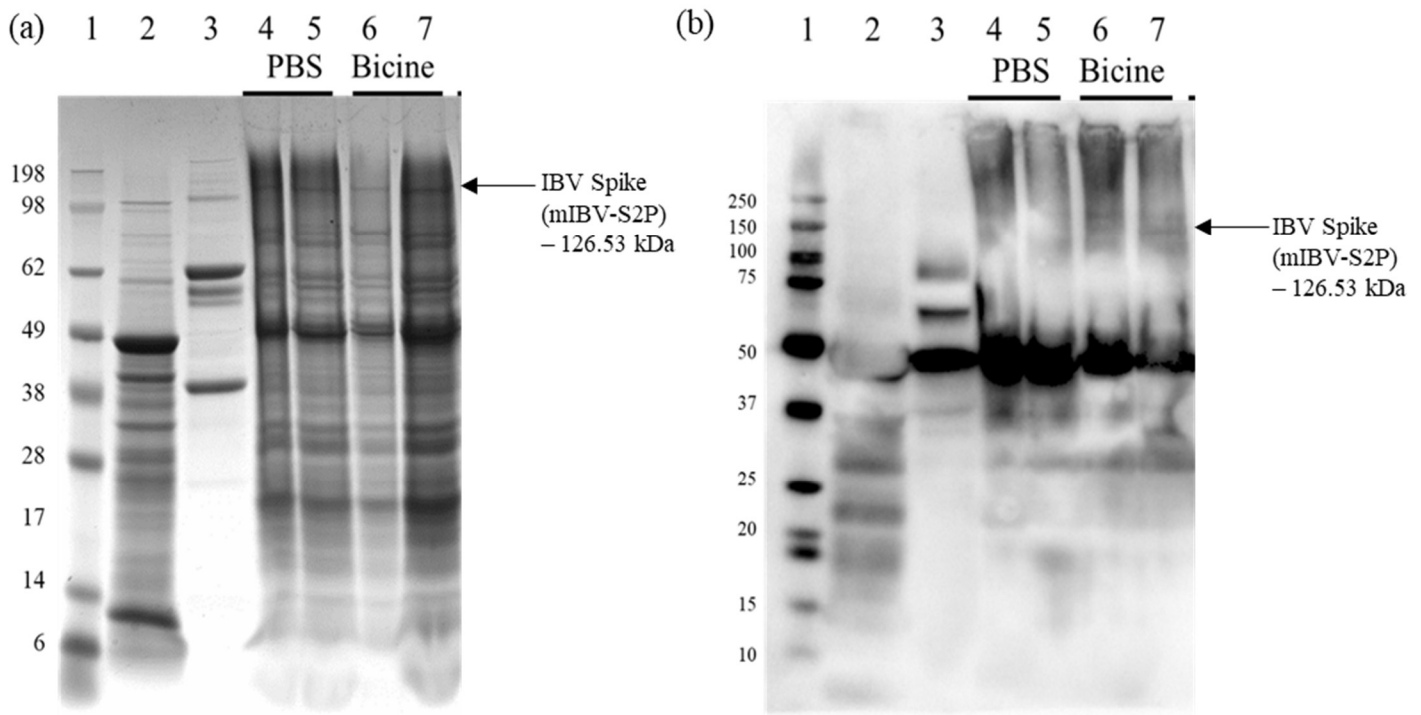


Figure 2.3. SDS-PAGE (a) and Western blot (b) of plant-produced IBV S protein (mIBV-S2P) purified in PBS or bicine buffer. Lane 1: molecular weight marker; Lane 2: plant-expressed empty pEAQ-HT vector; Lane 3: purified live QX-like IBV strain ck/ZA/3665/11; Lanes 4 and 5: mIBV-S2P:M:E:N Fractions 2 and 3; Lanes 6 and 7: mIBV-S2P:M:E:N Fractions 2 and 3. (Edited from Fig. S1).

mIBV-S2P: M: E: N

(2:1:1:1)

23 % coverage (95 % confidence) with 24 unique peptides

MGWSWIFLFLLSGAAGVHCNLFDSNNYVYYYQSAFRPPNGWHLQGGAYAVVNSTNHTSNAGSA
 QGCTVGVIKDVYNQSVASIAMTAPLQGMWFCTAYCNFSDTTVFVTHCYHIRISAMKNGSLFYNLT
VSVSKYPNFKSFQCVNNFTSVYLNGLDLVFTSNK**TTDVTSAGVYFKAGGPNYSIMKEFKVLAYFV**
NGTAQDVLCDNSPKGLLACQYNTGNFSDGFYPFTNSTLVR***EKFIVY***RESSFN~~TTLALTNFTFTNVS~~
 AQPNSGGVNTFHLYQTQTAQSGYYNFNLSFLSQFVYKASDFMYGSYHPSCSFRPETINSGLWFNSLS
 VSLTYGPLQGGCKQSVFSGK**ATCCYAYSYGPMACKGVYSGELRTNFECGLLVYVTKSDGSRIQ**
TRTEPLVLTQYNNITLDKCVAYNIYGRVGQGFITNVTDSAANFSYLADGGLAILDTSGAIDVFVV
 QGIYGLNYYK**VNPCEDVNQQFVVS**GGNIVGILTSRNETGSEQVENQFYVKLTNSSGGGGGSIGQN
 VTSCPYYVSYGR**FCIEPDGSLKMIVPEELK**QFVAPLLNITESVLIPNSFNLTVTDEYIQTRMDKVQINC
 LQYVCGNSLECR**KLFQQYGPVCDNLSVNSVSQKEDMELLSFYSSTKPK**GYDTPVLSNVSTGEF
 NISLLKTPISSSGR**SFIEDLLFTSVETVGLPTDAEYKKCTAGPLGTLK**DLICAREYNGLLVLPPIIT
 ADMQTMYTASLVGAMAFGGITSAAAIPFATQIQARINHLGITQSLLMKN**QEKIAASFNKAIGHMQE**
GFRSTSLALQQIQDVVNKQSAILTETMNSLNKNFGAITSVIQDIYAQLDPPQADAQVDRLITGR**LS**
LSVLASAKQSEYIRVSQQRELATK**KINECVKSQSNRYGFCGSGR**HVLSIPQNAPNGIVFIHFTYTPESF
 VNVTAIVGFCVNPANASQYAIVPANGRGVFIQVNGSYITARDMYMPRDITAGDIVTLTSCQANYVN
 VNK**TVINTFVEDDDFNFNDELSK**WWNDTKHELPDFDEFNYTVPVLNISNEIDRI**QEVIOGLNDSLID**
LETLSILKTYIKWPWYVWLAIFFAIIIFILILGWVFFMTGCCGCCCGCFGIPLMSKCGK**KSSYYTTFD**
NDVVTEQYRPKKSV

Figure 2.4. Protein confirmation using LC-MS/MS-based peptide sequencing of the modified IBV spike protein construct, mIBV-S2P. The percentage sequence coverage is indicated above with several unique peptides identified with > 90 % confidence. Peptides with > 95 % confidence are highlighted in **bold** text, those with 50 - 95 % confidence in *italics*, and those with < 50 % confidence are underlined. No peptides were identified for the non-highlighted regions of the sequence (grey).

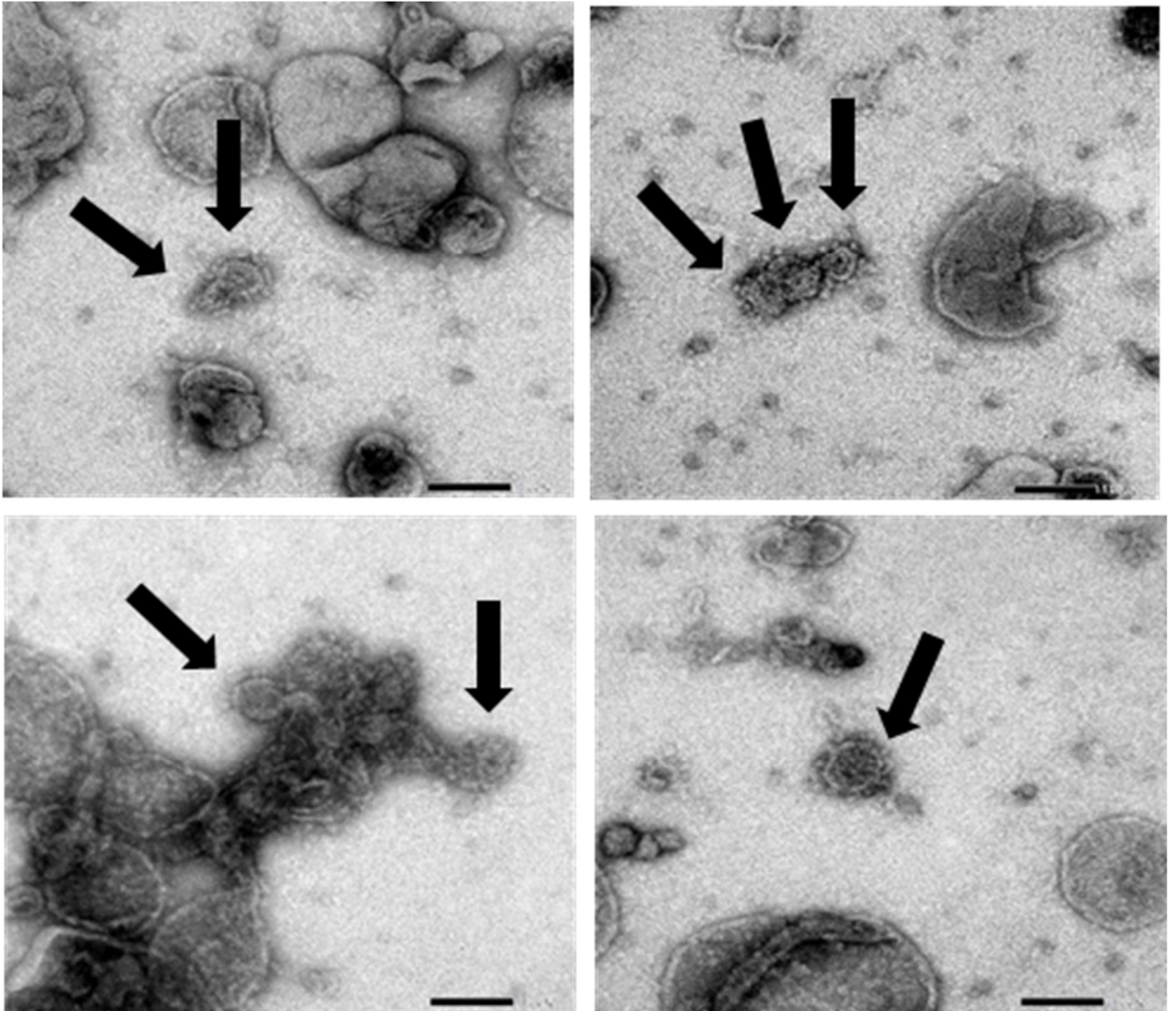


Figure 2.5. Negative-stained transmission electron microscopy images of plant-produced IBV virus-like particles expressed with the synthetic gene construct, mIBV-S2P in *N. benthamiana*. Arrows indicate VLPs.

2.4. Discussion

This chapter describes the first successful design, optimisation, and expression of VLPs displaying a full-length modified IBV spike protein (mIBV-S2P). The SDS-PAGE, Immunoblot, LC-MS/MS, as well as TEM results together allow it to be concluded that the construct mIBV-S2P, co-expressed with the IBV M, E, and/or N proteins, successfully expressed well enough in the *Nicotiana benthamiana* plants to produce VLPs resembling native IBV particles. Table S1 shows the levels of expression for each analytical technique. The VLPs ranged from 65 to 172 nm in diameter, the average being 111 nm. The spikes on their surface ranged from 11 to 24 nm in length, which mimics the typical morphology and size of IBV particles (Jackwood and de Wit, 2013).

Although plant-produced VLPs against IBV had not been described up until now, VLPs against IBV had previously been produced using the baculovirus-mediated insect cell expression system. The baculovirus-derived VLPs were shown to be highly immunogenic and offered better protection levels than an inactivated H120 IBV vaccine (Lv *et al.*, 2014; Wu *et al.*, 2019a; Liu *et al.*, 2013; Xu *et al.*, 2016). The successful production of IB VLPs in plants provides advantages not offered by other protein expression systems. These include cost-effectiveness, safety, scalability, and speedier production times (Peyret *et al.*, 2021; Theunemann *et al.*, 2013; Jordan, 2017). Several vaccine candidates against animal and human diseases have been developed using plant-based expression systems and demonstrated efficacy in their target species (Peyret *et al.*, 2021).

Given that a full-length native S protein was previously attempted and did not express well in plants or assemble VLPs (Sepotokele, 2020), it appears as though addition of the stabilising proline mutations (Pallesen *et al.*, 2017) was the key to improving protein expression and allowing VLPs to assemble. Although several modifications including replacing the native signal peptide with a murine signal peptide, removing the ER retention signal and substituting the TM and/or CT sequences with those of the IAV HA protein somewhat increased protein expression, those modifications alone were not enough to drive VLP assembly (Sepotokele, 2020). It therefore seems that the proline mutations added in this study were a critical requirement for the production of IB VLPs in plants. This was similar to the reports by Ward *et al.*, (2021) describing the assembly of SARS-CoV-2 by adding stabilising proline mutations to the S protein. Additionally, Ward *et al.*, (2021) also reported replacing the native signal peptide with a plant signal peptide which may have assisted with VLP assembly as done here.

In contrast, while previous attempts at expressing the native IBV spike protein with or without the other IBV structural proteins did not result in adequate protein expression or VLP assembly (Sepotokele, 2020), Ward and co-workers (2021) were able to express a native SARS-CoV-2 spike protein both alone, and with the envelope and membrane proteins.

Previously, co-expression with the M and E proteins appeared to elevate S protein expression compared to co-expression with just the M or just the E protein (Sepotokele, 2020). Ward and co-workers (2021) on the other hand, found that the level of VLPs assembled with just the S protein alone (2P stabilised) was three-fold higher than the levels obtained when the S protein was co-expressed with the M and E proteins.

In conclusion, the stabilising proline mutations in the S protein were the key to successful protein expression and IB VLP assembly in *N. benthamiana* plants for the first time.

CHAPTER 3

DESIGN, OPTIMISATION, AND EXPRESSION OF IBV SPIKE CONSTRUCTS MODIFIED WITH THE IAV HA2 PROTEIN

3.1. Introduction

Plants have been used for the production and development of virus-like particles (VLPs) against several animal viruses (Liu *et al.*, 2013b). One of the first and most successful instances of plant-produced VLP expression and production is that of Influenza A Virus (IAV) (D'Aoust *et al.*, 2008). Numerous viral glycoproteins tend to express in low amounts in plants. It is unknown why, but some hypothesise that it could be because of a shortage of vital chaperone proteins that are required to drive the folding of the glycoproteins. It could also be caused by an incompatibility between the glycoproteins and the endogenous plant chaperone proteins already present in the plant (Margolin *et al.*, 2018). Low glycoprotein expression was one of the challenges experienced previously (Sepotokele, 2020).

By contrast, not only is the expression of the unmodified haemagglutinin (HA) glycoprotein of IAV sufficient for VLP development (D'Aoust *et al.*, 2008), but several IAV HA proteins display high levels of expression in plants (Shoji *et al.*, 2011; D'Aoust *et al.*, 2008). The IAV HA glycoprotein is a trimer that is 13.5 nm in length (Boonstra *et al.*, 2018) and has a size of 72 kDa (D'Aoust *et al.*, 2008), with each of its monomers being 60 kDa in size prior to being glycosylated (Sriwilaijaroen and Suzuki, 2012). The trimer forms spike-shaped protrusions on the outside exterior of IAV (Isin *et al.*, 2002; Nayak *et al.*, 2010). Similar to the Infectious Bronchitis Virus (IBV) Spike protein, the IAV HA protein is also a type 1 integral transmembrane protein (Sriwilaijaroen and Suzuki, 2012). The HA0 homo-trimer is cleaved into its subunits HA1 and HA2 of 327 and 222 amino acids in length, respectively (Copeland *et al.*, 1986). The stalk part of the HA glycoprotein consists of HA1 as well as HA2 residues (forming a three stranded twisted coil of α -helices) (Wiley and Skehel, 1987), while its globular part consists only of HA1 residues (forming antiparallel β sheets) and is the receptor binding domain of the protein (Wilson and Skehel, 1981). This receptor binding site, along with the non-conserved antigenic binding loops surrounding it, is located on top of the RBD. Carbohydrate side chains are carried by these antigenic binding loops (Skehel and Wiley, 2000). Not only does the HA1 subunit participate in attachment and entry into the host cell (through receptor binding and fusion of the viral particle) but it is also involved in stimulating

host cell neutralising antibody responses (Nayak *et al.*, 2010; Sriwilaijaroen and Suzuki, 2012), and it is involved in the binding of the receptors and fusion of viral particle (Nayak *et al.*, 2010). The HA1 subunit consists of the fusion subdomains as well as the vestigial esterase (Rosenthal *et al.*, 1988; Wilson and Skehel, 1981). There are a minimum of five different characterised antigenic sites which overlap surrounding the receptor binding sites, and are found in the globular head of the H3 HA glycoprotein (Raymond *et al.*, 1986; Caton *et al.*, 1982). The sialic acid binding site as well as the epitopes to which the majority of neutralizing antibodies are directed, are located on the HA protein's globular head domain (Magadán *et al.*, 2013; Nayak *et al.*, 2010). These neutralizing antibodies are the most abundantly elicited post vaccination and infection and provide protective immunity (Nayak *et al.*, 2010; Neu *et al.*, 2016) although in humans, there have been protective antibodies elicited from the stalk region (Ekiert *et al.*, 2009; Margine *et al.*, 2013). The HA protein stem part of IAV is highly conserved among strains and between subtypes, and is the main target of universal IAV vaccines that are under development (Soltanialvar *et al.*, 2016).

The IAV Neuraminidase (NA) protein on the other hand, is a tetramer that is made up of four identical polypeptides. It accounts for between 10 and 20% of the total glycoproteins present on the surface of the virion (40 – 50 neuraminidase spikes, compared to 300 – 400 haemagglutinin spikes) (Moules *et al.*, 2010; Varghese *et al.*, 1983). The four NA monomers, of around 470 amino acids in size, are folded into four distinctive structural domains: the catalytic head, the stalk, as well as the transmembrane domain, and the cytosolic tail (McAuley *et al.*, 2019). The NA tetramer has been shown by cryoelectron tomography, to present itself as either local clusters, or isolated spikes that are surrounded by HA spikes on the viral surface (Harris *et al.*, 2006). The length of the NA stalk determines whether it protrudes less or more than the HA glycoprotein from the surface of the viral envelope, which can have an affect on enzymatic viral activity (Matsuoka *et al.*, 2009; Harris *et al.*, 2006; McAuley *et al.*, 2019). Lv *et al.*, (2014) previously experimented with using a linker to fuse the Infectious Bronchitis (IBV) S1 gene to the IAV neuraminidase (NA) protein transmembrane (TM) domain and cytosolic tail (CT). The co-expression of this fused protein with the IAV matrix 1 protein (M1) led to the formation of chimeric VLPs that looked similar to IAV particles. This experiment was performed using a baculovirus-mediated insect cell expression system. The chimeric VLPs elicited both humoral and cellular immunity and a neutralisation antibody response in mice and chickens that was higher than the responses elicited by an inactivated H120 vaccine (Lv *et al.*, 2014).

The similarities between the IAV HA glycoprotein and the IBV Spike protein, however, make it an ideal target for a modified IBV chimeric VLP vaccine candidate (similarities described in Sepotokele, 2020). The HA being a trimer like the S protein may allow the protein to fold in a similar way compared to using the NA protein which is a tetramer and might cause the protein to fold differently. Also using the insect cell expression system, Yin *et al.*, (2016) generated a fusion protein consisting of an IBV S1 protein fused to the HA2 subunit of IAV H3N2. This fusion protein offered better protection in chickens than an inactivated M41 vaccine after challenging with a virulent M41 IBV strain. It also offered better protection and had a higher immunogenicity than the S1 subunit alone (Yin *et al.*, 2016).

Modifications to the IBV spike protein previously involved substituting just the TM or both the TM and CT of the native IBV spike with the equivalent sequences of the IAV HA2 protein (Sepotokele, 2020). In addition to the modifications mentioned in Chapter 2, the modified constructs were further modified by substituting the transmembrane domain of the IBV spike protein with that of the IAV HA2 glycoprotein. While results showed that replacing the native IBV S protein TM and CT with the equivalent IAV HA protein sequences did slightly elevate glycoprotein expression as detected in the density gradient ultracentrifugation fractions, there were still no VLPs visualised under a transmission electron microscope (TEM) (Sepotokele, 2020).

Because of the low expression of the IBV S protein, I hypothesised that either substituting both the IBV S protein TM and CT sequences, or just the CT sequence with the equivalent sequence/s of the IAV HA protein may prove to be a useful strategy in improving the expression of the IBV S protein and producing IB VLPs.

The aim of this chapter was to produce VLPs against IBV in *Nicotiana benthamiana* plants through the transient expression and assembly of IBV Spike protein S1 hybrids modified using the IAV haemagglutinin protein HA2 subunit (H6 subtype) TM and/or CT sequences. The full-length IBV Spike (S) protein with stabilising mutations described in Chapter 2 was also further modified using the TM and/or CT of the IAV haemagglutinin protein HA2 subunit (H6 subtype). These were co-expressed with the IAV M1 and/or the IAV M2 protein to potentially enhance the expression and assembly of VLPs.

3.2. Materials and Methods

3.2.1. Design and Synthesis of Synthetic Gene Constructs



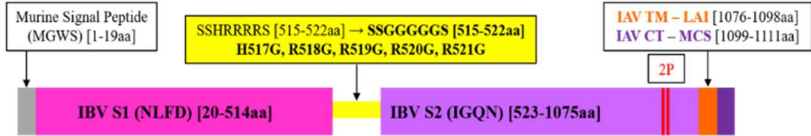
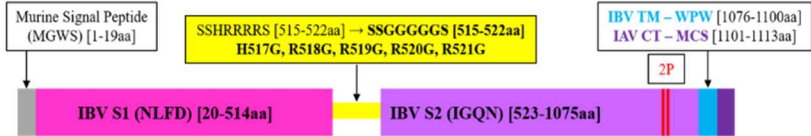
Synthetic gene sequences coding for the IBV S protein (ck/ZA/3665/11, QX-like strain, Abolnik, 2015) (Protein ID AKC34133), as well as the IAV Haemagglutinin (HA) protein (H6 subtype haemagglutinin) were acquired from the National Centre for Biotechnology Information (NCBI). Vector NTI software was used to design two separate hybrids of these gene sequences. The first hybrid contained the IBV S1 sequence fused to the IAV HA2 sequence via a linker (GGGSGGGGS), designated rIBV-S1-IAV-H6 (Table 3.1). The second hybrid contained the IBV S1 sequence fused to the TM/CT domain of the IAV HA2 sequence via a linker (GGGSGGGGS) designated rIBV-S1-IAV-H6^{TM/CT} (Table 3.1). *AgeI* and *XhoI* sites were added to the 5' and 3' ends of each gene, with a stop codon added downstream of each of the genes. Any other *AgeI* and *XhoI* sites in the gene sequences were mutated.

To improve VLP assembly in plants and to complement the IAV HA2 TM/CT, plant-codon optimised gene sequences coding for the IAV M1 (Protein ID ACD37431) and M2 (Protein ID ADL41185) (strain A/New Caledonia/20/1999 (H1N1)) proteins were already available to use for co-infiltration. The transient co-expression of the IAV M2 protein has previously been shown to potentially improve both the accumulation as well as the stability of recombinant proteins in the plant cell secretory pathway by regulating the pH of the cell (Jutras *et al.*, 2015).

These were synthesised previously to contain *AgeI* and *XhoI* restriction sites at the 5' and 3' ends, along with a stop codon downstream of each of the genes (Jutras *et al.*, 2015). Any additional *AgeI* and *XhoI* sites in the gene were mutated. The gene sequences were chicken codon-optimised for optimal expression in domestic chickens (*Gallus gallus*) unless otherwise stated and synthesised by BioBasic Canada Inc.

Primers were designed to modify the synthetic full-length IBV S protein (mIBV-S2P) designed in Chapter 2 (Integrated DNA Technologies Inc. (IDT)). These primers (Table 3.2) were designed with the intention of substituting the TM/CT domains of mIBV-S2P with the TM and CT sequences of the IAV HA2 protein subunit or substituting just the CT domain of mIBV-S2P with the CT domain of the IAV HA2 protein subunit. This resulted in two new synthetic gene sequences, mIBV-S2P-IAV-H6^{TM/CT} and mIBV-S2P-IAV-H6^{CTonly} (Table 3.1).

Table 3.1. Schematic diagrams of modified constructs designed in Chapter 3

Construct	Schematic Diagram	Modifications
rIBV-S1-IAV-H6		Native signal peptide (r), S1 Spike subunit, GGGGSGGGGS linker between IBV S1 and IAV HA2 subunit, IAV HA2 TM and CT
rIBV-S1-IAV-H6^{TM/CT}		Native signal peptide (r), S1 Spike subunit, GGGGSGGGGS linker between IBV S1, IAV HA2 TM and CT
mIBV-S2P-IAV-H6^{TM/CT}		Murine signal peptide (m), full length Spike protein (S), 2P mutation, SSGGGGGS linker between S1 and S2 subunits, IAV HA2 TM and CT
mIBV-S2P-IAV-H6^{CTonly}		Murine signal peptide (m), full length Spike protein (S), 2P mutation, SSGGGGGS linker between S1 and S2 subunits, IBV S TM , IAV HA2 CT

*(**LAI** – start of IAV **TM** sequence, **MCS** – start of IAV **CT** sequence, **WPW** – start of IBV **TM** sequence).

Table 3.2. Primers used for synthetic IAV construct design

Construct	Name	Sequence (5' – 3')
rIBV-S-H6 ^{TM/CT}	Fw	TTT ACC GGT ATG GGC TGG AGC TGG AAA CTC GAG TCA GAT GCA CAC TCT GCA CTG CAT GCT GCC GTT GCT GCA
	Rv	CAT CCA CAG GCC CAT AGC AAT GAT CAG TCC CAC CAG CAC CAG GCT GCT GCT CAC TGT GCT GTA GAT AGC CAG CTT AAT GTA GGT TTT CAG
mIBV-S2P-IAV-H6 ^{TM/CT}	Fw	TTT ACC GGT ATG GGC TGG AGC TGG GGA CTC GAG TCA GAT GCA CAC TCT GCA CTG CAT GCT GCC GTT GCT GCA
	IBV H6 CT tail Rv	CAT GAA GAA CAC CCA GCC CAG GAT

3.2.2. Cloning into pEAQ-HT Plant Expression Vector Plasmid

Synthesised genes rIBV-S1-IAV-H6 and rIBV-S1-IAV-H6^{TM/CT} were cloned into the pEAQ-HT expression vector, purified, and validated as in Chapter 2. Constructs mIBV-S2P-IAV-H6^{TM/CT} and mIBV-S2P-IAV-H6^{CTonly} were created by PCR amplification using the corresponding primer pairs in Table 3.2. PCR mixes were set up containing a final concentration of 0.3 μ M of each of the corresponding forward and reverse primers (Table 3.2), KAPA dNTP mix, 5X KAPA HIFI buffer, as well as the KAPA HIFI DNA polymerase enzyme (KAPA Biosystems) as instructed by the manufacturer. The PCR amplifications were performed using the GeneAmp 2720 Thermocycler (Applied Biosystems) with the following cycling conditions: 3 minutes initial denaturation at 95 °C (1 cycle); followed by 35 cycles of 20 sec denaturation at 98 °C, 30 sec annealing at 70 °C, and 210 sec extension at 72 °C; ending off with 5 minutes final extension at 72 °C (1 cycle). The resulting PCR products were separated on a 1 % agarose gel using the molecular weight marker GeneRuler ladder mix (SM0331) as a reference. The target bands corresponding to the right size were excised from the gel and purified using the ZymocleanTM Gel DNA Recovery Kit. The purified genes were then cloned into the pEAQ-HT expression vector, purified, and verified as in Chapter 2.

All the constructs in this chapter (Table 3.1) were co-infiltrated with either the IAV M1 construct, the IAV M2 construct, or both for comparison as opposed to with the IBV M, E, and N constructs used in Chapter 2.

3.3. Results

3.3.1. Cloning and Expression of Synthetic Gene Constructs

The synthetic gene constructs designed in Chapter 3 were successfully cloned into the pEAQ-HT expression vector which was successfully transformed into AGL-1 *Agrobacterium* and transiently co-expressed in *N. benthamiana* plants as in Table 3.3 with complementary structural or chaperone proteins. This was confirmed by colony PCR and Sanger sequencing. Table 3.3 shows the ratios of constructs to complementary protein/s. Glycerol stocks of sequence validated constructs were stored at -80°C until required for infiltrations. Three biological repeats were performed for constructs rIBV-S1-IAV-H6 and rIBV-S1-IAV-H6^{TM/CT}, four biological repeats for construct mIBV-S2P-IAV-H6^{TM/CT}, and construct mIBV-S2P-IAV-H6^{CTonly} was performed once, with different ratios, accessory proteins, and extraction buffers attempted.

Table 3.3. Gene construct co-infiltration ratios (Chapter 3)

Construct	Approximate mW (kDa)	Co-infiltrated with:	Ratio	
rIBV-S1-IAV-H6	82	IAV M1 and/or IAV M2	2:1	S:M1
			2:1	S:M2
			2:1:1	S:M1:M2
rIBV-S1-IAV-H6 ^{TM/CT}	61	IAV M1 and/or IAV M2	2:1	S:M1
			2:1	S:M2
			2:1:1	S:M1:M2
mIBV-S2P-IAV-H6 ^{TM/CT}	122	IAV M1 and/or IAV M2	2:1	S:M1
			2:1	S:M2
			4:1	S:M2
mIBV-S2P-IAV-H6 ^{CTonly}	123	IAV M2	2:1	S:M2
			4:1	S:M2

3.3.2. Protein Detection and Confirmation of Constructs rIBV-S1-IAV-H6 and rIBV-S1-IAV-H6^{TM/CT}

Preliminary results showed that constructs rIBV-S1-IAV-H6 and rIBV-S1-IAV-H6^{TM/CT} were not well expressed in the plants. There were SDS-PAGE bands that correlated to the expected sizes of the constructs, however, these bands were found in the negative control as well (pEAQ-HT vector backbone with no construct) suggesting that they may possibly be plant proteins or that the plant proteins are of a similar size to the constructs resulting in an overlap on the gel (Fig. 3.1 (a) and Fig. 3.2 (a)). The S protein was not detected by immunoblot using QX-like IBV-specific antisera (Fig. 3.1 (b) and Fig 3.2 (b)). This suggested that the protein was either not expressed at all, or was expressed in a quantity too low to be detected by immunoblotting. The antisera used was produced by chickens that had been vaccinated with commercial live-attenuated vaccines, and not with the homologous QX-like strain that the constructs were based on. The level of cross-protection found between the S protein of different serotypes is known to be low (Cavanagh, 2003) so it is possible that the antisera did not detect it simply because the serotypes were heterologous. Transmission electron microscope (TEM) analysis showed very few particles of the correct size that did resemble native IBV particles (Fig. 3.3). The SDS-PAGE and immunoblot results suggest that the constructs rIBV-S1-IAV-H6 and rIBV-S1-IAV-H6^{TM/CT} did not express well although the TEM results suggest that there was assembly of particles resembling the size and morphology of IBV particles. This was the same regardless of which buffer they were extracted in or which of their complementary proteins they were co-expressed with.

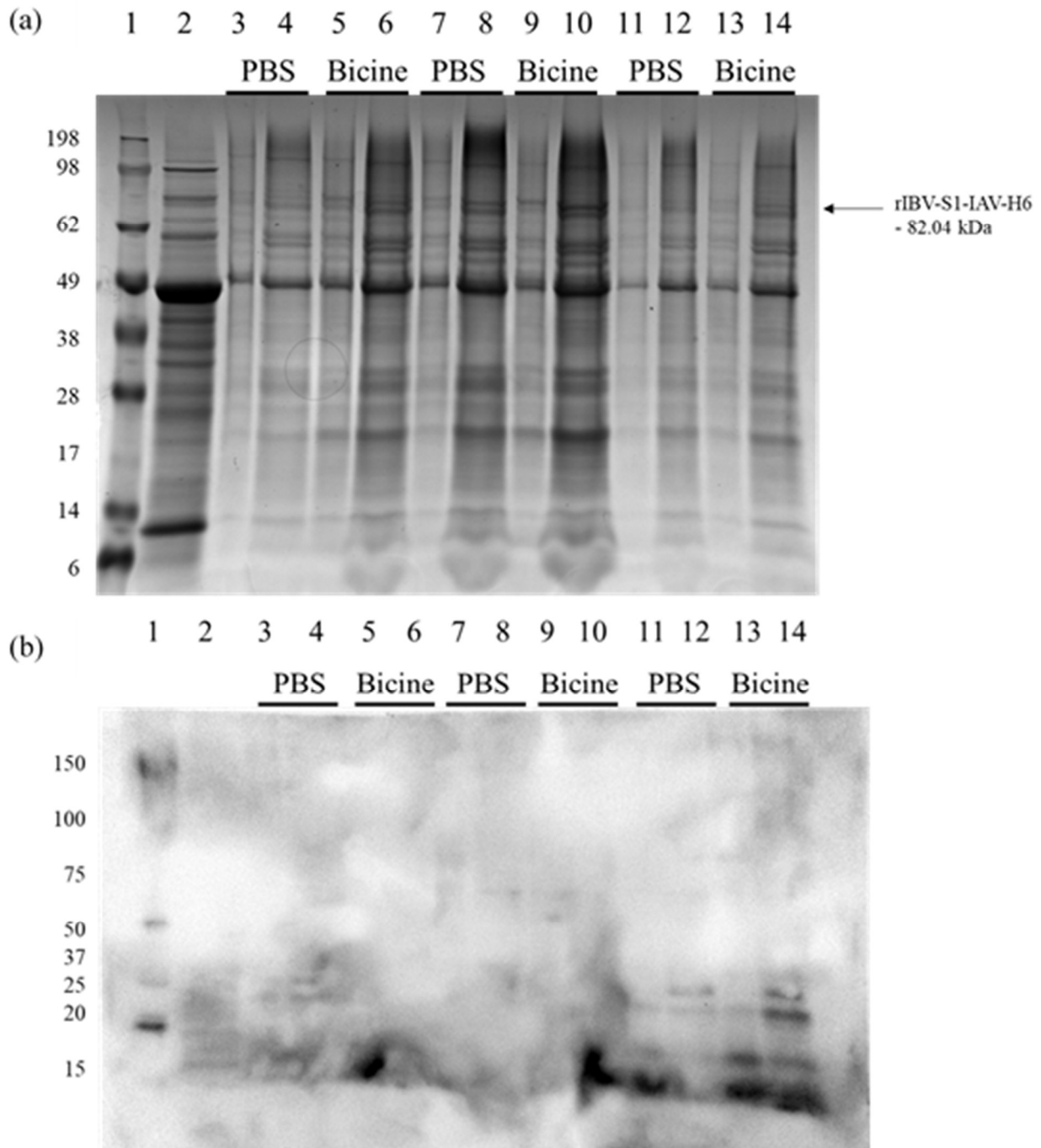


Figure 3.1. SDS-PAGE (a) and Western blot (b) of plant-produced rIBV-S1-IAV-H6 protein purified in PBS or bicine buffer. Lane 1: molecular weight marker; Lane 2: plant-expressed empty pEAQ-HT vector; Lanes 3 and 4: rIBV-S1-IAV-H6 :M1 :M2 Fractions 2 and 3; Lanes 5 and 6: rIBV-S1-IAV-H6 :M1 :M2 Fractions 2 and 3; Lanes 7 and 8: rIBV-S1-IAV-H6 :M1 Fractions 2 and 3; Lanes 9 and 10: rIBV-S1-IAV-H6 :M1 Fractions 2 and 3; Lanes 11 and 12: rIBV-S1-IAV-H6 :M2 Fractions 2 and 3; Lanes 13 and 14: rIBV-S1-IAV-H6 :M2 Fractions 2 and 3.

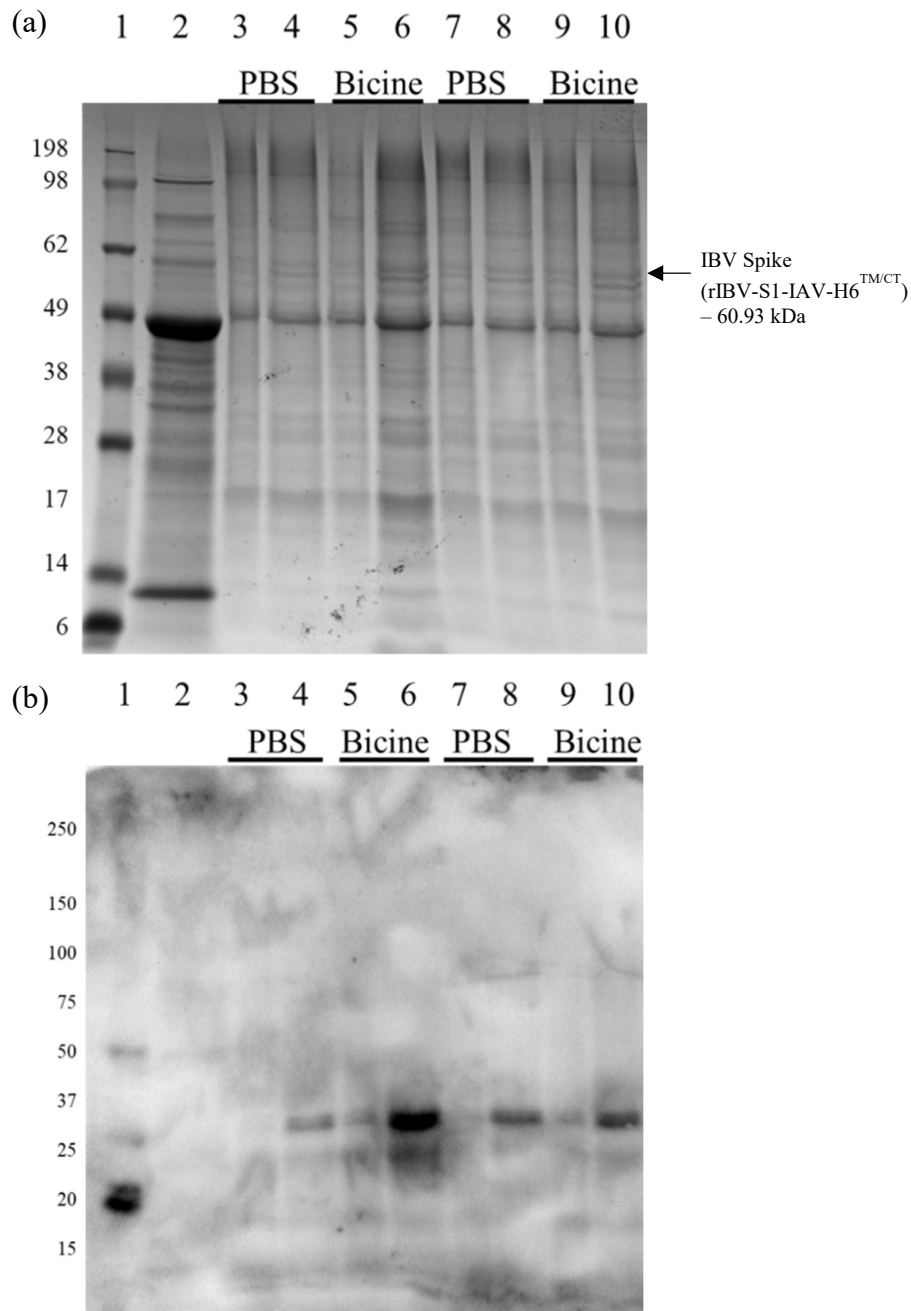


Figure 3.2. SDS-PAGE (a) and Western blot (b) of plant-produced rIBV-S1-IAV-H6^{TM/CT} protein purified in PBS or bicine buffer. Lane 1: molecular weight marker; Lane 2: plant-expressed empty pEAQ-HT vector; Lanes 3 and 4: rIBV-S1-IAV-H6^{TM/CT} :M1 :M2 Fractions 2 and 3; Lanes 5 and 6: rIBV-S1-IAV-H6^{TM/CT} :M1 :M2 Fractions 2 and 3; Lanes 7 and 8: rIBV-S1-IAV-H6^{TM/CT} :M2 Fractions 2 and 3; Lanes 9 and 10: rIBV-S1-IAV-H6^{TM/CT} :M2 Fractions 2 and 3. (Edited from Fig. S2).

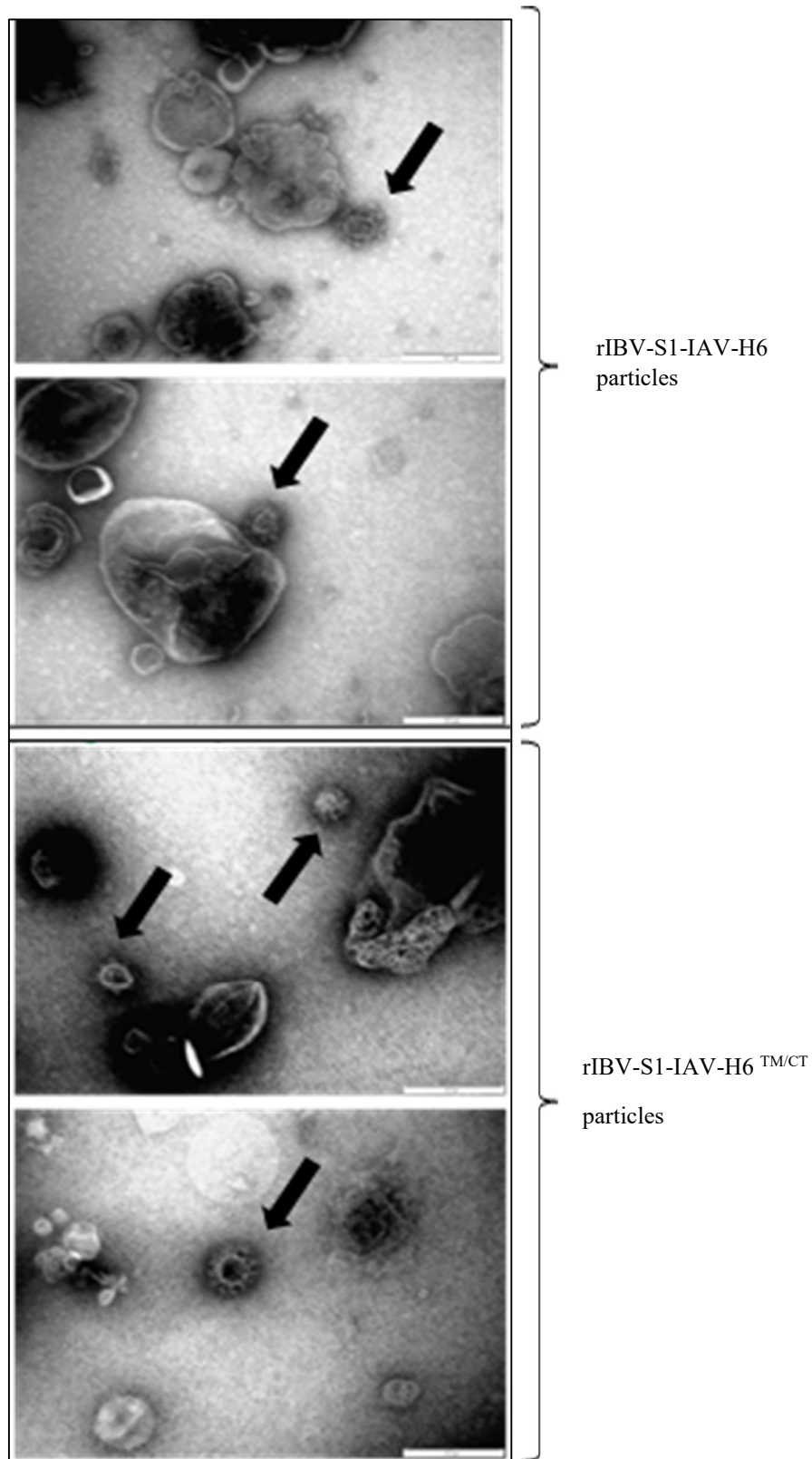


Figure 3.3. Negative-stained transmission electron microscopy images of plant-produced IBV virus-like particles expressed with the synthetic gene constructs rIBV-S1-IAV-H6 and rIBV-S1-IAV-H6^{TM/CT} in *N. benthamiana*. Arrows indicate VLPs.

3.3.3. Protein Detection and Confirmation of Construct mIBV-S2P-IAV-H6^{TM/CT}

In contrast the construct mIBV-S2P-IAV-H6^{TM/CT}, showed higher levels of protein expression in the plants. There were bands on the SDS-PAGE gel correlating to the expected sizes of the constructs (Fig. 3.4 (a)). The bands were noticeably higher than the band around the same size in the negative control as was the band in the positive control. This suggests that this was not a plant protein and was likely to be the S protein. Liquid chromatography mass spectrometry (LC-MS/MS) based peptide sequencing further confirmed it to be the IBV S protein (Fig. 3.5) with 25 peptides being detected at 25.8 % coverage. The IBV antisera was able to detect strong S protein specific bands in the Western blot (Fig. 3.4 (b)) compared to the rIBV-S1-IAV-H6 and the rIBV-S1-IAV-H6^{TM/CT} constructs where no S protein specific bands could be detected at all. This suggests that this construct (mIBV-S2P-IAV-H6^{TM/CT}) was able to more successfully express in the plants compared to the rIBV-S1-IAV-H6 and the rIBV-S1-IAV-H6^{TM/CT} constructs. The S protein specific bands for the (mIBV-S2P-IAV-H6^{TM/CT}) construct were also stronger than the ones detected for the mIBV-S2P construct expressed in Chapter 2. The S protein was not detected in the QX-like positive control (Fig. 3.4 (b)). This was most likely because the spike protein quantity in the in the purified virus used for the positive control was very low. It may also be because the flock that the virus was purified from was immunized with Mass-type IBV vaccines, and the level of cross-protection between the S protein of different serotypes is known to be low (Cavanagh, 2003). There was no noticeable difference between the protein expression levels when purified using PBS buffer compared with bicine buffer. The results were consistently similar for PBS and Bicine buffer when repeated; PBS was therefore chosen because it is the most commonly used buffer for biological research (Perchetti *et al.*, 2020). Visualisation under the TEM showed VLPs in the plant extracts that were infiltrated with the mIBV-S2P-IAV-H6^{TM/CT} construct (Fig. 3.6). These VLPs closely resembled native IBV particles and ranged from 67 nm to 164 nm in diameter, an average of 98 nm, with most of the particles falling between 80 nm and 100 nm in diameter. The spikes surrounding them ranged from 11 nm to 25 nm in length, typical of IBV particles (Jackwood and de Wit, 2013).

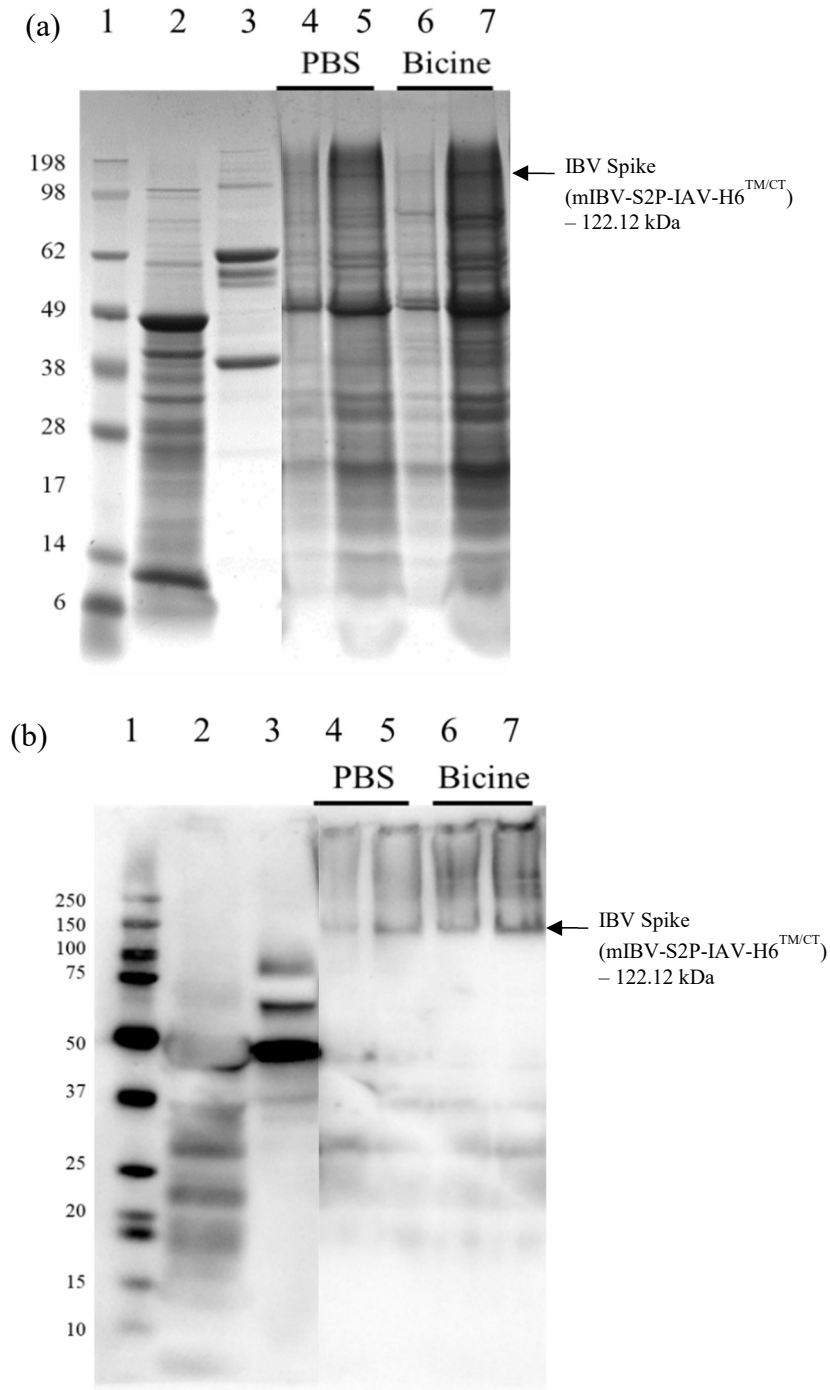


Figure 3.4. SDS-PAGE (a) and Western blot (b) of plant-produced IBV S protein (mIBV-S2P-IAV-H6^{TM/CT}) purified in PBS or bicine buffer. Lane 1: molecular weight marker; Lane 2: plant-expressed empty pEAQ-HT vector; Lane 3: purified live QX-like IBV strain ck/ZA/3665/11; Lanes 4 and 5: mIBV-S2P-IAV-H6^{TM/CT}:M2 Fractions 2 and 3; Lanes 6 and 7: mIBV-S2P-IAV-H6^{TM/CT}:M2 Fractions 2 and 3. (Edited from Fig. S1).

mIBV-S2P-IAV-H6^{TM/CT} : IAV M2 (2:1)

25.8 % coverage (95 % confidence) with 25 unique peptides

MGWSWIFLFLLSGAAGVHCNLFSDNNYVYYYQSAFRPPNGWHLQGGAYAVVNSTNHTSNAGSA
 QGCTVGVIKDVYNQSVASIAMTAPLQGMWFCTAYCNFSDTTVFVTHCYHIRISAMKNGSLFYNTL
 VSVSKYPNFKSFQCVNNFTSVYLNGLDLVFTSNK**TTDVTSAGVYFKAGGPNYSIMKEFKVLAYFV**
 NGTAQDVILCDNSPKGLLACQYNTGNFSDGFYPFTNSTLVRE**EKFIVYRE**SSFNNTLALTNFTFTNVSN
 AQPNSGGVNTFHLYQTQTAQSGYYNFNLSFLSQFVYKASDFMYGSYHPSCSFRPETINSGLWFNSLS
 VSLTYGPLQGGCKQSVFSGK**ATCCYAYSYKGPMAACKGVYSGELRTNFECGLLVYVTKSDGSRIQ**
TRTEPLVLTQYNNITLDKCVAYNIYGRVGGGFITNVTDSAANFSYLADGGGLAILDTSGAIDVFVVQ
 GIYGLNYYKVNPCEDVNQQFVVS~~GGNIVGILTSRNETGSEQVENQFYVKLTNSSGGGGGSIGQNV~~
 TSCPYPVSYGR**FCIEPDGSLKMIVPEELKQFVAPLLNITESVLIPNSFNLTVTDEYIQTRMDKVQINCL**
 QYVCGNSLECR**KLFQQYGPVCDNILSVNSVSQKEDMELLSFYSSTKPKGYDTPVLSNVSTGEF**
 NISLLLKTPISSSSGR**SFIEDLLFTSVETVGLPTDAEYKKCTAGPLGLTKDLICAREYNGLLVLPPIIT**
 ADMQTMYTASLVGAMAFGGITSAAAIPFATQIQARINHLGITQSLLMKN**QEKIAASFNKAIGHMQE**
GFRSTSLALQQIQDVVNKQSAILTETMNSLNKNFGAITSVIQDIYAQLDPPQADAQVDRLITGRL
SSLSVLASAKQSEYIRVSQQRELATKKINECVKSQSNRYGFCGSGRHVLSIPQNAPNGIVFIHFTYTPE
 SFVNVTAIVGFCVNPANASQYAIVPANGR**GVFIQVNGSYITAR**DMYMPRDITAGDIVTLTSCQANY
 VNVNK**TVINTFVEDDDFNFNDELSK**WWNDTKHELPDFDEFNYTVPVLNISNEIDRI**QEVIQGLND**
SLIDLETLSILKTYIKLAIYSTVSSSLVLVGLIHAMGLWMCSNGSMQCRVCI

Figure 3.5. Protein confirmation using LC-MS/MS-based peptide sequencing of the modified IBV spike protein construct, mIBV-S2P-IAV-H6^{TM/CT}. The percentage sequence coverage is indicated above with several unique peptides identified with > 90 % confidence. Peptides with > 95 % confidence are highlighted in **bold** text, those with 50 - 95 % confidence in *italics*, and those with < 50 % confidence are underlined. No peptides were identified for the non-highlighted regions of the sequence (grey).

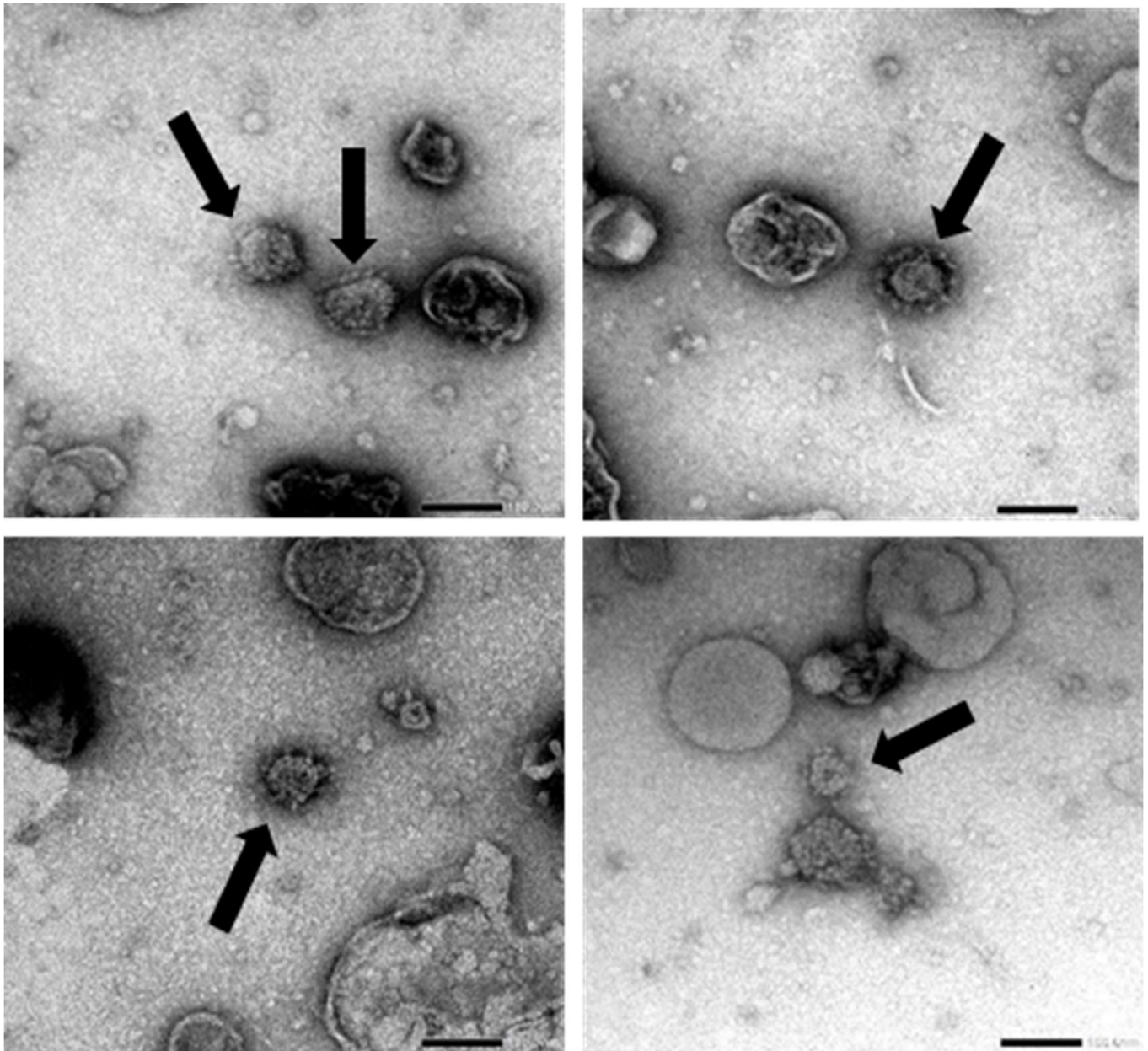


Figure 3.6. Negative-stained transmission electron microscopy images of plant-produced IBV virus-like particles expressed with the synthetic gene construct, mIBV-S2P-IAV-H6^{TM/CT} in *N. benthamiana*. Arrows indicate VLPs.

3.3.4. Protein Detection and Confirmation of Construct mIBV-S2P-IAV-H6^{CTonly}

An additional construct also derived from the mIBV-S2P construct was designed in an attempt to increase the levels of VLP expression. This construct had only the cytosolic tail (CT) of the IBV S protein substituted with that of the IAV HA2 protein designated mIBV-S2P-IAV-H6^{CTonly}.

For the mIBV-S2P-IAV-H6^{CTonly} construct, bands on the SDS-PAGE gel were observed which correlated to the expected S protein size (Fig. 3.7 (a)). These bands were again, noticeably higher than the band around the same size in the negative control as was the band in the positive control, suggesting that this was the S protein and not a plant protein. The SDS-PAGE gel also suggested that the highest protein content lay within fractions 3 – 6. The Western blot detected the strongest level of S protein specific bands at fractions 3 – 5 and the strongest detection was in the constructs infiltrated at a ratio of 4:1 (Fig. 3.7 (b)). This again shows that a higher construct to complementary protein ratio leads to higher protein expression in plants. The S protein was not detected in the QX-like positive control. Fraction 5 for each ratio was excised from the SDS-PAGE gel and analysed by liquid chromatography mass spectrometry (LC-MS/MS) based peptide sequencing, which further confirmed them to be the IBV S protein (Fig. 3.8). The number of peptides detected for the mIBV-S2P-IAV-H6^{CTonly}:M2 plant-produced VLPs at a 4:1 ratio were higher with more coverage than the ones produced by the same VLPs produced at a 2:1 ratio. The number of peptides detected for this construct were higher than the ones detected for the mIBV-S2P-IAV-H6^{TM/CT} construct developed previously, with more coverage. This shows that substituting just the cytosolic tail of the IBV S protein with that of the IAV HA2 protein leads to higher protein expression and more abundant VLP assembly than substituting both the transmembrane domain and the cytosolic tail. The TEM results showed that the most VLPs were found in fraction 5 and 6 as opposed to fractions 2 or 3 as found previously (Fig. 3.9). More VLPs were seen for the construct co-infiltrated at a ratio of 4:1 than for the same construct co-infiltrated at a ratio of 2:1 (Fig. 3.9).

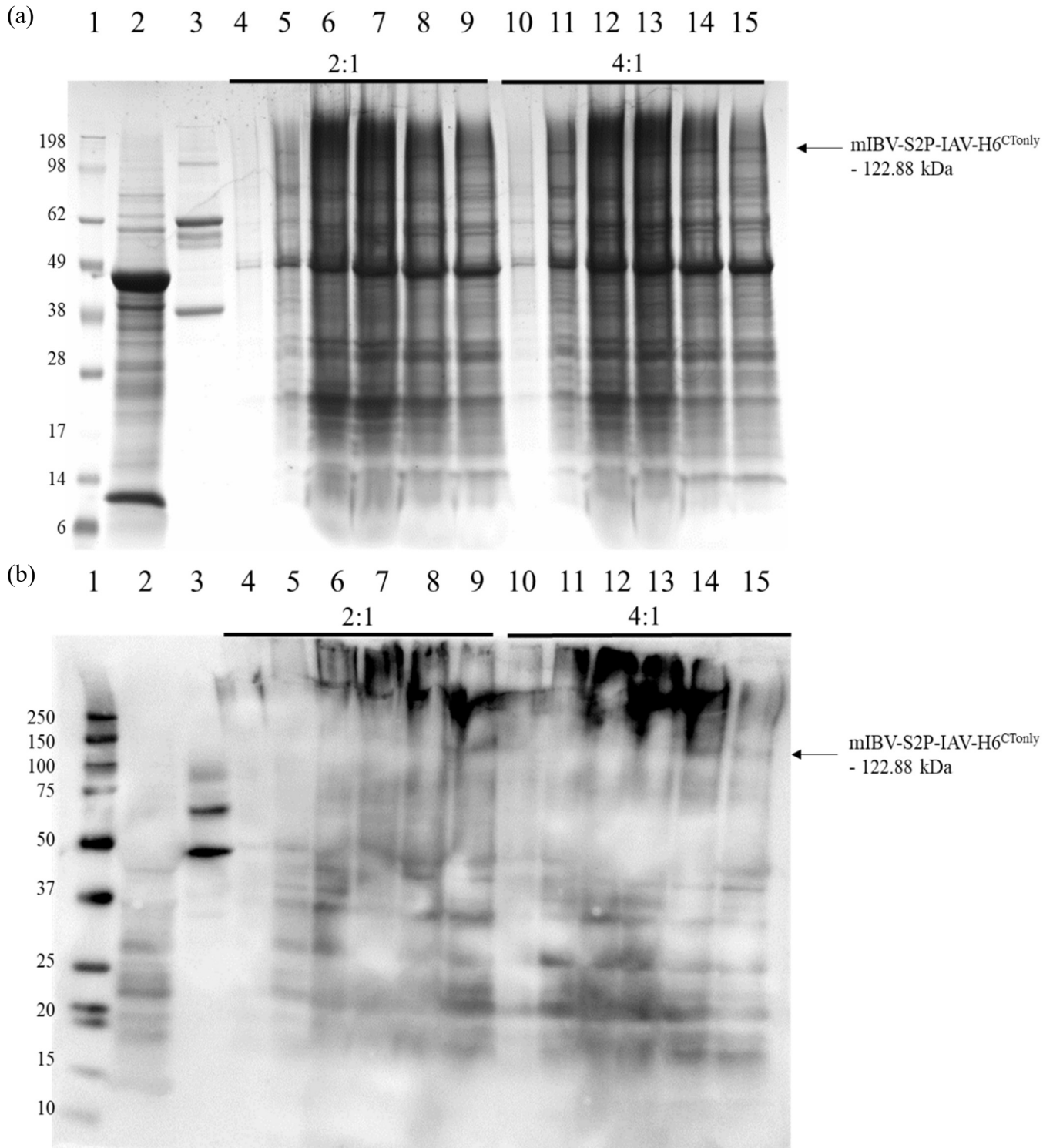


Figure 3.7. SDS-PAGE (a) and Western blot (b) of plant-produced mIBV-S2P-IAV-H6^{CTonly} protein co-infiltrated at different ratios with the IAV M2 protein. Lane 1: molecular weight marker; Lane 2: plant-expressed empty pEAQ-HT vector; Lane 3: purified live QX-like IBV strain ck/ZA/3665/11; Lanes 4 - 9: mIBV-S2P-IAV-H6^{CTonly}:M2 Fractions 1 - 6; Lanes 10 - 15: mIBV-S2P-IAV-H6^{CTonly}:M2 Fractions 1 - 6.

mIBV-S2P-IAV-H6^{CTonly} : M2 (2:1)

29.4 % coverage (95 % confidence) and 24 unique peptides

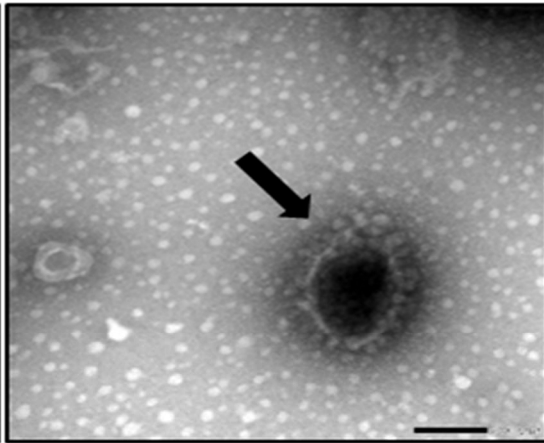
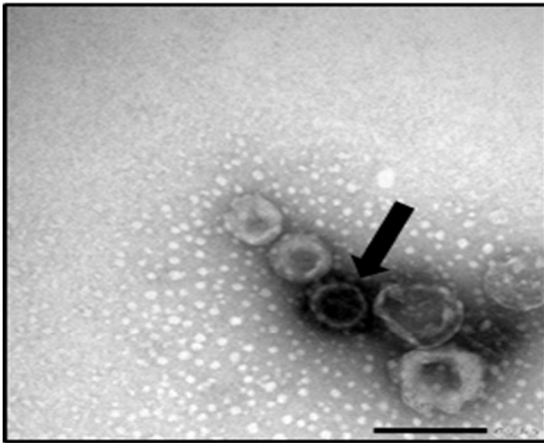
MGWSWIFLFLLSGAAGVHCNLFSDNNYVYYYQSAFRPPNGWHLQGGAYAVVNSTNHTSNAGSAQGCTV
 GVIKDVYNQSVASIAMTAPLQGMWFCAYCNFSDTTVFVTHCYHIRISAMKNGSLFYNLTVSVSKYPNFK
 SFQCVNNFTSVYLNGLDVFTSNK**TTDVTSAGVYFKAGGPVNYSIMKEFKVLAYFVNGTAQDVILCDNSPK**
 GLLACQYNTGNFSDGFYPFTNSTLVREKFIVYRESSFNTTLALTNFTFTNVSNAPNSGGVNTFHL YQTQTAQ
 SGYYNFNLSFLSQFVYKASDFMYGSYHPSCSFRPETINSGLWFNSLSVSLTYGPLQGGCKQSVFSGK**ATCCY**
AYSYKGPMACKGVYSGELRTNFECGLLVYVTKSDGSRIQTRTEPLVLTQYNNITLTKCVAYNIYGRV
 GQGFITNVTDSAANFSYLADGGLAILDTSGAIDVFVVQGIYGLNYYK**VNPCEDVNQQFVVS**GGNIVGILTSR
NETGSEQVENQFYVKLTNSSGGGGGSGIQNVTSQPYVSYGR**FCIEPDGSLKMIVPEELK**QFVAPLLNITESVLI
 PNSFNLTVTDEYIQTRMDKVQINCLQYVCGNSLECR**KLFQQYGPVCDNILSVNSVSQKEDMELLSFYSS**
KPKGYDTPVLSNVSTGEFNISLLLKTPISSSGRSFIEDLLFTSVETVGLPTDAEYKKCTAGPLGLTKDLICARE
 YNGLLVLPPIITADMQTMYTASLVGAMAFGGITSAAAIPFATQIQARINHLGITQSLLMKNQE**KIAASFNKAI**
GHMQEGFRSTSLALQQIQDVVNKQSAILTETMNSLNKNFGAITSVIQDIYAQLDPPQADAQVDRLITGR**LS**
SLSVLASAKQSEYIRVSQQRELATKKINECVKSQSNRYGFCGSGRHVLSIPQNAPNGIVFIHFTYTPESFVNVA
 IVGFCVNPNANASQYAIVPANGR**GVFIQVNGSYITARDMYMPRDITAGDIVTLTSCQANYVNVNKTVIN**TFV
EDDDFNFNDELSKWWNDTKHELPDFDEFNYTVPVLNISNEIDRIQEVIQGLNDSLIDLETLSILKTYIKWP
 WYVWLAIFFAIIFILILGWVFFMCSNGSMQCRVCI

mIBV-S2P-IAV-H6^{CTonly} : M2 (4:1)

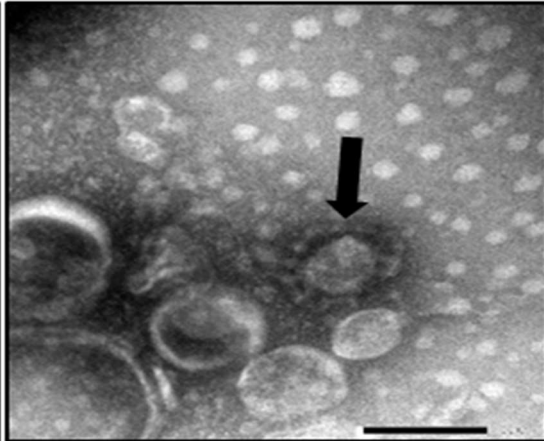
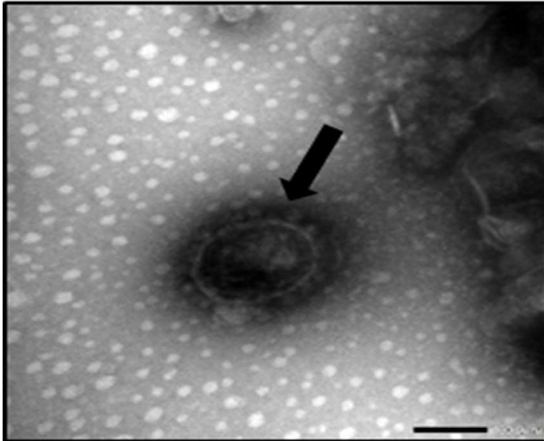
34.6 % coverage (95 % confidence) and 41 unique peptides

MGWSWIFLFLLSGAAGVHCNLFSDNNYVYYYQSAFRPPNGWHLQGGAYAVVNSTNHTSNAGSAQGCTV
 GVIKDVYNQSVASIAMTAPLQGMWFCAYCNFSDTTVFVTHCYHIRISAMKNGSLFYNLTVSVSKYPNFK
 SFQCVNNFTSVYLNGLDVFTSNK**TTDVTSAGVYFKAGGPVNYSIMKEFKVLAYFVNGTAQDVILCDNSP**
KGLLACQYNTGNFSDGFYPFTNSTLVREKFIVYRESSFNTTLALTNFTFTNVSNAPNSGGVNTFHL YQTQTA
 QSGYYNFNLSFLSQFVYKASDFMYGSYHPSCSFRPETINSGLWFNSLSVSLTYGPLQGGCKQSVFSGK**ATCC**
YAYSYKGPMACKGVYSGELRTNFECGLLVYVTKSDGSRIQTRTEPLVLTQYNNITLTKCVAYNIYGR
 VGQGFITNVTDSAANFSYLADGGLAILDTSGAIDVFVVQGIYGLNYYK**VNPCEDVNQQFVVS**GGNIVGILTSR
NETGSEQVENQFYVKLTNSSGGGGGSGIQNVTSQPYVSYGR**FCIEPDGSLKMIVPEELK**QFVAPLLNITESV
 LIPNSFNLTVTDEYIQTRMDKVQINCLQYVCGNSLECR**KLFQQYGPVCDNILSVNSVSQKEDMELLSFYSS**
TKPKGYDTPVLSNVSTGEFNISLLLKTPISSSGRSFIEDLLFTSVETVGLPTDAEYKKCTAGPLGLTKDLICA
 REYNGLLVLPPIITADMQTMYTASLVGAMAFGGITSAAAIPFATQIQARINHLGITQSLLMKNQE**KIAASFNK**
AIGHMQEGFRSTSLALQQIQDVVNKQSAILTETMNSLNKNFGAITSVIQDIYAQLDPPQADAQVDRLITGR
LSSLSVLASAKQSEYIRVSQQRELATKKINECVKSQSNRYGFCGSGRHVLSIPQNAPNGIVFIHFTYTPESFVN
 TAIVGFCVNPNANASQYAIVPANGR**GVFIQVNGSYITARDMYMPRDITAGDIVTLTSCQANYVNVNKTVIN**
TFVEDDDFNFNDELSKWWNDTKHELPDFDEFNYTVPVLNISNEIDRIQEVIQGLNDSLIDLETLSILKTYI
 KWVPYVWLAIFFAIIFILILGWVFFMCSNGSMQCRVCI

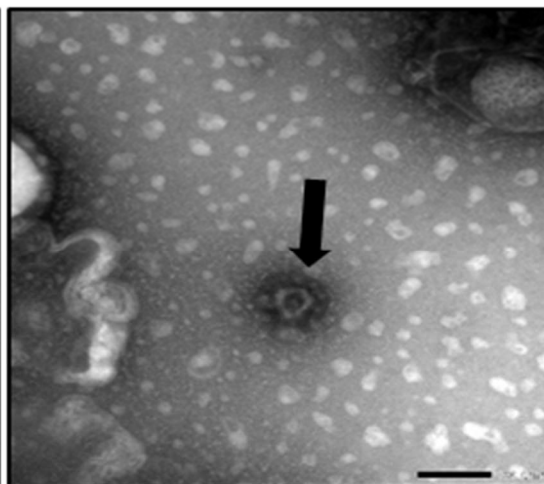
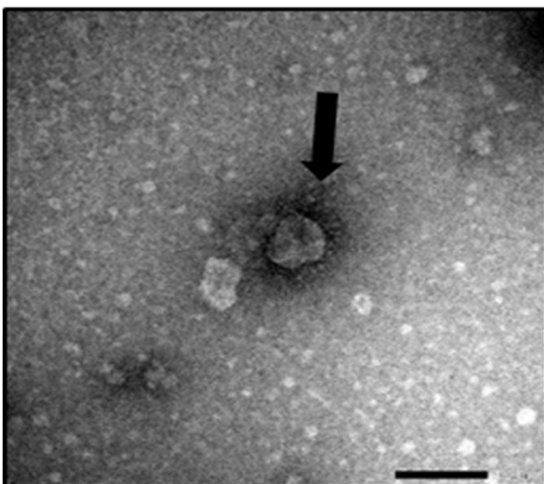
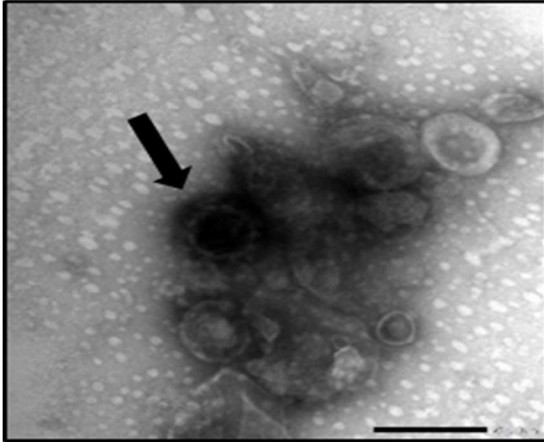
Figure 3.8. Protein confirmation using LC-MS/MS-based peptide sequencing of the modified IBV spike protein construct, mIBV-S2P-IAV-H6^{CTonly} co-expressed at different ratios with the IAV M2 protein. The percentage sequence coverage is indicated above with several unique peptides identified with > 90 % confidence. Peptides with > 95 % confidence are highlighted in **bold** text, those with 50 - 95 % confidence in *italics*, and those with < 50 % confidence are underlined. No peptides were identified for the non-highlighted regions of the sequence (grey).



mIBV-S2P-IAV-H6^{CTonly}
:M2 particles
(2:1 Ratio)
Fraction 3



mIBV-S2P-IAV-H6^{CTonly}
:M2 particles
(4:1 Ratio)
Fraction 3



mIBV-S2P-IAV-H6^{CTonly}
:M2 particles
(2:1 Ratio)
Fraction 6

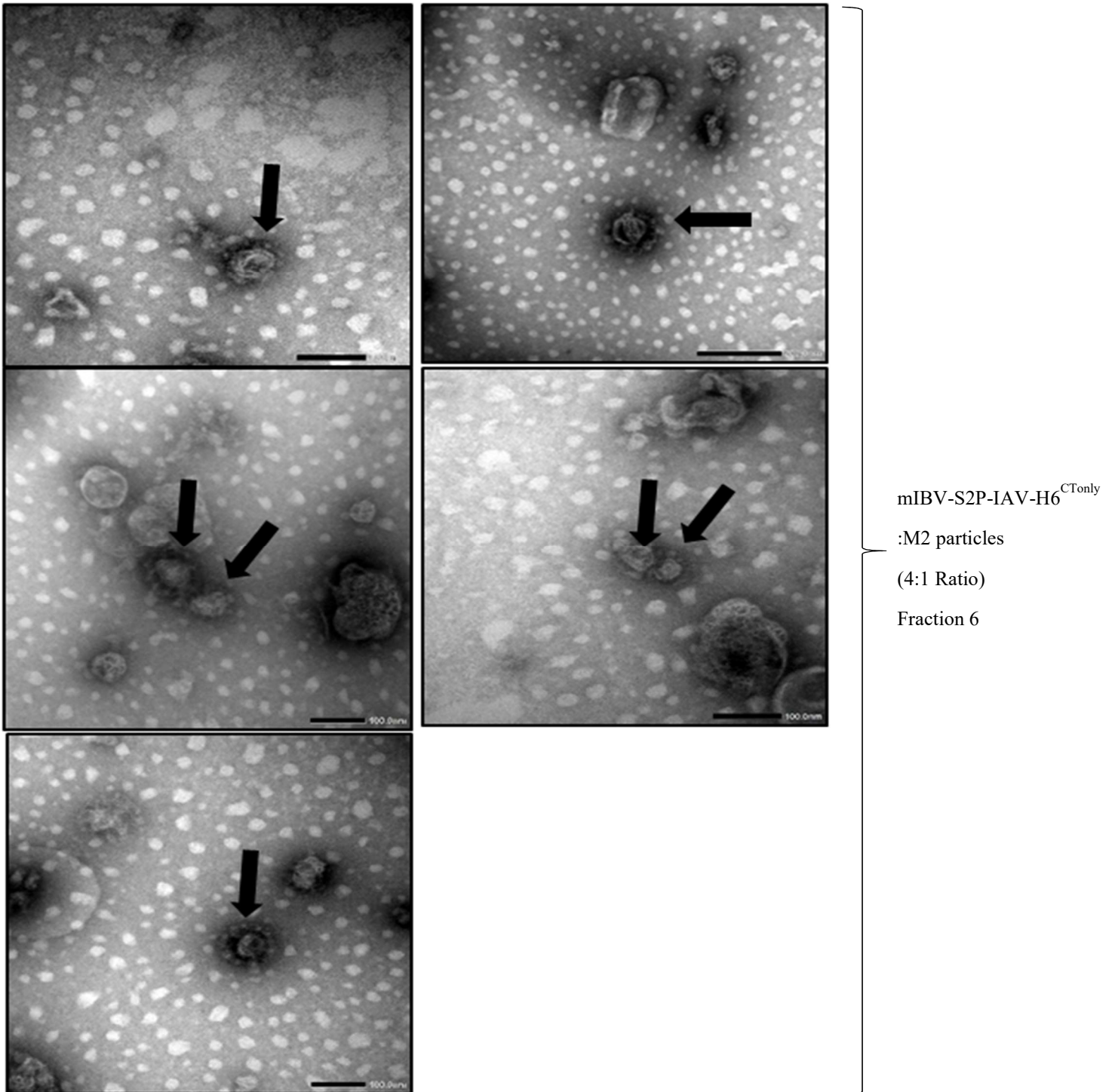


Figure 3.9. Negative-stained transmission electron microscopy images of plant-produced IBV virus-like particles expressed with the synthetic gene constructs mIBV-S2P-IAV-H6^{CTonly} in *N. benthamiana* in different ratios with IAV M2. Arrows indicate VLPs.

3.3.5. Effect of Ratio on Protein Expression and VLP Assembly

The constructs were infiltrated at different ratios with their complementary proteins in order to assess whether or not that would have an effect on protein expression and VLP assembly. Jutras *et al.*, (2015) co-infiltrated the IAV HA2 protein with the M2 protein at a ratio of 4:1 contrary to the 2:1 ratio that has been used so far and obtained good expression levels. Therefore, ratios of 2:1 and 4:1 were tested for the constructs to determine if changing the ratio would aid in improving protein expression levels.

Although increasing the ratio of the S protein to M2 seemingly enhanced the assembly of IB VLPs when TEM imaged, no difference could be seen in S protein expression on the SDS-PAGE gel (Fig. 3.10 (a)). There was strong interaction of the S protein specific bands with the antisera, however, there was no noticeable difference seen on the Western blot between the protein samples infiltrated at a ratio of 2:1 and those infiltrated at a ratio of 4:1 (Fig. 3.10 (b)). TEM showed very few assembled VLP particles in general, so it was difficult to observe differences in VLP abundance between the two ratios (Fig. 3.11). Results of the mIBV-S2P-IAV-H6^{CTonly} co-expression suggested that a higher number of VLPs may be found in later fractions, as opposed to fractions 2 and 3 that had been observed thus far. Although this is not always the case as seen by the level of protein separated on the SDS-PAGE gels, it was in the case of the mIBV-S2P-IAV-H6^{CTonly} construct.

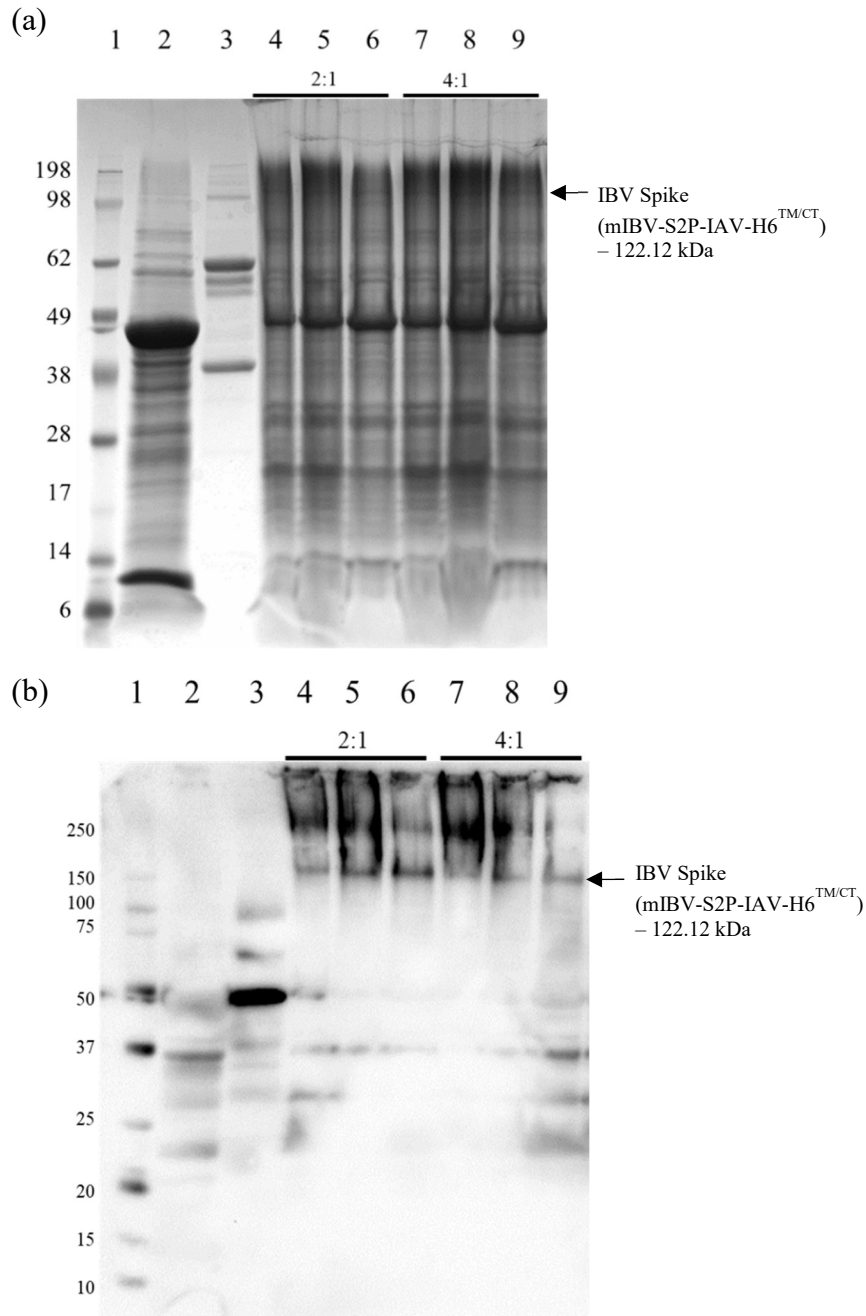


Figure 3.10. SDS-PAGE (a) and Western blot (b) of plant-produced IBV S protein (mIBV-S2P-IAV-H6^{TM/CT}) co-infiltrated at different ratios with the IAV M2 protein. Lane 1: molecular weight marker; Lane 2: plant-expressed empty pEAQ-HT vector; Lane 3: purified live QX-like IBV strain ck/ZA/3665/11; Lanes 4 - 6: mIBV-S2P-IAV-H6^{TM/CT}:M2 Fractions 2 - 4; Lanes 7 - 9: mIBV-S2P-IAV-H6^{TM/CT}:M2 Fractions 2 - 4. (Edited from Fig. S3).

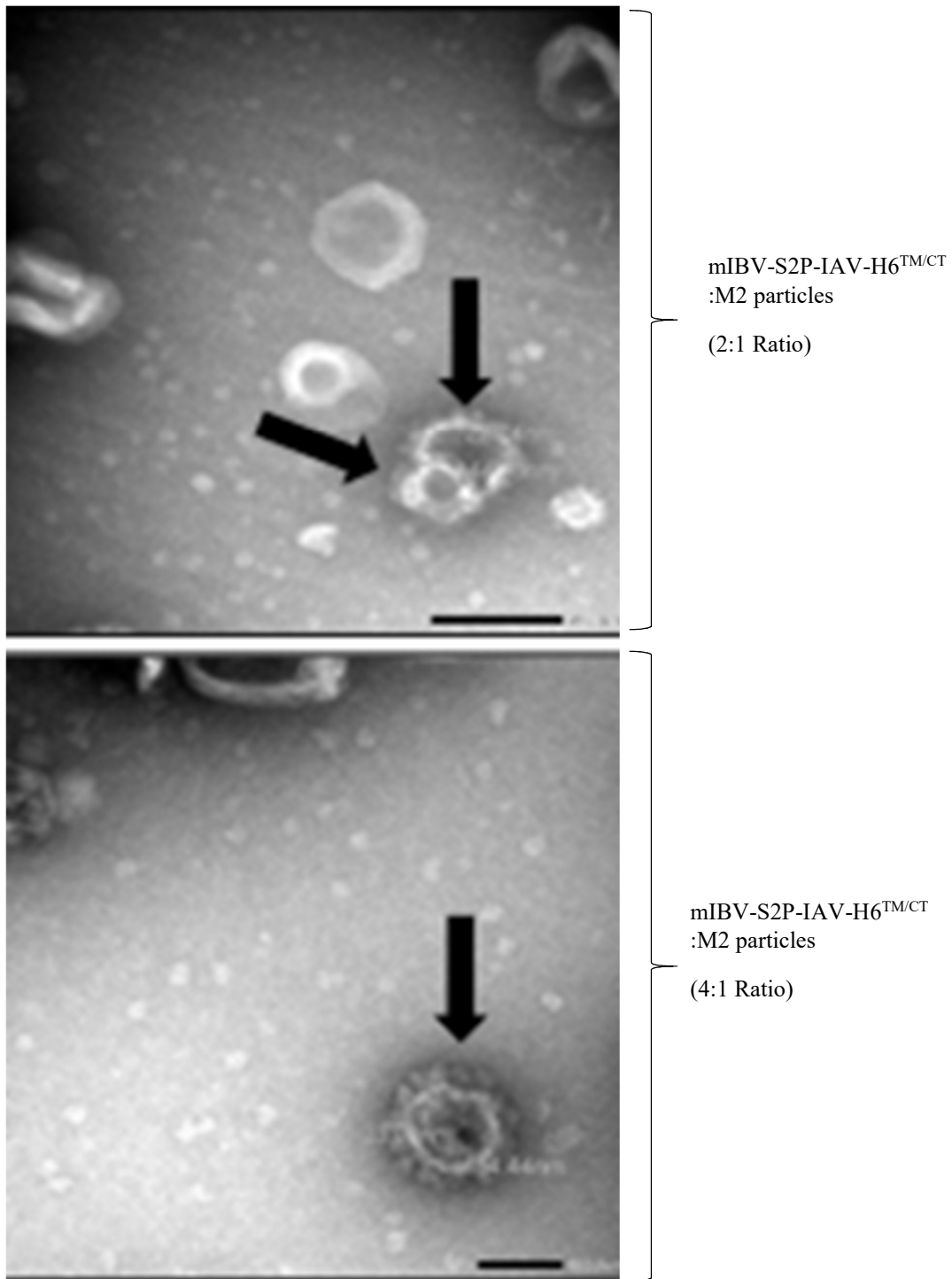


Figure 3.11. Negative-stained transmission electron microscopy images of plant-produced IBV virus-like particles expressed with the synthetic gene construct mIBV-S2P-IAV-H6^{TM/CT} in *N. benthamiana* at different ratios with its complementary protein IAV M2. Arrows indicate VLPs.

3.4. Discussion

In this chapter, several modifications were made to the IBV spike protein in an effort to increase protein expression and drive VLP assembly. These modifications were centred on replacing the native IBV spike protein TM sequence and/or the CT sequence, with corresponding TM and CT sequences of the IAV HA2 protein (H6 subtype). This was in part because both the IBV S protein and the IAV HA protein are both trimers, which would allow the protein to fold in a similar way compared to using the IAV NA protein which is a tetramer, and might hinder the normal folding of the viral particle. It was also chosen because of previous experiments involving substituting the native IBV TM and CT sequences with those of the HA that showed increase expression of the IBV S protein (Sepotokele, 2020).

The constructs whereby the IBV S1 subunit was fused to either the IAV HA2 protein subunit or to the IAV HA2 protein TM and CT sequences via a flexible linker (rIBV-S1-IAV-H6 and rIBV-S1-IAV-H6^{TM/CT}), did not express well in the plants, and although TEM visualisation showed particles somewhat similar to IB virus particles, the SDS-PAGE and immunoblot results did not confirm IBV spike protein expression. It is possible that S protein expression was too low to detect via immunoblotting since the antiserum used was produced by chickens that had been vaccinated with commercial live-attenuated vaccines, and not with the homologous QX-like strain used in this study. Because the level of cross-protection found between the S protein of different serotypes is known to be quite low (Cavanagh, 2003), it is possible that the antisera did not detect any protein because the serotypes were heterologous. It may be that a different or more serologically similar serum may have been required to more adequately detect any proteins that may have been present. However, as SDS-PAGE and Western blot techniques are the first tests for protein expression, and they did not confirm protein expression, the results were not convincing enough to warrant further pursuit, such as producing homologous antiserum in chickens. TEM was the only analytical technique that confirmed protein expression and VLP assembly. Therefore, it was concluded that the constructs rIBV-S1-IAV-H6 and rIBV-S1-IAV-H6^{TM/CT} expressed poorly in the plants. By contrast, Lv and co-workers (2014) were able to successfully produce this type of chimeric VLP vaccine using a baculovirus expression system by fusing the S1 protein to the IAV H5N1 neuraminidase protein TM and CT sequences (Lv *et al.*, 2014). This same approach but with the IAV HA2 of the H6 subtype was not successful in this study. Whether this was because of the protein expression system, subtype, or IAV protein used, or some other reason, remains unknown. Xu and co-workers were able to assemble highly immunogenic VLPs against IBV

by infecting Sf9 insect cells with a recombinant S protein construct, co-infected with the IBV M and E protein genes. Recombinant baculoviruses coded for the recombinant S protein that was produced by fusing the IBV S1 subunit to the IBV S2 subunit TM and CT sequences via a flexible linker (Xu *et al.*, 2016). This suggests that it is possible to produce VLPs expressing the IBV S1 subunit, however, it may be more challenging in plant expression systems because for reasons unclear, many viral glycoproteins do not express as well in plants (Margolin *et al.*, 2018).

The mIBV-S2P-IAV-H6^{TM/CT} construct, which was derived from mIBV-S2P (from Chapter 2), exhibited much higher levels of Spike protein expression confirmed by SDS-PAGE and immunoblotting, and resulted in the assembly of IB VLPs as seen under TEM. The results were further confirmed by LC-MS/MS analysis of the protein band of interest. Higher levels of protein expression were seen with this mIBV-S2P-IAV-H6^{TM/CT} construct than with the mIBV-S2P construct from Chapter 2. Previous attempts at expressing the native IBV spike protein with its native TM and/or CT sequences replaced with those of the IAV HA2 protein did to some extent elevate protein expression but not enough to form VLPs (Sepotokele, 2020). While the stabilising mutations (Pallesen *et al.*, 2017) were essential to successful VLP formation, substitution of the TM and/or CT sequences with the equivalent sequences of the IAV HA2 protein also played a role in increasing the levels of protein expression and the abundance of VLPs seen under TEM. Human SARS-CoV-2 plant-produced VLPs with native TM and CT sequences replaced with equivalent sequences from the HA protein from an H5 IAV subtype were successfully produced (Ward *et al.*, 2021; Peyret *et al.*, 2021). This begs the question of whether or not VLP expression may be dependent on the choice of IAV subtype. Co-infiltrating with the proteins specific to the TM and CT of the virus used is also critical in enhancing VLP assembly.

The transient co-expression of the IAV M2 protein was previously shown to potentially improve both the accumulation as well as the recombinant protein's stability within the secretory pathway of the plant cell by regulating the pH of the cells (Jutras *et al.*, 2015). However, the transient co-expression of the IAV M1 protein did not appear to be necessary for VLP formation in plants, and may potentially decrease it (Chen *et al.*, 2007). Co-infiltration with the IAV M2 protein showed improved protein expression and VLP formation than co-infiltration with the IAV M1 protein or with both the M1 and M2 proteins together shown mostly by the low number or lack of VLPs that were seen under TEM for the latter two.

Furthermore, co-infiltrating with a higher construct to complementary protein ratio (Jutras *et al.*, 2015) of 4:1 further improved protein expression compared to a ratio of 2:1 leading to a higher abundance of VLPs seen under TEM. Using PBS buffer for harvesting the leaves yielded higher S protein levels and more abundant VLPs than Bicine or Tris buffers. This could be because PBS buffer provided more adequate pH levels for protein and VLP stability than the other buffers. The conformations of proteins may be affected by a change in the conditions of a solutions, different pH levels, denaturants, and temperature (O'Brien *et al.*, 2013; Tanford and Roxby, 1972). Alexander and Collins, (1975) found that when IBV was grown in chick kidney cells at pH values ranging from 6 to 9, higher pH values resulted in faster release of the virus with a rapid drop in titre, while more acidic pH values reached maximum titres, showing a minimal reduction in infectivity for up to 49 hours after inoculation. The virus was also shown to be more stable in tissue culture medium of between pH 6 and 8, being more stable at acidic pH values (Alexander and Collins, 1975). It is therefore possible that the high pH values of Bicine buffer (pH 8.4) and Tris buffer (pH 8.0), affected the conformation of the virus particle thus affecting its stability during or after harvest compared to the more adequate pH 7.4 of PBS buffer.

Subsequently, the mIBV-S2P construct was again modified to substitute only the native cytosolic tail with that of the IAV HA2 protein (H6 subtype). This was a hypothesis based on the elevated expression levels seen when modifying the TM and CT domains. The resultant construct (mIBV-S2P-IAV-H6^{CTonly}) showed even higher levels of protein expression as well as more abundant VLPs under TEM than previously seen. Substituting just the CT of the IBV spike protein with that of the IAV HA2 protein led to higher protein expression levels than substituting both the TM domain and the CT. It is possible that retaining the native TM domain of the IBV S protein allowed the particle to assemble into a more natural conformation while still obtaining the benefits (elevated protein expression levels) of the IAV HA2 protein from its CT domain. Table S1 shows the levels of expression for each analytical technique. Together with the stabilising mutations suggested by Pallesen and co-workers (2017), as well as replacing the native signal peptide with a murine signal peptide, it is possible to obtain greater expression levels of the IBV S protein in plants than previously demonstrated (Sepotokele, 2020). Co-infiltrating with accessory proteins that complement the substituted TM and/or CT domains also improved protein expression, and increasing the ratio of construct to complementary protein led to the highest level of protein expression and a higher abundance of VLPs formed.

CHAPTER 4

DESIGN, OPTIMISATION, AND EXPRESSION OF NDV-F MODIFIED IBV SPIKE CONSTRUCTS AND PILOT IMMUNOGENICITY STUDY

4.1. Introduction

Of the viruses that have been considered as vaccine vectors for Infectious Bronchitis Virus (IBV), Newcastle disease virus (NDV) is one of the most promising because it is capable of inducing high levels of local as well as systemic immune responses. It is considered safe and would be capable of offering protection against both IBV and NDV as a bivalent vaccine (Shirvani *et al.*, 2018; Zhao *et al.*, 2017). NDV is an extremely infectious and economically significant disease that affects poultry (Taylor *et al.*, 1990). It exists as many genotypes and sub-genotypes but are broadly classified into three pathotypes by disease severity (Hanson and Brandly, 1955; Waterson *et al.*, 1967). The pathotype classifications are:

- Velogenic strains cause severe lethal disease in chickens of any ages. They are either neurotropic, which means they cause lesions in the nervous system and the respiratory tract, or viscerotropic, which means that they cause haemorrhagic lesions in the digestive tract (Taylor *et al.*, 1990).
- Mesogenic strains cause severe respiratory infections or lethal nervous system infections in younger chickens (Taylor *et al.*, 1990).
- Lentogenic strains cause minor infections in the respiratory tract (Taylor *et al.*, 1990).

NDV falls under the *Paramyxoviridae* family and is of the *Orthoavulavirus* type 1 genus (da Silva *et al.*, 2020). Viruses from this genus are enveloped, pleomorphic, and enclose a non-segmented, single-stranded, negative-sense RNA genome that is between 15 and 19 kb in size (Taylor *et al.*, 1990; Lamb and Kolakofsky, 2001). A lipid bilayer membrane surrounds the virion. On the surface of the virus particle are two glycoprotein spikes, both of which play a role in generating immunity (Avery and Niven, 1979; Merz *et al.*, 1980). These are the haemagglutinin-neuraminidase (HN) and the fusion (F) glycoproteins (Chen *et al.*, 1971).

The NDV Fusion (F) protein is a type 1 fusion protein (Colman and Lawrence, 2003; Heinz and Allison, 2001) that facilitates membrane fusion during viral infection (Scheid and Choppin, 1974; Gravel *et al.*, 2011). It is initially synthesised as the precursor protein F0, after which it is cleaved into F1 and F2 that are held together by disulphide bonds (Scheid and Choppin,

1977). The F protein is a homotrimer with intertwined monomers. It is wedge or triangle-shaped, and is divided into three domains, the head, neck, and stalk (Morrison, 2003). The head and neck domain contain F1 and F2 polypeptide sequences. The stalk region is a long coiled-coil trimer (171 – 221 amino acid region) that includes the cytosolic tail (CT) part of the HR1 domain (Morrison, 2003).

The LaSota strain of NDV has been commonly used as a safe and effective live-attenuated vaccine for over 60 years and as a recombinant vector vaccine against numerous avian diseases including IBV (Samal, 2011; Kim and Samal, 2016). Abozeid *et al.*, (2019) found that a recombinant NDV vector expressing the IBV Spike (S) protein was able to offer significant protection against challenge with the live IB virus in specific pathogen-free (SPF) chickens. A recombinant NDV expressing the IBV S1 subunit was shown to induce protective immunity against IBV challenge (Zhao *et al.*, 2017). In order to create this recombinant, an insert that consisted of the S1 subunit of IBV genetically fused to the transmembrane domain (TM) and cytosolic tail (CT) of the NDV F gene was cloned into a plasmid that contained the full-length cDNA of NDV (LaSota strain). The resultant plasmid was transfected into BSR T7/5 cells, resulting in a recombinant NDV containing an IBV S1 gene. As a live bivalent vaccine candidate, it induced effective haemagglutinin inhibition (HI) antibody responses against NDV and completely protected against NDV challenge; and it induced an antibody response against IBV and partially protected against IBV challenge. This protective efficacy was higher than that offered by commercial IBV (H120) vaccine (Zhao *et al.*, 2017). On the other hand, a recombinant NDV expressing the IBV (ArkDPI) S2 subunit was able to induce partial protection against IBV (Toro *et al.*, 2014). Toro *et al.*, (2014) hypothesised that overexposing the immune system of chickens to IBV S2 by making use of a vectored vaccine, and boosting with the whole virus, could offer protection against IBV strains with differing S1 sequences. The S2 gene of IBV (flanked by the start and end gene sequences of NDV) was inserted into a vector plasmid containing the full-length cDNA of NDV. The resultant plasmid was transfected into MVA/T7-infected HEp-2 cells resulting in a recombinant NDV containing the IBV S2 gene (Toro *et al.*, 2014). When boosted with a Mass strain of IBV, it was able to protect chickens against NDV and ArkDPI IBV challenge. The S2 sequence used in the study had an amino acid similarity that was at least 98.7 % similar to all available Ark S2 sequences and 94 % similar to the Mass strain that was used for boosting. This showed that boosting with the IBV Mass strain elicited an S2 memory response and was able to protect against ArkDPI challenge. Because the S2 subunit usually remains mostly unexposed during infection,

overexposing it may have induced an increase in the T and B cell-bearing receptors that interact with the epitopes on the S2 subunit increasing their affinity to them during vaccine challenge (Toro *et al.*, 2014). Shirvani *et al.*, (2018) however, found that not only did a recombinant NDV expressing the full-length S protein of IBV offer better protection against IBV than just one of the subunits as described by Zhao *et al.*, (2017) and Toro *et al.*, (2014), but it was also able to offer protection against both IBV and NDV challenge. This recombinant was developed by inserting the full-length IBV (Mass-41) S protein into a vector plasmid comprising the full-length NDV cDNA. This was done using reverse genetics. Recombinants containing only the S1 or S2 subunits were also developed. The recombinant containing the full S protein exhibited a decrease in the severity of clinical signs after IBV (Mass-41) and NDV challenge. It was able to stimulate the production of neutralizing IBV antibodies. It was found that the recombinant NDV that expressed only the S1 subunit resulted in the protein being retained in the cell. It was proposed that proper S1 protein folding required the assistance of the S2 subunit as a chaperone (Shirvani *et al.*, 2018). In a study that was done by Wu and coworkers (2019a), the native TM and CT sequences of the IBV S2 subunit were separately fused (using a flexible peptide (GlyGlySerSer or GGSS)) to either the IBV S1 subunit (to produce a recombinant S protein named rS) or to the NDV F protein ectodomain (to produce a recombinant F protein named rF). The two recombinant proteins rS and rF, along with the IBV M protein were expressed and assembled to form a chimeric IBV-NDV VLP vaccine using a baculovirus expression system (Wu *et al.*, 2019a). The resultant VLPs not only resembled a native IBV particle, but elicited efficient cellular and humoral immune responses in immunised SPF chickens. The chimeric IBV-NDV VLPs protected against challenge from both IBV and NDV and were able to fully protect against death (Wu *et al.*, 2019a).

The aim of this chapter was to produce IBV VLPs in *Nicotiana benthamiana* (*N. benthamiana*) plants through the transient expression and assembly of an IBV Spike protein S1 subunit hybrid modified using the NDV F protein TM and CT sequences. The IBV S1 subunit was fused to the TM and CT sequences of the NDV F protein in order to develop a VLP that can potentially protect against IBV.

The full-length IBV Spike protein with stabilising mutations described in Chapter 2 was also further modified to substitute the native IBV TM and/or CT with the equivalent sequences of the NDV F protein. These were co-expressed with the NDV matrix protein to potentially enhance the expression and assembly of VLPs.

4.2. Materials and Methods

4.2.1. Development, Optimisation, and Expression of Modified IBV Spike Constructs

4.2.1.1. Design and Synthesis of Synthetic Gene Constructs

Synthetic gene sequences coding for the IBV S protein (ck/ZA/3665/11, QX-like strain, Abolnik, 2015) (Protein ID AKC34133), as well as the NDV F protein (LaSota strain) (Protein ID MK310259) were acquired from the National Centre for Biotechnology Information (NCBI). Vector NTI software was used to design a hybrid of these gene sequences. The hybrid contained the IBV S1 sequence fused to the TM/CT domain of the NDV F sequence via a linker (GGGGSGGGGS) and was designated rIBV-S1-NDV-F^{TM/CT} (Table 4.1). *AgeI* and *XhoI* sites were added to the 5' and 3' ends, with a stop codon added downstream of the sequence. Any additional *AgeI* and *XhoI* sites in the gene were mutated.

To improve VLP assembly in plants and to complement the NDV F TM/CT, a chicken-codon optimised gene sequence coding for the NDV matrix (isolate turkey/South Africa/N2057/2013) (Protein ID KR815908), was already available to use for co-infiltration. This was synthesised previously to contain *AgeI* and *XhoI* restriction sites on the 5' and 3' ends, as well as a stop codon added downstream of each sequence. Any additional *AgeI* and *XhoI* restriction sites in the gene were mutated. The gene sequences were chicken codon-optimised for optimal expression in domestic chickens (*Gallus gallus*) unless otherwise stated, and synthesised by BioBasic Canada Inc.

Primers were designed to modify the synthetic full-length IBV S protein designed in Chapter 2 (Integrated DNA Technologies Inc. (IDT)). These primers (Table 4.2) were designed with the intention of substituting the TM/CT domains of mIBV-S2P with the TM/CT domains of the F protein of NDV or substituting just the CT domain of mIBV-S2P with the CT domain of the F protein of NDV. This resulted in two new synthetic gene sequences, mIBV-S2P-NDV-F^{TM/CT} and mIBV-S2P-NDV-F^{CTonly} (Table 4.1).

Table 4.1. Schematic diagrams of modified constructs designed in Chapter 4

Construct	Schematic Diagram	Modifications
rIBV-S1-NDV-F ^{TM/CT}		Native signal peptide (r), S1 Spike subunit, GGGGSGGGGS linker between IBV S1, NDV F TM and CT
mIBV-S2P-NDV-F ^{TM/CT}		Murine signal peptide (m), full length Spike protein (S), 2P mutation, SSGGGGGS linker between S1 and S2 subunits, NDV F TM and CT
mIBV-S2P-NDV-F ^{CTonly}		Murine signal peptide (m), full length Spike protein (S), 2P mutation, SSGGGGGS linker between S1 and S2 subunits, IBV S TM , NDV F CT

*(**LIT** – start of NDV **TM** sequence, **CYL** – start of NDV **CT** sequence, **WPW** – start of IBV **TM** sequence).

Table 4.2. Primers used for synthetic NDV construct design

Construct	Name	Sequence (5' – 3')
rIBV-S-H6 ^{TM/CT}	Fw	TTT ACC GGT ATG GGC TGG AGC TGG
	Rv	AAA CTC GAG TCA CAT CTT TGT TGT GGC TCT CAT CTG ATC CAG GGT GTT ATT GCC CAG CCA CAG CAG TGT TTT CTG CTG TGC
mIBV-S2P-NDV-F ^{TM/CT}	rIBV-S-F ^{TM/CT} Rv	CTT CTG CTT GTA CAT CAG GTA GCA GGC CAG GAT CAG GCT CAG GAT TCC GAA CAC CAG GGA GAT GAT TGT CAG CAC GAT GTA GGT GAT CAG CTT AAT GTA GGT TTT CAG
	rIBV-S-H6 ^{TM/CT} Fw	TTT ACC GGT ATG GGC TGG AGC TGG
mIBV-S2P-NDV-F ^{CTonly}	IBV NDV LaSota CT tail Rv	AAA CTC GAG TCA CAT CTT TGT TGT GGC TCT CAT CTG ATC CAG GGT GTT ATT GCC CAG CCA CAG CAG TGT TTT CTG CTG TGC CTT CTG CTT GTA CAT CAG GTA GCA GAA GAA CAC CCA GCC CAG GAT

4.2.1.2. Cloning into pEAQ-HT Plant Expression Vector Plasmid

The synthesised gene rIBV-S1-NDV-F^{TM/CT} was cloned into the pEAQ-HT expression vector, purified, and validated as in Chapter 2.

Constructs mIBV-S2P-NDV-F^{TM/CT} and mIBV-S2P-NDV-F^{CTonly} were created by PCR amplification using the corresponding primer pairs in Table 4.2. PCR mixes were set up to contain a final concentration of 0.3 μ M of each of the corresponding forward and reverse primers (Table 4.2), KAPA dNTP mix, 5X KAPA HIFI buffer, as well as KAPA HIFI DNA polymerase enzyme (KAPA Biosystems) according to manufacturer's directions. The PCR amplifications were performed using the GeneAmp 2720 Thermocycler (Applied Biosystems) with the following cycling conditions: 3 minutes initial denaturation at 95 °C (1 cycle); followed by 35 cycles of 20 sec denaturation at 98 °C, 30 sec annealing at 70 °C, and 210 sec extension at 72 °C; ending off with 5 minutes final extension at 72 °C (1 cycle). The resulting PCR products were separated on a 1 % agarose gel using the molecular weight marker GeneRuler ladder mix (SM0331) as a reference. The target bands of the right size were cut out from the gel and purified with the ZymocleanTM Gel DNA Recovery Kit. The purified genes were then cloned into the pEAQ-HT expression vector, purified, and verified as in Chapter 2.

All the constructs in this chapter were co-infiltrated with the NDV matrix construct as opposed to with the IBV M, E, and N constructs used in Chapter 2.

The results of this chapter showed that the construct mIBV-S2P-NDV-F^{TM/CT} produced the most abundant VLPs at the time of the trial, therefore it was subsequently used for the pilot immunogenicity study.

4.2.2. Preparation of VLP Batch for Pilot Immunogenicity Study

4.2.2.1. Agroinfiltration

The glycerol stocks for mIBV-S2P-NDV-F^{TM/CT} and NDV matrix were propagated on Luria Bertani (LB) agar plates in appropriate antibiotics until the OD₆₀₀ was ≤ 2 . The overnight cultures were prepared for infiltration as in Chapter 2.2.5 but with the *A. tumefaciens* suspensions combined to a final ratio of 4:1 (mIBV-S2P-NDV-F^{TM/CT}:matrix) before infiltrating.

4.2.2.2. Harvest of Leaf Material, Protein Extraction, and Purification

The infiltrated leaves were harvested at 6 days post infiltration, extracted in 1 X PBS buffer, purified by sucrose density ultracentrifugation, and the protein was confirmed by SDS-PAGE, immunoblot, and TEM as described in Chapter 2.

4.2.2.3. Protein Quantitation

4.2.2.3.1. Total Protein Quantitation

The total protein content was determined using the BCA protein assay kit (ThermoScientific). Bovine Serum Albumin (BSA) protein standards of known concentration were prepared and loaded onto a 96-well plate in triplicate alongside a 2-fold series dilution of fraction 3 of sucrose density ultracentrifugation purified VLP sample. The plate was treated as per manufacturer's instructions and read at 562 nm using an absorbance-based microplate reader. The concentration was determined using on the standard curve.

4.2.2.3.2. Spike Protein Quantitation

The partially purified mIBV-S2P-NDV-F^{TM/CT} VLPs were quantified using densitometry analysis on an SDS-PAGE gel. BSA protein standards of known concentration were prepared and then loaded onto a prepared 12 % SDS-PAGE gel alongside molecular weight markers SeeBluePlus2 (ThermoFisher Scientific) and PageRulerPlus (ThermoFisher Scientific). A sample of the dialysed VLPs was loaded onto the gel, which was run at 150 V. The gel was then stained with Coomassie Brilliant Blue Stain and analysed using the quantification software on the ChemiDocTM MP Imaging System (Bio-Rad) with the standards and the molecular weight markers serving as references.

The three fractions of the mIBV-S2P-NDV-F^{TM/CT}: matrix plant-produced VLPs that displayed the most abundant spike protein (fractions 3 – 5), according to SDS-PAGE and Western blot results, were pooled. The combined sample was dialysed in 1 X PBS buffer using a 3500 mW CO Slide-A-Lyzer® Dialysis Cassette (ThermoFisher Scientific, Product no. 66330) following manufacturer's instructions after which 15 % (w/v) trehalose dehydrate (Sigma-Aldrich) was

added to stabilise. The stabilised and partially purified sample was kept at 4 °C until the start of the immunogenicity study.

4.2.2.4. Pilot Immunogenicity Study

The immunogenicity study in SPF chickens took place in the Biosafety Level 3 facility at the University of Pretoria's Veterinary Faculty. All study procedures were approved by the Research and Animal Ethics Committees of the University of Pretoria (REC106-20), the CSIR (251/2018) and the Department of Agriculture, Land Reform, and Rural Development (12/11/1/1/MG).

4.2.2.4.1. Animals

Twenty 6-week old SPF White Leghorn Chickens (*Gallus gallus*) were purchased from Avi-Farms (Pty) Ltd, Pretoria. They were individually numbered with wing tags, and placed into an isolation room with the floor covered in sawdust to absorb excess waste, and perches were provided. The birds were allowed to roam freely within the room and were checked on regularly. Water and feed (Nova Feeds, Pretoria, South Africa) were both provided *ad libitum*. The room had adequate ambient light, therefore the lights were kept off in order to keep the chickens in natural daylight during the day and darkness at night.

4.2.2.4.2. Feed

The birds were fed pullet starter mash (Meadow Feeds, Doringkloof Pretoria) *ad libitum*. The composition of the feed is as follows:

- Protein: 190.0 g/kg
- Moisture: 120.0 g/kg
- Fibre: 70.0 g/kg
- Fat: 25.0 g/kg
- Calcium: 8-12 g/kg
- Total lysine: 7.0 g/kg
- Phosphorus: 6.0 g/kg

4.2.2.4.3. Vaccine Preparation

Two vaccine doses were prepared for comparison, a dose containing 5 µg of plant-produced VLPs and a dose containing 20 µg of plant-produced VLPs. On the day of immunization, the partially purified mIBV-S2P-NDV-F^{TM/CT} :matrix VLPs were diluted with sterile 1X PBS buffer and then mixed thoroughly with 10 % (v/v) of Emulsigen®-P Adjuvant (MVP, Phibro Animal Health, USA) for a total dose volume of 250 µl. Emulsigen-P is a dual adjuvant, antigen-friendly oil-in-water emulsion, which contains PolygenTM, which is a copolymer immunostimulant that demonstrates stimulated T-cell responses, which include interleukin 12 and γ -interferon. It contains micron sized oil droplets that are evenly dispersed ensuring maximum stability of the emulsion, as well as reduced viscosity and increased surface area for the antigens which reduces the final oil quantity required in the vaccine. Because it can be mixed with the antigen at any temperature, only mild mixing is required which enhances product immunogenicity and improves the safety profile of the vaccine. Because it contains less oil than water-in-oil-water or water-in-mineral-oil adjuvants (such as the MontanideTM ISA adjuvant), it easily passes through a 25 gauge needle making it less likely to cause a reaction at the injection site than other adjuvants (Abolnik *et al.*, 2022). Antigen presentation is improved by Emulsigen-P's depot effect which enhances immune responses as well as the efficacy of the vaccine (<https://mvpadjuvants.com/technical-bulletins/>). Emulsigen-P demonstrated stimulation of optimal immune responses in chickens that were vaccinated with plant-produced influenza A virus (IAV) VLPs, showing no adverse vaccination effects, when compared to other adjuvants (Abolnik *et al.*, 2022).

4.2.2.4.4. Experimental Design

The SPF chickens were randomly divided into two treatment groups of 10 birds each. One ml blood samples were collected from the wing veins of each bird prior to immunisation were used for baseline comparison. The first treatment group was vaccinated intramuscularly with the 5 µg VLP dose, while the second treatment group was vaccinated intramuscularly with the 20 µg VLP dose. Two weeks post-vaccination, blood samples were drawn from the wing veins of all the chickens before humanely euthanizing them by cervical dislocation.

4.2.2.4.5. Serology and HI Testing

Collected blood samples were left to clot at room temperature for an hour prior to being centrifuged at 3000 x g for 10 minutes at 22 °C. The sera were transferred to sterile tubes and tested using two commercial IBV antibody detection kits, namely the IDEXX IBV Antibody test kit (IDEXX Laboratories Inc., United States) and the BioChek IBV Antibody test kit (BioChek UK Ltd) (UP Department of Veterinary Tropical Diseases) following manufacturer's directions.

For the IDEXX kit, the following applied:

$$\text{Sample to positive ratio (S/P)} = \frac{\text{Sample mean} - \text{NCx}}{\text{PCx} - \text{NCx}}$$

With NCx being the average of the negative controls (valid at ≤ 0.150), and PCx being the average of the positive controls. $\text{PCx} - \text{NCx} > 0.075$ is considered valid. $\text{S/P} \leq 0.20$ is considered negative and $\text{S/P} > 0.20$ (titre greater than 396) is considered positive.

For the BioChek kit, the formulae used were the same with the following titre ranges applicable:

An S/P ratio of ≤ 0.149 (titre ≤ 624) is considered negative, an S/P ratio of $0.150 - 0.199$ (titre 925 – 833) is considered suspect, and an S/P ratio of ≥ 0.2 (titre ≥ 834) is considered positive.

To prepare the antigen required for the haemagglutination inhibition (HI) tests, allantoic fluid from SPF chicken eggs containing $10^{6.5}$ EID₅₀/0.1 ml (Egg infectious dose) of the live QX-like IBV strain chicken/ZA/3665/11 was centrifuged at 3000 rpm at 4 °C for 15 minutes. Five ml of the clarified fluid was mixed with 1 ml of a 1 U/ml neuraminidase solution derived from *Clostridium perfringens* (Abnova™ P5290, Taiwan). One ml aliquots were incubated overnight at 4 °C (Ruano *et al.*, 2000). HA and HI tests were performed using 1 % (v/v) chicken red blood cells (CRBC) as per the WOAHP-recommended method (WOAHP, 2019). The procedure was performed at room temperature instead of at 4 °C. The log₂ HI titre was recorded as the last well in the 2-fold titration of test serum where streaming of the CRBC in the tilted plate was

observed, relative to that observed in the control wells. Because there was a limited amount of antigen available, the HI tests were only performed on the sera from two weeks post immunisation. PBS and SPF negative serum were used as negative controls in each test. HI tests were performed by C. Abolnik.

4.2.2.4.6. Statistical Analysis

The un-paired T-test was used to analyse the pairwise mean comparisons between the two treatment groups using the GraphPad Prism v 9.4.1 software for Windows (la Jolla, CA, USA). A P-value of ≤ 0.05 was considered significant.

4.3. Results

4.3.1. Cloning and Expression of Synthetic Gene Constructs

The synthetic gene constructs designed in Chapter 4 were successfully cloned into pEAQ-HT, successfully transformed into AGL-1 *Agrobacterium* and transiently co-expressed in *N. benthamiana* plants as in Table 4.3 with complementary structural or chaperone proteins. This was confirmed by colony PCR and Sanger sequencing. Table 4.3 shows the ratios of constructs to complementary protein/s. Glycerol stocks of sequence validated constructs were stored at -80 °C until required for infiltrations. Three biological repeats were performed for construct rIBV-S1-NDV-F^{TM/CT}, six biological repeats for construct mIBV-S2P-NDV-F^{TM/CT}, and construct mIBV-S2P-IAV-H6^{CTonly} was performed once, with different ratios, accessory proteins, and extraction buffers attempted.

Table 4.3. Gene construct co-infiltration ratios (Chapter 4)

Construct	Approximate mW (kDa)	Co-infiltrated with:	Ratio	
rIBV-S1-NDV-F ^{TM/CT}	63	NDV matrix	2:1	S:matrix
mIBV-S2P-NDV-F ^{TM/CT}	124	NDV matrix	2:1	S:matrix
			4:1	S:matrix
			alone	S alone
mIBV-S2P-NDV-F ^{CTonly}	125	NDV matrix	2:1	S:matrix
			4:1	S:matrix
			alone	S alone

4.3.2. Protein Detection and Confirmation of Construct rIBV-S1-NDV-F^{TM/CT}

Preliminary results showed that construct rIBV-S1-NDV-F^{TM/CT} was poorly expressed in the plants. There were SDS-PAGE bands that corresponded to the expected construct sizes, however, these bands were present in the negative control as well (pEAQ-HT vector backbone with no construct) suggesting that they may possibly be plant proteins or that the plant proteins are of a similar size to the constructs resulting in an overlap on the gel (Fig. 4.1 (a)). The S protein was not detected by immunoblot using QX-like IBV-specific antisera (Fig. 4.1 (b)). This suggested that the protein was either not expressed at all, or was expressed in a quantity

too low to be detected by immunoblotting. The antisera used for the immunoblot was not homologous with the IBV strain used to develop the constructs, so the level of cross-protection may have been too low for detection (Cavanagh, 2003). Transmission electron microscope (TEM) analysis showed very few particles of the correct size that did resemble native IBV particles (Fig. 4.2). The SDS-PAGE and immunoblot results suggest that the construct rIBV-S1-NDV-F^{TM/CT} did not express well although the TEM results suggest that there was assembly of particles resembling the size and morphology of IBV particles. This was the same regardless of which buffer it was extracted in (PBS or bicine buffer).

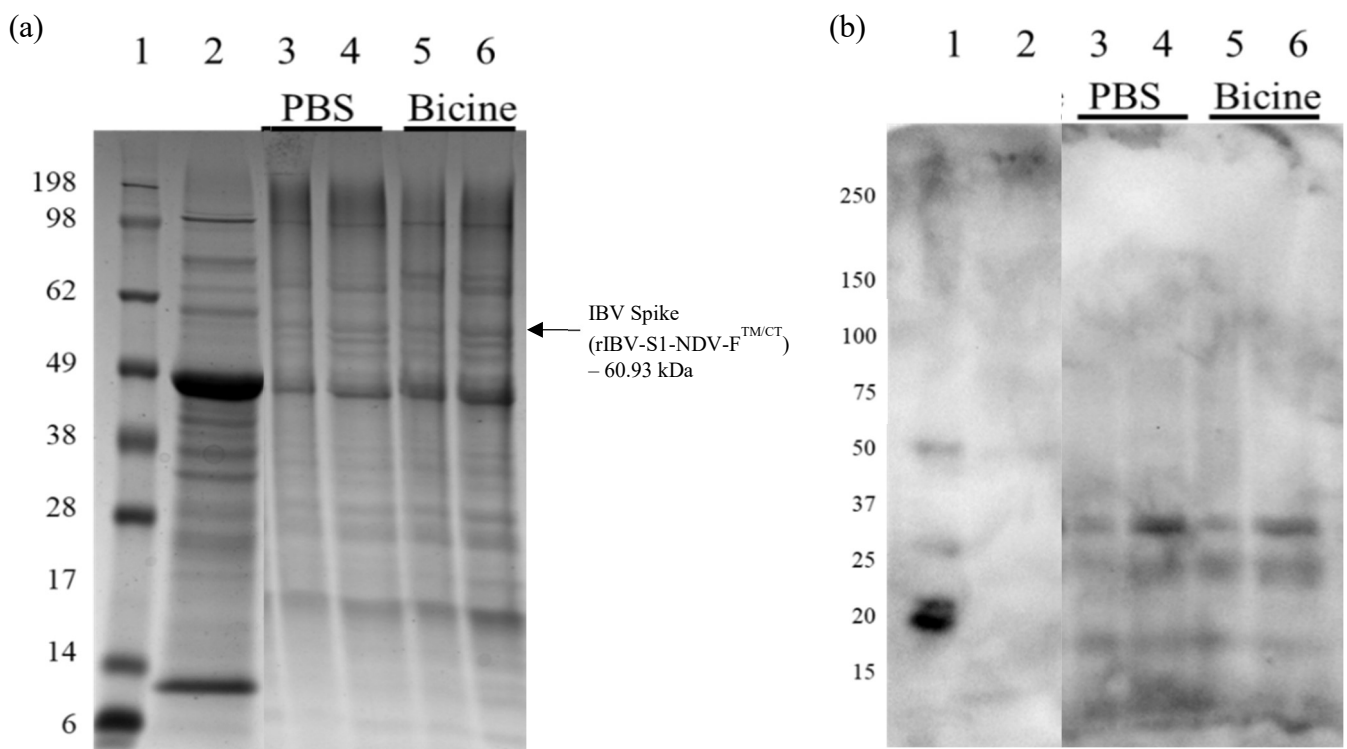


Figure 4.1. SDS-PAGE (a) and Western blot (b) of plant-produced rIBV-S1-NDV-F^{TM/CT} protein purified in PBS or bicine buffer. Lane 1: molecular weight marker; Lane 2: plant-expressed empty pEAQ-HT vector; Lanes 3 and 4: rIBV-S1-NDV-F^{TM/CT} :matrix Fractions 2 and 3; Lanes 5 and 6: rIBV-S1-NDV-F^{TM/CT} :matrix Fractions 2 and 3. (Edited from Fig. S2).

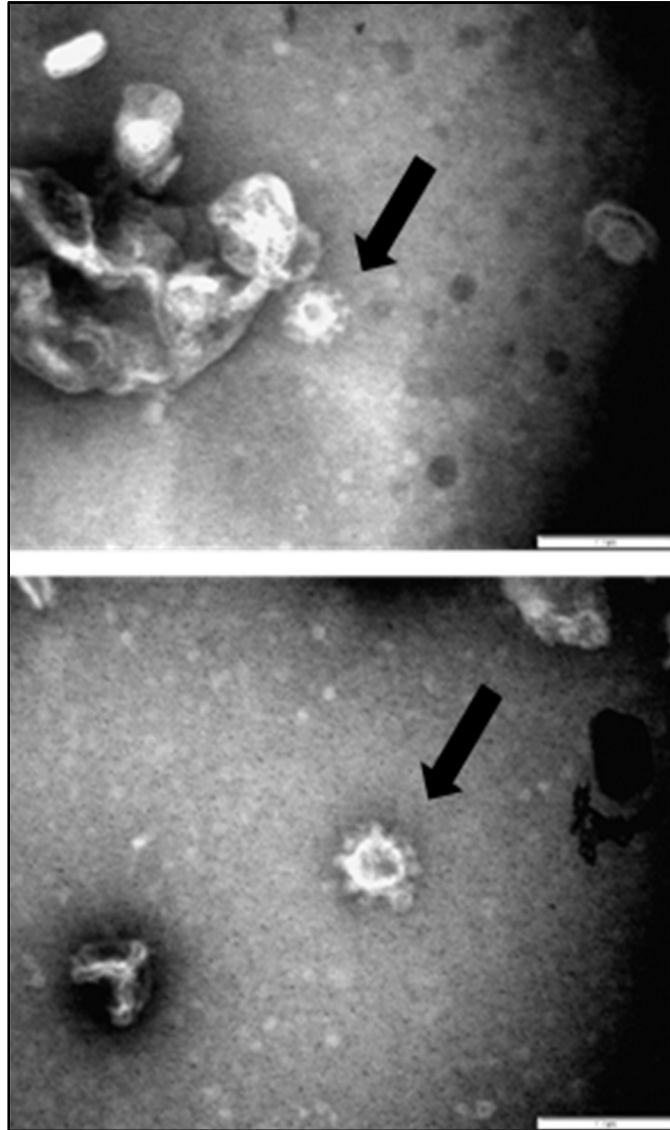


Figure 4.2. Negative-stained transmission electron microscopy images of plant-produced IBV virus-like particles expressed with the synthetic gene construct rIBV-S1-NDV-F^{TM/CT} in *N. benthamiana*. Arrows indicate VLPs.

TEM was the only analytical technique confirming protein expression and VLP assembly. The use of a more homologous antiserum may have allowed for better spike protein detection in the immunoblot.

4.3.3. Protein Detection and Confirmation of Construct mIBV-S2P-NDV-F^{TM/CT}

The construct mIBV-S2P-NDV-F^{TM/CT}, showed much higher levels of protein expression in the plants. There were bands on the SDS-PAGE gel correlating to the expected sizes of the constructs (Fig. 4.3 (a)). The bands were noticeably higher than the band around the same size in the negative control as was the band in the positive control. This suggests that this was not a plant protein and was likely to be the S protein. Liquid chromatography mass spectrometry (LC-MS/MS) based peptide sequencing further confirmed it to be the IBV S protein (Fig. 4.4) with 37 peptides being detected at 33.7 % coverage. The IBV antisera was able to detect strong S protein specific bands in the Western blot (Fig. 4.3 (b)) compared to the rIBV-S1-NDV-F^{TM/CT} construct where no S protein specific bands could be detected at all. This suggests that this construct was able to more successfully assemble VLPs in the plants than the rIBV-S1-NDV-F^{TM/CT} construct. The S protein specific bands for this construct were stronger than the ones detected for the mIBV-S2P-IAV-H6^{TM/CT} construct expressed in Chapter 3 and even stronger than the ones detected for the mIBV-S2P construct expressed in Chapter 2. The S protein was not detected in the QX-like positive control. The purified virus most likely had a low S protein quantity and because it was derived from a flock that was immunized with Mass-type IBV vaccines, was not homologous with the constructs. There was no obvious difference between the proteins purified using PBS buffer and the proteins purified using bicine buffer although the results were similar when repeated. However, PBS was chosen because it is the most commonly used buffer in biological research (Perchetti *et al.*, 2020). Visualisation under the TEM showed VLPs in the plant extracts that were infiltrated with the mIBV-S2P-NDV-F^{TM/CT} construct (Fig. 4.5). These VLPs closely resembled native IBV particles, and ranged from 67 nm to 147 nm in diameter, an average of 94 nm, with most of the particles falling between 90 nm and 105 nm in diameter. The spikes surrounding them ranged from 12 nm to 25 nm in length, typical of IBV particles (Jackwood and de Wit, 2013).

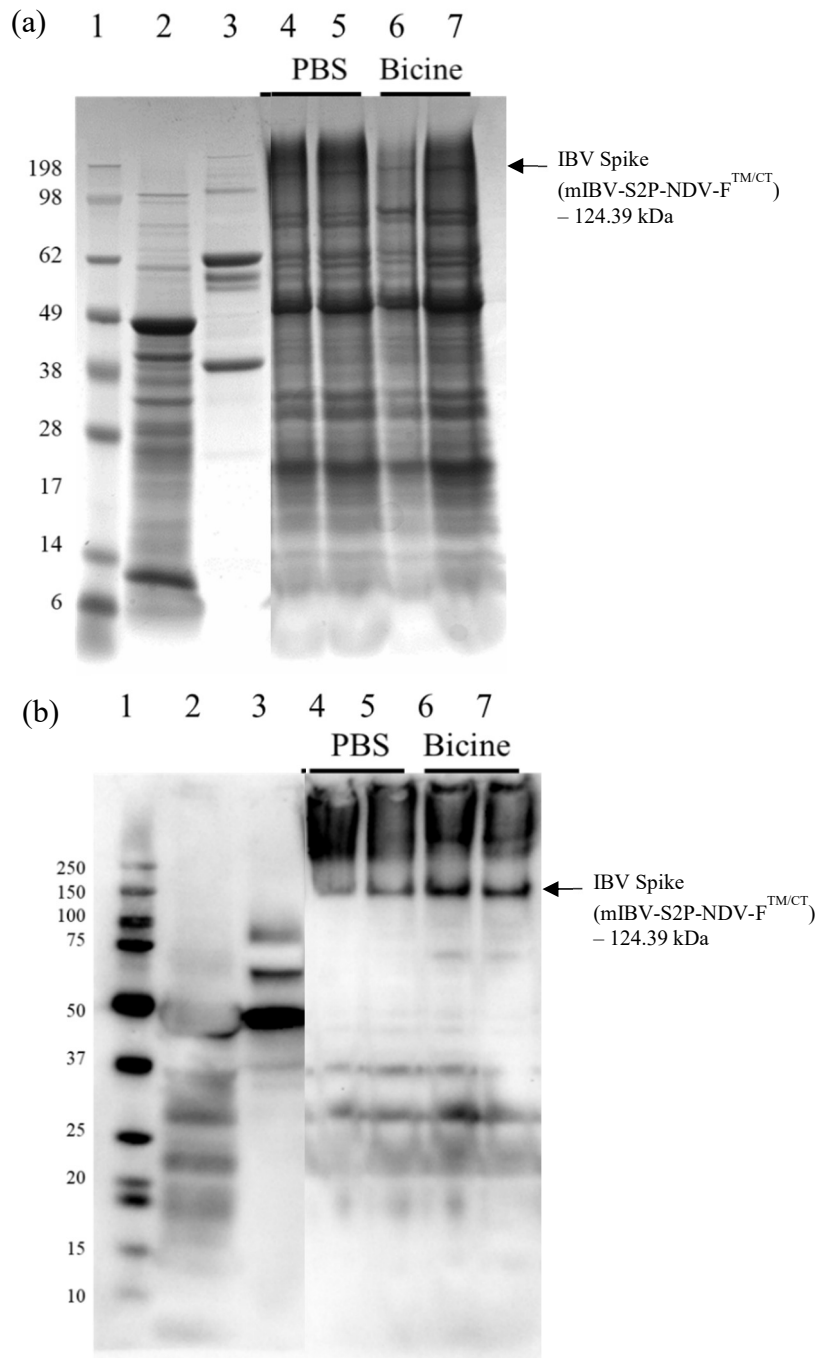


Figure 4.3. SDS-PAGE (a) and Western blot (b) of plant-produced IBV S protein (mIBV-S2P-NDV-F^{TM/CT}) purified in PBS or bicine buffer. Lane 1: molecular weight marker; Lane 2: plant-expressed empty pEAQ-HT vector; Lane 3: purified live QX-like IBV strain ck/ZA/3665/11; Lanes 4 and 5: mIBV-S2P-NDV-F^{TM/CT}:NDV matrix Fractions 2 and 3; Lanes 6 and 7: mIBV-S2P-NDV-F^{TM/CT}:NDV matrix Fractions 2 and 3. (Edited from Fig. S1).

mIBV-S2P-NDV-F^{TM/CT} : NDV matrix (2:1)

33.7% coverage at 95% confidence with 37 unique peptides

MGWSWIFLFLLSGAAGVHCNLFSDNNYVYYYQSAFRPPNGWHLQGGAYAVVNSTNHTSNAGSA
 QGCTVGVIKDVYNQSVASIAMTAPLQGMWFCTAYCNFSDTTVFVTHCYHIRISAMKNGSLFYNLT
VSVSKYPNFKSFQCVNNFTSVYLNGLDLVFTSNK**TTDVTSAGVYFKAGGPNYSIMKEFKVLAYFV**
NGTAQDVILCDNSPKGLLACQYNTGNFSDGFYPFTNSTLVREKFIVYRESSFNTTLALNTFTNVS
 NAQPNSGGVNTFHLYQTQTAQSGYYNFNLSFLSQFVYKASDFMYGSYHPSCSFRPETINSGLWFNSL
 SVSLTYGPLQGGCKQSVFSGK**ATCCYAYSYKGP**MACKGVYSGELRTNFECGLLVYVTKSDGSRIQ
 TRTEPLVLTQYNNITL**DKCVAYNIYGR**VGGFITNVTDSAANFSYLADGGLAILDTSGAIDVVFV
 VQGIYGLNYYKVN**PCEDVNQQFVVS**GGNIVGILTSRNETGSEQVENQFYVKLTNSSGGGGGSIGQ
 NVTSCPYYVSYGR**FCIEPDGSLKMIVPEELK**QFVAPLLNITESVLIPNSFNLTVTDEYIQTRMDK**VQIN**
CLQYVCGNSLECRKLFQQYGPVCDNLSVNSVSQKEDMELLSFYSSTKPKGYDTPVLSNVSTG
 EFNISLLKTPISSGRSFIEDLLFTSVETVGLPTDAEYKKCTAGPLGTLKDLICAREYNGLLVLPPII
 TADMQTMYTASLVGAMAFGGITSAAPFATQIQARINHLGITQSLLMKNQEKIAASFNKAIGHMQ
EGFRSTSLALQQIQDVVNKQSAILTETMNSLNKNFGAITSVIQDIYAQLDPPQADAQVDRLITGR
LSSLSVLASAKQSEYIRVSQQRELATKKINECVKSQSNRYGFCGSGRHVLSIPQNAPNGIVFIHFTYT
 PESFVNVTAVGFCVNPANASQYAIVPANGRGVFIOVNGSYYITARDMYMPRDITAGDIVTLTSCQAN
 YVNVNK**TVINTFVEDDDFNFNDEL**SKWWNDTKHELPDFDEFNYTVPVLNISNEIDRIQEVIQGLN
DSLIDLETLSILKTYIKLITYIVLTIISLVFGILSLILACYLMYKQKAQQK**TLLWLGNNTLDQMRATT**
KM

Figure 4.4. Protein confirmation using LC-MS/MS-based peptide sequencing of the modified IBV spike protein construct, mIBV-S2P-NDV-F^{TM/CT}. The percentage sequence coverage is indicated above with several unique peptides identified with > 90 % confidence. Peptides with > 95 % confidence are highlighted in **bold** text, those with 50 - 95 % confidence in *italics*, and those with < 50 % confidence are underlined. No peptides were identified for the non-highlighted regions of the sequence (grey).

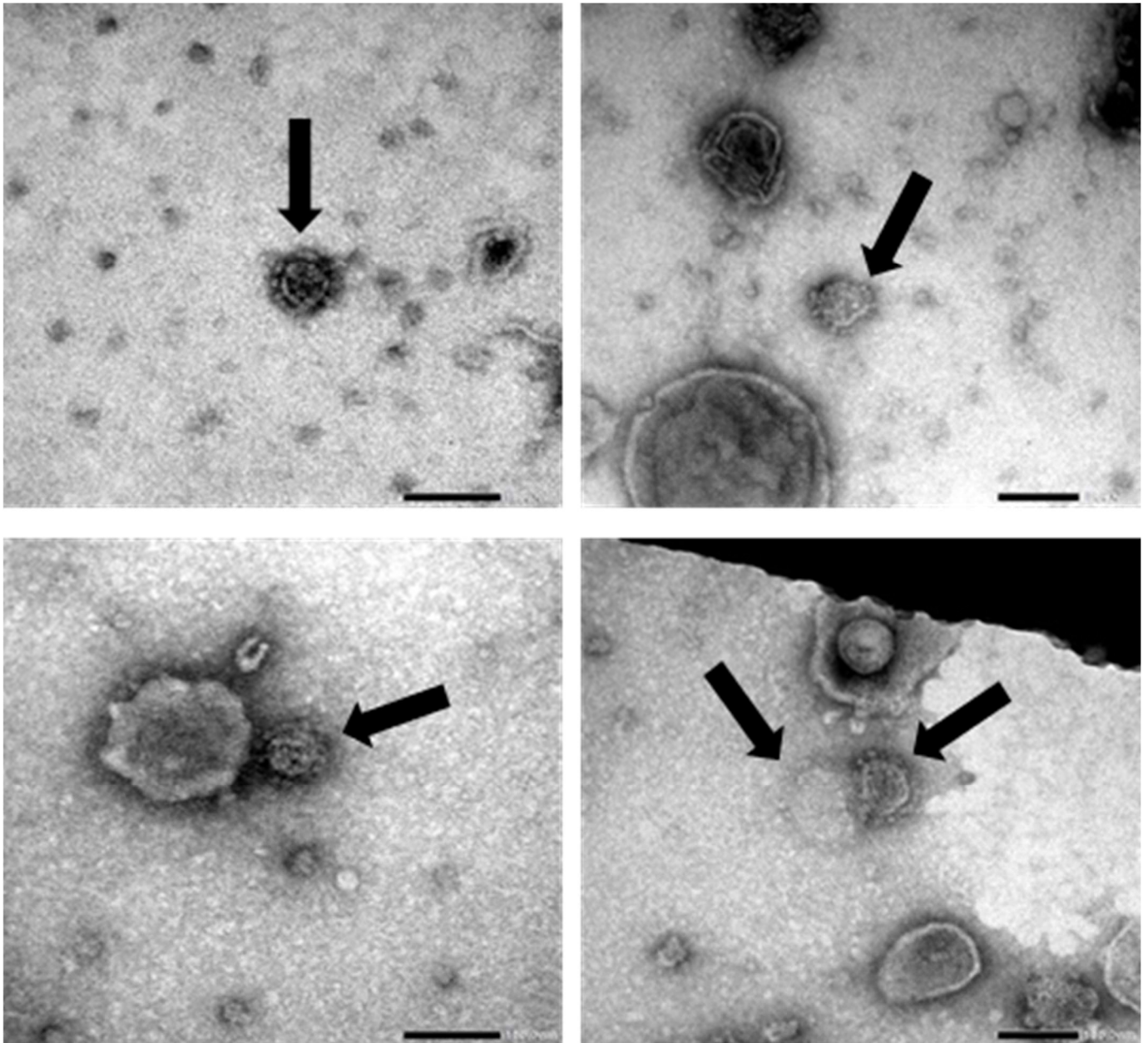


Figure 4.5. Negative-stained transmission electron microscopy images of plant-produced IBV virus-like particles expressed with the synthetic gene construct mIBV-S2P-NDV-F^{TM/CT} in *N. benthamiana*. Arrows indicate VLPs.

4.3.4. Protein Detection and Confirmation of Construct mIBV-S2P-NDV-F^{CTonly}

An additional construct also derived from the mIBV-S2P construct was designed to create more abundant VLPs. This construct had only the cytosolic tail (CT) of the IBV S protein substituted with that of the NDV F protein designated mIBV-S2P-NDV-F^{CTonly}.

For the mIBV-S2P-NDV-F^{CTonly} construct, there were bands on the SDS-PAGE gel which correlated to the expected sizes of the construct (Fig. 4.6 (a)). These bands were again, noticeably higher than the band around the same size in the negative control as was the band in the positive control, suggesting that this was the S protein and not a plant protein. The SDS-PAGE gel again suggested that the highest protein content lay within fractions 3 – 6. The Western blot detected the strongest level of S protein specific bands at fractions 3 – 5 (Fig. 4.6 (b)). The strongest detection was in the construct infiltrated without the NDV matrix protein, and the construct co-infiltrated at a 4:1 ratio with the NDV matrix protein had stronger S protein specific bands detected than the construct co-infiltrated at a 2:1 ratio. This again shows that a higher construct to complementary protein ratio leads to higher protein expression in plants although in this case, elimination of the complementary protein led to the highest protein expression. The S protein was not detected in the QX-like positive control. Fraction 5 for each ratio was excised from the SDS-PAGE gel and analysed by liquid chromatography mass spectrometry (LC-MS/MS) based peptide sequencing, which further confirmed them to be the IBV S protein (Fig. 4.7). The number of peptides detected for the mIBV-S2P-NDV-F^{CTonly}:matrix plant-produced VLPs at a 4:1 ratio were higher with more coverage than the ones produced by the same VLPs produced at a 2:1 ratio. The highest number of peptides detected with the most coverage were obtained when the construct was infiltrated on its own without the matrix protein. This suggests that the NDV matrix protein may not be necessary for the expression of the S protein. However, visualisation under a TEM, showed a higher abundance of VLPs when the construct was co-infiltrated with the matrix protein than when it was infiltrated alone (Fig. 4.8). This suggests that although not necessary for protein expression, the NDV matrix protein may assist in the assembly of VLPs. It is possible that a high quantity of the NDV matrix lowers protein expression, which was apparent in the high level of necrotic leaves seen in the days post-infiltration with the constructs co-infiltrated with the NDV matrix. The lower the NDV matrix content, the fewer necrotic leaves seen, but eliminating the NDV matrix entirely, decreased the level of VLP assembly seen. The number of peptides detected for this construct were higher than the ones detected for the mIBV-S2P-NDV-F^{TM/CT} construct developed previously, with more coverage. This shows that substituting just the cytosolic tail

of the IBV S protein with that of the NDV F protein leads to improved protein expression and VLP assembly than substituting both the transmembrane domain and the cytosolic tail. The TEM results showed abundant VLPs in fraction 3 (Fig. 4.8) although it is possible that more VLPs could have been present in the later fractions as seen for the mIBV-S2P-IAV-H6^{CTonly} construct in Chapter 3. A similar abundance of VLPs were seen for the construct co-infiltrated at a ratio of 4:1 as for the same construct co-infiltrated at a ratio of 2:1. Almost no convincing VLPs were seen for the construct infiltrated on its own. This suggests that the NDV matrix protein is necessary for VLP assembly.

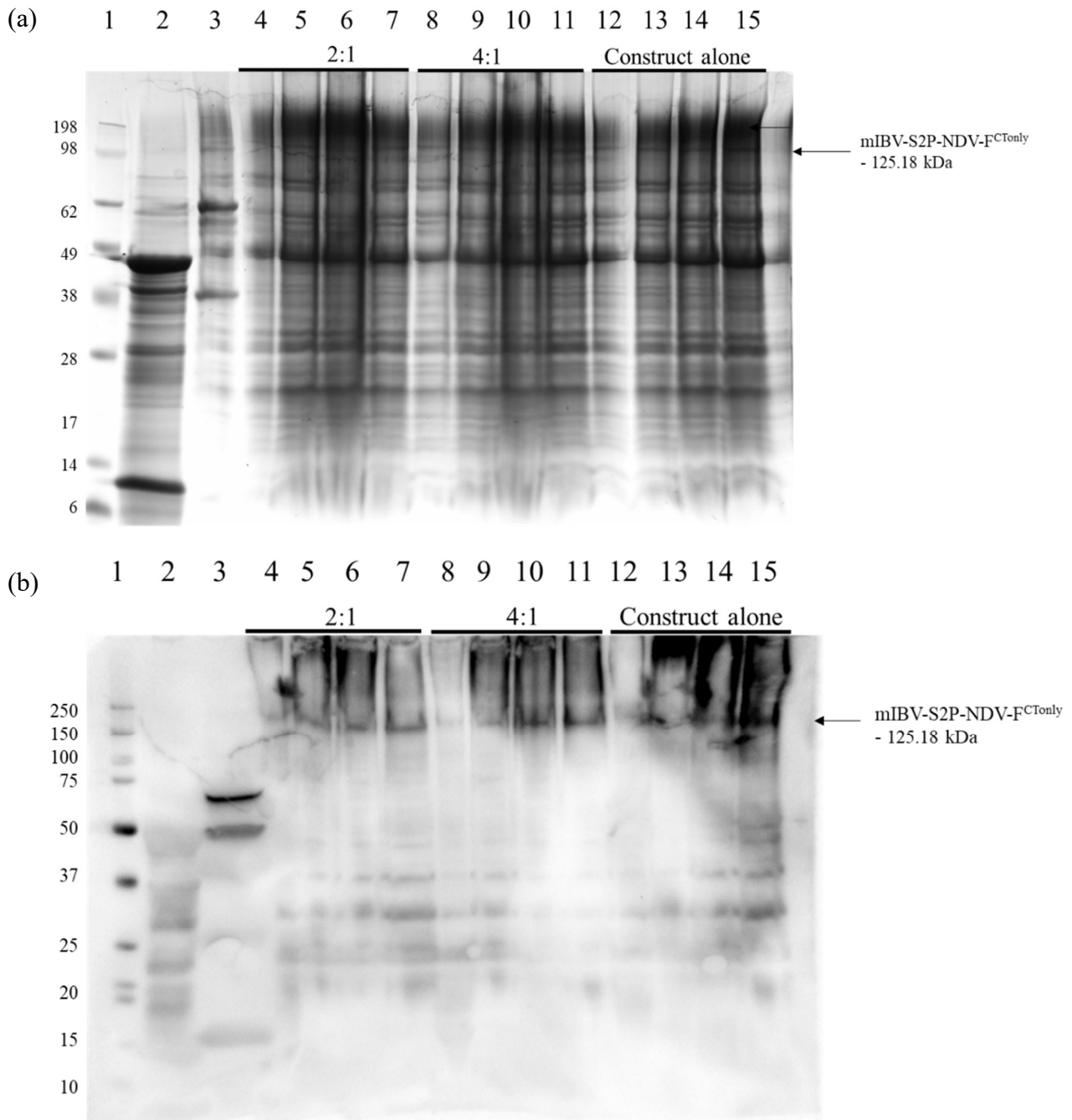


Figure 4.6. SDS-PAGE (a) and Western blot (b) of plant-produced mIBV-S2P-NDV-F^{CTonly} protein co-infiltrated at different ratios with the NDV matrix protein. Lane 1: molecular weight marker; Lane 2: plant-expressed empty pEAQ-HT vector; Lane 3: purified live QX-like IBV strain ck/ZA/3665/11; Lanes 4 - 7: mIBV-S2P-NDV-F^{CTonly}:matrix Fractions 2 - 5; Lanes 8 - 11: mIBV-S2P-NDV-F^{CTonly}:matrix Fractions 2 – 5; Lane 12 – 15: mIBV-S2P-NDV-F^{CTonly} alone Fractions 2 – 5.

mIBV-S2P-NDV-F^{CTonly} : Matrix (2:1)

23.3 % coverage (95 % confidence) and 22 unique peptides

MGWSWIFLFLLSGAAGVHCNLFSDNNYVYYYQSAFRPPNGWHLQGGAYAVVNSTNHTSNAGSA
 QGCTVGVIKDVYNQSVASIAMTAPLQGMWFCTAYCNFSDTTVFVTHCYHIRISAMKNGSLFYNLT
VSVSKYPNFKSFQCVNNFTSVYLNGLDLVFTSNKTTDVTSAAGVYFKAGGPVNYSIMKEFKVLAYFV
NGTAQDVILCDNSPKGLLACQYNTGNFSDGFYPFTNSTLVREKFIVYRESSFNTTLALTNFTFTNVS
 NAQPNSGGVNTFHLYQTQTAQSGYYNFNLSFLSQFVYKASDFMYGSYHPSCSFRPETINSGLWFNSL
 SVSLTYGPLQGGCKQSVFSGKATCCYAYSYKGPMAACKGVYSGELRTNFECGLLVYVTKSDGSRI
 QTRTEPLVLTQYNYNITLDKCVAYNIYGRVGQGFITNVTDSAANFSYLADGGLAILDTSGAIDVVF
 VQGIYGLNYYKVNPCEDVNQQFVVS^{GGNIVGILTSR}NETGSEQVENQFYVCLTNSSGGGGGSIGQ
 NVTSCPYVSYGRFCIEPDGSLKMIVPEELKQFVAPLLNITESVLIPNSFNLTVTDEYIQTRMDKVQIN
 CLQYVCGNSLECRKLFQQYGPVCDNILSVVNSVSQKEDMELLSFYSSTKPKGYDTPVLSNVSTG
 EFNISLLLKTPISSSGRSFIEDLLFTSVETVGLPTDAEYKKCTAGPLGTLKDLICAREYNGLLVLPPII
 TADMQTMYTASLVGAMAFGGITSAAPFATQIQARINHLGITQSLLMKNQEKIAASFNKAIGHMQ
 EGFRSTSLALQQIQDVVNKQSAILTETMNSLNKNFGAITSVIQDIYAQLDPPQADAQVDRITGR
LSSLSVLASAKQSEYIRVSQQRELATKKINECVKSQSNRYGFCGSGRHVLSIPQNAPNGIVFIHFTYTP
 ESFVNVTAVGFCVNPANASQYAIVPANGRGVFIQVNGSYYITARDMYMPRDITAGDIVTLTSCQAN
 YVNVNKTVINTFVEDDDDFNFNDELSKWWNDTKHELPDFDEFNYTVPVLNISNEIDRIQEVIOGLN
 DSLIDLETLSILKTYIKWPWYVWLAIFFAIIIFILILGWVFFCYLMYKQKAQQKTLLWLGNNTLDQMR
 ATTKM

mIBV-S2P-NDV-F^{CTonly} : Matrix (4:1)

26.4 % coverage (95 % confidence) and 31 unique peptides

MGWSWIFLFLLSGAAGVHCNLFSDNNYVYYYQSAFRPPNGWHLQGGAYAVVNSTNHTSNAGSA
 QGCTVGVIKDVYNQSVASIAMTAPLQGMWFCTAYCNFSDTTVFVTHCYHIRISAMKNGSLFYNLT
VSVSKYPNFKSFQCVNNFTSVYLNGLDLVFTSNKTTDVTSAAGVYFKAGGPVNYSIMKEFKVLAYFV
NGTAQDVILCDNSPKGLLACQYNTGNFSDGFYPFTNSTLVREKFIVYRESSFNTTLALTNFTFTNVS
 NAQPNSGGVNTFHLYQTQTAQSGYYNFNLSFLSQFVYKASDFMYGSYHPSCSFRPETINSGLWFNS
 LSVSLTYGPLQGGCKQSVFSGKATCCYAYSYKGPMAACKGVYSGELRTNFECGLLVYVTKSDGSRI
 QTRTEPLVLTQYNYNITLDKCVAYNIYGRVGQGFITNVTDSAANFSYLADGGLAILDTSGAIDVVF
 VVQGIYGLNYYKVNPCEDVNQQFVVS^{GGNIVGILTSR}NETGSEQVENQFYVCLTNSSGGGGGSIGQ
 NVTSCPYVSYGRFCIEPDGSLKMIVPEELKQFVAPLLNITESVLIPNSFNLTVTDEYIQTRMDKVQIN
 CLQYVCGNSLECRKLFQQYGPVCDNILSVVNSVSQKEDMELLSFYSSTKPKGYDTPVLSNVSTG
 EFNISLLLKTPISSSGRSFIEDLLFTSVETVGLPTDAEYKKCTAGPLGTLKDLICAREYNGLLVLPPII
 TADMQTMYTASLVGAMAFGGITSAAPFATQIQARINHLGITQSLLMKNQEKIAASFNKAIGHMQ
EGFRSTSLALQQIQDVVNKQSAILTETMNSLNKNFGAITSVIQDIYAQLDPPQADAQVDRITGR
LSSLSVLASAKQSEYIRVSQQRELATKKINECVKSQSNRYGFCGSGRHVLSIPQNAPNGIVFIHFTYTP
 PESFVNVTAVGFCVNPANASQYAIVPANGRGVFIQVNGSYYITARDMYMPRDITAGDIVTLTSCQA
 NYVNVNKTVINTFVEDDDDFNFNDELSKWWNDTKHELPDFDEFNYTVPVLNISNEIDRIQEVIOGLN
 NDSLIDLETLSILKTYIKWPWYVWLAIFFAIIIFILILGWVFFCYLMYKQKAQQKTLLWLGNNTLD
QMRATTKM

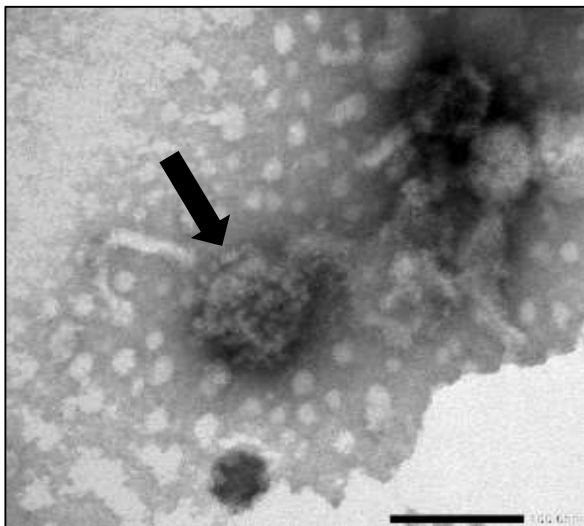
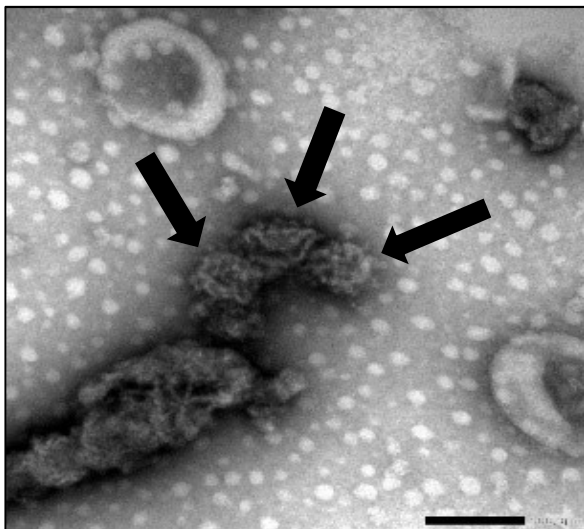
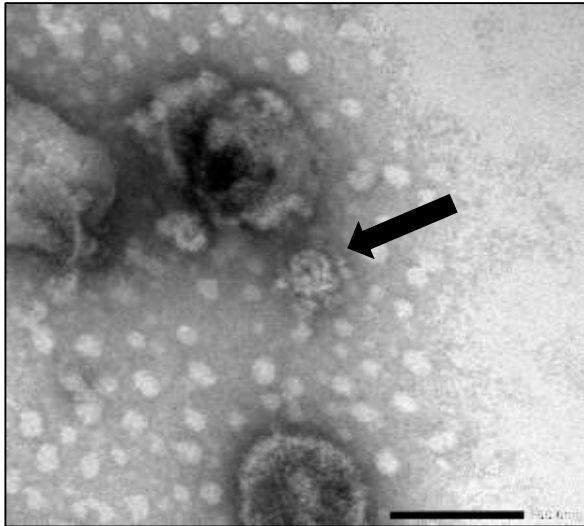
mIBV-S2P-NDV-F^{CTonly}

alone

34.8 % coverage (95 % confidence) and 33 unique peptides

MGWSWIFLFLLSGAAGVHCNLFSDNNYVYYYQSAFRPPNGWHLQGGAYAVVNSTNHTSNAGSA
 QGCTVGVIKDVYNQSVASIAMTAPLQGMWFCTAYCNFSDTTVFVTHCYHIRISAMKNGSLFYNLT
VSVSKYPNFKSFQCVNNFTSVYLNGLVFTSNKTTDVTSAGVYFKAGGPNYSIMKEFKVLAYF
VNGTAQDVLCDNSPKGLLACQYNTGNFSDGFYPTNSTLVREKFIVYRESSFNTTLALTNFTFTNV
 SNAQPNSGGVNTFHLYQTQTAQSGYYNFNLSFLSQFVYKASDFMYGSYHPSCSFRPETINSGLWFNS
 LSVSLTYGPLQGGCKQSVFSGKATCCYAYSYKGPMAACKGVYSGELRTNFECGLLVYVTKSDGSRI
 QTRTEPLVLTQYNYNNITLDKCVAYNIYGRVGQGFITNVTDSAANFSYLADGGLAILDTSGAIDVF
 VVQGIYGLNYKVNPCEDVNQQFVVSAGGNIVGILTSRNETGSEQVENQFYVKLNTSSGGGGGSIG
 QNVTSCPYPVSYGRFCIEPDGSLKMIVPEELKQFVAPLLNITESVLIPNSFNLTVTDEYIQTRMDKVQI
 NCLQYVCGNSLECRKLFQQYGPVCDNILSVVNSVSQKEDMELLSFYSSTKPKGYDTPVLSNVST
GEFNISLLLKTPISSGRSFIEDLLFTSVETVGLPTDAEYKKCTAGPLGTLKDLICAREYNGLLVLP
 IITADMQTMYTASLVGAMAFGGITSAAAIPFATQIQARINHLGITQSLLMKNQEKIAASFNK AIGHM
 QEGFRSTSLALQQIQDVVNKQSAILTETMNSLNKNFGAITSVIQDIYAQLDPPQADAQVDRITG
 RLSSLSVLASAKQSEYIRVSQQRELATK KINECVKSQSNRYGFCGSGRHVLSIPQNAPNGIVFIHFTY
 TPESFVNVTAVGFCVNPANASQYAIVPANGRGVFIQVNGSYYITARDMYMPRDITAGDIVTLTSCQ
ANYVNVNKTVINTFVEDDDFNFNDELSKWWNDTKHELPDFDEFNYTVPVLNISNEIDRIQEVIQ
GLNDSLIDLETLSILKTYIKWPWYVWLAIFFAIIIFILIGWVFFCYLMYKQKAQQKTLLWLGNNTL
DQMRATTKM

Figure 4.7. Protein confirmation using LC-MS/MS-based peptide sequencing of the modified IBV spike protein construct, mIBV-S2P-NDV-F^{CTonly} co-expressed at different ratios with the NDV matrix protein. The percentage sequence coverage is indicated above with several unique peptides identified with > 90 % confidence. Peptides with > 95 % confidence are highlighted in **bold** text, those with 50 - 95 % confidence in *italics*, and those with < 50 % confidence are underlined. No peptides were identified for the non-highlighted regions of the sequence (grey).

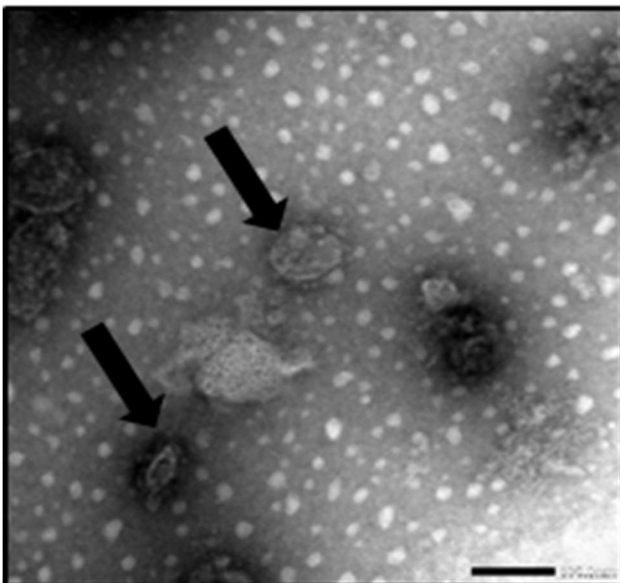
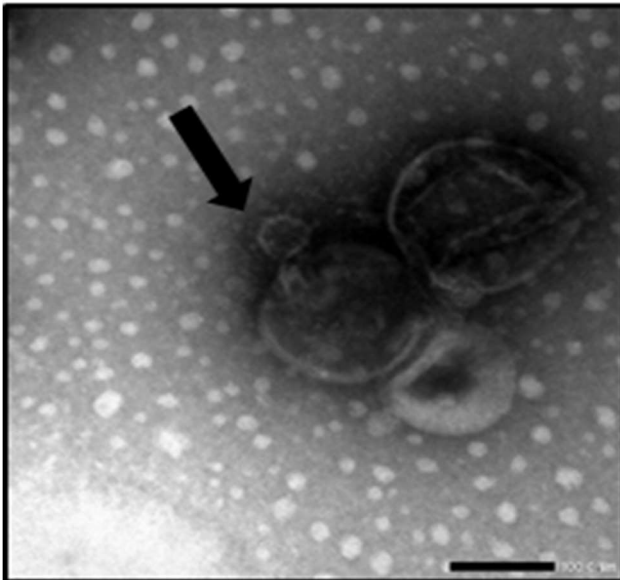
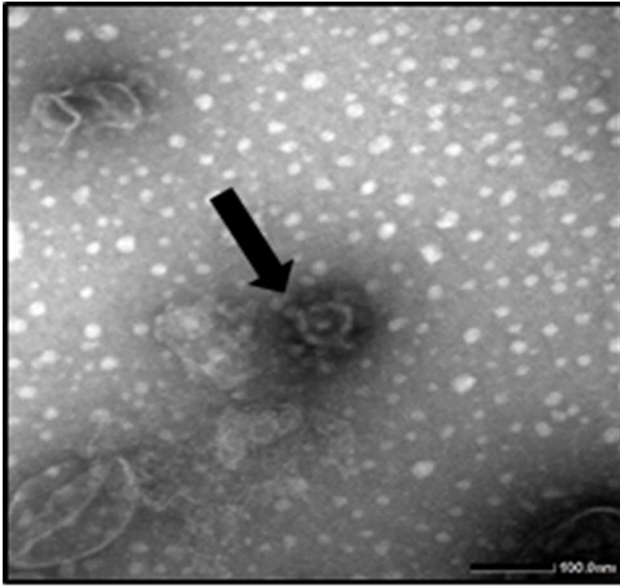


mIBV-S2P-NDV-F^{CTonly}

:matrix particles

(2:1 Ratio)

Fraction 3



mIBV-S2P-NDV-F^{CTonly}:matrix
particles

(4:1 Ratio)

Fraction 3

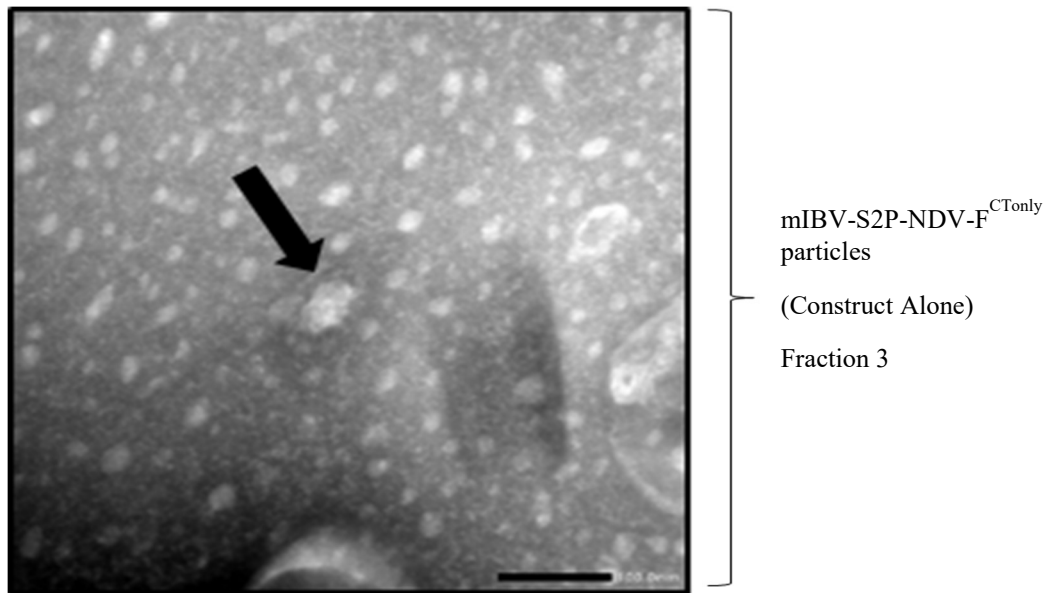


Figure 4.8. Negative-stained transmission electron microscopy images of plant-produced IBV virus-like particles expressed with the synthetic gene construct mIBV-S2P-NDV-F^{CTonly} in *N. benthamiana* in different ratios with NDV matrix. Arrows indicate VLPs.

4.3.5. Effect of Ratio on Protein Expression and VLP Assembly

The constructs were infiltrated at different ratios with their complementary proteins to assess whether or not that would have an effect on protein expression and VLP assembly. Therefore, ratios of 2:1 and 4:1 as well as the construct infiltrated on its own were tested for the constructs to determine if changing the ratio would aid in improving protein expression levels.

The results showed that increasing the ratio of construct to complementary protein increased protein expression and led to the assembly of VLPs in higher abundance. No difference could be seen in S protein expression on the SDS-PAGE gel (Fig. 4.9 (a)). For the mIBV-S2P-NDV-F^{TM/CT} construct, the immunoblot suggested that infiltrating the construct on its own may have led to an even higher level of protein expression (Fig 4.9 (b)), while TEM showed more abundant VLPs for the constructs infiltrated at a ratio of 4:1 with the NDV matrix protein (Fig. 4.10). This suggested that although not an essential requirement for protein expression and VLP assembly, co-infiltration with the NDV matrix protein did enhance the assembly of VLPs in the plants.

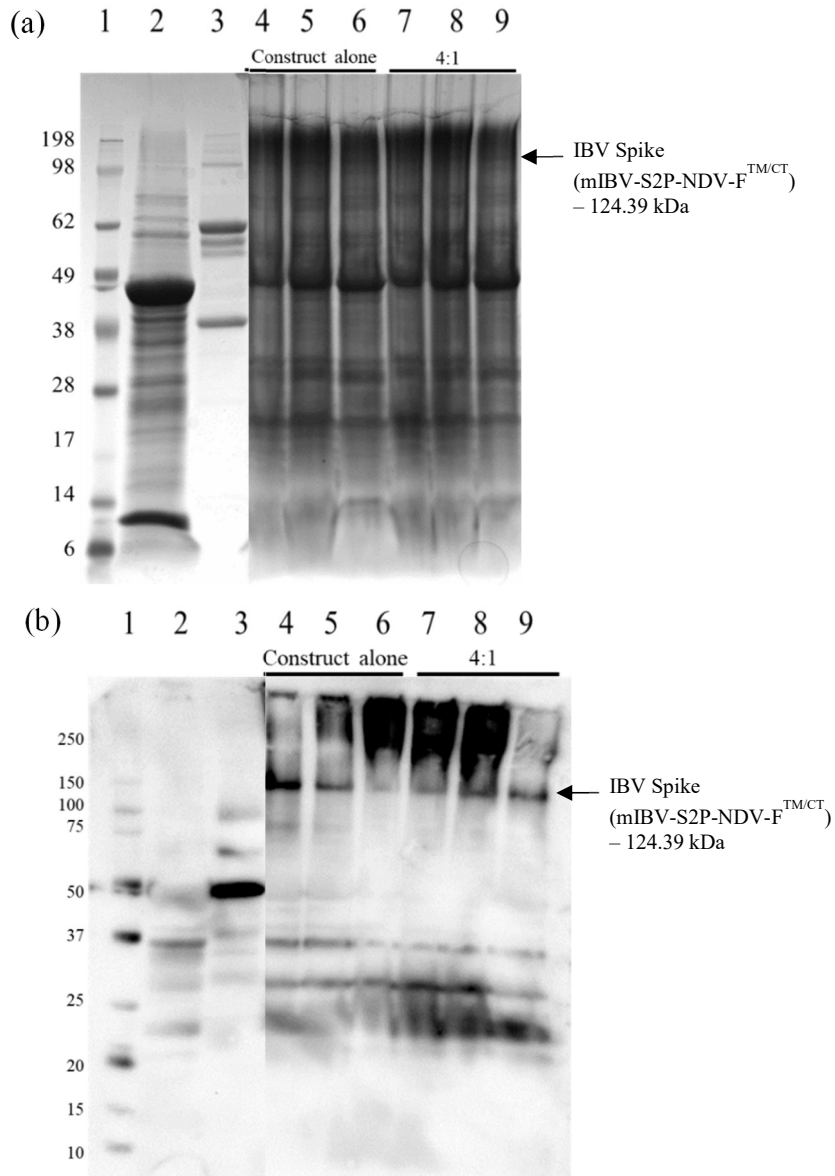
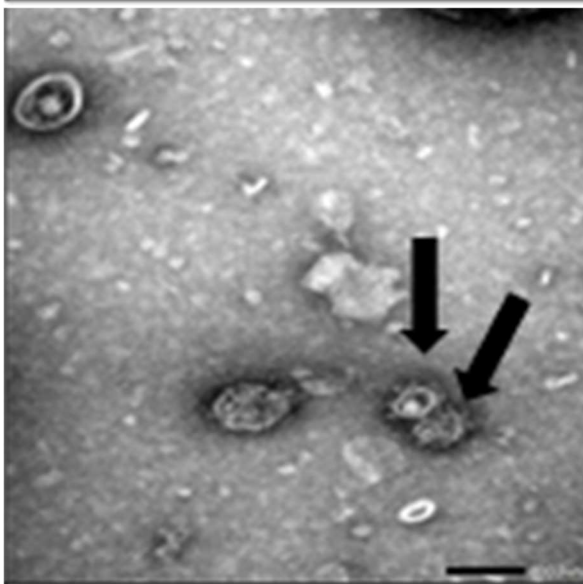
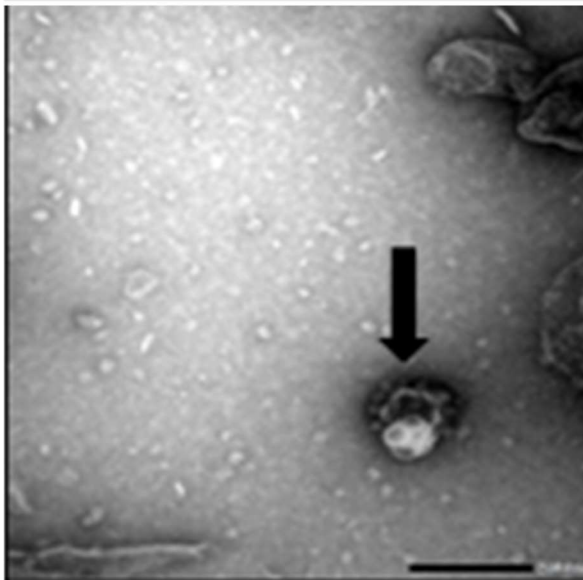
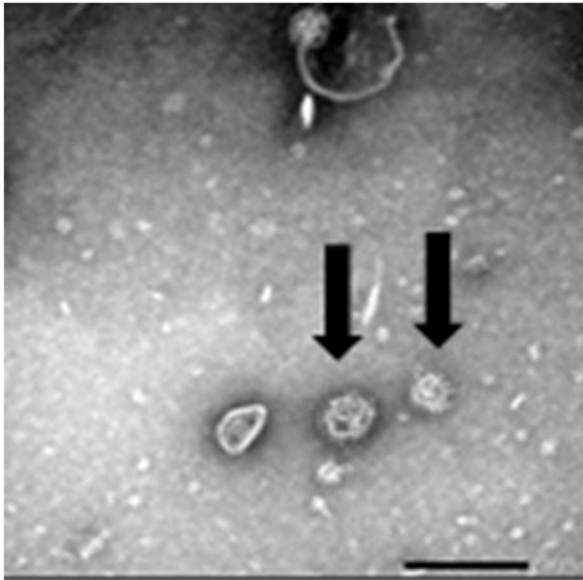


Figure 4.9. SDS-PAGE (a) and Western blot (b) of plant-produced IBV S protein (mIBV-S2P-NDV-F^{TM/CT}) co-infiltrated at different ratios with the NDV matrix protein. Lane 1: molecular weight marker; Lane 2: plant-expressed empty pEAQ-HT vector; Lane 3: purified live QX-like IBV strain ck/ZA/3665/11; Lanes 4 - 6: mIBV-S2P-NDV-F^{TM/CT} alone Fractions 2 - 4; Lanes 7 - 9: mIBV-S2P-NDV-F^{TM/CT}:matrix Fractions 2 - 4. (Edited from Fig. S3).



mIBV-S2P-NDV-FTM/CT
particles
(Construct only)

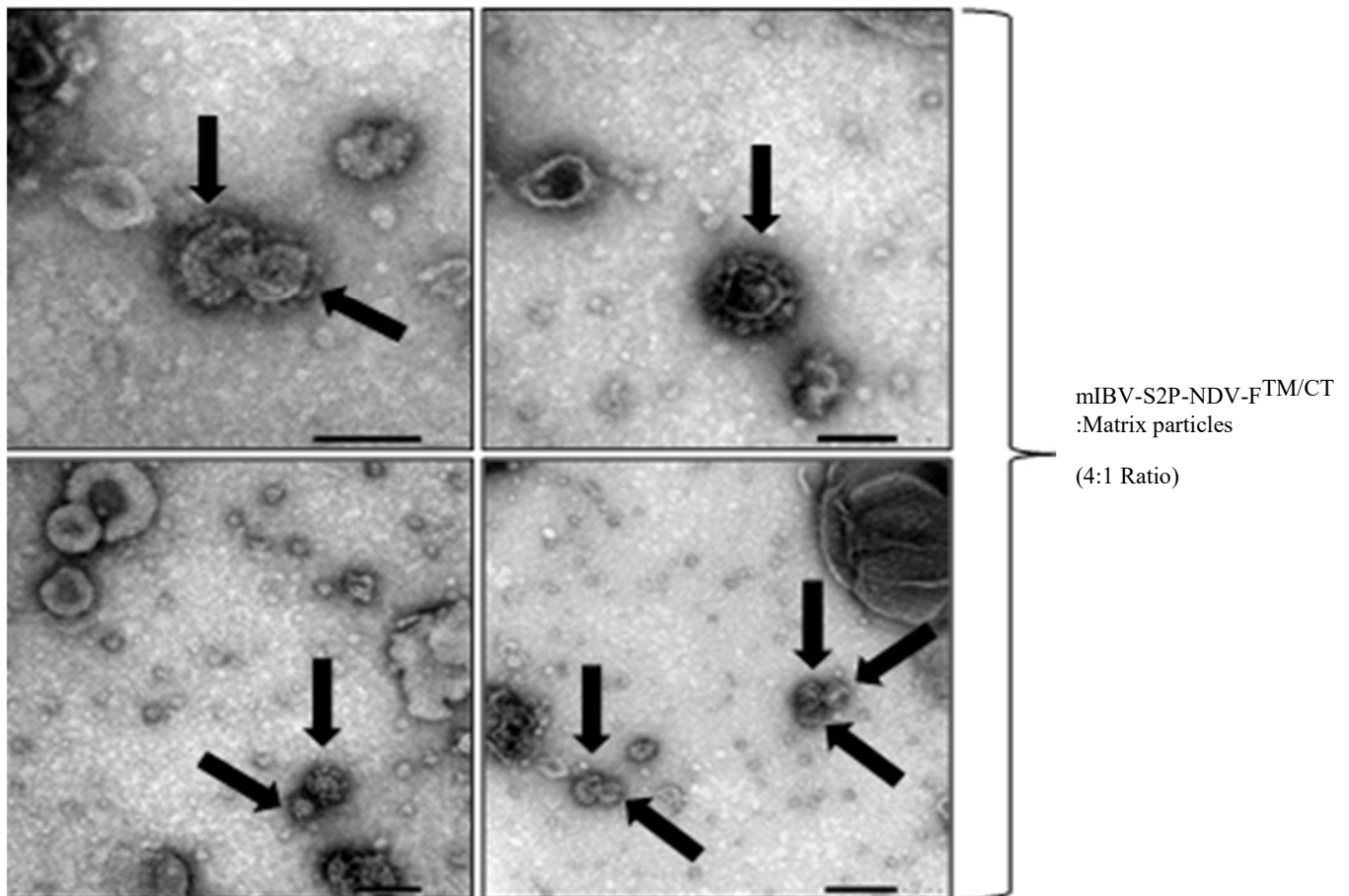


Figure 4.10. Negative-stained transmission electron microscopy images of plant-produced IBV virus-like particles expressed with the synthetic gene construct mIBV-S2P-NDV-F^{TM/CT} in *N. benthamiana* in different ratios with its complementary protein, NDV matrix. Arrows indicate VLPs.

4.3.6. Pilot Immunogenicity Study Results

4.3.6.1. Protein Detection and Confirmation of mIBV-S2P-NDV-F^{TM/CT}

The synthetic gene construct pEAQ-HT-mIBV-S2P-NDV-F^{TM/CT} in AGL-1 was successfully agro-infiltrated into *N. benthamiana* plants at a ratio of 4:1 with the pEAQ-HT-NDV matrix protein gene construct. The leaves were harvested with either PBS or Bicine buffer for comparison in order to confirm if a difference could be seen now that there was noticeably higher levels of protein expression at this stage compared to preliminary stages. SDS-PAGE, and immunoblotting confirmed the presence of the S protein band at 124 kDa corresponding to the size of the mIBV-S2P-NDV-F^{TM/CT} gene construct (Fig. 4.11 (a) and Fig. 4.11 (b)). There

was little difference between the samples harvested using PBS and with the samples harvested using bicine buffer. The bands were noticeably higher than the band around the same size in the negative control as was the band in the positive control. This suggests that this was not a plant protein and was likely to be the S protein. The S protein was not detected in the QX-like positive control. TEM confirmed the presence of several VLPs resembling native IBV particles for the samples harvested with PBS buffer and fewer VLPs for the samples harvested with bicine buffer.

The BCA protein assay kit determined the total protein content in the PBS-purified VLP sucrose fraction 3 to be 734 $\mu\text{g/ml}$. The sample (harvested in PBS buffer) was dialysed overnight in 1 X PBS buffer and stabilised with 15 % trehalose. Densitometry analysis determined the concentration of the S protein 124 kDa band to be approximately 101 $\text{ng}/\mu\text{l}$ (Fig. S4). The purified mIBV-S2P-NDV-F^{TM/CT}:matrix VLPs that were harvested in PBS buffer were used for the immunogenicity study.

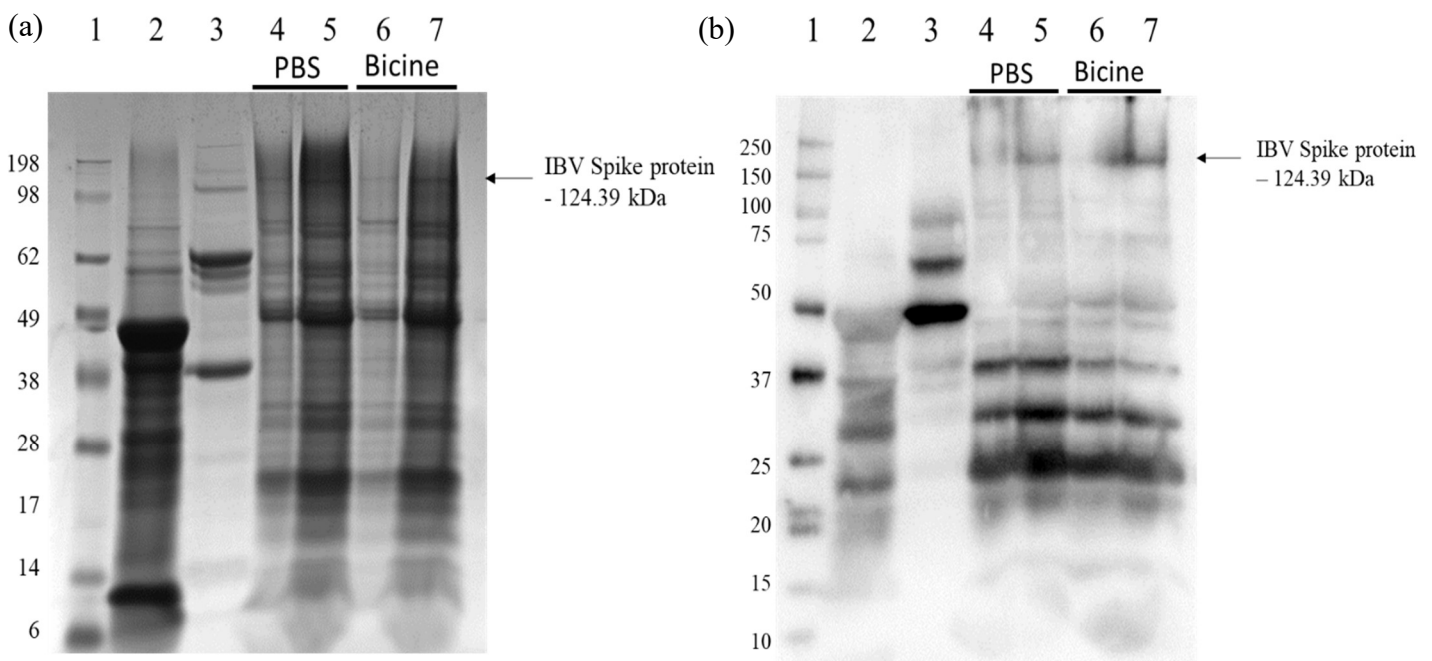


Figure 4.11. SDS-PAGE (a) and Western blot (b) of plant-produced mIBV-S2P-NDV-F^{TM/CT} protein co-infiltrated at a 4:1 ratio with the NDV matrix protein harvested in PBS and bicine buffers. Lane 1: molecular weight marker; Lane 2: plant-expressed empty pEAQ-HT vector; Lane 3: purified live QX-like IBV strain ck/ZA/3665/11; Lanes 4 and 5: mIBV-S2P-NDV-F^{TM/CT}:matrix Fractions 2 and 3; Lanes 6 and 7: mIBV-S2P-NDV-F^{TM/CT}:matrix Fractions 2 and 3.

4.3.6.2. HI Testing

All 20 of the serum samples taken prior to vaccinating the SPF chickens tested negative for the presence of IBV-specific antibodies with a commercial ELISA antibody test kit. This verified that the SPF chickens had not been exposed to IBV prior to the start of the trial. Fourteen days after immunisation, the ten chickens that had been immunised with 5 µg of the VLP preparation showed seroconversion with HI titres that ranged from 8 log₂ to 10 log₂ with a geometric mean titre (GMT) of 9.1 log₂ (Table 4.4). The ten chickens that had been immunised with 20 µg of the VLP preparation showed significantly higher ($P \leq 0.001$) HI titres ranging from 10 log₂ to 12 log₂ with a GMT of 10.5 log₂ (Fig. 4.12).

Table 4.4. Log₂ HI titres at 14 days post vaccination

Treatment Group	Bird no.	14d post vaccination Log ₂ HI titre
Group 1 - 5 µg IB VLP dose	10356	9
	10357	10
	10358	9
	10359	9
	10360	9
	10361	8
	10362	10
	10363	9
	10364	9
	10365	9
	GMT:	9,1
Group 2 - 20 µg IB VLP dose	10366	10
	10367	11
	10368	12
	10369	10
	10370	10
	10371	11
	10372	11
	10373	10
	10374	10
	10375	10
	GMT:	10,5

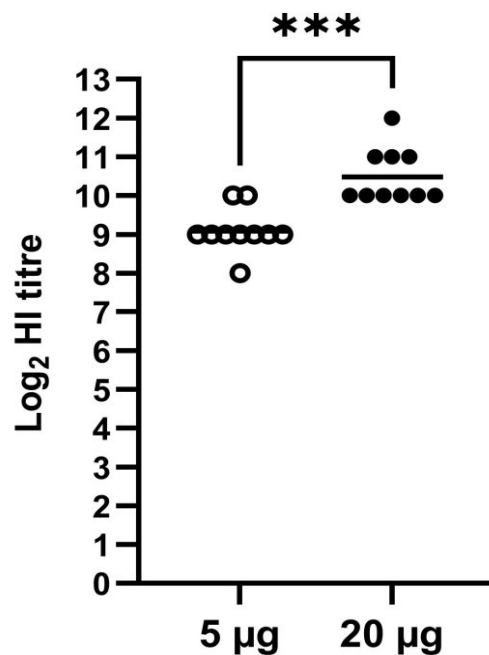


Figure 4.12. Haemagglutination inhibition (HI) titres for the chicken sera two weeks after a single immunisation with 5 µg and 20 µg doses of the mIBV-S2P-NDV-F^{TM/CT}:matrix VLPs. The bar shows the geometric mean titre (GMT), and the asterisks indicate the statistical significance *** ($P \leq 0.001$).

No adverse vaccine effects were seen at the injection site in any of the chickens throughout the trial. All 20 of the serum samples taken after 2 weeks tested negative using two commercial ELISA kits. This was unsurprising as the kits are optimised to detect the highly conserved IBV structural proteins that are common in all serotypes of IBV. This VLP preparation did not include the M, E, and N proteins as the modified mIBV-S2P-NDV-F^{TM/CT} protein was co-infiltrated with the NDV matrix protein to complement the TM domain and CT of the NDV F protein used.

4.4. Discussion

In this chapter, several variations of the IBV spike protein were made to investigate the factors that elevate protein expression and drive the assembly of VLPs. These modifications were centred on replacing the native IBV S protein TM and/or CT sequences, with corresponding TM and CT sequences of the Newcastle Disease Virus (NDV) Fusion protein.

The construct whereby the IBV S1 subunit was fused to the NDV F protein TM and CT sequences via a flexible linker (rIBV-S1-NDV-F^{TM/CT}) expressed poorly in the plants, and although TEM visualisation showed particles somewhat similar to IB virus particles, the SDS-PAGE and immunoblot results did not confirm IBV spike protein expression. Similar to the results found in Chapter 3, it is possible that S protein expression was too low to detect via immunoblotting or that the antiserum used was mismatched. Therefore, it was concluded that the construct rIBV-S1-NDV-F^{TM/CT} expressed poorly in the plants. By contrast, Wu and co-workers (2019a) created two fusion proteins by separately fusing the IBV S protein TM and CT sequences to either the IBV S1 subunit, or to the NDV F protein. Co-expressing both fusion proteins and the IBV M protein, a chimeric VLP vaccine was successfully produced using a baculovirus expression system that was able to fully protect against IBV or NDV challenge and induce efficient cellular and humoral immune responses in chickens (Wu *et al.*, 2019a). Again, this shows that it is possible to assemble VLPs expressing the IBV S1 subunit, but it may be more challenging in plant expression systems due to the low expression of viral glycoproteins *in planta* (Margolin *et al.*, 2018). Recombinant NDVs expressing either the IBV S1 subunit (fused to the TM and CT of the NDV F protein) (Zhao *et al.*, 2017) or the IBV S2 subunit (Toro *et al.*, 2014) were able to protect against IBV or NDV challenge and induce effective antibody responses against IBV. However, Shirvani and co-workers (2018) found that a recombinant NDV expressing the full-length S protein offered better protection than just one of the subunits. In fact, it was found that the recombinant NDV expressing only the S1 subunit of IBV resulted in retention of the protein in the cell, and it was speculated that correct folding of the S1 protein required the presence of the S2 subunit (Shirvani *et al.*, 2018). Perhaps the rIBV-S1-NDV-F^{TM/CT} construct was not able to fold correctly without the S2 subunit of IBV resulting in low protein expression.

The mIBV-S2P-NDV-F^{TM/CT} construct which was derived from mIBV-S2P (from Chapter 2), exhibited even higher levels of spike protein expression confirmed by SDS-PAGE and immunoblot, and resulted in the assembly of even more VLPs seen under TEM. These results

were further confirmed by LC-MS/MS analysis of the protein band of interest. Higher levels of protein expression were seen with this mIBV-S2P-NDV-F^{TM/CT} construct than with the mIBV-S2P-IAV-H6^{TM/CT} construct from Chapter 3 and even more so than the mIBV-S2P construct from Chapter 2. While the stabilising mutations (described by Pallesen *et al.*, 2017) were the driving force behind successful VLP formation, substitution of the TM and/or CT sequences with those of the NDV F protein also played a role in increasing the levels of protein expression and led to the most abundant IB VLPs (confirmed by TEM) produced thus far. The highest levels of S protein expression and plant-produced IB VLPs assembly were seen when the full-length IBV S protein was modified with the two stabilising proline mutations in the S2 subunit, as well as when the only native CT was substituted with that of the NDV F protein, and co-infiltrated with the NDV matrix protein (mIBV-S2P-NDV-F^{CTonly}:matrix). The second highest levels were seen with the S protein modified with the two stabilising proline mutations in the S2 subunit, as well as when the native TM and CT were substituted with the equivalent sequences of the NDV F protein, and co-infiltrated with the NDV matrix protein (mIBV-S2P-NDV-F^{TM/CT}:matrix). The latter was the most successful construct at the time of the pilot immunogenicity study, and as such was selected for use in the study.

While the mIBV-S2P-NDV-F^{TM/CT} construct was able to form IB VLPs without co-expressing with the NDV matrix protein, the number of VLPs seen under TEM were very few. VLP abundance was noticeably higher under TEM when the construct was co-infiltrated with the NDV matrix protein. The NDV matrix protein is known to have a crucial part in both the assembly as well as budding of viral particles from the cell membrane (Battisti *et al.*, 2012).

Similar to the findings presented in Chapter 3, co-infiltrating with a higher construct to complementary protein ratio (Jutras *et al.*, 2015) of 4:1 further improved protein expression compared to a ratio of 2:1. For the mIBV-S2P-NDV-F^{TM/CT} construct specifically, co-infiltrating with a higher level of the NDV matrix protein led to necrosis of the leaf tissue and a lower yield, while a lower level of the NDV matrix improved protein expression and VLP assembly while decreasing leaf necrosis. Harvesting the leaves with PBS buffer yielded higher S protein levels and more abundant VLPs than harvesting with Bicine or Tris buffers.

Subsequently, the mIBV-S2P construct was again modified to substitute only the native cytosolic tail with that of the NDV F protein. This was a hypothesised based on the elevated expression levels seen when modifying the TM and CT domains. The resultant construct (mIBV-S2P-NDV-F^{CTonly}) showed the highest levels of protein expression as well as the most

abundant VLPs under TEM than previously seen. Substituting just the CT of the IBV S protein with that of the NDV F protein leads to higher protein expression levels than substituting both the transmembrane domain and the cytosolic tail. It is possible that retaining the native transmembrane domain of the IBV S protein was allowed the particle to assemble into a more natural conformation while still getting the benefits (elevated protein expression levels) of the NDV F protein from its CT domain. Together with the stabilising mutations suggested by Pallesen and co-workers (2017), as well as replacing the native signal peptide with a murine signal peptide, it is possible to achieve high enough expression levels of the IBV spike protein in plants than seen previously (Sepotokele, 2020). Co-infiltrating with accessory proteins that complement the substituted TM and/or CT domains also improved protein expression, and increasing the ratio of construct to complementary protein leads to the highest level of protein expression and a higher abundance of VLPs formed. Table S1 shows the levels of expression for each analytical technique.

Higher levels of protein expression and VLP assembly were seen for the constructs that had their native TM and/or CT substituted with equivalent sequences of the NDV F protein than for those that had the IAV HA2 protein TM and/or CT sequences. The TM and CT sequences of the IAV HA2 protein were slightly shorter in length (36 amino acids) than those of the NDV F protein (53 amino acids). This resulted in the constructs containing the NDV F protein TM and/or CT sequences being closer to the molecular weight of the constructs with the native S protein, while the constructs containing the TM and/or CT of the IAV HA2 protein were noticeably smaller in size. Perhaps this allowed the constructs containing the NDV F protein to fold into a conformation more closely resembling the native IBV spike protein, but with the properties of the NDV F protein that allowed for elevated levels of protein expression and VLP assembly.

The IB VLPs produced with the mIBV-S2P-NDV-F^{TM/CT} construct co-infiltrated with the NDV matrix protein were formulated into a vaccine with the addition of the Emulsigen-P adjuvant. Emulsigen-P was chosen for its ability to stimulate peak immune responses without any adverse vaccine effects at the injection site (Abolnik *et al.*, 2022). In the immunogenicity study, the SPF chickens that were vaccinated with the Emulsigen-P adjuvanted IB VLPs displayed no adverse vaccine effects. Traditional inactivated virus vaccines formulated with an oil emulsion sometimes cause lesions or reactions at the injection site that can lead to downgrades of the animal carcass (Temiz *et al.*, 2021; Cook *et al.*, 2012). With Emulsigen-P, the final vaccine formulation has a reduced oil quantity and lower viscosity, which means, because it can pass

easily through a 25-gauge needle during immunisation, there is a lower likelihood of reactions occurring at the site of injection (Abolnik *et al.*, 2022).

For the single-dose immunogenicity study, the plant-produced IB VLP vaccine preparation containing 5 µg of Spike protein was able to elicit a strong humoral immune response in SPF chickens after two weeks and induced S-protein specific antibodies which were detected by an HI test. A 20 µg VLP preparation elicited even stronger humoral immune responses and induced higher levels of S-specific antibodies. The construct used to produce the VLPs for the vaccine (mIBV-S2P-NDV-F^{TM/CT}) was co-infiltrated with the NDV matrix protein rather than the IBV structural proteins (M, E, and N). Therefore, two commercial IBV ELISA antibody detection kits (commonly optimised to detect the more highly conserved structural proteins that are common in all IBV serotypes) were not able to detect any antibodies that may have been elicited by this produced VLP vaccine. This may theoretically prove to be a useful feature for DIVA, in which flocks that have been vaccinated with live-attenuated or inactivated whole virus vaccines could be distinguished from flocks that have only been vaccinated with plant-produced VLP vaccines. In practice, however, an ideal vaccination program would most likely involve the use of a combination of live-attenuated and VLP vaccines in a prime-boost vaccination strategy (de Wit *et al.*, 2011).

CHAPTER 5

EFFICACY OF PLANT-PRODUCED IB VLPS IN SPF CHICKENS AGAINST HOMOLOGOUS CHALLENGE WITH A LIVE VIRUS

5.1. Introduction

The efficacy of a veterinary vaccine is determined by its specific ability to cause a reduction in disease under carefully-controlled, randomised clinical trials, based on a defined protocol by the manufacturer (WOAH, 2012). Its effectiveness on the other hand is determined by its ability to cause a reduction in disease within the field (Parida, 2009; Simon and Vonkorff, 1995). While the terms “efficacy” and “effectiveness” are often used interchangeably, the effectiveness of a vaccine depends on its efficacy (Asokan, 2009). One of the clearest methods for evaluating vaccine efficacy is a double blind, randomised control study. Cohort and case control observational studies are useful for effectively comparing the efficacy of vaccines (Asokan, 2009). Different vaccines can be compared using challenge studies as a standardised platform. These, however, do not accurately factor in the variation found in field conditions such as the immune status of the bird due to other pathogens in the flock or their nutrition (Knight-Jones *et al.*, 2014). Nonetheless, their effectiveness requires thorough evaluation, given the economic and health implications of their use (Asokan, 2009).

Veterinary vaccines undergo rigorous immunogenicity and safety evaluations to obtain market authorization. This is usually performed on a restricted number of the target species individuals (European pharmacopoeia, 2012). *In vivo* challenge or sero-conversion studies are used to assess a vaccines ability to protect against disease, and various measures of efficacy are used to express the corresponding results (WOAH, 2012).

a) Challenge studies

These can be used to compare unvaccinated and vaccinated individuals in a controlled experimental setting after challenge with the pathogen of interest (Knight-Jones *et al.*, 2014). Veterinary vaccine evaluation is heavily reliant on these studies. The assessment of vaccine protection is performed using the lowest vaccine antigen level allowed and challenging with a pathogen of high level (Knight-Jones *et al.*, 2014). This gives some level of confidence that the vaccine may be able to protect in extreme situations as well. The advantage of challenge studies is that participant and pathogen characteristics can

be controlled which minimises the differences that can be found between vaccinated and unvaccinated groups. Various vaccines can be compared for the same disease along with the effect of different variables on the ability of the vaccine to protect against disease (Knight-Jones *et al.*, 2014).

b) Randomised controlled trials

These trials are considered inferior to challenge studies with regards to evaluating the efficacy of veterinary vaccines (WOAH, 2012). Because the market for veterinary vaccines is small compared to that of human vaccines, the associated cost of larger randomised controlled trials may be problematic (Van Aarle, 2010; Meeusen *et al.*, 2007). Cluster randomised designs might be more useful than these trials because large groups of livestock are vaccinated together as opposed to both vaccinated and unvaccinated animals being present in the same group (Knight-Jones *et al.*, 2014).

c) Observational studies

This type of study is not commonly used for animal populations, but several examples of its practice include cohort studies, outbreak studies, case-control studies, relative effectiveness, and vaccine programme impact (Knight-Jones *et al.*, 2014). The performance of the vaccine under programmatic circumstances is evaluated. These are circumstances where the health of the individual will vary, along with how the vaccine is stored and delivered (Knight-Jones *et al.*, 2014). In observational studies, individuals that are vaccinated differ from vaccinated individuals in a way that might confuse the effects of the vaccine (Knight-Jones *et al.*, 2014).

To assess the efficacy of a veterinary vaccine, the statistical validation of vaccination-challenge studies needs to be demonstrated in the host animal. Usually, the youngest or most sensitive animals are used. The studies are ideally performed using seronegative animals under controlled conditions (WOAH, 2018b).

The assessment of live-attenuated vaccines requires at least ten specific pathogen free (SPF) chickens at the youngest age recommended for vaccination. The vaccines are administered either by eye drop or intranasally using the recommended dosage. A control group containing ten unvaccinated birds of the same type are kept separately. All the groups are then challenged 3-4 weeks later (or at a time interval that lines up with the duration or onset of immunity). A

tracheal swab is taken from each chicken 4-5 days post-challenge and placed in antibiotic broth and tested for Infectious Bronchitis Virus (IBV) by inoculating into embryonated eggs. Alternatively, birds are killed 4-6 days post challenge, tracheas are removed and examined for ciliary motility. An extensive loss of ciliary activity indicates that the bird was unable to resist challenge. If a minimum of 80 % of the vaccinated birds that were challenged show no signs of IBV in their trachea, and at least 80 % of the control birds show signs of IBV, then the live-attenuated vaccine is considered suitable for use as a vaccine (WOAH, 2018a).

The assessment of inactivated vaccines whose intended use is to protect against respiratory disease requires twenty 4-week-old SPF chickens to be vaccinated according to recommendations. A control group of twenty unvaccinated birds of the same type are kept together with the first group. When antibody responses are determined after 4 weeks, the unvaccinated birds should have no response. All the groups are challenged and killed after 4-7 days. Either tracheas are removed and assessed for ciliary activity, or tracheal swabs are examined for the recovery of the challenge virus. A minimum of 80 % of the control birds should show complete ciliostasis, while a similar amount of the vaccinated birds should have unaffected tracheal cilia. In the control birds, at least 90 % of the tracheal swabs should test positive for isolation of the challenge virus, while the same amount should be negative for viral isolation in the vaccinated birds (WOAH, 2018a).

A challenge study was therefore chosen as it was most useful for testing the vaccine produced in this thesis.

Different criteria have been used for the evaluation of vaccine protection (Darbyshire and Peters, 1984; Jackwood *et al.*, 2007; Lee *et al.*, 2010). In the USA, vaccine efficacy is evaluated by detecting the challenge virus, while in Europe, the evaluation of tracheal ciliostasis determines vaccine efficacy (Jackwood *et al.*, 2015). The evaluation of ciliary activity can be used to effectively measure immunity to IBV (Andrade *et al.*, 1982).

A method adapted from Cook *et al.*, (1999) for ciliary motility scoring has been used to assess vaccine protection against IBV. For this method, birds are euthanised and necropsied post IBV challenge. The tracheas are carefully removed and tracheal rings that are approximately 1 mm in thickness are cut from them. Three rings are cut from the distal section, four from the middle section, and three from the proximal section (Adeyemi *et al.*, 2018). Each of these rings are then prepared and examined under a low magnification light microscope and given a score between 0 and 4 as follows (Darbyshire, 1979; Adeyemi *et al.*, 2018; Cook *et al.*, 1999):

0 – 100 % beating cilia

1 – 75 % beating cilia

2 – 50 % beating cilia

3 – 25 % beating cilia

4 – 0 % beating cilia

The sum of all of the scores given for each of the ten rings determined the ciliostasis score. The maximum ciliostasis score that could be given was 40. A ciliostasis score higher than 20 indicated a lack of protection (Cavanagh *et al.*, 1997).

A total average score for each tracheal ring was calculated and the average protection score per group was determined using this formula:

Average Protection Score

$$= 100 - \frac{\text{total of the individual scores for the group}}{\text{the number of individuals in the group} \times 20} \times 100$$

An average protection score of 50 or higher is considered protected. A minimum of 50 % of the tracheal sections need to demonstrate ciliary movement to confirm that a vaccine offered protection against viral challenge (Andrade *et al.*, 1982).

Vaccinating with two live-attenuated vaccines that are antigenically distinct (i.e., 4-91 and a Mass-type) can offer wide cross-protection against a variety of different types of IBV (Terregino *et al.*, 2008; de Wit *et al.*, 2011). Priming with live-attenuated IBV vaccines before using inactivated IBV vaccines has demonstrated increased levels of protection particularly during the laying period of commercial laying chickens (Box *et al.*, 1988; de Wit *et al.*, 2011).

The development of plant-produced VLP vaccines against IBV offers crucial benefits such as speed, safety, and scalability. This technology is particularly relevant in producing variant vaccines which are closely antigenically-matched to a field strain that is circulating at a given time. There are several live-attenuated and inactivated IBV vaccines that are registered for use in South Africa (IVS, 2019). Many of the inactivated vaccines contain H-52, Mass 41 as well

as other killed pathogens such as infectious bursal disease and Newcastle disease virus. There is no plant-produced IBV variant vaccine registered for use in South Africa as of yet.

A challenge model for the ck/ZA/3665/11 QX-like strain was used which was developed at the University of Pretoria (Abolnik, 2014). The objective of the challenge model was to determine the time dependent for tracheal ciliary movement, the clinical signs (including any kidney histopathology), and the viral shedding of the QX-like strain assessed by qRT-PCR. There were three groups of twenty chickens each, two of which were challenged by eye drop with a $10^{4.0}$ EID₅₀/dose (Group 1) or a $10^{4.5}$ EID₅₀/dose (Group 2) of the challenge virus (Abolnik, 2014). The third group was an unchallenged control. On days 3, 5, 7, and 10 post challenge, five birds were removed from each of the groups, humanely euthanized, and necropsied. Their tracheas were immediately removed for ciliary motility scoring, their kidneys were collected in formalin for histopathology, and swabs were taken in duplicate for qRT-PCR (Abolnik, 2014). The birds appeared clinically healthy throughout the trial, and ciliary motility was severely affected for both challenge groups, peaking between days 5 and 7, before the onset of recovering on day 10. Viral replication began to be established around day 3 while oropharyngeal shedding peaked on day 5 post infection for both challenged groups (Abolnik, 2014). Virus was still being excreted on day 10 for both challenge groups. The QX-like strain did not appear to be nephropathogenic. Overall, the challenge model determined that after challenge with this strain of IBV, chickens should be sacrificed on day 7 after infection for ciliary motility scoring and quantification of viral shedding (Abolnik, 2014).

The immunogenicity of the IB VLPs (developed with the mIBV-S2P-NDV-F^{TM/CT} construct co-infiltrated at a 4:1 ratio with the NDV matrix protein) was demonstrated in Chapter 4 and its efficacy was investigated in this Chapter using the described challenge model (Abolnik, 2014).

The aim of this chapter was to assess the efficacy of the plant-produced infectious bronchitis VLPs (mIBV-S2P-NDV-F^{TM/CT}:matrix) in a challenge study with a live homologous virus using SPF chickens. The efficacy of the VLP vaccine was contrasted against the efficacy of a vaccine mixture containing IBV 4-91 and IBV Ma5 live-attenuated vaccines.

5.2. Materials and Methods

5.2.1. Production of IB VLPs

The mIBV-S2P-NDV-F^{TM/CT} and NDV matrix constructs in AGL-1 were co-infiltrated into *N. benthamiana* plants, harvested, extracted and purified as described in Chapter 4 for the immunogenicity study. VLPs were extracted, purified, and stored at 4 °C until ready for use.

5.2.2. Efficacy Study

The efficacy study in SPF chickens took place in the Biosafety Level 3 facility at the Veterinary Faculty of the University of Pretoria.

All study procedures were approved by the University of Pretoria Research and Animal Ethics Committees (REC106-20), the CSIR (251/2018) and the Department of Agriculture, Land Reform, and Rural Development (12/11/1/1/MG).

Ciliary motility scoring was used to evaluate the efficacy of the VLP vaccines produced in this study as the QX-like challenge virus (ck/ZA/3665/11) does not produce obvious clinical signs (e.g., respiratory signs, depression) in infected SPF chickens under experimental conditions. The protective efficacy was also measured by the ability of the VLP vaccines to reduce oropharyngeal and cloacal shedding of the challenge virus (Abolnik, 2014).

5.2.2.1. Animals

Sixty 3-week old SPF White Leghorn Chickens (*Gallus gallus*) were purchased from Avi-Farms (Pty) Ltd, Pretoria. They were divided into four treatment groups and individually numbered with wing tags (Table 5.1).

5.2.2.2. Housing, Feed, and Water

Ten chickens were housed in each of 6 isolators as follows:

Table 5.1. Treatment Groups for the Efficacy Study

	Treatment Group	No. of Birds	Isolator
Group A	Live vaccine + VLP vaccine, challenged	20	1 and 2
Group B	Live vaccine + Live vaccine, challenged	20	3 and 4
Group C	Unvaccinated challenged	10	5
Group D	Unvaccinated unchallenged	10	6

In isolation room 1, there is a negative pressure cascade maintaining the isolators under a negative pressure of between 90 and 100 Pa. Each of the isolators is fitted with HEPA-filtered and pre-filtered (for the dust from bird feathers and feed). Additional HEPA filters and pre-filters were installed for inlet and outlet of the air in Isolation room 1. The isolator temperatures were set to 26 °C to make them comfortable for the chickens. Isolation room has adequate ambient light. Therefore, the lights in the isolators as well as in Isolation room 1 were kept off to keep the chickens in natural daylight and darkness at night. Perches were placed in each of the isolators.

Water was provided to the chickens by drinking nipples connected to a header tank. To prevent backflow, the inlet water supply to the header tanks was raised above water level. The header tanks were designed to fill automatically.

The chickens were observed daily. The pressure and temperature of the isolators and in the isolation facility were monitored daily and recorded. The water levels were monitored daily and feed replenished through the double-door hatches. Feed (Nova Feeds, Pretoria, South Africa) was provided to the birds *ad libitum*.

5.2.2.3. Preparation of Live-attenuated Vaccines

The use of a combination of antigenically distinct live-attenuated vaccines has been shown to offer broad cross-protection against a number of IBV serotypes (Valastro *et al.*, 2016; Terregino *et al.*, 2008). The two live-attenuated vaccines used to prime the chickens in the first group and vaccinate the chickens (both prime and boost) in the second group were IB Ma5 (Nobilis, MSD Animal Health, South Africa), and IBV 4-91 (Nobilis, MSD Animal Health, South Africa). This vaccine combination is used by poultry veterinarians to control QX-like variant infections in South Africa. Each dose

of the freeze dried IB Ma5 contains at least $10^{3.5}$ EID₅₀ IBV strain Ma5 (Massachusetts) and each dose of the freeze dried IB 4-91 contains at least $10^{3.6}$ EID₅₀ IBV strain 4-91. The two live-attenuated vaccines were reconstituted in 10 ml in Diluvac (Nobilis, MSD Animal Health, South Africa) and 1 ml of each reconstituted vaccine was mixed with 10 ml of Diluent Oculo Nasal (Intervet, MSD Animal Health, South Africa). The vaccine preparation was kept at 4 °C until use.

5.2.2.4. Preparation of VLP Vaccine

The partially-purified mIBV-S2P-NDV-F^{TM/CT}:matrix VLPs were quantified by densitometry as described in Chapter 4. On the day of immunization, the partially purified mIBV-S2P-NDV-F^{TM/CT}:matrix VLPs were diluted with sterile 1X PBS buffer and then mixed thoroughly with 10 % (v/v) of Emulsigen®-P Adjuvant (MVP, Phibro Animal Health, USA) for a total 20 µg dose volume of 250 µl. The vaccine preparation was kept at 4 °C until use.

5.2.2.5. Challenge Virus

The ck/ZA/3665/11 QX-like strain was acquired from UP's poultry virus repository, where it was propagated and titrated in SPF eggs at the Department of Veterinary Tropical Diseases by virologist Ms Karen Ebersohn. Immediately before viral challenge, the virus ($10^{6.5}$ EID₅₀/0.1 ml in allantoic fluid) was diluted to a challenge dosage of 10^6 EID₅₀/0.06 ml corresponding to a single 30 µl drop in each eye. The diluted challenge virus was kept at 4 °C until use.

5.2.2.6. Experimental Design

Day 1 (3 weeks old): Primary Immunization

At the start of the trial, 1 ml of blood was drawn from the wing vein of all of the birds. The unvaccinated chickens (Groups C and D) were thereafter placed in separate isolators. The birds belonging to Groups A and B were immunized via eye drop with the prepared live-attenuated vaccine (Fig. 5.1). One drop was placed in each eye of each bird. Thereafter the birds were placed in separate isolators, with ten birds housed in each.

Day 21 (6 weeks old): Booster Immunization

Blood (1 ml) was drawn from the wing veins of the birds belonging to Groups A and B. Birds belonging to Group B were immunized again via eye drop with the prepared live-attenuated vaccine. The birds were thereafter placed back into their isolators. Birds belonging to Group A were immunized intramuscularly in the breast with 0.25 ml of the prepared VLP vaccine using sterile 11-gauge needles (Fig. 5.1). The birds were then placed back into their isolators.

Day 42 (9 weeks old): Challenge

Blood (1 ml) was drawn from the wing veins of the birds belonging to Groups A and B. The chickens in Groups A, B, and C were then challenged with the prepared challenge virus via eye drop (Fig. 5.1). The birds were monitored every day after challenge (Days 43 – 49) for clinical signs.

Day 45 (3 days post challenge):

Oropharyngeal and cloacal samples were taken from all of the birds using sterile plastic applicator rayon-tipped swabs (Copan Diagnostics Inc. Murrieta, California, USA) (Fig. 5.1). The swabs were placed in tubes containing 2 ml of Viral Transport Media (VTM) (brain-heart broth, 0.1 mg/ml enrofloxacin, 1 mg/ml penicillin-streptomycin, 0.1 mg/ml doxycycline, and 10 % glycerol). The tubes were stored at 4 °C until analysis.

Day 47 (5 days post challenge):

Oropharyngeal and cloacal swabs were taken again and stored at 4 °C until analysis (Fig. 5.1).

Day 49 (7 days post challenge) and final day of trial:

Oropharyngeal and cloacal swabs were taken again and stored at 4 °C until analysis. Blood (1 ml) was drawn from the wing veins of all the birds before they were humanely euthanized by cervical dislocation. Their tracheas were removed and prepared for ciliary motility scoring which was performed within an hour of euthanasia (Fig. 5.1).

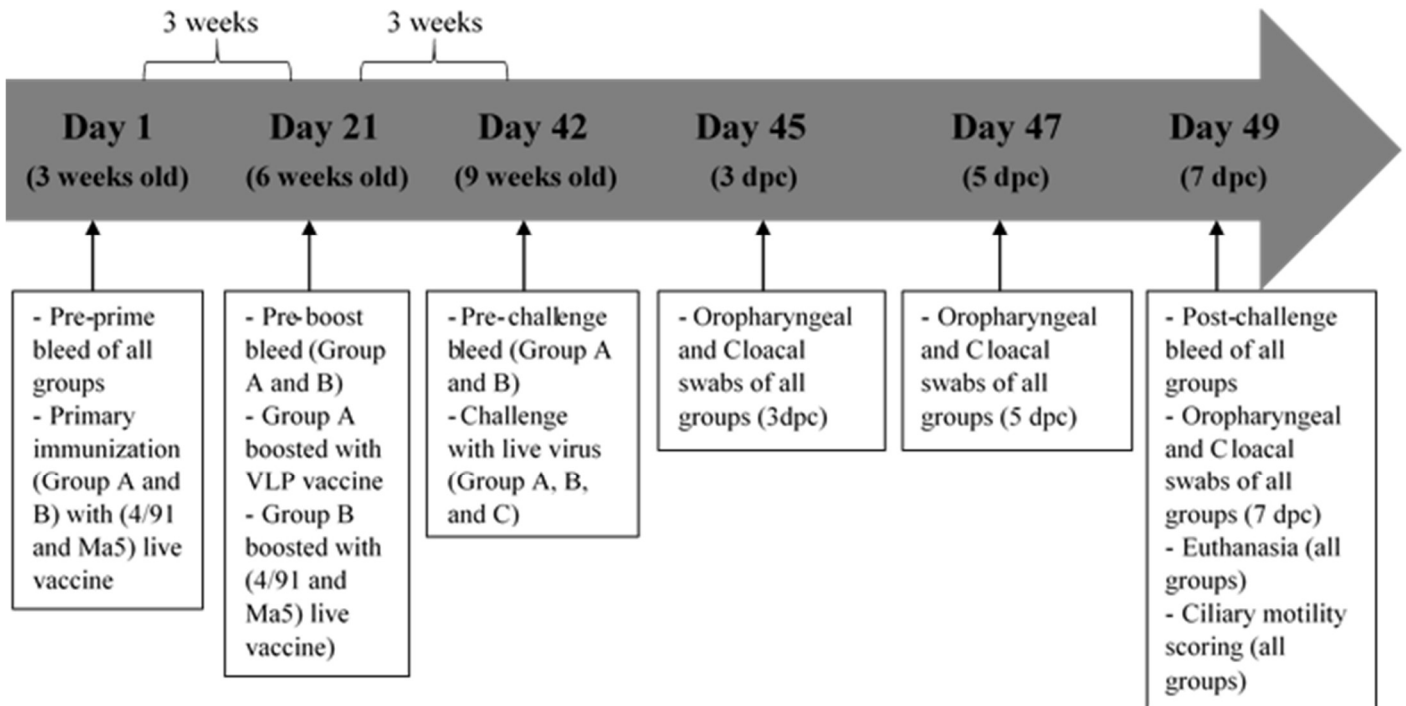


Figure 5.1. Experimental design of the efficacy study (49 days).

The chickens were monitored daily throughout the course of the trial for clinical signs of IBV post viral challenge as well as for adverse vaccine effects.

5.2.2.7. Serology and HI Testing

The blood samples taken at each point in the trial were left to clot for an hour at room temperature after they were drawn. The samples were centrifuged at 3000 x g for 10 minutes at 22 °C and the sera collected in tubes. These were stored until ready for testing. Once all the sera had been collected, the serology and HI tests were carried out as described in Chapter 4.

5.2.2.8. Quantitative Real-time Reverse Transcription PCR

The viral RNA was extracted from 200 µl of the vortexed swab fluid using the IndiMag Pathogen Kits according to the suggested method in an IndiMag 48 instrument (Indical BioSciences). The extracted viral RNA was subjected to qRT-PCR.

QX-like IBV-specific RNA was detected using the primers, probe and method described in Abolnik (2014), in a StepOnePlus™ (Applied Biosystems) instrument using the Vetmax™ –Plus One Step RT-PCR kit (Applied Biosystems). The probe was designed to specifically detect only sequences from the QX type IBV and exclude all other serotypes. Each of the qRT-PCR reactions were made up of the following: 4 µl of the extracted viral RNA, 0.15 µl (5 pmol/µl) IBV QX Probe labelled MGB-FAM, 0.5 µl (12.5 pmol/µl) of each forward and reverse primer, 6 µl of the 2 X RT-PCR buffer, 0.5 µl of the 25 X RT-PCR enzyme mix, made up to a final volume of 13 µl with nuclease-free water. The cycling conditions for the PCR reaction were: 1 cycle of 48 °C for 10 min, 1 cycle of 95 °C for 10 min, 40 cycles of 95 °C for 15 sec, and 60 °C for 45 sec.

Two-fold serial dilutions from 10^0 to 10^{-8} of RNA extracted from 250 µl of the viral challenge material ($10^{6.5}$ EID₅₀/ml) were used as positive controls and included in triplicate in each qRT-PCR run. The positive control samples were used to generate a standard curve that was used to extrapolate the EID₅₀ viral quantities for each sample. The limit of detection could, however, not be determined using this method. Therefore, samples that had a titre higher than 15.93 EID₅₀/ml (the lowest detected titre) were considered positive for QX IBV.

Nuclease-free water as well as the extracted RNA of IB Ma5 and IB 4-91 strains were used as negative controls.

5.2.2.9. Ciliary Motility Scoring

Within an hour of euthanasia, tracheal rings were prepared and visualized under light microscopes. A score between 0 and 4 was given to each of the ten tracheal rings and the sum of the ten rings for each bird was calculated as the ciliostasis score. The equation given in the introduction of this chapter was used to calculate the average protection score for each group.

The scores were assigned by myself, Prof. Celia Abolnik, Ms. Michaela Hayes, Dr. Tanja Smith, and Ms. Leandri Wandrag. Each score was double-checked by a second scorer in order to reduce the level of subjectivity of the scoring process.

5.2.2.10. Statistical Analysis

The HI results were statistically compared by un-paired T-test using the GraphPad Prism v 9.4.1 software for Windows (La Jolla, Ca, United States of America) with a P-value of < 0.05 being considered significant. For the qRT-PCR results, the statistical tests were performed on the untransformed data, but the results were presented as Log_{10} values in the figures to make comparison easier. The mean antibody titres and viral RNA between the groups were analysed using one-way analysis of variance (ANOVA) which was followed by Tukey's multiple comparison test. The mean antibody titres of each group on the different days post challenge were compared by paired student's T-test with a P-value of < 0.05 being considered significant.

5.3. Results

5.3.1. Production of IB VLPs

The synthetic gene construct pEAQ-HT-mIBV-S2P-NDV-F^{TM/CT} in AGL-1 was successfully agro-infiltrated into *N. benthamiana* plants at a 4:1 ratio with the pEAQ-HT-NDV-matrix protein gene construct. Leaves were harvested with either PBS, Bicine or Tris buffers for comparison in order to confirm if a difference could be seen now that there was noticeably higher levels of protein expression at this stage compared to preliminary stages. SDS-PAGE, and immunoblotting confirmed the presence of the S protein band at 124 kDa corresponding to the size of the mIBV-S2P-NDV-F^{TM/CT} gene construct (Fig. 5.2 (a) and Fig. 5.2 (b)). The IBV QX chicken antisera reacted more strongly with S protein specific bands in the samples harvested with PBS than with Tris or Bicine buffers (Fig. 5.2 (b)). This suggested that there was a higher protein content in the constructs harvested with PBS buffer. The bands were noticeably higher than the band around the same size in the negative control as was the band in the positive control. This suggests that this was not a plant protein and was likely to be the S protein. The S protein was not detected in the QX-like positive control. No VLPs were visualised under the TEM for the samples harvested with Tris and Bicine buffers (data not shown). TEM confirmed the presence of VLPs resembling native IBV particles for the samples harvested with PBS buffer (Fig. 5.3).

The three samples (harvested in the three different buffers) were dialysed overnight in 1 X PBS buffer and stabilised with 15 % trehalose. Densitometry analysis showed very low S protein concentrations for the samples harvested in Tris and Bicine buffer. The levels were undetectable (data not shown) with the quantification software. The purified mIBV-S2P-NDV-F^{TM/CT}:matrix VLPs that were harvested in PBS buffer were used for the *in vivo* challenge study. This time, densitometry analysis determined the concentration of the purified S protein 124 kDa band to be approximately 62 ng/μl (Fig. S5).

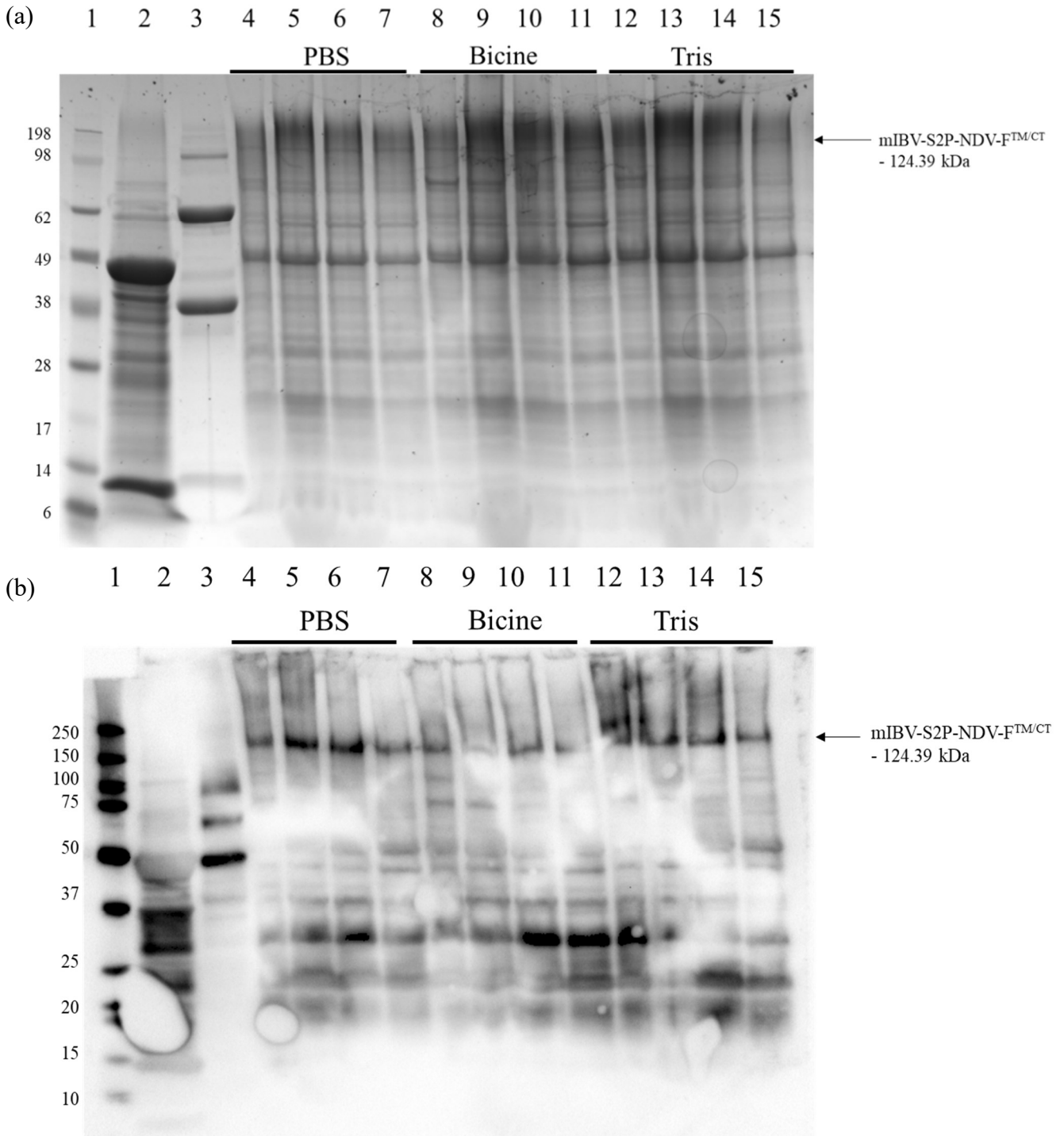


Figure 5.2. SDS-PAGE (a) and Western blot (b) of plant-produced mIBV-S2P-NDV-F^{TM/CT} protein co-infiltrated at a 4:1 ratio with the NDV matrix protein harvested in PBS, Bicine, or Tris Buffers. Lane 1: molecular weight marker; Lane 2: plant-expressed empty pEAQ-HT vector; Lane 3: purified live QX-like IBV strain ck/ZA/3665/11; Lanes 4 - 7: mIBV-S2P-NDV-F^{TM/CT}:matrix Fractions 3 - 6; Lanes 8 - 11: mIBV-S2P-NDV-F^{TM/CT}:matrix Fractions 3 - 6; Lanes 12 - 15: mIBV-S2P-NDV-F^{TM/CT}:matrix Fractions 3 - 6.

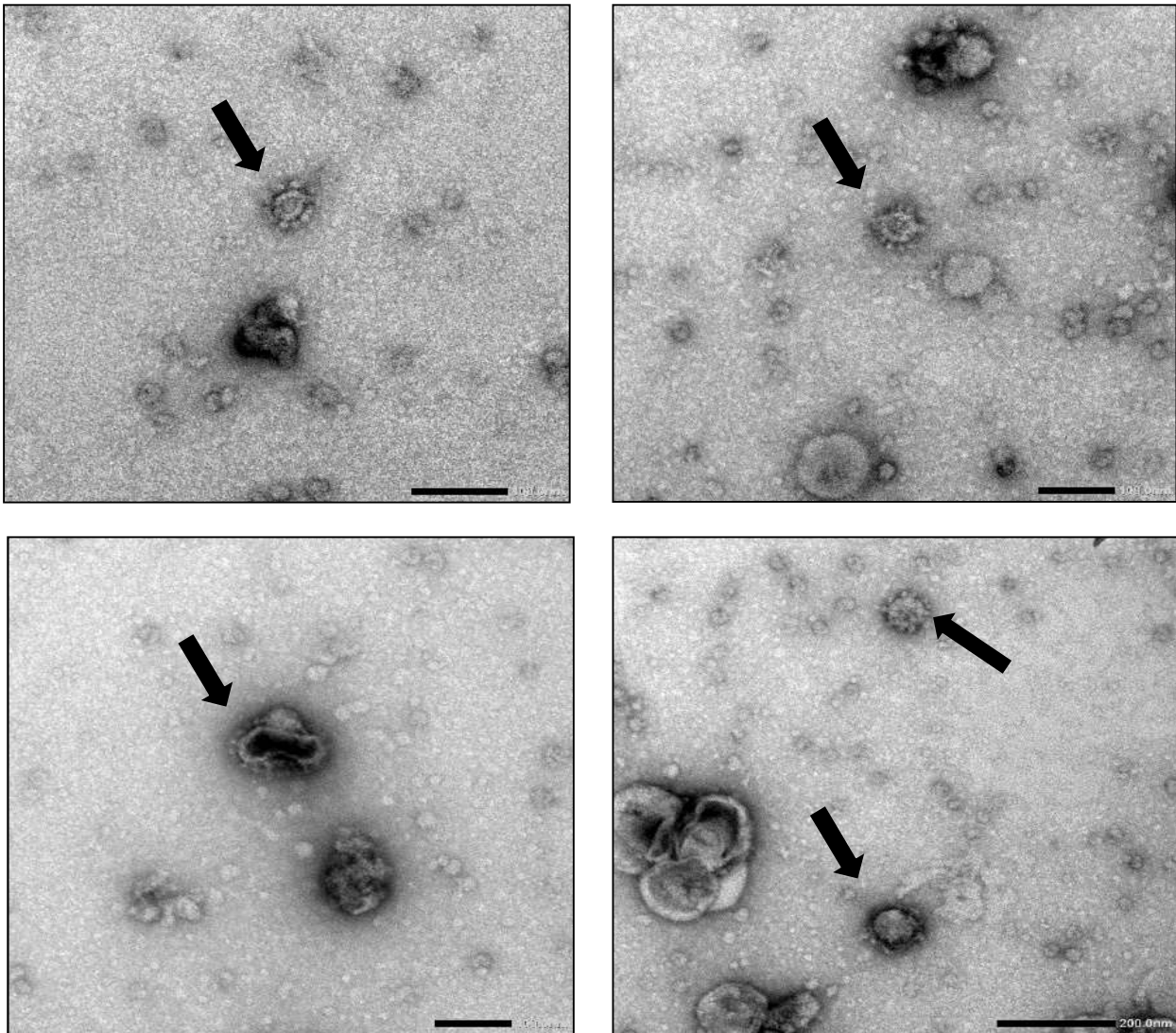


Figure 5.3. Negative-stained transmission electron microscopy images of plant-produced IBV virus-like particles expressed with the synthetic gene constructs mIBV-S2P-NDV-F^{TM/CT} in *N. benthamiana* in different ratios with NDV matrix. Arrows indicate VLPs.

5.3.2. Serology Testing

An incident regarding a malfunctioning header tank resulted in the unfortunate loss of 8 chickens in Group A. Two more chickens died from a lack of oxygen due to load shedding (power cuts) causing the generators in the BSL3 facility to malfunction resulting in inadequate pressure control. A nonconformance was raised and contingency measures were put in place to avoid any further losses before the trial ended. In total, 10 chickens from Group A were lost. Thus, only the results from 10 randomly selected chickens belonging to Group B were used.

Table 5.2. Serology test results. (Positive results highlighted in grey)

Blood Sample Collection Date		Pre-prime bleed (Day 1)			Pre-boost bleed (Day 21)			Pre-challenge bleed (Day 42)			Post-challenge bleed (Day 49)		
Treatment Group	Bird no.	S/P	Log ₁₀ titre	Titre	S/P	Log ₁₀ titre	Titre	S/P	Log ₁₀ titre	Titre	S/P	Log ₁₀ titre	Titre
Group A: Live vaccine + VLP vaccine, challenged	10241	0,02	1,79	61,51	0,86	3,59	3906,55	1,39	3,82	6592,89	2,67	4,13	13421,64
	10244	0,13	2,71	514,77	1,09	3,70	5024,36	1,43	3,83	6765,41	2,51	4,10	12507,80
	10245	0,02	1,79	61,51	0,31	3,10	1269,57	0,11	2,60	401,55	2,07	4,01	10148,45
	10246	0,02	1,86	72,76	0,61	3,43	2686,58	0,72	3,51	3202,47	2,73	4,14	13744,42
	10247	0,03	1,93	84,16	1,67	3,91	8035,35	1,17	3,74	5464,02	1,93	3,97	9387,99
	10248	0,02	1,86	72,76	0,85	3,59	3857,06	0,61	3,43	2670,58	2,14	4,02	10513,84
	10249	0,01	1,27	18,57	0,62	3,44	2750,65	0,61	3,43	2670,58	1,73	3,92	8354,76
	10250	0,02	1,79	61,51	0,55	3,38	2384,01	0,75	3,53	3365,17	2,32	4,06	11498,87
	10252	0,08	2,46	291,41	0,51	3,34	2210,25	0,42	3,25	1773,21	2,15	4,03	10597,04
	10254	0,12	2,66	459,95	0,32	3,13	1344,96	0,16	2,81	638,91	1,36	3,81	6432,64
	Mean	0,05	2,01	169,89	0,74	3,46	3346,93	0,74	3,39	3354,48	2,16	4,02	10660,74
Group B: Live vaccine + Live vaccine, challenged	10264	0,04	2,12	130,93	0,46	3,30	1990,74	0,73	3,51	3251,21	1,83	3,95	8861,93
	10265	0,01	1,27	18,57	0,57	3,39	2479,23	0,53	3,36	2289,09	1,83	3,95	8878,33
	10267	0,01	1,60	39,54	0,20	2,91	811,22	0,29	3,08	1194,55	1,66	3,90	7963,84
	10270	0,03	2,03	107,34	1,13	3,72	5243,81	0,46	3,30	1990,74	2,30	4,06	11415,12
	10272	0,05	2,22	166,99	0,93	3,63	4254,38	1,90	3,97	9251,24	2,41	4,08	11968,84
	10274	0,11	2,62	420,51	0,33	3,14	1375,21	0,63	3,44	2766,68	2,20	4,04	10880,29
	10276	0,08	2,48	304,14	0,38	3,20	1588,48	0,43	3,26	1835,14	1,31	3,79	6177,51
	10277	0,03	1,93	84,16	0,74	3,52	3300,01	0,62	3,43	2718,60	1,98	3,98	9651,94
	10279	0,05	2,25	179,16	0,23	2,96	913,19	0,26	3,02	1045,69	1,72	3,92	8289,50
	10280	0,05	2,28	191,40	1,49	3,85	7076,85	0,63	3,44	2766,68	1,92	3,97	9355,03
	Mean	0,05	2,08	164,27	0,65	3,36	2903,31	0,65	3,38	2910,96	1,92	3,96	9344,23

Table 5.2. Serology test results CONTINUED

Blood Sample Collection Date		Pre-prime bleed (Day 1)			Pre-boost bleed (Day 21)			Pre-challenge bleed (Day 42)			Post-challenge bleed (Day 49)		
Treatment Group	Bird no.	S/P	Log ₁₀ titre	Titre	S/P	Log ₁₀ titre	Titre	S/P	Log ₁₀ titre	Titre	S/P	Log ₁₀ titre	Titre
Group C: Unvaccinated Challenged Control	10281	0,01	1,60	39,54		NT	NT		NT	NT	0,37	3,19	1536,22
	10282	0,02	1,86	72,76		NT	NT		NT	NT	0,94	3,63	4309,58
	10283	0,02	1,86	72,76		NT	NT		NT	NT	1,14	3,72	5291,62
	10284	0,02	1,79	61,51		NT	NT		NT	NT	1,16	3,73	5417,47
	10285	0,11	2,64	433,63		NT	NT		NT	NT	1,02	3,67	4681,72
	10286	0,02	1,79	61,51		NT	NT		NT	NT	0,79	3,55	3543,00
	10287	0,01	1,46	28,89		NT	NT		NT	NT	0,60	3,42	2626,40
	10288	0,01	1,46	28,89		NT	NT		NT	NT	0,13	2,70	498,25
	10289	0,02	1,70	50,42		NT	NT		NT	NT	0,88	3,60	3986,11
	10290	0,01	1,60	39,54		NT	NT		NT	NT	0,64	3,45	2819,80
	Mean	0,03	1,78	88,94								0,77	3,47
Group D: Unvaccinated Unchallenged Control	10291	0,04	2,08	119,09		NT	NT		NT	NT	-0,01	0	0
	10292	0,02	1,70	50,42		NT	NT		NT	NT	0,02	1,91	81,75
	10293	0,03	1,98	95,69		NT	NT		NT	NT	0,17	2,82	655,26
	10294	0,03	2,03	107,34		NT	NT		NT	NT	0,11	2,64	433,95
	10295	0,02	1,86	72,76		NT	NT		NT	NT	0,02	1,69	48,98
	10296	0,03	2,03	107,34		NT	NT		NT	NT	0,03	2,02	104,26
	10297	0,03	1,98	95,69		NT	NT		NT	NT	0,02	1,85	70,67
	10298	0,02	1,79	61,51		NT	NT		NT	NT	0,03	1,97	92,95
	10299	0,02	1,70	50,42		NT	NT		NT	NT	0,08	2,45	283,05
	10300	0,01	1,60	39,54		NT	NT		NT	NT	-0,01	0	0
	Mean	0,02	1,88	79,98								0,05	1,73

5.3.2.1. Pre-prime Bleed (Day 1)

All serum samples that were taken prior to vaccinating the chickens tested negative for the presence of IBV-specific antibodies with the IDEXX IBV antibody ELISA test kit (Table 5.2). The sample to positive (S/P) ratio was negative for all the Day 1 bleeds (≤ 0.20) with mean antibody titres of 169.9, 164.3, 88.95, and 79.98 for Groups A to D respectively (Fig. 5.4). This verified that the SPF chickens had not been exposed to IBV prior to the trial.

5.3.2.2. Pre-boost Bleed (Day 21)

Three weeks after both vaccinated groups received a single dose of mixed Mass/4-91 live-attenuated vaccines, the mean S/P for Group A was positive with a mean antibody titre of 3347 and the mean S/P for Group B was positive with a mean antibody titre of 2903, but there was no statistical difference between the means of the two groups ($P > 0.05$) (Fig. 5.4).

5.3.2.3. Pre-challenge Bleed (Day 42)

Three weeks after vaccinated chickens initially primed with the mixed live-attenuated vaccines were re-immunized with either VLP vaccine or mixed live-attenuated vaccines again, the mean S/P for Group A was positive with a mean antibody titre of 3354.49 and the mean S/P for Group B was positive with a mean antibody titre of 2911, but there was no statistical significance between the means of the two groups ($P > 0.05$) (Fig. 5.4). There was no statistical difference in the IBV group-specific antibodies elicited by the birds that were primed with the live-attenuated vaccine and boosted with the VLP vaccine compared to those elicited by the birds that were immunized with the live-attenuated vaccine both times.

5.3.2.4. Post-challenge Bleed (Day 49)

At the end of the trial, the mean S/P for Group A was positive with a mean antibody titre of 10660.74 and the mean S/P for Group B was positive with a mean antibody titre of 9344. Even though Group A appeared to elicit antibody titres that were higher than those for Group B, the difference was not significant ($P > 0.05$). The mean S/P for

Group C was positive with a mean antibody titre of 3471.02, while the mean S/P for Group D was negative with a mean antibody titre of 177.1 (Fig. 5.4). Birds from both vaccinated groups (A and B) elicited significantly higher ($P > 0.0001$) IBV antibody levels than the unvaccinated birds. The unvaccinated unchallenged control tested negative for the presence of IBV antibodies at the end of the trial showing no exposure to IBV throughout the trial (Table 5.2).

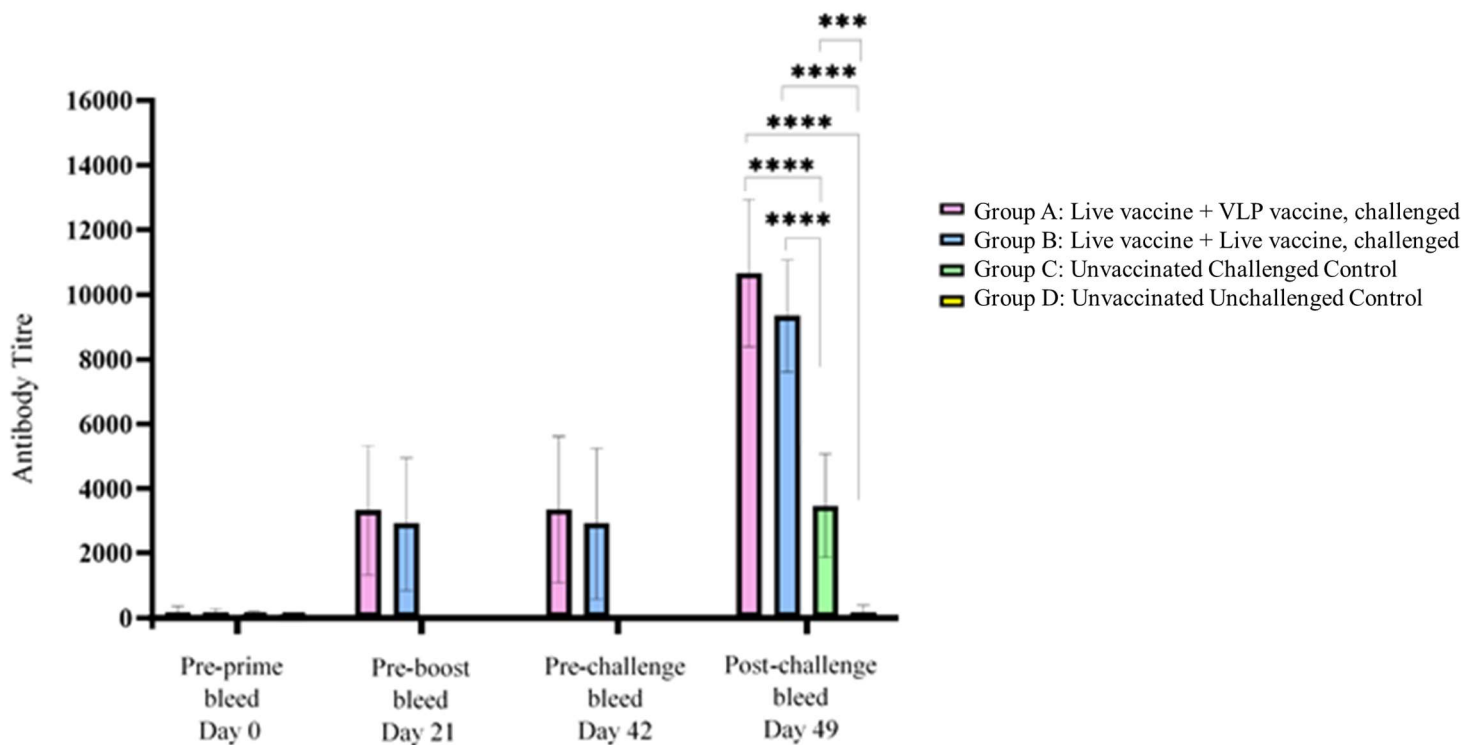


Figure 5.4. Antibody titres \pm standard deviation for the chicken sera taken at 4 different time points during the trial. The asterisks indicate the statistical significance *** ($P \leq 0.001$), **** ($P \leq 0.0001$). Only significant differences are indicated on the graph ($P \leq 0.05$).

5.3.3. HI Testing

The sera from the blood samples taken on Day 42 (Pre-challenge bleed) were treated as described above. The ten chickens from Group A showed seroconversion with HI titres ranging from $6 \log_2$ to $7 \log_2$ with a geometric mean titre (GMT) of $6.8 \log_2$ and the ten chickens from Group B showed seroconversion with HI titres ranging from $6 \log_2$ to $8 \log_2$ with a GMT of $7.2 \log_2$ (Table 5.3). There was no statistical difference between the GMTs of Group A and Group B ($P > 0.05$) (Fig. 5.5).

Table 5.3. Log₂ HI titres for the blood samples taken prior to viral challenge

Treatment Group	Bird no.	Pre-challenge Log₂ HI titre
Group A: Live vaccine + VLP vaccine, challenged	10241	6
	10244	6
	10245	7
	10246	7
	10247	7
	10248	7
	10249	7
	10250	7
	10252	7
	10254	7
	GMT:	6,8
Group B: Live vaccine + Live vaccine, challenged	10264	8
	10265	7
	10267	8
	10270	7
	10272	8
	10274	7
	10276	7
	10277	7
	10279	7
	10280	6
	GMT:	7,2

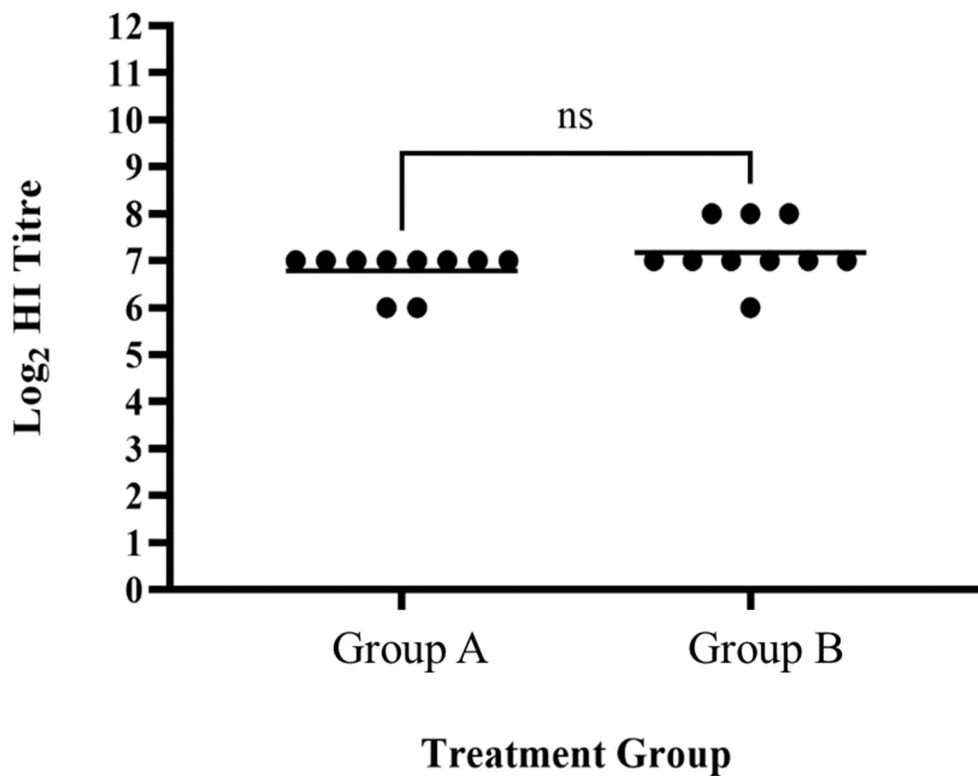


Figure 5.5. Haemagglutination inhibition (HI) log₂ titres for the chicken sera in Groups A and B taken on day 42 (pre-challenge). The bar shows the geometric mean titre (GMT), and the statistical significance is notated “ns” (P > 0.05).

5.3.4. qRT-PCR Results

To assess the vaccine’s ability to reduce viral shedding, oropharyngeal and cloacal swabs were taken on days 3, 5, and 7 post challenge with the live virus. The viral RNA was extracted and tested for the presence of IBV QX-like specific RNA. This was a genotype-specific qRT-PCR assay designed to only detect the QX-like serotype, to the exclusion of all other serotypes including the live-attenuated vaccine strains.

5.3.4.1. Oropharyngeal Viral Shedding

Table 5.4. Individual qRT-PCR results for the oropharyngeal swabs

Treatment Group	Bird no.	3 dpc		5 dpc		7 dpc	
		Quantity (EID ₅₀ /ml)	Log ₁₀ (EID ₅₀ /ml)	Quantity (EID ₅₀ /ml)	Log ₁₀ (EID ₅₀ /ml)	Quantity (EID ₅₀ /ml)	Log ₁₀ (EID ₅₀ /ml)
Group A: Live vaccine + VLP vaccine, challenged	10241	179,28	2,25	0	0	1146,39	3,06
	10244	5296,69	3,72	0	0	798,39	2,90
	10245	101357,60	5,01	9182,43	3,96	2367,52	3,37
	10246	381,20	2,58	0	0	0	0
	10247	76512,80	4,88	25127,72	4,40	0	0
	10248	7284,89	3,86	1342,05	3,13	0	0
	10249	15961,25	4,20	467,24	2,67	0	0
	10250	169813,64	5,23	15509,57	4,19	849,55	2,93
	10252	69536,64	4,84	1491,57	3,17	570,63	2,76
	10254	4979,08	3,70	0	0	251,12	2,40
		45130,31	4,03	5312,06	2,15	598,36	1,74
Group B: Live vaccine + Live vaccine, challenged	10264	91664,85	4,96	276,34	2,44	54,96	1,74
	10265	8768,66	3,94	1111,04	3,05	114,21	2,06
	10267	17039,64	4,23	490,51	2,69	0	0
	10270	51998,34	4,72	230,95	2,36	42,22	1,63
	10272	11532,95	4,06	299,15	2,48	0	0
	10274	31612,60	4,50	103,60	2,02	31,49	1,50
	10276	73,59	1,87	148,23	2,17	195,05	2,29
	10277	2289,79	3,36	109,61	2,04	61,60	1,79
	10279	128019,27	5,11	4595,54	3,66	135,36	2,13
	10280	4788,72	3,68	151,62	2,18	54,92	1,74
		34778,84	4,04	751,66	2,51	68,98	1,49

Table 5.4. Individual qRT-PCR results for the oropharyngeal swabs CONTINUED

Treatment Group	Bird no.	3 dpc		5 dpc		7 dpc	
		Quantity (EID ₅₀ /ml)	Log ₁₀ (EID ₅₀ /ml)	Quantity (EID ₅₀ /ml)	Log ₁₀ (EID ₅₀ /ml)	Quantity (EID ₅₀ /ml)	Log ₁₀ (EID ₅₀ /ml)
Group C: Unvaccinated Challenged Control	10281	541948,75	5,73	305323,84	5,48	20403,64	4,31
	10282	247804,59	5,39	294193,41	5,47	33879,38	4,53
	10283	289909,25	5,46	50322,24	4,70	24579,80	4,39
	10284	36584,17	4,56	1069940,25	6,03	7855,70	3,90
	10285	1446638,63	6,16	1343351,00	6,13	138556,97	5,14
	10286	272777,06	5,44	150562,98	5,18	25601,25	4,41
	10287	65896,81	4,82	150627,44	5,18	16489,17	4,22
	10288	419920,84	5,62	166550,88	5,22	18028,89	4,26
	10289	499273,78	5,70	496545,63	5,70	7103,47	3,85
	10290	319693,31	5,50	574348,31	5,76	5589,62	3,75
			414044,72	5,44	460176,60	5,48	29808,79
Group D: Unvaccinated Unchallenged Control	10291	0	0	0	0	0	0
	10292	0	0	0	0	0	0
	10293	0	0	0	0	0	0
	10294	0	0	0	0	0	0
	10295	0	0	0	0	0	0
	10296	0	0	0	0	0	0
	10297	0	0	0	0	0	0
	10298	0	0	0	0	0	0
	10299	0	0	0	0	0	0
	10300	0	0	0	0	0	0
			0	0	0	0	0

At 3 days post challenge (dpc), the mean group titre of Group A was 4.03 log₁₀ EID₅₀/ml, the mean group titre of Group B was 4.04 log₁₀ EID₅₀/ml, the mean group titre of Group C was 5.44 log₁₀ EID₅₀/ml, and there was no viral shedding detected in Group D (Table 5.4). There was no statistical difference between the means of Group A and Group B (Fig. 5.6). There was significantly less virus shed in Group A ($P \leq 0.01$) and Group B ($P \leq 0.001$) than in the unvaccinated challenged control Group C (Fig. 5.6).

At 5 dpc, the mean group titre of Group A was 2.15 log₁₀ EID₅₀/ml, the mean group titre of Group B was 2.51 log₁₀ EID₅₀/ml, and the mean group titre of Group C was 5.49 log₁₀ EID₅₀/ml (Table 5.4). Although there appeared to be more virus shed from Group B than Group A, there was no statistical difference between the two means (Fig. 5.6). There was significantly less virus shed in Group A ($P \leq 0.001$) and Group B ($P \leq 0.001$) than in the unvaccinated challenged control Group C (Fig. 5.6).

At 7 dpc, the mean group titre of Group A was 1.74 log₁₀ EID₅₀/ml, the mean group titre of Group B was 1.49 log₁₀ EID₅₀/ml, and the mean group titre of Group C was 4.28 log₁₀ EID₅₀/ml (Table 5.4). While there seemed to be slightly more viral shedding for Group A, than for Group B, there was no statistical difference between the means of the two groups (Fig. 5.6). There was significantly less virus shed in Group A ($P \leq 0.05$) and Group B ($P \leq 0.01$) than in the unvaccinated challenged control Group C (Fig. 5.6).

Oropharyngeal Swabs

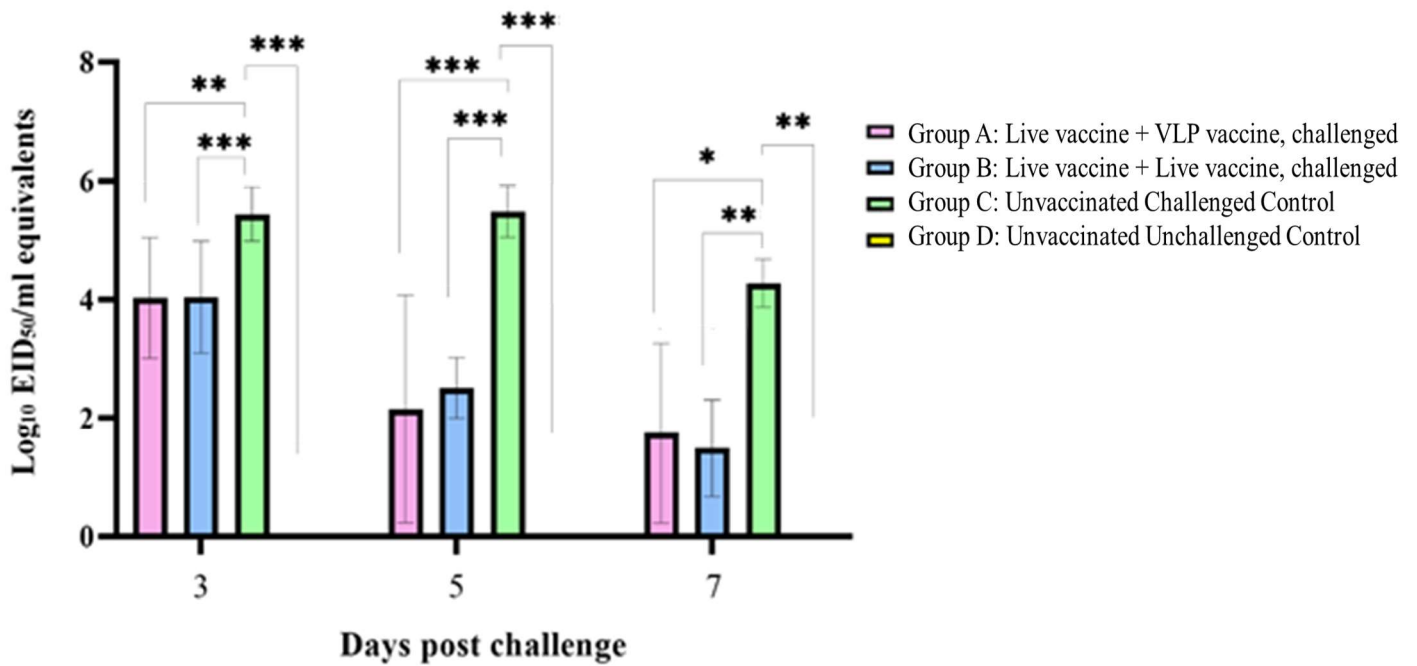


Figure 5.6. Viral RNA log₁₀ EID₅₀/ml equivalents ± standard deviation for the oropharyngeal swabs taken at 3, 5, and 7 days post challenge. The asterisks indicate the statistical significance * (P ≤ 0.05), ** (P ≤ 0.01), *** (P ≤ 0.001), **** (P ≤ 0.0001). Only significant differences are indicated on the graph (P ≤ 0.05).

Table 5.5. Fold differences between the mean titres of each group on the different days post challenge for the oropharyngeal swabs. Significant p-values are highlighted ($P < 0.05$).

		Days post challenge					
		3 dpc vs 5 dpc			5 dpc vs 7 dpc		
Group A	Mean titres (EID ₅₀ /ml)	45130,31	5312,06		decrease	5312,06	
	Fold Difference	8,50		8,88			
	P value	0,04		0,12			
Group B	Mean titres (EID ₅₀ /ml)	34778,84	751,66	decrease	751,66	68,98	decrease
	Fold Difference	46,27			10,90		
	P value	0,03			0,15		
Group C	Mean titres (EID ₅₀ /ml)	414044,72	460176,60	increase	460176,60	29808,79	decrease
	Fold Difference	1,11			15,44		
	P value	0,71			0,01		

There was a significant (***) $P \leq 0.001$ reduction in viral shedding between 3 and 5 dpc for Group A. While there was a reduction in viral shedding between days 5 and 7 for Group A, it was not significant ($P > 0.05$) (Table 5.5).

For Group B, there was a significant (***) $P \leq 0.001$ reduction in viral shedding from day 3 to day 5 post challenge, followed by reduction in viral shedding from day 5 to day 7 post challenge that was not significant (Table 5.5).

There was a slight increase in viral shedding (not significant ($P > 0.05$)) for Group C between days 3 and 5 post challenge, followed by a significant ($P \leq 0.001$) reduction in viral shedding between days 5 and 7 post challenge (Table 5.5).

Group D showed no viral shedding on days 3, 5, or 7 post challenge (Fig. 5.6).

These results show that vaccinating the birds, either with the live-attenuated vaccine and boosting with the VLP vaccine, or vaccinating twice with the live-attenuated vaccine was able to reduce viral shedding from day 3 to day 7 post challenge, although more so between days 3 and 5 post viral challenge. Not vaccinating the birds leads to increased viral shedding between days 3 and 5 which only begins to decrease after day 7. It was, however, beyond the scope of this work to determine the endpoint of viral shedding.

5.3.4.2. Cloacal Viral Shedding

Table 5.6. Individual qRT-PCR results for the cloacal swabs

Treatment Group	Bird no.	3 dpc		5 dpc		7 dpc	
		Quantity (EID ₅₀ /ml)	Log ₁₀ (EID ₅₀ /ml)	Quantity (EID ₅₀ /ml)	Log ₁₀ (EID ₅₀ /ml)	Quantity (EID ₅₀ /ml)	Log ₁₀ (EID ₅₀ /ml)
Group A: Live vaccine + VLP vaccine, challenged	10241	0	0	0	0	0	0
	10244	0	0	0	0	0	0
	10245	0	0	887,38	2,95	0	0
	10246	0	0	1822,67	3,26	0	0
	10247	0	0	0	0	0	0
	10248	0	0	5294,02	3,72	1739,86	3,24
	10249	287,66	2,46	0	0	2935,41	3,47
	10250	0	0	0	0	0	0
	10252	0	0	0	0	0	0
	10254	0	0	0	0	0	0
			28,77	0,25	800,41	0,99	467,53
Group B: Live vaccine + Live vaccine, challenged	10264	0	0	0	0	0	0
	10265	0	0	0	0	4073,69	3,61
	10267	0	0	0	0	0	0
	10270	0	0	15929,18	4,20	7030,33	3,85
	10272	63,47	1,80	45,72	1,66	0	0
	10274	0	0	0	0	0	0
	10276	0	0	0	0	0	0
	10277	0	0	0	0	809,13	2,91
	10279	0	0	0	0	0	0
	10280	0	0	191,10	2,28	1823,26	3,26
			6,35	0,18	1616,60	0,81	1373,64

Table 5.6. Individual qRT-PCR results for the cloacal swabs CONTINUED

Treatment Group	Bird no.	3 dpc		5 dpc		7 dpc	
		Quantity (EID ₅₀ /ml)	Log ₁₀ (EID ₅₀ /ml)	Quantity (EID ₅₀ /ml)	Log ₁₀ (EID ₅₀ /ml)	Quantity (EID ₅₀ /ml)	Log ₁₀ (EID ₅₀ /ml)
Group C: Unvaccinated Challenged Control	10281	15,93	1,20	43,25	1,64	1869,11	3,27
	10282	0	0	6347,43	3,80	41476,40	4,62
	10283	111513,07	5,05	31,47	1,50	4545,92	3,66
	10284	536,67	2,73	0	0	0	0
	10285	218,51	2,34	44,61	1,65	56846,61	4,75
	10286	393,60	2,60	43,07	1,63	0	0
	10287	34,78	1,54	0	0	164478,55	5,22
	10288	0	0	203,78	2,31	19538,41	4,29
	10289	28,50	1,45	259587,94	5,41	12332,07	4,09
	10290	0	0	140705,81	5,15	31383,62	4,50
			11274,11	1,69	40700,73	2,31	33247,07
Group D: Unvaccinated Unchallenged Control	10291	0	0	0	0	0	0
	10292	0	0	0	0	0	0
	10293	0	0	0	0	0	0
	10294	0	0	0	0	0	0
	10295	0	0	0	0	0	0
	10296	0	0	0	0	0	0
	10297	0	0	0	0	0	0
	10298	0	0	0	0	0	0
	10299	0	0	0	0	0	0
	10300	0	0	0	0	0	0
			0	0	0	0	0

At 3 dpc, the mean group titre of Group A was 0.25 log₁₀ EID₅₀/ml, the mean group titre of Group B was 0.18 log₁₀ EID₅₀/ml, the mean group titre of Group C was 1.69 log₁₀ EID₅₀/ml, and there was no viral shedding detected in Group D (Table 5.6). Although there appeared to be more virus shed from Group C than from Group A or B, there were no statistical differences between the means of Groups A, B, and C (Fig. 5.7).

At 5 dpc, the mean group titre of Group A was 0.99 log₁₀ EID₅₀/ml, the mean group titre of Group B was 0.81 log₁₀ EID₅₀/ml, the mean group titre of Group C was 2.31 log₁₀ EID₅₀/ml and there was no viral shedding detected in Group D (Table 5.6). While there appeared to be more virus shed from Group C than from Groups A or B, there were no statistical differences between the means of Groups A, B, and C (Fig. 5.7).

At 7 dpc, the mean group titre of Group A was 0.67 log₁₀ EID₅₀/ml, the mean group titre of Group B was 1.36 log₁₀ EID₅₀/ml, the mean group titre of Group C was 3.44 log₁₀ EID₅₀/ml, and there was no viral shedding detected in Group D (Table 5.6). There appeared to be more virus shed from Group B than from Group A, but there was no statistical difference between the means of the two groups. There was significantly less virus shed in Group A ($P \leq 0.05$) and Group B ($P \leq 0.05$) than in Group C (Fig. 5.7)

Cloacal Swabs

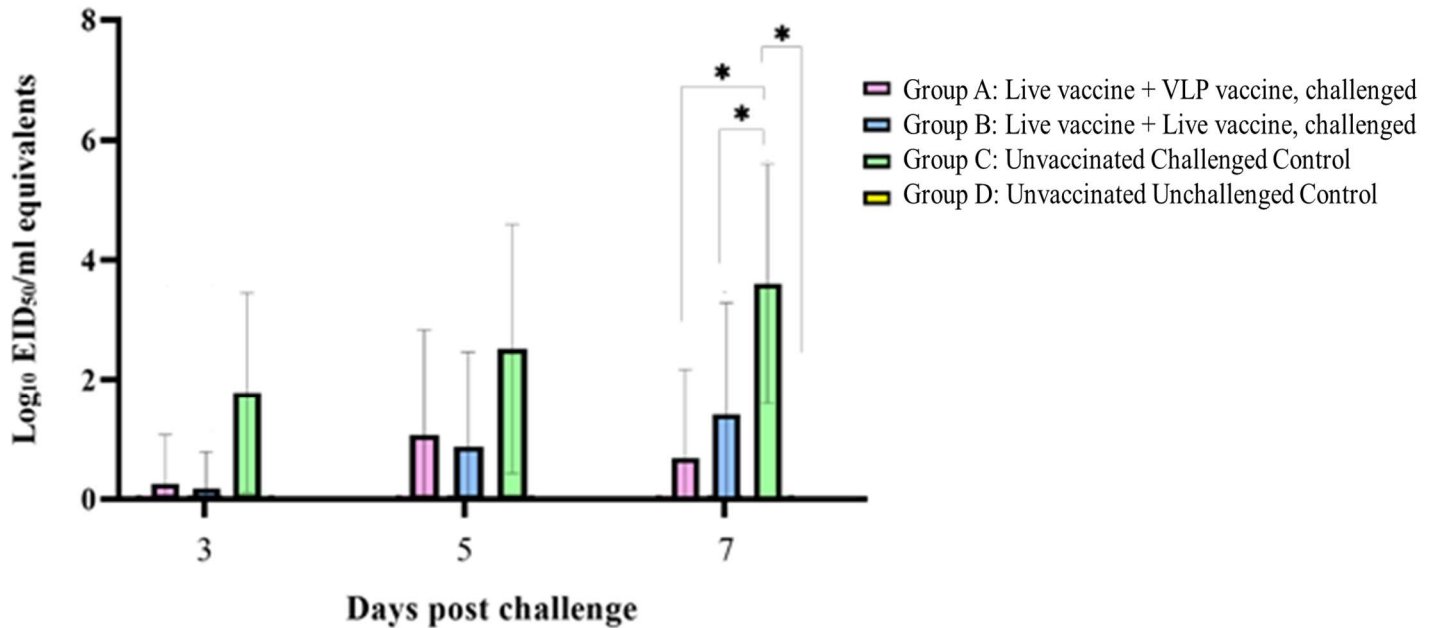


Figure 5.7. Viral RNA \log_{10} EID₅₀/ml equivalents \pm standard deviation for the cloacal swabs taken at 3, 5, and 7 days post challenge. The asterisks indicate the statistical significance * ($P \leq 0.05$), ** ($P \leq 0.01$) *** ($P \leq 0.001$) **** ($P \leq 0.0001$). Only significant differences are indicated on the graph ($P \leq 0.05$).

Both of the vaccinated groups (A and B) were able to substantially reduce viral cloacal shedding at 3, 5, and 7 days post challenge, compared to the unvaccinated challenged group (C), but this was only significant on day 7. The reduction of cloacal viral shedding appeared to be greater in Group A than in Group B on day 7, though the difference was not significant.

Table 5.7. Fold differences between the mean titres of each group on the different days post challenge for the cloacal swabs. Significant p-values are highlighted ($P < 0.05$).

		Days post challenge					
		3 dpc vs 5 dpc			5 dpc vs 7 dpc		
Group A	Mean titres (EID ₅₀ /ml)	28,77	800,41	increase	800,41	467,53	decrease
	Fold Difference	27,82			1,71		
	P value	0,19			0,54		
Group B	Mean titres (EID ₅₀ /ml)	6,35	1616,60	increase	1616,60	1373,64	decrease
	Fold Difference	254,72			1,18		
	P value	0,34			0,82		
Group C	Mean titres (EID ₅₀ /ml)	11274,11	40700,73	increase	40700,73	33247,07	decrease
	Fold Difference	3,61			1,22		
	P value	0,38			0,83		

There was no significant ($P > 0.05$) reduction in viral shedding between 3, 5, and 7 dpc for Group A. The viral shedding appeared to increase from day 3 to day 5, and then decrease on day 7 (Table 5.7).

For Group B, the viral shedding from day 3 through to day 7 appeared to increase, but the increase was not significant ($P > 0.05$) (Table 5.7).

The viral shedding for Group C increased from day 3 through to day 5, although the increase was not significant ($P > 0.05$) (Table 5.7).

Group D showed no viral shedding on days 3, 5, or 7 post challenge (Fig. 5.7).

These results show that while vaccinating the birds with the live-attenuated vaccine and boosting with the VLP vaccine was able to decrease viral shedding (particularly on day 7), vaccinating twice with the live-attenuated vaccine showed an increase in viral shedding from day 3 to day 7 post challenge, although the viral shedding was still lower than that seen in the unvaccinated challenged group (C). Not vaccinating the birds leads to increased viral shedding between days 3 and 5 which only begins to decrease after day 7.

5.3.5. Ciliary Motility Scoring

Table 5.8. Ciliary motility scores

Group A: Live vaccine + VLP vaccine, challenged													
Bird no.	Upper			Middle				Lower			Ciliostasis Score (Out of 40)	Average Protection Score	Total # of +ve birds
241	0	0	2	0	0	0	0	1	1	1	5		
244	0	1	0	0	0	0	0	0	1	0	2		
245	2	0	2	0	0	2	2	0	2	2	12		
246	0	0	0	0	0	1	0	1	1	1	4		
247	0	0	0	0	0	0	0	2	2	0	2		
248	0	0	0	0	0	0	0	0	0	0	0		
249	0	0	0	0	0	0	0	2	0	0	2		
250	0	2	0	0	0	0	0	0	0	0	2		
252	0	1	1	0	0	0	0	0	0	0	2		
254	1	1	0	0	0	2	2	2	1	2	11		
											42	79	10/10 (100 %)
Group B: Live vaccine + Live vaccine, challenged													
Bird no.	Upper			Middle				Lower			Ciliostasis Score (Out of 40)	Average Protection Score	Total # of +ve birds
264	3	3	2	0	0	1	0	1	1	1	12		
265	0	0	1	2	0	0	1	1	0	2	7		
267	1	0	1	1	0	0	0	0	1	0	4		
270	1	1	1	2	2	2	1	1	2	2	15		
272	0	0	0	0	0	0	0	0	0	1	1		
274	1	0	1	0	0	0	1	0	0	0	3		
276	2	2	2	0	0	0	1	1	1	1	10		
277	0	1	0	0	1	0	0	0	0	0	2		
279	0	0	0	1	1	0	0	0	0	1	3		
280	0	1	2	2	1	2	1	0	0	0	9		
											66	67	10/10 (100 %)

Table 5.8. Ciliary motility scores CONTINUED

Group C: Unvaccinated Challenged Control													
Bird no.	Upper			Middle				Lower			Ciliostasis Score (Out of 40)	Average Protection Score	Total # of +ve birds
281	2	3	3	3	3	3	3	2	3	3	28		
282	2	3	3	3	3	3	3	3	3	3	29		
283	4	4	4	4	3	4	4	4	4	4	39		
284	4	3	3	3	3	4	4	3	2	3	32		
285	3	3	3	3	3	3	3	4	4	3	32		
286	4	4	4	4	4	3	3	4	4	4	38		
287	4	4	4	3	3	3	4	4	4	4	37		
288	3	3	3	3	3	3	3	3	3	4	31		
289	3	3	3	3	4	3	3	4	4	3	33		
290	2	2	3	4	3	4	4	4	4	3	33		
											332	-66	0/10 (0 %)
Group D: Unvaccinated Unchallenged Control													
Bird no.	Upper			Middle				Lower			Ciliostasis Score (Out of 40)	Average Protection Score	Total # of +ve birds
291	0	0	0	0	0	0	0	0	0	0	0		
292	0	0	0	0	0	0	0	0	0	0	0		
293	0	0	0	0	0	2	2	2	0	0	6		
294	1	0	0	0	0	0	1	0	0	0	2		
295	0	0	0	0	0	0	0	0	0	0	0		
296	1	3	1	0	0	0	0	0	0	0	5		
297	2	0	4	0	3	0	0	3	4	0	16		
298	0	4	0	2	0	0	0	0	0	0	6		
299	0	0	0	0	0	0	0	0	0	0	0		
300	0	0	0	0	0	0	0	0	0	0	0		
											29	85,5	10/10 (100 %)

All the individual birds in Groups A (Live vaccine + VLP vaccine, challenged), B (Live vaccine + Live vaccine, challenged), and D (Unvaccinated Unchallenged Control) obtained a ciliostasis score lower than 20 (Table 5.8). All the birds in Group C (Unvaccinated Challenged Control) obtained a ciliostasis above 20, which indicated a lack of protection. The average protection score for the birds in Group A was 79, while the average protection score for the birds in Group B was 67 (Table 5.8). This suggested that the birds in Group A were more protected against ciliary damage than the birds in Group B, although both vaccinated groups were well protected. The average protection score for the birds in Group D was 85.5, which was unsurprising as the birds had not been exposed to any live virus (Table 5.8). The average protection score for the birds in Group C was -66 (Table 5.8); these birds were unvaccinated and challenged with the live virus, and although the ciliary motility was severely affected, the birds showed no obvious respiratory signs, but this is not unusual for SPF birds infected with IBV under experimental conditions.

5.3.6. Clinical Signs

None of the birds showed any clinical signs of infection at any point after viral challenge. There were also no noticeable adverse vaccine effects post vaccination throughout the trial.

5.4. Discussion

In this chapter, a novel plant-produced IB VLP vaccine was assessed for its efficacy in conferring protective immunity against live IBV challenge with a homologous QX-like challenge virus in SPF chickens. This was done using a prime-boost vaccination strategy using a combination of live-attenuated vaccines (Ma5 and 4-91) for comparison, since the combination of live-attenuated and inactivated variant IB vaccines is a standard practice in the field.

It had previously been determined that this QX-like challenge virus does not produce obvious clinical signs in SPF chickens when challenged under experimental conditions (Abolnik, 2014), therefore, the lack of clinical signs seen in this study was anticipated. The safety of this novel vaccine was demonstrated, as seen by a lack of adverse vaccine side-effects in the chickens. Live-attenuated vaccines also induce local immunity and protect the upper respiratory tract from infection, therefore, the challenge virus may not have been able to invade the trachea to cause infection (Abd El-Hamid *et al.*, 2018). The mix of live-attenuated vaccines used in this trial is commonly used in South Africa to protect flocks against QX-like variants.

Both of the vaccinated groups were able to elicit strong IBV group-specific antibody responses in the chickens after immunisation which were greatly increased after challenge with the live virus. While not statistically significant, there appeared to be a higher antibody response to viral challenge in the birds that were primed with the live-attenuated vaccine and boosted with the plant-produced VLP vaccine than in the birds that received two immunisations with the live-attenuated vaccine. While live-attenuated vaccines are able to elicit strong local immunity that is able to protect the respiratory tract from infection and keep that protection at a high level for an extended period of time (i.e., during the laying period), inactivated vaccines are reportedly able to induce high levels of serum antibody and protect the kidneys, internal tissues, and reproductive tract (Jackwood and de Wit, 2013). In particular, inactivated variant vaccines (such as VLPs), offer higher levels of protection against challenge with live IBV variant strains than inactivated vaccines produced from classical variants (Ladman *et al.*, 2002). This may explain the higher antibody response seen after viral challenge, as the VLP vaccine was homologous with the live IBV challenge strain. The IDEXX IBV antibody test kit was used to detect group-specific IBV antibodies (which would detect the more abundant IBV proteins that exist in all serotypes, such as IBV-N, and IBV-M). Because this is not a genotype-specific ELISA, these results are not an accurate reflection of the serotype-specific immunity afforded

by the VLP vaccine which would provide more S protein specific antibodies capable of protecting against antigenically-matched IBV variants. By comparison, the live-attenuated vaccines, which contained abundant and conserved M and N proteins (the VLP vaccine does not), would likely have been strongly detected by this ELISA kit regardless of how serotypically different the vaccine strain was to the challenge virus. This ELISA essentially only binds antibody to group-specific antigens, and does not accurately measure S-specific antibodies, which may explain why there was no significant difference between the antibody titres of the two groups prior to challenge. An S protein specific ELISA may have provided a more accurate measurement of the neutralising S protein specific antibodies that were elicited by the VLP vaccine, however, as of yet, there is no S protein specific ELISA commercially available. Attempts were made to develop an S-protein specific ELISA by expressing either the S1 subunit or conserved S-protein epitopes in *N. benthamiana* plants were unsuccessful (data not shown). Yin *et al.*, (2021) synthesised and used a 20-mer peptide, SCPYVSYGRFCIQPDGSIKQ found in the S2 subunit of the IBV spike protein (CK/CH/2010/JT1 strain), as the coating antigen for an S-protein peptide-based ELISA (pELISA). The pELISA demonstrated the ability to detect antibodies against different IBV serotypes, and was highly specific, sensitive, and accurate when compared to a commercially available ELISA kit (Yin *et al.*, 2021). Wu and co-workers (2019b) identified several conserved peptide epitopes in the S2 subunit of the spike protein of several IBV strains and identified 16R in the S2 subunit as a key amino acid that mediates S2 protein antigenicity. The peptides with the 16R were shown to react with sera against a variety of IBV strains, while a commercially available IBV antibody test kit was not able react with sera against all IBV strains (Wu *et al.*, 2019b). Attempts at expressing synthetic designs of these epitopes in this study for the purpose of developing an S-protein peptide-based ELISA, were unsuccessful (data not shown). Serotype-specific antibodies may be passed on to progeny which is beneficial in the long term (Jackwood and de Wit, 2013) and because humoral immunity results in the generation of memory B-cells, there would be potential lifelong immunity against re-infection (Janeway *et al.*, 2001). In a recent study by de Wit and co-workers (2022) investigating the efficacy of an IBV vaccination programme that included two live-attenuated vaccines and three different inactivated vaccines available commercially, with each of them containing antigen against a minimum of one IBV strain, it was found that efficient priming with a live virus contributes immensely to the protection offered against IBV (de Wit *et al.*, 2022). The use of inactivated IBV vaccines offered significant protection against five IBV challenge strains. There was an increase in the titre of virus neutralising (VN) antibodies against all the IBV

antigens following boosting with the inactivated vaccine at 15 weeks. All three of the inactivated vaccines were able to induce both homologous and heterologous virus-neutralising antibody responses (de Wit *et al.*, 2022). The birds that had only received the live-attenuated vaccine showed increased VN titres against all five antigens when compared to the birds that had not been vaccinated, but the increase was much lower than the increase detected in the birds that had also been boosted with one of the three inactivated vaccines (de Wit *et al.*, 2022). It is possible that similar results could have been obtained for this study, had a VN test or a serotype-specific ELISA been used instead of the group specific ELISA used in this study. The level of VN antibodies may not have been accurately measured by the ELISA thus giving the impression that the group vaccinated with the live-attenuated and boosted with the VLP vaccine gave similar antibody responses to the group that received two immunisations with the live-attenuated vaccine.

The HI test showed that both vaccinated groups showed seroconversion with high HI titres but the difference between the two groups was not statistically significant. This was surprising as the virus used for the HI test was homologous with the VLP vaccine. The HI test measures S protein specific antibodies, and may be highly specific to a particular IBV strain following a single exposure, however, once birds have been exposed to the virus multiple times (i.e. following vaccination, as was the case in this study), there are varying levels of cross-reactions with different serotypes, which makes it difficult to differentiate between different strains (Cook *et al.*, 1987; Gelb and Jackwood, 2008). Because the HI test can detect cross-reactive antibodies, it suffers from a lack of sensitivity, because it is essentially a serotype-specific reaction. It has further been found, that even in SPF flocks, a small number of birds within the flock may exhibit a non-specific titre of 2^4 , although this is usually in birds that are over 1 year in age, and because the sera from those birds have been in contact with several IBV strains contain antibodies that may display cross-reactivity against strains that are antigenically distinct, a cut-off of 2^4 would most likely be too low (a titre of 2^4 or higher is considered positive for the HI test) (WOAH, 2018a).

Both of the vaccinated groups were able to substantially reduce oropharyngeal and cloacal shedding compared to the unvaccinated challenged control group with the most significant reduction in cloacal shedding being apparent on day 7 post challenge. Group A (Live vaccine + VLP vaccine, challenged) appeared to provide better reduction in cloacal shedding at day 7 than Group B (Live vaccine + Live vaccine, challenged), though the difference was not statistically significant. Challenging vaccinated chickens with a homologous virus has been

shown to result in less viral shedding for shorter periods of time, than in unvaccinated birds, while the extent of protection against heterologous challenge tends to vary (Jackwood and de Wit, 2013; Cook *et al.*, 1986; Pensaert and Lambrechts, 1994). There have been previous reports of IBV persisting long terms specifically in the cecal tonsils as well as in faeces (Naqi *et al.*, 2003). A study showed that IBV strain Delmarva (DMV)/1639 demonstrated continuous cloacal viral shedding even after 16 weeks, which was linked to high viral loads in the cecal tonsils (Hassan *et al.*, 2021). In this study, the birds in the unvaccinated challenged control group displayed increasing levels of cloacal viral shedding from day 3 to 7, with significant amounts of virus still being shed at that point. This persistent cloacal shedding can potentially aid in the persistent spread of IBV by means of fomites, which highlights the need to vaccinate chickens against IBV to prevent viral spread and to protect the chickens from respiratory and reproductive disease. The ability of a vaccine to significantly reduce viral shedding from the cloaca is therefore important and valuable in preventing the further spread of disease.

The birds that were primed with the live-attenuated vaccine and boosted with the VLP vaccine had a higher average ciliary protection score than the birds that received two immunisations with the live-attenuated vaccine, while the birds in the unvaccinated challenged control group demonstrated a complete lack of protection. While both vaccines offered adequate protection against viral challenge (Andrade *et al.*, 1982), it appears that the plant-produced VLP vaccine was superior to the live-attenuated vaccine in protecting the tracheal cilia after viral infection, which is important in a flock where other pathogens that infect the trachea are also present.

While vaccine efficacy is determined by the vaccine's ability to cause a reduction in disease under carefully controlled conditions (WOAH, 2012), its effectiveness is determined by its ability to cause a reduction in disease within the field (Parida, 2009; Simon and Vonkorff, 1995). In other words, this study was able to determine the efficacy of the VLP vaccine, however, its effectiveness would need to be determined by vaccinating a flock that is not under strictly controlled conditions. Challenge studies under strictly controlled conditions do not factor in the variation that will inevitably be found under field conditions (Knight-Jones *et al.*, 2014). This includes the variation that will be experienced when mass vaccinating entire flocks (Jackwood and de Wit, 2013) as well as the bird type, flock size, management of vaccine intake by each bird, susceptibility to other pathogens, or exposure to secondary bacterial infections (Cook *et al.*, 1986; Matthijs *et al.*, 2003).

FINAL CONCLUSIONS AND FUTURE PERSPECTIVES

The control of Infectious Bronchitis Virus (IBV) is highly dependent on developing adequate vaccination strategies. This involves knowing what strain is circulating in a particular region, identifying protectotype vaccines that are capable of protecting against more than one variant of IBV at a time, and being able to keep up with emerging variants as they arise (Butcher *et al.*, 2022). Because IBV has a high rate of mutation, new variants emerge faster than most vaccine production lines are able to keep up with (de Wit *et al.*, 2011). Every time a new variant emerges, new vaccines need to be made that can protect against them (Meeusen *et al.*, 2007).

Vaccines that are egg-based have disadvantages including animal ethics issues that stem from the sacrifice of live embryos during the process of vaccine production, safety, as well as ensuring access to an adequate supply of SPF eggs available for attenuation (Vaughn *et al.*, 2009). It also takes time to isolate and adapt field viruses to the high titre growth properties that are required to produce inactivated variant vaccines (Vaughn *et al.*, 2009) and it can take up to a year to produce live-attenuated vaccines (Jordan, 2017).

IBV VLPs produced in plants have the potential to replace traditional whole inactivated virus vaccines due to their ability to be modified to closely match any circulating variant in the field, if the spike (S) protein sequence is known. The process of developing plant-produced VLPs is much easier, safer and more cost-effective than the process of developing live-attenuated or traditional whole inactivated virus vaccines. Once the S protein gene sequence of interest is obtained, which nowadays is easily achieved with direct next generation sequencing on clinical samples without the need to isolate the virus, bulk doses of VLPs can very quickly be manufactured and purified within just two weeks of infiltrating the agrobacterium cultures containing the cloned synthetic spike gene (Lai and Chen, 2012; Huang *et al.*, 2009).

VLPs can be produced in plants within 1 – 2 weeks of obtaining the S protein gene sequence for the strain of interest (Ukrami *et al.*, 2017; Huang *et al.*, 2009; Lai and Chen, 2012). They can induce both humoral and cellular immunity (Ukrami *et al.*, 2017; Zdanowicz and Chroboczek, 2016), compared to traditional whole inactivated virus vaccines which only induce humoral immunity (Bande *et al.*, 2016). While a prime-boost vaccination strategy offers the most optimal protection against IBV challenge (Box *et al.*, 1988; de Wit *et al.*, 2011), the VLP vaccine produced in this study was shown to induce high levels of serum antibody against the IBV spike protein on its own after a single immunisation in chickens. In contrast, traditional

whole inactivated virus vaccines are not as effective at stimulating local and cell-mediated immunity as well as modified live-attenuated IBV vaccines do on their own without prior priming with a live-attenuated vaccine (Butcher *et al.*, 2022).

In this study, the first successful production of Infectious Bronchitis Virus VLPs using a plant-based protein expression system was achieved. IB VLPs were successfully produced using *Agrobacterium*-mediated gene transfer in *Nicotiana benthamiana* plants and the resultant VLPs closely resembled native IBV particles in size and morphology. Modifying the native S protein with stabilising proline mutations (Pallesen *et al.*, 2017), and modifying the native TM and CT sequences with those of the NDV F protein allowed for the highest levels of protein expression and the most abundant VLP assembly. This VLP vaccine was able to induce high HI titres in chickens within two weeks after immunising with just 5 µg (S protein content) of the VLP preparation. In a prime-boost vaccination study, the VLP vaccine led to seroconversion with high HI titres in chickens comparable to those induced in the birds vaccinated twice with the live-attenuated vaccine. Comparably high levels of S protein specific antibodies were detected in both the VLP vaccinated birds and the birds vaccinated with the live-attenuated vaccine compared to the unvaccinated challenged control. The VLP vaccine was able to reduce both oropharyngeal and cloacal viral shedding in chickens after challenge with the live virus at a level comparable to the reduction seen in the chickens vaccinated with the live-attenuated vaccine, however, the birds that were vaccinated with the live-attenuated vaccine and boosted with the VLP vaccine displayed higher ciliary motility scores after viral challenge than those that were twice vaccinated with the live-attenuated vaccine, which suggested that the VLP vaccine was able to protect the respiratory system more effectively than the live-attenuated vaccine was. There were no clinical signs seen in any of the chickens after challenge which is unsurprising as the QX-like challenge virus (ck/ZA/3665/11) does not produce observable clinical signs in SPF chickens that have been challenged under experimental conditions (Abolnik, 2014).

While the results suggest that the level of protection offered by the VLP vaccine and the live-attenuated vaccine were similar, the added advantages offered by the VLP vaccine, such as safety, modifiability, and production speed compared to the method required to produce live-attenuated vaccines gives the VLP vaccine an edge over the live-attenuated vaccine

Overall, vaccinating the birds, either with the live-attenuated vaccine followed by the VLP vaccine, or with two immunisations of the live-attenuated vaccine, was able to fully protect the

birds from respiratory infection, substantially reduce both oropharyngeal and cloacal shedding, and elicit high titres of IBV group-specific antibodies capable of protecting the birds from IBV infection. The VLP vaccine was able to elicit S-specific antibodies (being homologous with the challenge virus), however, the assays used in this study were neither sensitive enough (HI) nor specific enough (ELISA and HI) to accurately measure the level produced. Therefore, while the study was able to determine that the VLP did afford protection against viral challenge, it was unable to accurately determine the extent of protection offered. More specific tests (such as an S-specific) ELISA would most likely be able to give more insight to the level of neutralising antibodies elicited by the VLP vaccine versus the live-attenuated vaccine.

While IB VLPs have been produced in a baculovirus-mediated insect cell expression system, plant-produced VLPs are less complex, prompt to produce, cost-effective, and a safe vaccine alternative. Plant-based transient protein expression is the safest, quickest, and most affordable recombinant protein platform at present (D'Aoust *et al.*, 2008). While traditional pharmaceutical manufacturing methods are found to be inadequate, plant-based expression systems can be utilized in situations requiring prompt responses and are easily scalable (Rybicki, 2009; Stoger *et al.*, 2014). They allow new vaccines to be produced quickly that are able to keep up with new emerging variants, making them particularly appealing in developing countries that do not currently have the infrastructure for producing pharmaceuticals traditionally and are thus most negatively affected by infectious diseases (Ma *et al.*, 2013; Hefferon, 2013; Rybicki *et al.*, 2013).

Currently, the yield of the QX-like IBV VLP vaccine produced in this study was calculated to be 3352 single 5 µg doses per kilogram of leaf material harvested from the plants. Further optimisation of extraction and purification methods has the potential to improve this yield. Many viral glycoproteins tend to be expressed in low levels, which may possibly be because of a shortage of essential viral molecular chaperone proteins that are needed to enhance proper protein folding (Margolin *et al.*, 2018). In coronaviruses, the M protein has been reported to interact with cytoskeletal elements (Wang *et al.*, 2009). This interaction suggests that actin plays a role in the replication cycle of IBV (Kong *et al.*, 2010). Studies done by Kong *et al.*, (2010) revealed that tubulin and actin formed part of the IBV particle which pointed to their role in moving necessary viral components to sites of assembly. Actin and tubulin are categorised as the key folding substrates for Chaperonin containing TCP-1 (CCT). In eukaryotic cytosolic chaperones, CCT is thought to play a part in assisting a small set of proteins with their folding. This means that it might be indispensable for the assembly of IBV

proteins (Kong *et al.*, 2010). Heat-shock proteins (HSPs) have multiple functions including driving protein folding and unfolding, preventing cytosolic protein accumulation, participating in signalling and vesicular transport processes. The majority of HSPs are considered molecular chaperones and many viruses make use of the host cell's molecular chaperones for many steps in the viral life cycle including entry, replication, and assembly (Mayer, 2005; Maggioni and Braakman, 2005). Li *et al.*, (2020) reported that HSP90 β had a stabilising effect on the nucleoprotein of MERS-CoV. HSP90 β was found to be crucial for viral replication. It was also shown that viral proteins were highly dependent on HSP90. When the HSP90 β was removed from the MERS-CoV gene sequence, the result was suppressed replication, as well as inhibited spread of the virus (Li *et al.*, 2020). IBV particles have been shown to incorporate HSP70 and HSP90 (Kong *et al.*, 2010) therefore it is possible that co-expression with HSP90 might enhance the expression of IB VLPs, although further studies would be needed to confirm this. A study performed by Margolin *et al.*, (2020) revealed that the co-expression of human calreticulin as a chaperone resulted in a dramatic increase in the expression of the SARS CoV-2 spike protein (Margolin *et al.*, 2020). Co-expression with a molecular chaperone may lead to improved expression levels, and increased VLP yield. Further optimisation of the neuraminidase treatment method for the VLPs in order to grant them haemagglutination ability may also prove useful for quantifying the VLPs more accurately using HA tests (Ruano *et al.*, 2000). It may be possible to determine the concentration of a particular VLP-associated protein using Western blots, provided a purified protein version of the VLP protein of interest is available, or if a known concentration of a source of the particular protein is available, and lastly, an antibody that is specific to the protein of interest is required (McGinnes and Morrison, 2014). Quantification may also be achieved by the detection of radioactively labelled proteins within the VLP proteins. This would require radioactively labelled VLPs to be generated (McGinnes and Morrison, 2014).

While the method of administration is still the same as for traditional whole inactivated virus vaccines, namely by intramuscular injection, there are numerous other means of administration that can be investigated which would make the mass-application of plant-produced vaccines more accessible in future. For example, powdered vaccine formulations that can be used for quicker and easier mucosal vaccination in larger flocks (Tomar *et al.*, 2018).

The ability to accurately assess the comparative efficacy of the IBV VLP vaccines here was limited by the circumstances produced in the highly controlled environment of isolators, where the birds are pressure and temperature controlled, which is very different from the

circumstances seen under field conditions. Bwala and co-workers (2018) designed a co-infection challenge model with the QX-like IB virus in order to assess the protective efficacy of *Mycoplasma gallisepticum* (MG) in chickens against a virulent MG field strain found in South Africa. Co-infecting the chickens with the QX-like IBV strain was done to mimic field conditions where flocks would typically be challenged by a number of other disease-causing microorganisms. The co-infection model allowed the protective effects of two MG vaccines to be assessed with more pronounced clinical signs (unlike the lack of clinical signs seen under controlled conditions), both macro and micro pathological lesions, as well as the quantitative distribution of tissue of the pathogens after challenge (Bwala *et al.*, 2018). Both MG vaccines were able to cause a reduction in clinical signs after infection with both the virulent MG and the IBV strain, both showed decreased protection against clinical disease, decreased tracheal lesion scores as well as mucosal thickness, with surprising non-specific protection against challenge with IBV. This could be a useful model for assessing the VLP vaccines in future. It would also be interesting to see if the mIBV-S2P VLP vaccines with native TM and/or CT sequences replaced with the equivalent IAV HA or NDV F protein sequences produced in this study (or different modifications thereof that would potentially expose antigenic parts of the IAV or NDV sequences) would offer any protection against those two pathogens were they included in a co-infection model with IBV. The chimeric IBV-NDV VLP vaccine produced by Wu and co-workers was able to offer protection against both NDV and IBV challenge (Wu *et al.*, 2019a). Further animal trials would need to be done in order to assess such a co-infection challenge model, or to assess the ability of the chimeric vaccines produced in this study to offer dual protection.

The use of a virus-neutralising test may offer a more accurate measurement of the level of virus-neutralising antibodies elicited by the VLP vaccine than the ELISA or the HI test was able to, however, as mentioned, these are only available for a limited number of serotypes. It may also be possible to successfully produce an S protein specific ELISA using conserved epitopes that is capable of measuring the level of S protein specific antibodies elicited by the vaccine. This would require the identification of conserved epitopes in the spike protein and their successful expression and purification for their use as the antigen in the ELISA assay.

Determining humoral immunity is vital for the control of poultry viral diseases, but it does not relate to the level of protection offered against IBV (Collisson *et al.*, 2000). Studies have shown that the evaluation of cellular immune responses is important for identifying the level of immune protection against viral avian diseases. Cell-mediated immunity plays a critical role in

controlling viral infections in avian species (Hao *et al.*, 2021). Increased activity of cytotoxic T lymphocytes (CTL) in splenocytes are associated with a decrease in IBV viral load in the kidneys and lungs of infected chickens (Collisson *et al.*, 2000). These cytotoxic T cells are important in the early phases of IBV immune responses and are responsible for the *in vivo* clearance of the virus (Liu *et al.*, 2012; (Collisson *et al.*, 2000). There are methods for assessing T-cell immunity in infected or vaccinated chickens including intracellular cytokine staining (ICS), enzyme-linked immunospot assay (ELISPOT), proliferation assays, as well as adapted and validated flow cytometry, which are all safe to use in birds (Hao *et al.*, 2021). The initial replication of IBV occurs in the Harderian Glands (HG) (Chousalkar *et al.*, 2007) which is where IBV specific IgA antibodies would be secreted following exposure to IBV (van Ginkel *et al.*, 2008). Conjunctiva-associated lymphoid tissues (CALT) may also be associated with mucosal immune protection in the eyes of infected birds (van Ginkel *et al.*, 2012) and may be the main site for the assessment of cytotoxic IBV immune responses.

South Africa has a history (longer than 20 years) of research into molecular pharming which is supported by major government-linked funders (Murad *et al.*, 2020). The Technology Innovation Agency (TIA) and the Department of Science and Innovation (DSI) have made substantial grants to two of the groups that are involved in this area of research, being the type of novel biotechnology that interests South Africa's National Bio-Economy Strategy (<https://mg.co.za/special-reports/2022-05-13-towards-true-impact-by-the-technology-innovation-agency-in-line-with-south-africas-bio-economy-strategy/#:~:text=The%20strategy%20seeks%20to%20use,financial%20resources%2C%20in%20infrastructure%20and%20knowledge>). Bio Pharms is a small-scale biopharming facility in Cape Town that is used as a model for the government to invest in new technologies (Murad *et al.*, 2020). CapeBio™ is South Africa's leading biotechnology company, with a proprietary large-scale bio-manufacturing process for enzymes and kits used in the field of molecular research (<https://capebios.com/about-us/>). The regulation and approval of pharmaceuticals in S.A. have been well-established. With all this in mind, although South Africa still has a long way to go in improving its capacity for producing plant vaccines, there are projects in the pipelines, as well as companies capable of meeting the supply and demand for resources needed to make significant advances in plant molecular pharming.

The results of this research demonstrate the safety and efficacy of the plant-produced VLP vaccine produced in this study and suggest that it may be a very promising alternative to vaccines currently available for IBV control. Plant-produced IB VLP vaccines have great

potential to improve the health of poultry worldwide. The ability to very speedily produce safe homologous variant vaccines against IBV cost-effectively and scale them up to meet agricultural needs, even in low to middle income countries, offers a much needed solution for dealing with continuously emerging IBV variants.

REFERENCES

- Abd El-Hamid, H. S., Ellakany, H. F., Ibrahim, M. S., Tahoun, A. Y., Elbestawy, A. R., Elgohary, H. K. (2018). Evaluation of Protection Spectrum Provided Against Two Infectious Bronchitis Virus Isolates Using Some Commercially Available Vaccines. *Alexandria Journal of Veterinary Sciences*. Vol **57** (1). 98 – 105.
- Abdel-Moneim, A. S. (2017). Coronaviridae: Infectious Bronchitis Virus. In: Bayry, J. (eds) *Emerging and Re-emerging Infectious Diseases of Livestock*. Springer, Cham.
- Abolnik, C. (2014). Challenge model for an IBV QX-like strain isolated in RSA. Technical Report, University of Pretoria.
- Abolnik, C. (2015). Genomic and single nucleotide polymorphism analysis of infectious bronchitis coronavirus. *Infection, genetics and evolution* **32**. 416-424.
- Abolnik, C., O’Kennedy, M., Murphy, M. A., and Wandrag D. B. R. (2022). Efficacy of a plant-produced clade 2.3.4.4 H5 influenza virus-like particle vaccine in layer hens. *Veterinary Vaccine* **1**. 1 – 10.
- Abozeid, H. H., Paldurai, A., Varghese, B. P., Khattar, S. K., Afifi, M. A., Zouelfakkar, S., El-Deeb, A. H., El-Kady, M. F., and Samal, S. K. (2019). Development of a recombinant Newcastle disease virus-vectored vaccine for infectious bronchitis virus variant strains circulating in Egypt. *Vet Res*. **50** (1). 12.
- Adams, G. (2020) A beginner’s guide to RT-PCR, qPCR and RT-qPCR. *Biochem (Lond)* **42** (3). 48–53.
- Adeyemi, M., Bwala, D. G., and Abolnik, C. (2018). Comparative evaluation of the pathogenicity of *Mycoplasma gallinaceum* in chickens. *Avian Diseases* **62**. 1-7.
- Ahmed, H. N. (1954). Incidence and treatment of some infectious viral respiratory diseases of poultry in Egypt. [PhD thesis]. Egypt: Faculty of Veterinary Medicine, Cairo University.
- Alexander, D. H., and Collins, M. S. (1975). Effect of pH on the growth and cytopathogenicity of avian infectious bronchitis virus in chick kidney cells. *Arch Virol*. **49** (4). 339-348.
- Andoh, K., Suenaga, K., Sakaguchi, M., Yamazaki, K., and Honda, T. (2015). Decreased neutralizing antigenicity in IBV S1 protein expressed from mammalian cells. *Virus Res*. **208**. 164-170.
- Andrade, L. F., Villegas, P., Fletcher, O. J., and Laudencia, R. (1982). Evaluation of Ciliary Movement in Tracheal Rings to Assess Immunity against Infectious Bronchitis Virus. *Avian Diseases* **26** (4). 805-815.
- Archetti, I., and Horsfall, F. L. (1950). Persistent antigenic variation of influenza A viruses after incomplete neutralization *in vivo* with heterologous immune serum. *J Exp Med*. **92**. 441–462.

- Asokan, G. V. (2009). Epidemiological assessment of vaccine efficacy. *Veterinary World* **2** (3). 118-122.
- Avery, R. J., and Niven, J. (1979). Use of antibodies to purified Newcastle disease virus glycoproteins for strain comparisons and characterizations. *Infect. Immun.* **26**. 795-801.
- Bande, F., Arshad, S. S., Bejo, M. H., Moeini, H., and Omar, A. R. (2015). Progress and challenges toward the development of vaccines against avian infectious bronchitis. *Journal of Immunology Research*. Vol. **2015**. 1-12.
- Bande, F., Arshad, S. S., Bejo, M. H., Kadkhodaei, S., and Omar, A. R. (2016). Prediction and In Silico Identification of Novel B-Cells and T-Cells Epitopes in the S1-Spike Glycoprotein of M41 and CR88 (793/B) Infectious Bronchitis Virus Serotypes for Application in Peptide Vaccines. *Advances in Bioinformatics* **2016**. 1-5.
- Battisti, A. J., Meng, G., Winkler, D. C., McGinnes, L. W., Plevka, P., Steven, A. C., Morrison, T. G., and Rossmann, M. G. (2012). Structure and assembly of a paramyxovirus matrix protein. *Proc Natl Acad Sci* **109**. 13996-14000.
- Bijlenga, G., Cook, J. K., Gelb Jr, J., and de Wit, J. J. (2004). Development and use of the H strain of avian infectious bronchitis virus from the Netherlands as a vaccine: a review. *Avian Pathology* **33**. 55 - 557.
- Binns, M. M., Boursnell, M. E., Cavanagh, D., Pappin, D. J., and Brown, T. D. (1985). Cloning and sequencing of the gene encoding the spike protein of the coronavirus IBV. *Journal of General Virology* **66** (pt 4). 719-726.
- Blokhina, E. A., Kupriyanov, V. V., Ravin, N. V., and Skryabin, K. G. (2013). The Method of Noncovalent in vitro Binding of Target Proteins to Virus-Like Nanoparticles Formed by Core Antigen of Hepatitis B. Virus. *Dokl Akad Nauk* **448**. 719–721.
- Bochkov, Y. A., Batchenko, G. V., Shcherbakova, L. O., Borisov, A. V., and Drygin, V. V. (2006). Molecular epizootiology of avian infectious bronchitis in Russia. *Avian Pathology* **35**. 379 - 393.
- Boonstra, S. Blijleven, J. S., Roos, W. H., Onck, P. R., van der Giessen, E., and van Oijen, A. M. (2018). Hemagglutinin-Mediated Membrane Fusion: A Biophysical Perspective. *Annual review of biophysics* **47**. 153-173.
- Bosch, B. J., van der Zee, R., de Haan, C. A., and Rottier, P. J. (2003). The coronavirus spike protein is a class I virus fusion protein: structural and functional characterization of the fusion core complex. *Journal of virology* **77**. 8801–8811.
- Boursnell, M. E. G., Brown, T. D. K., Foulds, I. J., Green, P. F., Tomley, F. M., and Binns, M. M. (1987). Completion of the sequence of the genome of the coronavirus avian infectious bronchitis virus. *Journal of General Virology* **68**. 57-77.
- Box, P. G., Beresford, A. V., and Roberts, B. (1980). Protection of laying hens against infectious bronchitis with inactivated emulsion vaccines. *Vet Rec* **106**. 264-268.
- Box, P. G., and Ellis, K. R. (1985). Infectious bronchitis in laying hens: interference with response to emulsion vaccine by attenuated live vaccine. *Avian Pathol* **14**. 9-22.

- Box, P. G., Holmes, H. C., Finney, P. M., and Froymann, R. (1988). Infectious bronchitis in laying hens: the relationship between haemagglutination inhibition antibody levels and resistance to experimental challenge. *Avian Pathol.* **17**. 349–361.
- Britton, P., Evans, S., Dove, B., Davies, M., Casais, R., and Cavanagh, D. (2005). Generation of a recombinant avian coronavirus infectious bronchitis virus using transient dominant selection. *J. Virol. Methods* **123**. 203–211.
- Broadfoot, D. I., Pomeroy, B. S., and Smith Jr, W. M. (1954). Effect of infectious bronchitis on egg production. *J Am Vet Med Assoc* **124**. 128-130.
- Butcher, G. D., Winterfield, R. W., and Shapiro, D. P. (1990). Pathogenesis of H13 nephropathogenic infectious bronchitis virus. *Avian Dis* **34**. 916-921.
- Butcher, G. D., Shapiro, D. P., and Miles, R. D. (2022). Infectious Bronchitis Virus: Classical and Variant Strains. *Veterinary Medicine* VM127.
- Bwala, D. G., Solomon, P., Duncan, N., Wandrag, D. B. R., and Abolnik, C. (2018). Assessment of *Mycoplasma gallisepticum* vaccine efficacy in a co-infection challenge model with QX-like infectious bronchitis virus. *Avian Pathology*.
- Callison, S. A., Hilt, D. A., Boynton, T. O., Sample, B. F., Robison, R., Swayne, D. E., and Jackwood, M. W. (2006). Development and evaluation of a real-time Taqman RT-PCR assay for the detection of infectious bronchitis virus from infected chickens. *Journal of Virol Methods* **138**. 60-65.
- Casais, R., Thiel, V., Siddell, S.G., Cavanagh, D., and Britton, P. (2001). Reverse genetics system for the avian coronavirus infectious bronchitis virus. *J. Virol.* **75**. 12359-12369.
- Casais, R., Dove, B., Cavanagh, D., and Britton, P. (2003). Recombinant avian infectious bronchitis virus expressing a heterologous spike gene demonstrates that the spike protein is a determinant of cell tropism. *Journal of Virology* **77**. 9084-9089.
- Castilho, A., Strasser, R., Stadlmann, J., Grass, J., Jez, J., Gattinger, P., Kunert, R., Quendler, H., Pabst, M., Leonard, R., Altmann, F., and Steinkellner, H. (2010). In planta protein sialylation through overexpression of the respective mammalian pathway. *J. Biol. Chem.* **285**. 15923-15930.
- Castilho, A., and Steinkellner, H. (2012). Glyco-engineering in plants to produce human-like N-glycan structures. *Biotechnology Journal* **7**. 1088-1098.
- Caton, A. J., Brownlee, G. G., Yewdell, J. W., and Gerhard, W. (1982). The antigenic structure of the influenza virus A/PR/8/34 hemagglutinin (H1 subtype). *Cell* **31**. 417-427.
- Cavanagh, D., Davis, P. J., Darbyshire, J. H., and Peters, R. W. (1986). Coronavirus IBV: virus retaining spike glycopolyptide S2 but not S1 is unable to induce virus-neutralizing or haemagglutination-inhibiting antibody, or induce chicken tracheal protection. *Journal of General Virology* **67** (pt 7). 1435-1442.
- Cavanagh, D., Elus, M. M., and Cook, J. K. A. (1997). Relationship between sequence variation in the S1 spike protein of infectious bronchitis virus and the extent of cross-protection *in vivo*. *Avian Pathology* **26** (1). 63-74.

- Cavanagh, D. (2001). A nomenclature for avian coronavirus isolates and the question of species status. *Avian Pathol.* **30**. 109–115.
- Cavanagh, D. (2003). Severe acute respiratory syndrome vaccine development: experiences of vaccination against avian infectious bronchitis coronavirus. *Avian Pathology* **32**. 567-582.
- Cavanagh, D. (2007). Coronavirus avian infectious bronchitis virus. *Veterinary Research* **38**. 281-297.
- Cavanagh, D., and Gelb Jr, J. (2008). Infectious Bronchitis. In Saif, Y. M., Fadly, A. M., Glisson, J. R., McDougald, L. R., Nolan, L. K., Swayne, D. E. (Eds). *Diseases of Poultry*. Wiley-Blackwell, Ames, IA, USA, 117 - 135.
- Chen, B. J., Leser, G. P. Morita, E. and Lamb, R. A. (2007). Influenza virus hemagglutinin and neuraminidase, but not the matrix protein, are required for assembly and budding of plasmid-derived virus-like particles. *J. Virol.* **81**. 7111–7123.
- Chen, C., Compans, R. W., and Choppin, P. W. (1971). Parainfluenza virus surface projections: glycoproteins with hemagglutinin and neuraminidase activities. *J. Gen. Virol.* **11**. 53-58.
- Chen, Q., Dent, M., Hurtado, J., Stahnke, J., McNulty, A., Leuzinger, K., and Lai, H. (2006). Transient protein expression by agroinfiltration in lettuce. *Methods Mol Biol* **1385**. 55-67.
- Chilton, M. D., Drummond, M. H., Merlo, D. J., Sciaky, D., Montoya, A. L., Gordon, M. P., and Nester, E. W. (1977). Stable incorporation of plasmid DNA into higher plant cells: the molecular basis of crown gall tumorigenesis. *Cell* **11**(2). 263-271.
- Chong, K. T., and Apostolov, K. (1982). The pathogenesis of nephritis in chickens induced by infectious bronchitis virus. *J Comp Pathol* **92**. 199-211.
- Chousalkar, K. K., Roberts, J. R., and Reece, R. (2007). Comparative histopathology of two serotypes of infectious bronchitis virus (T and N1/88) in laying hens and cockerels. *Poult. Sci.* **86**. 50–58.
- Christie, P. J. (2009). Agrobacterium and plant cell transformation. *Encyclopaedia of Microbiology* (Third edition). Academic press. 1-16.
- Collisson, E. W., Pei, J., Dzielawa, J., and Seo, S. H. (2000). Cytotoxic T lymphocytes are critical in the control of infectious bronchitis virus in poultry. *Developmental & Comparative Immunology.* **24**. 187–200.
- Colman, P. M., and Lawrence, M. C. (2003). The structural biology of type 1 viral membrane fusion. *Nat. Rev. Mol. Cell Biol.* **4**. 309–316.
- Compton, S. R., Barthold, S. W., and Smith, A. L. (1993). The cellular and molecular pathogenesis of coronaviruses. *Lab Anim Sci.* **43**. 15–28.
- Cook, J. K. A., Smith, H.W., and Huggins, M. B. (1986). Infectious bronchitis immunity: its study in chickens experimentally infected with mixtures of infectious bronchitis virus and *Escherichia coli*. *J Gen Virol.* **67**. 1427–1434.

- Cook, J. K. A., Brown, A. J., and Bracewell, C. D. (1987). Comparison of the hemagglutination inhibition test and the serum neutralization test in tracheal organ cultures for typing infectious bronchitis virus strains. *Avian Pathol.* **16**. 505–511.
- Cook, J. K. A., Orbell, S. J., Woods, M. A., and Huggins, M. B. (1999). Breadth of protection of the respiratory tract provided by different live-attenuated infectious bronchitis vaccines against challenge with infectious bronchitis viruses of heterologous serotypes. *Avian Pathol.* **28**. 477–485.
- Cook, J. K. A., Jackwood, M., and Jones, R. C. (2012). The long view: 40 years of infectious bronchitis research. *Avian Pathology* **41**. 239-250.
- Copeland, C.S., Doms, R.W., Bolzau, E.M., Webster, R.G. and Helenius, A. (1986). Assembly of influenza hemagglutinin trimers and its role in intracellular transport. *Journal of Cellular Biology* **103**. 1179 – 1191.
- Corse, E., and Machamer, C. E. (2003). The cytoplasmic tails of infectious bronchitis virus E and M proteins mediate their interaction. *Virology* **312**. 25-34.
- Cumming, R. B. (1963). Infectious avian nephrosis (uraemia) in Australia. *Austral Vet J* **39**. 145-147.
- Cumming, R. B. (1969). The control of avian infectious bronchitis/ nephrosis in Australia. *Austral Vet J* **45**. 200-203.
- D'Aoust, M., Lavoie, P., Couture, M. M., Trépanier, S., Guay, J., Dargis, M., Mongrand, S., Landry, N., Ward, B. J., and Vézina, L. (2008). Influenza virus-like particles produced by transient expression in *Nicotiana benthamiana* induce a protective immune response against a lethal viral challenge in mice. *Plant Biotechnology Journal* **6**. 930-940.
- da Silva, A. P., Aston, A. E., Chiwanga, G. H., Birakos, A., Muhairwa, A. P., Kayang, B. B., Kelly, T., Zhou, H., and Gallardo, R. A. (2020). Molecular characterization of Newcastle disease viruses isolated from chickens in Tanzania and Ghana. *Viruses* **12** (916). 1-14.
- Darbyshire, J. H. (1979). Assessment of cross-immunity dm chickens to strains of avian infectious bronchitis virus using tracheal organ cultures. *Avian Pathol.* **9**. 179-183.
- Darbyshire, J. H., and Peters, R. W. (1984). Sequential development of humoral immunity and assessment of protection in chickens following vaccination and challenge with avian infectious bronchitis virus. *Res. Vet. Sci.* **37**. 77–86.
- Darteil, R., Bublot, M., Laplace, E., Bouquet, J.F., Audonnet, J.C., and Rivière, M. (1995). Herpesvirus of turkey recombinant viruses expressing infectious bursal disease virus (IBDV) VP2 immunogen induce protection against an IBDV virulent challenge in chickens. *Virology* **211**. 481–490.
- de Groot, R. J., Baker, S. C., Baric, R., Enjuanes, L., Gorbalenya, A. E., Holmes, K. V., Perlman, S., Poon, L., Rottier, P. J. M., Talbot, P. J., Woo, P. C. Y., and Ziebuhr, J. (2011). Coronaviridae, in: King, A.M.Q., Adams, M.J., Carstens, E.B., Lefkowitz, E.J. (Eds.), *Virus Taxonomy: Ninth Report of the International Committee on Taxonomy of Viruses*. Elsevier Academic Press, San Diego. 774-796.

de Groot, R. J., Baker, S. C., Baric, R., Enjuanes, L., Gorbalenya, A. E., Holmes, K. V., Perlman, S., Poon, L., Rottier, P. J. M., Talbot, P. J., Woo, P. C. Y., and Ziebuhr, J. (2012). *Family Coronaviridae*. Academic Press: San Diego, CA, USA.

de Haan, C. A., Vennema, H., and Rottier, P. J. (2000). Assembly of the coronavirus envelope: Homotypic interactions between the M proteins. *Journal of Virology* **74**. 4967-4978.

de Wit, J. J., (2000). Detection of infectious bronchitis. *Avian Pathol.* **29**. 71–93.

de Wit, J. J., Cook, J. K., and van der Heijden, H. M. (2011). Infectious bronchitis virus variants: a review of the history, current situation and control measures. *Avian Pathology* **40**. 223-235.

de Wit, J. J. S., and Cook, J. K. A. (2014). Factors influencing the outcome of infectious bronchitis vaccination and challenge experiments. *Avian Pathology* **43** (6). 485-497.

de Wit, J. J. S., and Cook, J. K. A. (2019). Spotlight on avian pathology: infectious bronchitis virus. *Avian Pathology*. **48** (5). 393-395.

de Wit, J. J. S., de Herdt, P., Cook, J. K. A., Andreopoulou, M., Jorna, I., and Koopman, H. C. R. (2022). The inactivated infectious bronchitis virus (IBV) vaccine used as booster in layer hens influences the breadth of protection against challenge with IBV variants. *Avian Pathology* Vol. **51** (3). 244-256.

Dennis, S. J., O'Kennedy, M. M., Rutkowska, D., Tsekoa, T., Lourens, C. W., Hitzeroth, I. I., Meyers, A. E., and Rybicki, E. P. (2018a). Safety and immunogenicity of plant-produced African horse sickness virus-like particles in horses. *Vet Res.* **49** (1). 105.

Dennis, S. J., Meyers, A. E., Guthrie, A. J., Hitzeroth, I. I., and Rybicki, E. P. (2018b). Immunogenicity of plant-produced African horse sickness virus-like particles: implications for a novel vaccine. *Plant Biotechnol J.* **16** (2). 442-450.

Dhinaker Raj, G., and Jones, R. C. (1997). Infectious bronchitis virus: Immunopathogenesis of infection in the chicken. *Avian Pathol.* **26**. 677–706.

Eissa, Y. M., Zaher, A., Nafai, E. (1963). Studies on respiratory diseases. Isolation of infectious bronchitis virus. *J Arab Vet Med Ass* **23**. 381.

Ekiert, D. C., Bhabha, G., Elsliger, M. A., Friesen, R. H., Jongeneelen, M., Throsby, M., Goudsmit, J., and Wilson, I. A. (2009). Antibody recognition of a highly conserved influenza virus epitope. *Science* **324**. 246-251.

El-Houadfi, M., and Jones, R. C. (1985). Isolation of avian infectious bronchitis viruses in Morocco including an enterotropic variant. *Vet Rec* **116**. 445.

Enjuanes, L., Zuñiga, S., Castaño-Rodríguez, C., Gutierrez-Alvarez, J., Canton, J., and Sola, I. (2016). Molecular basis of coronavirus virulence and vaccine development. *Adv. Virus Res.* **96**. 245-286.

Etteradossi, N., and Britton, P. (2013). Avian infectious bronchitis. In: Biological Standards Commission, editor. Manual of diagnostic tests and vaccines for terrestrial animals. Paris World Organization for Animal Health.

European pharmacopoeia. (2012) Evaluation of efficacy of veterinary vaccines and immunosera. Ch. 5.2.7, 8th edition, Version 8.2).

Falchieri, M., Lupini, C., Cecchinato, M., Catelli, E., Kontolaimou, M., and Naylor, C. J. (2013). Avian metapneumoviruses expressing Infectious Bronchitis virus genes are stable and induce protection. *Vaccine* **31**. 2565–2571.

Fan, W., Tang, N., Dong, Z., Chen, J., Zhang, W., Zhao, C., He, Y., Li, M., Wu, C., Wei, T., Huang, T., Mo, M., and Wei, P. (2019). Genetic Analysis of Avian Coronavirus Infectious Bronchitis Virus in Yellow Chickens in Southern China over the Past Decade: Revealing the Changes of Genetic Diversity, Dominant Genotypes, and Selection Pressure. *Viruses* **11**, 898.

Faulkner, O. B., Estevez, C., Yu, Q., and Suarez, D. L. (2013). “Passive antibody transfer in chickens to model maternal antibody after avian influenza vaccination”. *Veterinary Immunology and Immunopathology* **152** (3-4). 341–347.

Faye, L., Boulaflous, A., Benchabane, M., Gomord, V., and Michaud, D. (2005). Protein modifications in the plant secretory pathway: current status and practical implications in molecular pharming. *Vaccine* **23**. 1770-1778.

Gallardo, R. A. (2021). Infectious bronchitis virus variants in chickens: evolution, surveillance, control and prevention. *Austral J Vet Sci* **53**. 55-62.

Gelb, J. Jr., Perkins, B. E., Rosenberger, J. K. and Allen, P. H. (1981). Serologic and cross-protection studies with several infectious bronchitis virus isolates from Delmarva-reared broiler chickens. *Avian Diseases* **25**. 655–666.

Gelb, J. Jr., and Jackwood, M. W. (2008). Infectious Bronchitis. In: A laboratory manual for the isolation, identification and characterization of avian pathogens. 5th ed. L. Dufour-Zavala, D. E. Swayne, J. R. Glisson, J. E. Pearson. W. M. Reed, M. W. Jackwood, and P. Woolcock, eds. *American Association of Avian Pathologists*, Kennett Square, PA. 146 - 149.

Giritch, A., Marillonnet, S., Engler, C., van Eldik, G., Botterman, J., Klimyuk, V., and Gleba, Y. (2006). Rapid high-yield expression of full-size IgG antibodies in plants coinfecting with noncompeting viral vectors. *Proc Natl Acad Sci* **103** (40). 14701-14706.

Godet, M., L'Haridon, R., Vautherot, J. F., and Laude, H. (1992). TGEV corona virus ORF4 encodes a membrane protein that is incorporated into virions. *Virology*. **188** (2). 666-675.

Gong, F., Giddings, T. H., Meehl, J. B., Staehelin, L. A., and Galbraith, D. W. (1996). Z-membranes: Artificial organelles for overexpressing recombinant integral membrane proteins. *Proc. Natl. Acad. Sci. USA* **93**. 2219-2223.

Goodin, M. M., Zaitlin, D., Naidu, R. A., and Lommel, S. A. (2008). *Nicotiana benthamiana*: Its history and future as a model for plant-pathogen interactions. *Molecular Plant-Microbe Interactions* **21** (8). 1015-1026.

Gravel, K. A., McGinnes, L. W., Reitter, J., and Morrison, T. G. (2011). The transmembrane domain sequence affects the structure and function of the Newcastle Disease Virus fusion protein. *Journal of Virology* **85** (7). 3486-3497.

- Gui, M., Song, W., Zhou, H., Xu, J., Chen, S., Xiang, Y., and Wang, X. (2017). Cryo-electron microscopy structures of the SARS-CoV spike glycoprotein reveal a prerequisite conformational state for receptor binding. *Cell research* **27**. 119–129.
- Guo, Z., Wang, H., Yang, T., Wang, X., Lu, D., Li, Y., and Zhang, Y. (2010). Priming with a DNA vaccine and boosting with an inactivated vaccine enhance the immune response against infectious bronchitis virus. *J. Virol. Methods* **167**. 84–89.
- Haagmans, B. L., van den Brand, J. M. A., Raj, V. S., Volz, A., Wohlsein, P., Smits, S. L., Schipper, D., Bestebroer, T. M., Okba, N., Fux, R., Bensaid, A., Foz, D. S., Kuiken, T., Baumgärtner, W., Segalés, J., Sutter, G., and Osterhaus, A. D. M. E. (2016). An orthopoxvirus-based vaccine reduces virus excretion after MERS-CoV infection in dromedary camels. *Science* **351**. 77–81.
- Hagemeyer, M. C., Verheije, M. H., Ulasli, M., Shaltiel, I. A., de Vries, L. A., Reggiori, F., Rottier, P. J., and de Haan, C. A. (2010). Dynamics of coronavirus replication-transcription complexes. *J Virol.* **84**. 2134–2149.
- Hager, K. J., Pérez Marc, G., Gobeil, P., Diaz, R. S., Heizer, G., Llapur, C., Makarkov, A. I., Vasconcellos, E., Pillet, S., Riera, F., Saxena, P., Geller Wolff, P., Bhutada, K., Wallace, G., Aazami, H., Jones, C. E., Polack, F. P., Ferrara, L., Atkins, J., Boulay, I., Dhaliwall, J., Charland, N., Couture, M. M. J., Jiang-Wright, J., Landry, N., Lapointe, S., Lorin, A., Mahmood, A., Moulton, L. H., Pahmer, E., Parent, J., Séguin, A., Tran, L., Breuer, T., Ceregido, M. A., Koutsoukos, M., Roman, F., Namba, J., D’Aoust, M. A., Trepanier, S., Kimura, Y., Ward, B. J. CoVLP Study Team (2022). Efficacy and Safety of a Recombinant Plant-Based Adjuvanted Covid-19 Vaccine. *The New England Journal of Medicine*, **386** (22), 2084–2096.
- Hanada K., Suzuki, Y., and Gojobori, T. (2004). A large variation in the rates of synonymous substitution for RNA viruses and its relationship to a diversity of viral infection and transmission modes. *Molecular Biology and Evolution* **21**. 1074 – 1080.
- Hanson, R. P., and Brandly. C. A. (1955). Identification of vaccine strains of Newcastle disease virus. *Science* **122**. 156-157.
- Hao, X., Zhang, F., Yang, Y. Y., and Shang, S. (2021). The evaluation of cellular immunity to avian viral diseases: Methods, Applications, and Challenges. *Frontiers in Microbiology* **12**.
- Harris, A., Cardone, G., Winkler, D. C., Heymann, J. B., Brecher, M., White, J. M., and Steven, A. C. (2006). Influenza virus pleiomorphy characterized by cryoelectron tomography. *Proc. Natl. Acad. Sci. U. S. A.* **103**.19123–19127.
- Hassan, M. S. H., Ali, A., Buharideen, S. M., Goldsmith, D., Coffin, C. S., Cork, S. C., van der Meer, F., Boulianne, M., and Abdul-Careem, M. F. (2021). Pathogenicity of the Canadian Delmarva (DMV/1639) Infectious Bronchitis Virus (IBV) on Female Reproductive Tract of Chickens. *Viruses*. **13** (12). 2488.
- Hefferon, K. (2013). Plant-derived pharmaceuticals for the developing world. *Biotechnol. J.* **8**. 1193-1202.
- Heinz, F. X., and Allison, S. L. (2001). The machinery for flavivirus fusion with host cell membranes. *Curr. Opin. Microbiol.* **4**. 450–455.

- Hodgson, T., Casais, R., Dove, B., Britton, P., and Cavanagh, D. (2004). Recombinant infectious bronchitis coronavirus Beaudette with the spike protein gene of the pathogenic M41 strain remains attenuated but induces protective immunity. *J. Virol.* **78**. 13804–13811.
- Hofstad, M. S. (1975). Immune response to infectious bronchitis vims. *Am. J. vet. Res.* **36**, 520-521.
- Hopkins, S. R., and Yoder, H. W. (1986). Reversion to virulence of chicken-passaged infectious bronchitis vaccine virus. *Avian Dis* **30**. 221-223.
- Huang, Z., Chen, Q., Hjelm, B., Arntzen, C., and Mason, H. (2009). A DNA replicon system for rapid high-level production of virus-like particles in plants. *Biotechnol. Bioeng.* **103**. 706-714.
- Ignjatovic, E. J., and Ashton, F. (1996). Detection and differentiation of avian infectious bronchitis viruses using a monoclonal antibody-based ELISA. *Avian Pathology* **25**. 721-736.
- Index of Veterinary Specialities (IVS) Desk Reference. April-June 2019, Vol **57** No.2.
- Isin, B., Doruker, P., and Bahar, I. (2002). Functional motions of influenza virus hemagglutinin: a structure-based analytical approach. *Biophys. J.* **82**. 569–581.
- Jackwood, M. W., Yousef, N. M., and Hilt, D. A. (1997). Further development and use of a molecular serotype identification test for infectious bronchitis virus. *Avian Dis.* **41**. 105–110.
- Jackwood, M. W., Hilt, D. A., and Brown, T. P. (2003). Attenuation, safety, and efficacy of an infectious bronchitis virus GA98 serotype vaccine. *Avian Dis.* **47**. 627–632.
- Jackwood, M. W., Hilt, D. A., Williams, S. M., Woolcock, P., Cardona, C., and O’Connor, R. (2007). Molecular and serologic characterization, pathogenicity, and protection studies with infectious bronchitis virus field isolates from California. *Avian Dis.* **51**. 527–533.
- Jackwood, M. W., Hilt, D. A., Sellers, H. S., Williams, S. M., and Lasher, H.N. (2010). Rapid heat-treatment attenuation of infectious bronchitis virus. *Avian Pathol.* **39**. 227–233.
- Jackwood, M. W. (2012). Review of infectious bronchitis virus around the world. *Avian Diseases Digest* **56**. 634 - 641.
- Jackwood, M. W., Hall, D., and Handel, A. (2012). Molecular evolution and emergence of avian gammacoronaviruses. *Infect. Genet. Evol* **12**. 1305-1311.
- Jackwood, M. W., and de Wit, J. J. S. (2013). Infectious Bronchitis. *Diseases of Poultry*. Chapter **4**. 139 - 153.
- Jackwood, M. W., Jordan, B. J., Roh, H., Hilt, D. A., and Williams, S. M. (2015). Evaluating Protection against Infectious Bronchitis Virus by Clinical Signs, Ciliostasis, Challenge Virus Detection, and Histopathology. *Avian Diseases* **59** (3). 368-374.
- Janeway, C. A Jr., Travers, P., Walport, M., and Shlomchik, M. J. (2001). Immunobiology: The Immune System in Health and Disease. 5th edition. New York: Garland Science. *The Humoral Immune Response*. Chapter **9**.

- Jansen, T., Hofmans, M. P., Theelen, M. J., Manders, F., and Schijns, V. E. (2006). Structure- and oil type-based efficacy of emulsion adjuvants. *Vaccine*. **24**. 5400–5405.
- Jara, M., Crespo, R., Roberts, D. L., Chapman, A., Banda, A., and Machado, G. (2021). Development of a Dissemination Platform for Spatiotemporal and Phylogenetic Analysis of Avian Infectious Bronchitis Virus. *Frontiers in Veterinary Science* **8**. Article 624233. 1-12.
- Jayaram, H., Fan, H., Bowman, B. R., Ooi, A., Jayaram, J., Collisson, E. W., Lescar, J., and Prasad, B. V. (2006). X-ray structures of the N- and C- terminal domains of a coronavirus nucleocapsid protein: implications for nucleocapsid formation. *Journal of Virology* **80**. 6612-6620.
- Jayaram, J., Youn, S., and Collisson, E. W. (2005). The virion N protein of infectious bronchitis virus is more phosphorylated than the N protein from infected cell lysates. *Virology*. **339** (1). 127-135.
- Jazayeri, S. D., and Poh, C. L. (2019). Recent advances in delivery of veterinary DNA vaccines against avian pathogens. *Vet Res* **50**. 78.
- Jennings, G. T., and Bachmann, M. F. (2008). The coming of age of virus-like particle vaccines. *Biol Chem* **389**. 521-536.
- Jia, W., Karaca, K., Parrish, C. R., and Naqi, S. A. (1995). A novel variant of avian infectious bronchitis virus resulting from recombination among three different strains. *Arch Virol* **140** (2). 259-71.
- Jiang, L., Wang, N., Zuo, T., Shi, X., Poon, K. M. V., Wu, Y., Gao, F., Li, D., Wang, R., Guo, J., Fu, L., Yuen, K., Zheng, B., Wang, X., and Zhang, L. (2014). Potent neutralization of MERS-CoV by human neutralizing monoclonal antibodies to the viral spike glycoprotein. *Sci Transl. Med.* **6**. 234 - 259.
- Johnson, M. A., Pooley, C., Ignjatovic, J., and Tyack, S. G. (2003). A recombinant fowl adenovirus expressing the S1 gene of infectious bronchitis virus protects against challenge with infectious bronchitis virus. *Vaccine*. **21**. 2730–2736.
- Jordan, B. (2017). Vaccination against infectious bronchitis virus: A continuous challenge. *Vet Microbiol.* **206**. 137-143.
- Jung, J., Zahmanova, G., Minkov, I., and Lomonosoff, G. P. (2022). Plant-based expression and characterization of SARS-CoV-2 virus-like particles presenting a native spike protein. *Plant Biotechnology Journal* **20**. 1363-1372.
- Jutras, P. V., D’Aoust, M., Couture, M. M., Vézina, L., Goulet, M., Michaud, D., and Sainsbury, F. (2015). Modulating secretory pathway pH by proton channel co-expression can increase recombinant protein stability in plants. *Biotechnology Journal* **10**. 1-9.
- Kant, A., Koch, G., van Roozelaar, D. J., Kusters, J. G., Poelwijk, F. A., and van der Zeijst, B. A. (1992). Location of antigenic sites defined by neutralizing monoclonal antibodies on the S1 avian infectious bronchitis virus glycopolyptide. *Journal of General Virology* **73** (Pt 3). 591-596.

- Karaca, K., Naqi, S., and Gelb Jr, J. (1992). Production and characterization of monoclonal antibodies to three infectious bronchitis virus serotypes. *Avian Dis.* **36**. 903–915.
- Keeler Jr, C. L., Reed, K. L., Nix, W. A., and Gelb Jr, J. (1998). Serotype identification of avian infectious bronchitis virus by RT-PCR of the peplomer (S-1) gene. *Avian Dis.* **42**. 275–284.
- Khataby, K., Kasmi, Y., Souiri, A., Loutfi, C., and Ennaji, M. M. (2020). Avian Coronavirus: Case of Infectious Bronchitis Virus Pathogenesis, Diagnostic Approaches, and Phylogenetic Relationship Among Emerging Strains in Middle East and North Africa Regions. *Emerging and Reemerging Viral Pathogens.* 729–744.
- Kim, S. H., and Samal, S. K. (2016). Newcastle disease virus as a vaccine vector for development of human and veterinary vaccines. *Viruses.* **8**. 183.
- Kirchdoerfer, R. N., Cottrell, C. A., Wang, N., Pallesen, J., Yassine, H. M., Turner, H. L., Corbett, K. S., Graham, B. S., McLellan, J. S., and Ward, A. B. (2016). Pre-fusion structure of a human coronavirus spike protein. *Nature* **531**. 118–121.
- Kirchdoerfer, R. N., Wang, N., Pallesen, J., Wrapp, D., Turner, H. L., Cottrell, C. A., Corbett, K. S., Graham, B. S., McLellan, J. S., and Ward, A. B. (2018). Stabilized coronavirus spikes are resistant to conformational changes induced by receptor recognition or proteolysis. *Scientific Reports* **8**. 1-11.
- Klumperman, J., Locker, J. K., Meijer, A., Horzinek, M. C., Geuze, H. J., and Rottier, P. J. (1994). Coronavirus M proteins accumulate in the Golgi complex beyond the site of virion budding. *Journal of virology*, **68** (10). 6523-6534.
- Knight-Jones, T. J. D., Edmond, K., Gubbins, S., and Paton, D. J. (2014). Veterinary and human vaccine evaluation methods. *Proc. R. Soc. B.* **281**. 1-10.
- Knoetze, A. D., Moodley, N., and Abolnik, C. (2014). Two genotypes of infectious bronchitis virus are responsible for serological variation in KwaZulu-Natal poultry flocks prior to 2012. *Onderstepoort Journal of Veterinary Research* **81**. 1-10.
- Koch, G., Hartog, L., Kant, A., and van Roozelaar, D. J. (1990). Antigenic domains on the peplomer protein of avian infectious bronchitis virus: correlation with biological functions. *Journal of General Virology* **71** (pt 9). 1929-1935.
- Kong, Q., Xue, C., Ren, X., Zhang, C., Li, L., Shu, D., Bi, Y., and Cao, Y. (2010). Proteomic analysis of purified coronavirus infectious bronchitis virus particles. *Proteome Science* **8** (29). 1-10.
- Kung, Y., Lee, K., Chiang, H., Huang, S., Wu, C., and Shih, S. (2022). Molecular Virology of SARS-CoV-2 and Related Coronaviruses. *Microbiology and Molecular Biology Reviews.* Vol. **86**, (No. 2). 1-21.
- Kusters J. G., Jager, E. J., Niesters, H. G. M., and van der Zeijst, B. A. M. (1990). Sequence evidence for RNA recombination in field isolates of avian coronavirus infectious bronchitis virus. *Vaccine* **8**. 605 - 608.

- Kwon, H. M., Jackwood, M. W., and Gelb, J. (1993). Differentiation of infectious-bronchitis virus serotypes using polymerase chain-reaction and restriction-fragment-length-polymorphism analysis. *Avian Dis* **37**. 194-202.
- Ladman, B. S., Pope, C. R., Ziegler, A. F., Swieczkowski, T., Callahan, C. J., Davison, S., and Gelb Jr, J. (2002). Protection of chickens after live and inactivated virus vaccination against challenge with nephropathogenic infectious bronchitis virus PA/ Wolgemuth/ 98. *Avian Dis* **46**. 938-944.
- Ladman, B. S., Loupos, A. B., and Gelb Jr, J. (2006). Infectious bronchitis virus S1 gene sequence comparison is a better predictor of challenge of immunity in chickens than serotyping by virus neutralization. *Avian Pathology* **35**. 127-133.
- Lai, H., and Chen, Q. (2012). Bioprocessing of plant-derived virus-like particles of Norwalk virus capsid protein under current Good Manufacture Practice regulations. *Plant Cell Rep* **31**. 573-584.
- Lai, M. M., and Cavanagh, D. (1997). The molecular biology of coronaviruses. *Adv Virus Res* **48**. 1-100.
- Lamb, R. A., and Kolakofsky, D., (2001). in: D.M. Knipe, P.M. Howley (Eds.). *Fields Virology*, 3rd ed., vol. 1, Lippincott-Williams & Wilkins, Philadelphia. 1305– 1340.
- Lan, J., Yao, Y., Deng, Y., Chen, H., Lu, G., Wang, W., Bao, L., Deng, W., Wei, Q., Gao, G. F., Qin, C., and Tan, W. (2015). Recombinant receptor binding domain protein induces partial protective immunity in rhesus macaques against Middle East respiratory syndrome coronavirus challenge. *EBioMedicine* **2**. 1438-1446.
- Lee, C. W., Hilt, D. A., and Jackwood, M. W. (2003). Typing of field isolates of infectious bronchitis virus based on the sequence of the hypervariable region in the S1 gene. *J. Vet. Diagn. Investig.* **15** (4). 344–348.
- Lee, H. J., Youn, H. N., Kwon, J. S., Lee, Y. J., Kim, J. H., Lee, J. B., Park, S. Y., Choi, I. S., and Song, C. S. (2010). Characterization of a novel live attenuated infectious bronchitis virus vaccine candidate derived from a Korean nephropathogenic strain. *Vaccine* **28**. 2887–2894.
- Leuzinger, K., Dent, M., Hurtado, J., Stahnke, J., Lai, H., Zhou, X., and Chen, Q. (2013). Efficient agroinfiltration of plants for high level transient expression of recombinant proteins. *Journal of Visualized experiments* **77**. 50521.
- Lewicki, D. N., and Gallagher, T. M. (2002). Quaternary structure of coronavirus spikes in complex with carcinoembryonic antigen-related cell adhesion molecule cellular receptors. *J. Biol. Chem* **277**. 19727-19734.
- Li, C., Chu, H., Liu, X., Chiu, M. C., Zhao, X., Wang, D., Wei, Y., Hou, Y., Shuai, H., Cai, J., Chan, J. F., Zhou, J., and Yuen, K. Y. (2020). Human coronavirus dependency on host heat shock protein 90 reveals an antiviral target. *Emerging Microbes and Infections*. **9** (1). 2663–72.
- Li, F. (2016). Structure, function, and evolution of coronavirus spike proteins. *Annu Rev Virol* **3**. 237–261.

- Li, H., Wang, Y., Han, Z., Wang, Y., Liang, S., Jiang, L., Hu, Y., Kong, X., and Liu, S. (2016). Recombinant duck enteritis viruses expressing major structural proteins of the infectious bronchitis virus provide protection against infectious bronchitis in chickens. *Antiviral Research* **130**. 19 - 26.
- Li, W., Joshi, M. D., Singhanian, S., Ramsey, K. H., and Murthy, A. K. (2014). Peptide vaccine: Progress and challenges. *Vaccines (Basel)* **2** (3). 515-536.
- Lin, Z., Kato, A., Kudou, Y., and Ueda, A. (1991). A new typing method for the avian infectious bronchitis virus using polymerase chain reaction and restriction enzyme fragment length polymorphism. *Archives of virology*. Vol **116** (1-4). 19-31.
- Liu, F., Wu, X., Li, L., Ge, S., Liu, Z., and Wang, Z. (2013b). Virus-like particles: Promising platforms with characteristics of DIVA for veterinary vaccine design. *Comparative Immunology, Microbiology and Infectious Diseases* **36**. 343–352.
- Liu, G., Wang, Q., Liu, N., Xiao, Y., Tong, T., Liu, S., and Wu, D. (2012). Infectious bronchitis virus nucleoprotein specific CTL response is generated prior to serum IgG. *Vet. Immunol. Immunopathol.* **148**. 353–358.
- Liu, G., Lv, L., Yin, L., Li, X., Luo, D., Liu, K., Xue, C., and Cao, Y. (2013a). Assembly and immunogenicity of coronavirus-like particles carrying infectious bronchitis virus M and S proteins. *Vaccine* **31**. 5524-5530.
- Liu, H. J., Lee, L. H., Shih, W. L., Lin, M. Y., and Liao, M. H. (2003). Detection of infectious bronchitis virus by multiplex polymerase chain reaction and sequence analysis. *Journal of Virological Methods* **109**. 31-37.
- Liu, S., Xu, Q., Han, Z., Liu, X., Li, H., and Guo, H. (2014). Origin and characteristics of the recombinant novel avian infectious bronchitis coronavirus isolate ck/CH/LJL/111054. *Infect Genet Evol* **23**. 189-195.
- Liu, Y. V., Massare, M. J., Barnard, D. L., Kort, T., Nathan, M., Wang, L., and Smith, G. (2011). Chimeric severe acute respiratory syndrome coronavirus (SARS-CoV) S glycoprotein and influenza matrix 1 efficiently form virus-like particles (VLPs) that protect mice against challenge with SARS-CoV. *Vaccine* **29**. 6606–6613.
- Lohr, J. E. (1988). Differentiation of IBV strains. Hygiene and Pathology, Proc. 1st Int. Symp. On Infectious Bronchitis, World's Poultry Science Association, European group no. 7, Rauschholzhausen, Germany. 199-207.
- Lv, L., Li, X., Liu, G., Li, R., Liu, Q., Shen, H., Wang, W., Xue, C., and Cao, Y. (2014). Production and immunogenicity of chimeric virus-like particles containing the spike glycoprotein of infectious bronchitis virus. *J. Vet. Sci* **15** (2). 209-216.
- Ma, C., Wang, L., Tao, X., Zhang, N., Yang, Y., Tseng, C. T. K., Li, F., Zhou, Y., Jiang, S., and Du, L. (2014b). Searching for an ideal vaccine candidate among different MERS coronavirus receptor-binding fragments—the importance of immunofocusing in subunit vaccine design. *Vaccine* **32**. 6170–6176.

- Ma, J. K., Christou, P., Chikwamba, R., Haydon, H., Paul, M., Ferrer, M. P., Ramalingam, S., Rech, E., Rybicki, E., Wigdorovitz, A., Yang, D. C., and Thangaraj, H. (2013). Realising the value of plant molecular pharming to benefit the poor in developing countries and emerging economies. *Plant Biotechnology Journal* **11**. 1029-1033.
- Maeda, J., Maeda, A., and Makino, S. (1999). Release of coronavirus E protein in membrane vesicles from virus-infected cells and E protein-expressing cells. *Virology*. **263** (2). 265-272.
- Maeda, J., Repass, J. F., Maeda, A., and Makino, S. (2001). Membrane topology of coronavirus E protein. *Virology*. **281** (2). 163-169.
- Magadán, J. G., Khurana, S., Das, S. R., Frank, G. M., Stevens, J., Golding, H., Bennink, J. R., and Yewdell, J. W. (2013). Influenza A Virus Hemagglutinin Trimerization Completes Monomer Folding and Antigenicity. *Journal of Virology* **87** (17). 9742-9753.
- Maggioni, C., and Braakman, I. (2005). Synthesis and quality control of viral membrane proteins. *Curr Top Microbiol Immunol* **285**. 175-198.
- Mamedov, T., Yuksel, D., Ilgin, M., Gürbüzasan, I., Gulec, B., Mammadova, G., Say, D., and Hasanova, G. (2020). Engineering, production and characterization of Spike and Nucleocapsid structural proteins of SARS-CoV-2 in *Nicotiana benthamiana* as vaccine candidates against COVID-19. bioRxiv.
- Margine, I., Hai, R., Albrecht, R. A., Obermoser, G., Harrod, A. C., Banchereau, J., Palucka, K., García-Sastre, A., Palese, P., Treanor, J. J., and Krammer, F. (2013). H3N2 influenza virus infection induces broadly reactive hemagglutinin stalk antibodies in humans and mice. *Journal of Virology* **87**. 4728-4737.
- Margolin, E., Chapman, R., Williamson, A., Rybicki, E. P., and Meyers, A. E. (2018). Production of complex viral glycoproteins in plants as vaccine immunogens. *Plant Biotechnology Journal* **16**. 1531-1545.
- Masters, P. S. (2006). The molecular biology of coronaviruses. *Adv. Virus Res.* **66**. 193–292.
- Masters, P., and Perlman, S. (2013). Coronaviridae. In: Howley, P., Knipe, D. M., (Eds). *Fields Virology*. Kluwer, Wolters. Chapter **28**. 825–858.
- Matsuoka, Y., Swayne, D. E., Thomas, C., Rameix-Welti, M. A., Naffakh, N., Warnes, C., Altholtz, M., Donis, R., and Subbarao, K. (2009). Neuraminidase stalk length and additional glycosylation of the hemagglutinin influence the virulence of influenza H5N1 viruses for mice. *J. Virol.* **83**. 4704–4708.
- Matthijs, M. G., van Eck, J. H., Landman, W. J., and Stegeman, J. A. (2003). Ability of Massachusetts-type infectious bronchitis virus to increase colibacillosis susceptibility in commercial broilers: a comparison between vaccine and virulent field virus. *Avian Pathol.* **32**. 473–481.
- Matthijs, M. G., Bouma, A., Velkers, F. C., van Eck, J. H., and Stegeman, J. A. (2008). Transmissibility of infectious bronchitis virus H120 vaccine strain among broilers under experimental conditions. *Avian Dis.* **52**. 461–466.

- Mayer, M. P. (2005). Recruitment of Hsp70 chaperones: a crucial part of viral survival strategies. *Rev Physiol Biochem Pharmacol.* **153.** 1-46.
- McAuley, J. L., Gilbertson, B. P., Trifkovic, S., Brown, L. E., and McKimm-Breschkin, J. L. (2019). Influenza Virus Neuraminidase Structure and Functions. *Frontiers in Microbiology: Virology.* Vol **10** (39).
- McGinnes, L. W., and Morrison, T. G. (2014). Newcastle disease virus-like particles: Preparation, Purification, Quantification, and Incorporation of Foreign Glycoproteins. *Curr Protoc Microbiol* **30.** 1-28.
- McKinley, E. T., Hilt, D. A., and Jackwood, M. W. (2008). Avian coronavirus infectious bronchitis attenuated live vaccines undergo selection of subpopulations and mutations following vaccination. *Vaccine* **26.** 1274–1284.
- McMartin, D. A. (1993). Infectious bronchitis. In J.B. McFerran & M.S. McNulty (Eds.), *Virus Infections of Vertebrates. Virus Infections of birds*, Vol **4.** 249–275.
- Meeusen, E. N. T., Walker, J., Peters, A., Pastoret, P-P., and Jungersen, G. (2007). Current status of veterinary vaccines. *Clin. Microbiol. Rev.* **20.** 489–510.
- Merz, D. C., Scheid, A., and Choppin, P. (1980). Importance of antibodies to the fusion glycoprotein of paramyxoviruses in the prevention of spread of infection. *J. Exp. Med.* **151.** 275-288.
- Mett, V., Musiychuk, K., Bi, H., Farrance, C. E., Horsey, A., Ugulava, N., Shoji, Y., de la Rosa, P., Palmer, G.A., Rabindran, S., Streatfield, S. J., Boyers, A., Russel, M., Mann, A., Lambkin, R., Oxford, J. S., Schild, G. C., and Yusibov, V. (2008). A plant-produced influenza subunit vaccine protects ferrets against virus challenge. *Influenza Other Respir. Viruses* **2.** 33–40.
- Mokoena, N. B., Moetlhoa, B., Rutkowska, D. A., Mamputha, S., Dibakwane, V. S, Tsekoa, T. L., and O'Kennedy, M. M. (2019). Plant-produced Bluetongue chimaeric VLP vaccine candidates elicit serotype-specific immunity in sheep. *Vaccine.* **37** (41). 6068-6075.
- Morgan, R.W., Gelb Jr., J., Schreurs, C.S., Lutticken, D., Rosenberger, J.K., and Sondermeijer, P.J. (1992). Protection of chickens from Newcastle and Marek's diseases with a recombinant herpesvirus of turkeys vaccine expressing the Newcastle disease virus fusion protein. *Avian Dis.* **36.** 858–870.
- Morley, A. J., and Thomson, D. K. (1984). Swollen-head syndrome in broiler chickens. *Avian Dis* **28.** 238-243.
- Morrison, T. G. (2003). Structure and function of a paramyxovirus fusion protein. *Biochimica et Biophysica Acta* **1614.** 73-84.
- Mou, H., Raj, V. S., van Kuppeveld, F. J., Rottier, P. J., Haagmans, B. L., and Bosch, B. J. (2013). The receptor binding domain of the new Middle East respiratory syndrome coronavirus maps to a 231-residue region in the spike protein that efficiently elicits neutralizing antibodies. *J. Virol.* **87.** 9379–9383.

- Moules, V., Ferraris, O., Terrier, O., Giudice, E., Yver, M., Rolland, J. P., Bouscambert-Duchamp, M., Bergeron, C., Ottman, M., Fournier, E., Traversier, A., Boule, C., Rivoire, A., Lin, Y., Hay, A., Valette, M., Marquet, R., Rosa-Calatrava, M., Naffakh, N., Schoehn, G., and Lina, B. (2010). In vitro characterization of naturally occurring influenza H3NA-viruses lacking the NA gene segment: toward a new mechanism of viral resistance? *Virology* **404**. 215–224.
- Mousavi, P., Mostafavi-Pour, Z., Morowvat, M. H., Nezafat, N., Zamani, M., Berenjian, A., and Ghasemi, Y. (2017). In silico analysis of several signal peptides for the excretory production of reteplase in *Escherichia coli*. *Curr. Proteom.* **14** (4). 326–335.
- Moustafa, K., Makhzoum, A., and Tremouillaux-Giller, J. (2016). Molecular farming on rescue of pharma industry for next generations. *Crit. Rev. Biotechnol* **36**. 840-850.
- Murad, S., Fuller, S., Menary, J., Moore, C., Pinneh, E., Szeto, T., Hitzlerith, I., Freire, M., Taychakhoonavudh, S., Phoolcharoen, W., and Ma, J. K. C. (2020). Molecular pharming for low and middle income countries. *Current opinion in Biotechnology* **61**. 53-59.
- Muthumani, K., Falzarano, D., Reuschel, E. L., Tingey, C., Flingai, S., Villarreal, D. O., Wise, M., Patel, A., Izmily, A., Aljuaid, A., Seliga, A. M., Soule, G., Morrow, M., Kraynyak, K. A., Khan, A. S., Scott, D. P., Feldmann, F., LaCasse, R., White, K. M., Okumura, A., Ugen, K. E., Sardesai, N. Y., Kim, J. J., Kobinger, G., Feldmann, H., and Weiner, D. B. (2015). A synthetic consensus anti-spike protein DNA vaccine induces protective immunity against Middle East respiratory syndrome coronavirus in nonhuman primates. *Sci. Transl. Med.* **7**. 301-132.
- Naqi, S., Gay, K., Patalla, P., Mondal, S., and Liu, R. (2003). Establishment of persistent avian infectious bronchitis virus infection in antibody-free and antibody-positive chickens. *Avian Dis.* **47**. 594–601.
- Narayanan, K., Chen, C. J., Maeda, J., and Makino, S. (2003). Nucleocapsid-independent specific viral RNA packaging via viral envelope protein and viral RNA signal. *J Virol.* **77** (5). 2922-2927.
- Nayak, B., Kumar, S., DiNapoli, J. M., Paldurai, A., Perez, D. R., Collins, P. L., and Samal, S. K. (2010). Contributions of the Avian Influenza Virus HA, NA., and M2 Surface Protein to the Induction of Neutralizing Antibodies and Protective Immunity. *Journal of Virology* **84** (5). 2408-2420.
- Neu, K. E., Henry Dunand, C. J., and Wilson, P. C. (2016). Heads, stalks and everything else: how can antibodies eradicate influenza as a human disease? *Curr Opin Immunol* **42**. 48-55.
- Nix, W. A., Trorber, D. S., Kingdom, B. F., Keeler, J. C. L., and Gelb, J. J. (2000). Emergence of subtype strains of the Arkansas serotype of infectious bronchitis virus in Delmarva broiler chickens. *Avian Disease.* **44**. 568–581.
- Noad, R., and Roy, P. (2003). Virus-like particles as immunogens. *Trends in Microbiol* **11**. 438-444.
- O'Brien, E. P., Brooks, B. R., and Thirumalai, C. (2013). Effects of pH on proteins: Predictions for ensemble and single molecule pulling experiments. *J Am Chem Soc* **134** (2). 979-987.

- Ohmuro-Matsuyama, Y., and Yamaji, H. (2017). Modifications of a signal sequence for antibody secretion from insect cells. *Cytotechnology*. 1–8.
- O'Kennedy, M. M., Coetzee, P., Koekemoer, O., du Plessis, L., Lourens, C. W., Kwezi, L., du Preez, I., Mamputha, S., Mokoena, N. B., Rutkowska, D. A., Verschoor, J. A., and Lemmer, Y. (2022). Protective immunity of plant-produced African horse sickness virus serotype 5 chimaeric virus-like particles (VLPs) and viral protein 2 (VP2) vaccines in IFNAR^{-/-} mice. *Vaccine*. **40** (35). 5160-5169.
- Ong, H. K., Tan, W. S., and Ho, K. L. (2017). Virus like particles as a platform for cancer vaccine development. *Peer J*. 1-31.
- Oshop, G. L., Elankumaran, S., and Heckert, R. A. (2002). DNA vaccination in the avian. *Vet. Immunol. Immunopathol* **89**. 1–12.
- Pallesen, J., Wang, N., Corbett, K. S., Wrapp, D., Kirchdoerfer, R. N., Turner, H. L., Cottrell, C. A., Becker, M. M., Wang, L., Shi, W., Kong, W., Andres, E. L., Kettenbach, A. N., Denison, M. R., Chappel, J. D., Graham, B. S., Ward, A. B., and McLellan, J. S. (2017). Immunogenicity and structures of a rationally designed prefusion MERS-CoV spike antigen. *Proceedings of the National Academy of Sciences of the United States of America* **114**. E7348–e7357.
- Parida S. (2009). Vaccination against foot-and-mouth disease virus: strategies and effectiveness. *Expert Rev. Vaccines* **8**. 347–365.
- Pawar, K. R., and Waghmare, S. G. (2016). Agroinfiltration – effective method of gene transfer. *Biotech articles* (<https://www.biotecharticles.com/Biotech-Research-Article/Agroinfiltration-Effective-Method-of-Gene-Transfer-3735.html>).
- Pensaert, M., and Lambrechts, C. (1994). Vaccination of chickens against a Belgian nephropathogenic strain of infectious bronchitis virus B1648 using attenuated homologous and heterologous strains. *Avian Pathology* **23**. 631 – 641.
- Perchetti, G. A., Huang, M, Peddu, V., Jerome, K. R., and Greninger, A. L. (2020). Stability of SARS-CoV-2 in Phosphate-Buffered Saline for Molecular Detection. *Journal of Clinical Microbiology* **58** (8).
- Perlman, S., Gallagher, T., and Snijder, E. J. (2008). *Nidoviruses*. ASM Press, Washington, DC.
- Peyret, H., Steele, J. F. C., Jung, J. W., Theuenemann, E. C., Meshcheriakova, Y., and Lomonosoff, G. P. (2021). Producing Vaccines against Enveloped Viruses in Plants: Making the Impossible, Difficult. *Vaccines* **9** (7). 780.
- Pogue, G. P., Vojdani, F., Palmer, K. E., Hiatt, E., Hume, S., Phelps, J., Long, L., Bohorova, N., Kim, D., Pauly, M., Velasco, J., Whaley, K., Zeitlin, L., Garger, S. J., White, E., Bai, Y., Haydon, H., and Bratcher, B. (2010). Production of pharmaceutical-grade recombinant aprotinin and a monoclonal antibody product using plant-based transient expression systems. *Plant Biotechnology Journal* **8**. 638-654.

- Promkuntod, N., van Eijndhoven, R. E., de Vrieze, G., Grone, A., and Verheije, M. H. (2014). Mapping of the receptor-binding domain and amino acids critical for attachment in the spike protein of avian coronavirus infectious bronchitis virus. *Virology* **448**. 26-32.
- Qin, Y., Tu, K., Teng, Q., Feng, D., Zhao, Y., and Zhang, G. (2021). Identification of novel T-cell epitopes on infectious bronchitis virus N protein and development of a multi-epitope vaccine. *Journal of Virology*, **95** (17).
- Qin, Y., Teng, Q., Feng, D., Pei, Y., Zhao, Y., and Zhang, G. (2022). Development of a Nanoparticle Multiepitope DNA Vaccine against Virulent Infectious Bronchitis Virus Challenge. *The Journal of Immunology*, **208** (6). 1396-1405.
- Raamsman, M. J. B., Locker, J. K., de Hooge, A., de Vries, A. A. F., Griffiths, G., Vennema, H., and Rottier, P. J. M. (2000). Characterization of Coronavirus mouse hepatitis virus strain A59 small membrane protein E. *J. Virol.* **74**. 2333–2342.
- Raymond, F. L., Caton, A. J., Cox, N. J., Kendal, A. P., and Brownlee, G. G. (1986). The antigenicity and evolution of influenza H1 haemagglutinin, from 1950–1957 and 1977–1983: two pathways from one gene. *Virology* **148**. 275–287.
- Roh, H. J., Jordan, B. J., Hilt, D. A., and Jackwood, M. W. (2014). Detection of infectious bronchitis virus with the use of real-time quantitative reverse transcriptase–PCR and correlation with virus detection in embryonated eggs. *Avian Diseases*, **58** (3). 398-403.
- Rosenthal, P., Zhang, X., and Formanowski, F. (1988). Structure of the haemagglutinin-esterase-fusion glycoprotein of influenza C virus. *Nature* **396**.
- Ruano, M., El-Attrache, J., and Villegas, P. (2000). A rapid-plate hemagglutination assay for the detection of infectious bronchitis virus. *Avian diseases* **44**. 99 - 104.
- Ruch, T. R., and Machamer, C. E. (2011). The hydrophobic domain of infectious bronchitis virus E protein alters the host secretory pathway and is important for release of infectious virus. *Journal of Virology* **85**. 675-685.
- Rutkowska, D. A., Mokoena, N. B., Tsekoa, T. L., Dibakwane, V. S., and O'Kennedy, M. M. (2019). Plant-produced chimeric virus-like particles - a new generation vaccine against African horse sickness. *BMC Vet Res.* **15** (1). 432.
- Rybicki, E. P. (2009). Plant-produced vaccines: promise and reality. *Drug Discov. Today* **14**. 16-24.
- Rybicki, E. P. (2010). Plant-made vaccines for humans and animals. *Plant Biotechnology Journal* **8**. 620-637.
- Rybicki, E. P., Hitzeroth, I. I., Meyers, A., Dus Santos, M. J., and Wigdorovitz, A. (2013). Developing country applications of molecular farming: case studies in South Africa and Argentina. *Curr. Pharm. Des.* **19**. 5612-5621.
- Sainsbury, F., and Lomonosoff, G. P. (2008). Extremely high level and rapid transient protein production in plants without the use of viral replication. *Plant Physiology*. **148**. 1212 - 1218.

- Sainsbury, F., Thuenemann, E. C., and Lomonossoff, G. P. (2009). pEAQ: Versatile expression vectors for easy and quick transient expression of heterologous proteins in plants. *Plant Biotechnology Journal*. **7**. 682 - 693.
- Sainsbury, F., Cañizares, M. C., and Lomonossoff, G. P. (2010). Cowpea mosaic virus: The plant virus-based biotechnology workhorse. *Annual Review of Phytopathology*, **48**. 437 - 455.
- Sainsbury, F., Saxena, P., Geisler, K., Osbourn, A., and Lomonossoff, G. P. (2012). Using a virus-derived system to manipulate plant natural product biosynthetic pathways. *Methods in Enzymology*. Volume **517**. Chapter 9. 185 - 202.
- Saléry, M. (2017). Autogenous vaccines in Europe: national approaches to authorisation. *Regulatory rapporteur, Topra*, **14** (6). 27-32.
- Samal, S. K. (Norfolk Caister Academic Press, 2011). Newcastle disease and related avian paramyxoviruses. In *The Biology of Paramyxoviruses*. (ed. Samal, S. K.) 69-114.
- Schalk, A.F., and M.C. Hawn. (1931). An apparent new respiratory disease of baby chicks. *J Am Vet Med Assoc*. **78**. 413–422.
- Scheid, A., and Choppin, P. W. (1974). Identification of biological activities of paramyxovirus glycoproteins. Activation of cell fusion, hemolysis, and infectivity by proteolytic cleavage of an inactive precursor protein of Sendai virus. *Virology* **57**. 475-490.
- Scheid, A., and Choppin, P. W. (1977). Two disulfide-linked polypeptide chains constitute the active F protein of paramyxoviruses. *Virology* **80**. 54-66.
- Seo, S. H., Wang, L., Smith, R., and Collisson, E. W. (1997). The carboxyl-terminal 120-residue polypeptide of infectious bronchitis virus nucleocapsid induces cytotoxic T lymphocytes and protects chickens from acute infection. *J Virol*. **71** (10). 7889-7894.
- Septokele, K. M. (2020). Towards producing infectious bronchitis virus-like particles in plants as potential vaccine candidates. MSc Thesis, University of Pretoria. Accessible at: <https://repository.up.ac.za/handle/2263/86941>.
- Seyfi Abad Shapouri, M. R., Mayahi, M., Assasi, K., and Charkhkar, S. (2004). A survey of the prevalence of infectious bronchitis virus type 4/91 in Iran. *Acta Veterinaria Hungarica* **52**. 163-166.
- Sheludko, Y. V., Sindarovska, Y. R., Gerasymenko, I. M., Bannikova, M. A., and Kuchuk, N. V. (2007). Comparison of several *Nicotiana* species as hosts for high scale *Agrobacterium* mediated transient expression. *Biotechnol Bioeng* **96**. 608–614.
- Shevchenko, A., Tomas, H., Havlis, J., Olsen, J. V., and Mann, M. (2007). In-gel digestion for mass spectrometric characterization of proteins and proteomes. *Nature Protocols* **1** (6). 2856-2860.
- Shirvani, E., Paldurai, A., Manoharan, V. K., Varghese, B. P., and Samal, S. K. (2018). A recombinant Newcastle disease virus (NDV) expressing S protein of infectious bronchitis virus (IBV) protects chickens against IBV and NDV. *Scientific reports* **8**. 1-14.

- Shoji, Y., Chichester, J. A., Jones, M., Manceva, S. D., Damon, E., Mett, V., Musiychuk, K., Bi, H., Farrance, C., Shamloul, M., Kushni, N., Sharma, S., and Yusibov, V. (2011). Plant-based rapid production of recombinant subunit hemagglutinin vaccines targeting H1N1 and H5N1 influenza. *Hum. Vaccin.* **7** (Suppl). 41-50.
- Siegrist, C. A. (2001). Neonatal and early life vaccinology. *Vaccine* **19**. 3331–3346.
- Simon, G. E., and Vonkorff, M. (1995). Recognition, management, and outcomes of depression in primary care. *Arch Fam Med* **4** (2). 99-105.
- Skehel, J. J., and Wiley, D. C. (2000). Receptor binding and membrane fusion in virus entry: The influenza hemagglutinin. *Annu. Rev. Biochem.* **69**. 531–569.
- Skwarczynski, M., and Toth, I. (2016). Peptide-based synthetic vaccines. *Chem. Sci.* **7** (2). 842-854.
- Smith, T., O’Kennedy, M. M., Wandrag, D. B. R., Adeyemi, M., and Abolnik, C. (2019). Efficacy of a plant-produced virus-like particle vaccine in chickens challenged with Influenza A H6N2 virus. *Plant Biotechnology Journal*. 1-11.
- Soltanialvar, M., Bagherpour, A., and Akbarnejad, F. (2016). Roll of hemagglutinin gene in the biology of avian influenza virus. *Asian Pacific Journal of Tropical Disease* **6** (6). 443-446.
- Song, C. S., Lee, Y. J., Lee, C. W., Sung, H. W., Kim, J. H., Mo, I. P., Izumiya, Y., Jang, H. K., and Mikami, T. (1998). Induction of protective immunity in chickens vaccinated with infectious bronchitis virus S1 glycoprotein expressed by a recombinant baculovirus. *Journal of General Virology* **79** (Pt. 4). 719–723.
- Song, F., Fux, R., Provacia, L. B., Volz, A., Eickmann, M., Becker, S., Osterhaus, A. D. M. E., Haagmans, B. L., and Sutter, G. (2013). Middle East respiratory syndrome coronavirus spike protein delivered by modified vaccinia virus Ankara efficiently induces virus-neutralizing antibodies. *J. Virol.* **87**. 11950–11954.
- Sriwilajaroen, N., and Suzuki, Y. (2012). Molecular basis of the structure and function of H1 hemagglutinin of influenza virus. *Proc Jpn Acad Ser B Phys Biol Sci.* **88** (6). 226-249.
- Stander, J., Chabeda, A., Rybicki, E. P., and Meyers, A. E. (2021). A Plant-Produced Virus-Like Particle Displaying Envelope Protein Domain III Elicits an Immune Response Against West Nile Virus in Mice. *Front Plant Sci.* **12**. 738619.
- Stoger, E., Fischer, R., Moloney, M., and Ma, J. K. (2014). Plant molecular pharming for the treatment of chronic and infectious diseases. *Annu. Rev. Plant Biol.* **65**. 743-768.
- Strasser, R., Stadlmann, J., Schähs, M., Stiegler, G., Quendler, H., Mach, L., Glössl, J., Weterings, K., Pabst, M., and Steinkellner, H. (2008). Generation of glycol-engineered *Nicotiana benthamiana* for the production of monoclonal antibodies with a homogeneous human-like N-glycan structure. *Plant Biotechnology Journal* **6**. 392-402.
- Su, X., Schmitz, G., Zhang, M, Mackie, R. I., and Cann, I. K. O. (2012). Chaperone – Heterologous gene expression in filamentous fungi. *Advances in Applied Microbiology*, academic press vol **81**. 1-61.

- Tan, Y. W., Fung, T. S., Shen, H., Huang, M., and Liu, D. X. (2018). Coronavirus infectious bronchitis virus non-structural proteins 8 and 12 form stable complex independent of the non-translated regions of viral RNA and other viral proteins. *Virology* **513**. 75-84.
- Tanford, C., and Roxby, R. (1972). Interpretation of protein titration curves. Application to lysozyme. *Biochemistry*. **11**. 2192–2198.
- Tang, J., Zhang, N., Tao, X., Zhao, G., Guo, Y., Tseng, C. T. K., Jiang, S., Du, L., and Zhou, Y. (2015). Optimization of antigen dose for a receptor-binding domain-based subunit vaccine against MERS coronavirus. *Hum. Vaccin. Immunother.* **11**. 1244–1250.
- Taylor, J., Edbauer, C., Rey-Senelongue, A., and Bouquet, J. (1990). Newcastle disease virus fusion protein expressed in a fowlpox virus recombinant confers protection in chickens. *Journal of Virology* **64** (4). 1441-1450.
- Temiz, S. A., Abdelmaksoud, A., Dursun, R., and Vestita, M. (2021). Acral chilblain-like lesions following inactivated SARS-CoV-2 vaccination. *Int J Dermatol.* **60** (9). 1152-1153.
- Terregino, C., Toffan, A., Beato, M. S., De Nardi, R., Vascellari, M., Meini, A., Ortali, G., Mancin, M., and Capua, I. (2008). Pathogenicity of a QX strain of infectious bronchitis virus in specific pathogen free and commercial broiler chickens, and evaluation of protection induced by a vaccination programme based on the Ma5 and 4/91 serotypes. *Avian Pathology* **37**. 487 - 493.
- Thekiso, M. M. O., Mbat, P. A., and Bisschop, S. P. R. (2003). Diseases of free-ranging chickens in the Qwa-Qwa district of the Northeastern Free State province of South Africa. *J S Afr Vet Assoc* **74**. 14-16.
- Theuenemann, E. C., Meyers, A. E., Verwey, J., Rybicki, E. P., and Lomonosoff, G. P. (2013). A method for rapid production of heteromultimeric protein complexes in plants: assembly of protective bluetongue virus-like particles. *Plant Biotechnology Journal*. 1-8.
- Toffan A., Monne, I., Terregino, C., Cattoli, G., Hodobo, C. T., Gadaga, B., Makaya, P. V., Mdlongwa, E., and Swiswa, S. (2011). QX-like infectious bronchitis virus in Africa. *Vet Rec* **169**. 589.
- Tomar, J., Biela, C., deHaan, C. A. M., Rottier, P. J. M., Petrovsky, N., Frijlink, H. W., Huckriede, A., Hinrichs, W. L. J., and Peeters, B. (2018). Passive inhalation of dry powder influenza vaccine formulations completely protects chickens against H5N1 lethal virus challenge. *European Journal of Pharmaceutics and Biopharmaceutics* **133**. 85-95.
- Toro, H., Zhang, J. F., Gallardo, R. A., van Santen, V. L., van Ginkel, F. W., Joiner, K. S., and Breedlove, C. (2014a). S1 of distinct IBV population expressed from recombinant adenovirus confers protection against challenge. *Avian Dis.* **58** (2). 211-215.
- Toro, H., Zhao, W., Breedlove, C., Zhang, Z., Yu, Q., and Van Santen, V. (2014b). Infectious bronchitis virus S2 expressed from recombinant virus confers broad protection against challenge. *Avian Dis.* **58** (1). 83-89.
- Tschofen, M., Knopp, D., Hood, E., and Stoger, E. (2016). Plant molecular farming: Much more than medicines. *Annu. Rev. Anal. Chem* (Palo Alto Calif) **9**. 271-294.

- Ujike, M., and Taguchi, F. (2015). Incorporation of Spike and Membrane glycoproteins into coronavirus virions. *Viruses* **7**. 1700-1725.
- Ukrami, A., Sakurai, A., Ishikawa, M., Yap, M. L., Flores-Garcia, Y., Haseda, Y., Aoshi, T., Zavala, F. P., Rossman, M. G., Kuno, S., Ueno, R., and Akahata, W. (2017). Development of a novel virus-like particle vaccine platform that mimics the immature form of alphavirus. *Clinical and Vaccine Immunology* Vol **24**. Issue 7. 1-14.
- Vagnozzi, A., Zavala, G., Riblet, S.M., Mundt, A., and Garcia, M. (2012). Protection induced by commercially available live-attenuated and recombinant viral vector vaccines against infectious laryngotracheitis virus in broiler chickens. *Avian Pathol.* **41**. 21–31.
- Valastro, V., Holmes, E. C., Britton, P., Fusaro, A., Jackwood, M. W., Cattoli, G., and Monne, I. (2016). S1 gene-based phylogeny of infectious bronchitis virus: An attempt to harmonize virus classification. *Infect Genet Evol.* **39**. 349-364.
- Van Aarle, P. (2010). Immunological correlates of vaccine-derived protection against FMD: the regulatory perspective. In *Vaccine efficacy: immunological correlates of vaccine derived protection*, Fondation Merieux, Veyrier-du-Lac, France, 20–22 September 2010.
- van Eck, J. H. (1983). Effects of experimental infection of fowl with EDS'76 virus, infectious bronchitis virus and/ or fowl adenovirus on laying performance. *Vet Q* **5**. 11-25.
- van Ginkel, F. W., van Santen, V. L., Gulley, S. L., and Toro, H. (2008). Infectious bronchitis virus in the chicken harderian gland and lachrymal fluid: viral load, infectivity, immune cell responses, and effects of viral immunodeficiency. *Avian Dis.* **52**. 608–617.
- van Ginkel, F. W., Gulley, S. L., Lammers, A., Hoerr, F. J., Gurjar, R., and Toro, H. (2012). Conjunctiva-associated lymphoid tissue in avian mucosal immunity. *Dev. Comp. Immunol.* **36**. 289–297.
- van Roeckel, H., Bullis, K. L., Flint, O. S., and Clarke, M. K. (1942). Poultry disease control service. Massachusetts Agricultural Experiment Station. MA Annual Report. Bulletin **388**. 99-103.
- Varghese, J. N., Laver, W. G., and Colman, P. M. (1983). Structure of the influenza virus glycoprotein antigen neuraminidase at 2.9 Å resolution. *Nature* **303**. 35–40.
- Vaughn, D. W., Whitehead, S. S., and Durbin, A. P. (2009). In, “Vaccines for Biodefense and Emerging and Neglected Diseases”. 285-324.
- Volz, A., Kupke, A., Song, F., Jany, S., Fux, R., Shams-Eldin, H., Schmidt, J., Becker, C., Eickmann, M., Becker, S., and Sutter, G. (2015). Protective efficacy of recombinant modified vaccinia virus Ankara delivering Middle East Respiratory Syndrome coronavirus spike glycoprotein. *J. Virol.* **89**. 8651–8656.
- Walls, A. C., Tortorici, M. A., Bosch, B., Frenz, B., Rottier, P. J., M., DiMaio, F., Rey, F. A., and Veisler, D. (2016a). Cryo-electron microscopy structure of a coronavirus spike glycoprotein trimer. *Nature* **531**. 114–117.

Walls, A. C., Tortorici, M. A., Frenz, B., Snijder, J., Li, W., Rey, F. A., DiMaio, F., Bosch, B., and Veessler, D. (2016b). Glycan shield and epitope masking of a coronavirus spike protein observed by cryo-electron microscopy. *Nat Struct Mol Biol*, **10**.1038.

Walls, A. C., Tortorici, M. A., Snijder, J., Xiong, X., Bosch, B., Rey, F. A., and Veessler, D. (2017). Tectonic conformational changes of a coronavirus spike glycoprotein promote membrane fusion. *Proceedings of the National Academy of Sciences of the United States of America* **114**. 11157–11162.

Walls, A. C., Xiong, X., Park, Y., Tortorici, A., Snijder, J., Quispe, J., Cameroni, A., Gopal, R., Dai, M., Lanzavecchia, A., Zamboni, M., Rey, F. A., Corti, D., and Veessler, D. (2019). Unexpected receptor functional mimicry elucidates activation of coronavirus fusion. *Cell* **176**. 1026-1039.

Wang, J., Fang, S., Xiao, H., Chen, B., Tam, J. P., and Liu, D. X. (2009). Interaction of the coronavirus infectious bronchitis virus membrane protein with betaactin and its implication in virion assembly and budding. *PLoS One* **4**. e4908.

Wang, L., Shi, W., Joyce, M. G., Modjarrad, K., Zhang, Y., Leung, K., Lees, C. R., Zhu, T., Yassine, H. M., Kanekiyo, M., Yang, Z., Chen, X., Becker, M. M., Freeman, M., Vogel, L., Johnson, J. C., Olinger, G., Todd, J. P., Bagci, U., Solomon, J., Mollura, D. J., Hensley, L., Jahrling, P., Denison, M. R., Rao, S. S., Subbarao, K., Kwong, P. D., Mascola, J. R., Kong, W., and Graham, B. S. (2015). Evaluation of candidate vaccine approaches for MERS-CoV. *Nat. Commun.* **6**. 7712.

Ward, B. J., Gobeil, P., Séguin, A., Atkins, J., Boulay, I., Charbonneau, P. Y., Couture, M., D'Aoust, M. A., Dhaliwall, J., Finkle, C., Hager, K., Mahmood, A., Makarkov, A., Cheng, M. P., Pillet, S., Schimke, P., St-Martin, S., Trépanier, S., and Landry, N. (2021). Phase 1 randomized trial of a plant-derived virus-like particle vaccine for COVID-19. *Nat Med*. **27**(6). 1071-1078.

Waterson, A. P., Pennington, T. H., and Allen, W. H. (1967). Virulence in Newcastle disease virus. A preliminary study. *Br. Med Bull.* **23**. 138-143.

Wickramasinghe, I. N. A., de Vries, R. P., Grone, A., de Haan, C. A., and Verheije, M. H. (2011). Binding of avian coronavirus spike proteins to host factors reflects virus tropism and pathogenicity. *Journal of Virology* **85**. 8903-8912.

Wickramasinghe, I. N. A., van Beurden, S. J., Weerts, E. A. W. S., and Verheije, M. H. (2014). The avian coronavirus spike protein. *Virus Research* **194**, 37 - 48.

Wiley, D. C., and Skehel, J. J. (1987). The structure and function of the hemagglutinin membrane glycoprotein of influenza virus. *Annu. Rev. Biochem.* **56**. 365–394.

Williams, A. K., Wang, L., Sneed, L. W., and Collisson, E. W. (1992). Comparative analysis of the nucleocapsid genes of several strains of infectious bronchitis virus and other coronaviruses. *Virus Res.* **25**. 213–222.

Wilson, I., and Skehel, J. (1981). Structure of the haemagglutinin membrane glycoprotein of influenza virus at 3 Å resolution. *Nature* **289**. 366–373.

Wilson, L., Gage, P., and Ewart, G. (2006). Hexamethylene amiloride blocks E protein ion channels and inhibits coronavirus replication. *Virology*. **353** (2). 294-306.

WOAH. (https://www.woah.org/en/what-we-do/standards/codes-and-manuals/terrestrial-code-online-access/?id=169&L=1&htmfile=chapitre_oie_listed_disease.htm).

WOAH (2012). Manual of diagnostic tests and vaccines for terrestrial animals 2012. Paris: World Organisation for Animal Health).

WOAH. (2018a). Terrestrial Manual. Avian Infectious Bronchitis. (Chapter 3.3.2.).

WOAH. (2018b). Terrestrial Manual. Principles of veterinary vaccine production. (Chapter 1.1.8.).

Wong, M. L., and Medrano, J. F. (2005). Real-time PCR for mRNA quantitation. *Biotechniques*, **39** (1). 75-85.

World Bank & TAFS-Forum. (2011). World livestock disease atlas: A quantitative analysis of global animal health data (H. S. N. The World Bank, Washington, DC 20433, USA Ed.). (Available online - accessed July 2022).

Wu, X., Zhai, X., Lai, Y., Zuo, L., Zhang, Y., Mei, X., Xiang, R., Kang, Z., Zhou, L., and Wang, H. (2019a). Construction and immunogenicity of novel chimeric virus-like particles bearing antigens of infectious bronchitis virus and Newcastle disease virus. *Viruses* **11** (254). 1-13.

Wu, Q., Lin, Z., Qian, K., Shao, H., Ye, J., and Qin, A. (2019b). Peptides with 16R in S2 protein showed broad reactions with sera against different types of infectious bronchitis viruses. *Veterinary Microbiology* **236**. 2-5.

Xu, L., Ren, M., Sheng, J., Ma, T., Han, Z., Zhao, Y., Sun, J., and Liu, S. (2019). Genetic and biological characteristics of four novel recombinant avian infectious bronchitis viruses isolated in China. *Virus Res.* **263**. 87-97.

Xu, P., Wu, X., Wang, H., Ma, B., Ding, M., and Yang, X. (2016). Assembly and immunogenicity of baculovirus-derived infectious bronchitis virus-like particles carrying membrane, envelope and the recombinant spike proteins. *Biotechnol Lett* **38**. 299-304.

Yang, T., Wang, H. N., Wang, X., Tang, J. N., Gao, R., Li, J, Guo, Z. C., and Li, Y. L. (2009a). Multivalent DNA vaccine enhanced protection efficacy against infectious bronchitis virus in chickens. *Journal of Veterinary Medical Science*, **71** (12). 1585-1590.

Yang, T., Wang, H. N., Wang, X., Tang, J. N., Lu, D., Zhang, Y. F., Guo, Z. C., Li, Y. L., Gao, R., and Kang, R. M. (2009b). The protective immune response against infectious bronchitis virus induced by multi-epitope based peptide vaccines. *Bioscience, Biotechnology, and Biochemistry* **73**. 1500 - 1504.

Yang, X., Zhou, Y., Li, J., Fu, L., Ji, G., Zeng, F., Zhou, L., Gao, W., and Wang, H. (2016). Recombinant infectious bronchitis virus (IBV) H120 vaccine strain expressing the hemagglutinin-neuraminidase (HN) protein of Newcastle disease virus (NDV) protects against IBV and NDV challenge. *Archives of Virology* **161**. 1209 - 1216.

- Yin, L., Zeng, Y., Wang, W., Wei, Y., Xue, C., and Cao, Y. (2016). Immunogenicity and protective efficacy of recombinant fusion proteins containing spike protein of infectious bronchitis virus and hemagglutinin of H3N2 influenza virus in chickens. *Virus Research* **223**. 206-212.
- Yin, L., Wu, Q., Lin, Z., Qian, K., Shao, H., Wan, Z., Liu, Y., Ye, J., and Qin, A. (2021). A peptide-based enzyme-linked immunosorbent assay for detecting antibodies against avian infectious bronchitis virus. *Frontiers in Veterinary Science* **7** (Article 619601). 1-7.
- Yu, D., Han, Z., Xu, J., Shao, Y., Li, H., Kong, X., and Liu, S. (2010). A novel B-cell epitope of avian infectious bronchitis virus N protein. *Viral Immunol.* **23** (2). 189-199.
- Yu, L., Jiang, Y., Low, S., Wang, Z., Nam, S. J., Liu, W., and Kwang, J. (2001). Characterization of three infectious bronchitis virus isolates from China associated with proventriculus in vaccinated chickens. *Avian Dis.* **45**. 416–424.
- Zdanowicz, M., and Chroboczek, J. (2016). Virus-like particles as drug vectors. *Acta biochimica Polonica* Vol **63**. No 3. 469–473.
- Zhang, N., Channappanavar, R., Ma, C., Wang, L., Tang, J., Garron, T., Tao, Z., Tasneem, S., Lu, L., Tseng, C. K., Zhou, Y., Perlman, S., Jiang, S., and Du, L. (2016). Identification of an ideal adjuvant for receptor-binding domain-based subunit vaccines against Middle East respiratory syndrome coronavirus. *Cell. Mol. Immunol.* **13**. 180–190.
- Zhang, Y., Wang, H. N., Wang, T., Fan, W. Q., Zhang, A. Y., Wei, K., Tian, G. B., and Yang, X. (2010). Complete genome sequence and recombination analysis of infectious bronchitis virus attenuated vaccine strain H120. *Virus Genes* **41**. 377 - 388.
- Zhao, Y., Zhang, H., Zhao, J., Zhong, Q., Jin, J. H., and Zhang, G. Z. (2016). Evolution of infectious bronchitis virus in China over the past two decades. *J. Gen. Virol.* **97**. 1566–1574.
- Zhao, R., Sun, J., Qi, T., Zhao, W., Han, Z., Yang, X., and Liu, S. (2017). Recombinant Newcastle disease virus expressing the infectious bronchitis virus S1 gene protects chickens against Newcastle disease virus and infectious bronchitis virus challenge. *Vaccine* **35** (18). 2435-2442.
- Zhou, J., Wu, J., Cheng, L., and Zheng, X. (2003). Expression of immunogenic S1 glycoprotein of infectious bronchitis virus in transgenic potatoes. *Journal of Virology* **77** (16). 9090-9093.
- Zhou, J., Cheng, L., Zheng, X., Wu, J., Shang, S., Wang, J., and Chen, J. (2004). Generation of the transgenic potato expressing full-length spike protein of infectious bronchitis virus. *Journal of Biotechnology* **111**. 121-130.
- Ziebuhr, J., Snijder, E. J., and Gorbalenya, A. E. (2000). Virus-encoded proteinases and proteolytic processing in the nidovirales. *Journal of General Virology* **81**. 853 - 879.

APPENDIX



agriculture, land reform & rural development

Department:
Agriculture, Land Reform and Rural Development
REPUBLIC OF SOUTH AFRICA

Directorate Animal Health, Department of Agriculture, Land Reform & Rural Development
Private Bag X133, Pretoria 0001

Enquiries: Mr Henry Gokals • Tel: +27 12 319 7532 • Fax: +27 12 319 7470 • E-mail: Henry.G@dairrd.gov.za
Reference: 12/15/15/16/ 1700/MO

Prof Celia Abolnik
University of Pretoria
Onderstepoort
0100
E-mail: celia.abolnick@up.ac.za

Dear Prof Celia Abolnik,

RE: PERMISSION TO DO RESEARCH IN TERMS OF SECTION 20 OF THE ANIMAL DISEASES ACT, 1984 (ACT NO. 35 OF 1984)

Your application received per email on, requesting permission under Section 20 of the Animal Disease Act, 1984 (Act No. 35 of 1984) to perform a research project or study, refers. I am pleased to inform you that permission is hereby granted to perform the following study, with the following conditions:

Conditions:


1. This permission does not relieve the researcher of any responsibility which may be placed on him by any other act of the Republic of South Africa;
2. The study is approved as per the application form dated 31 July 2020 and the correspondence thereafter. Written permission from the Director: Animal Health must be obtained prior to any deviation from the conditions approved for this study under this Section 20 permit. Please apply in writing to Henry.G@dairrd.gov.za
3. All potentially infectious material utilised, collected or generated during the study are to be destroyed at the completion of the study. A registered waste removal company must dispose the material generated from the study. Records must be kept for five years for auditing purposes;
4. Plant based infectious bronchitis (IB) plant based virus like particles (VLP) will be produced at the Council for Scientific and Industrial Research (CSIR). IB virus will not be used at this stage, but genes encoding for selected capsid

- proteins will be imported from Biostasis in Canada. A veterinary import permit must be obtained prior to importation;
5. The synthesised VLP will be taken to University of Pretoria Poultry BSL3 facility for a vaccination and challenge study;
 6. The chickens to be used in the study must be sourced from an area not under any veterinary restrictions. A letter from the state responsible of the area where the chickens will originate from must be obtained;
 7. The vaccination must only utilise VLP vaccine candidate and commercial IB vaccine. Chickens will be challenged using a local IB virus strain;
 8. All material generated by this study must be disposed at the BSL3 facility. All chickens used in the study should be euthanized;
 9. The researcher is permitted to retain constructs containing genes of interest beyond the duration of this study and should be stored at CSIR Biosciences facility. Any further use or distribution of these stored samples is subject to obtaining a separate Section 20 approval;
 10. If required, an application for an extension must be made by the responsible researcher at least one month prior to the expiry of this Section 20 approval.

Title of research/study: The production of plant-expressed virus like particle vaccines against infectious bronchitis coronavirus and efficacy in chickens.

Researcher: Miss Kamogelo Mmapitso Sepotokale
Institution: University of Pretoria,
Our ref Number: 12/11/1/1/MG
Your ref:
Expiry date: 31 December 2023

Kind regards,



DR. MPHO MAJA
DIRECTOR OF ANIMAL HEALTH
Date: 2021-03-08

SUBJECT: The production of plant-expressed virus like particle vaccines against infectious bronchitis coronavirus and efficacy in chickens



Faculty of Veterinary Science
Animal Ethics Committee

10 March 2021

**Approval Certificate
New Application**

AEC Reference No.: REC106-20
Title: The production of plant-expressed virus-like particle vaccines against infectious bronchitis coronavirus and efficacy in chickens
Researcher: Miss KM Sepotokele
Student's Supervisor: Prof O Abolnik

Dear Miss KM Sepotokele,

The New Application as supported by documents received between 2020-07-28 and 2021-03-05 for your research, was approved by the Animal Ethics Committee on its quorate meeting of 2021-03-05.

Please note the following about your ethics approval:

1. The use of species is approved:

Species	Number
Poultry (<i>Gallus gallus</i>)	168
Sample Blood	1008 (2 ml each)
Cloacal and Tracheal	3024 (swabs)

2. Ethics Approval is valid for 1 year and needs to be renewed annually by 2022-03-10.
3. Please remember to use your protocol number (REC 106-20) on any documents or correspondence with the AEC regarding your research.
4. Please note that the AEC may ask further questions, seek additional information, require further modification, monitor the conduct of your research, or suspend or withdraw ethics approval.
5. All incidents must be reported by the PI by email to Ms Marieze Rheeder (AEC Coordinator) within 3 days, and must be subsequently submitted electronically on the application system within 14 days.
6. The committee also requests that you record major procedures undertaken during your study for own-archiving, using any available digital recording system that captures in adequate quality, as it may be required if the committee needs to evaluate a complaint. However, if the committee has monitored the procedure previously or if it is generally can be considered routine, such recording will not be required.

Ethics approval is subject to the following:

- The ethics approval is conditional on the research being conducted as stipulated by the details of all documents submitted to the Committee. In the event that a further need arises to change who the investigators are, the methods or any other aspect, such changes must be submitted as an Amendment for approval by the Committee.

We wish you the best with your research.
Yours sincerely


Prof. V. Naidoo

CHAIRMAN: UP-Animal Ethics Committee

Room 6-11, Arnold Theiler Building, Onderstepoort
Private Bag 836, Onderstepoort 0110, South Africa
Tel +27 12 529 8434
Fax +27 12 529 8321
Email: marissa.rheeder@up.ac.za

Fakhele Masetsheng
Lefapha la Dinonane ka Bongakadifiso



Faculty of Veterinary Science
Animal Ethics Committee

13 September 2022

**Approval Certificate
Annual Renewal
(EXT1)**

AEC Reference No.: REC105-20 Line 1
Title: The production of plant-expressed virus-like particle vaccines against infectious bronchitis coronavirus and efficacy in chickens
Researcher: Miss KM Sepotokale
Student's Supervisor: Prof C Abonik

Dear Miss KM Sepotokale,

The **Annual Renewal** as supported by documents received between 2022-07-13 and 2022-08-29 for your research, was approved by the Animal Ethics Committee on its quorate meeting of 2022-08-29.

Please note the following about your ethics approval

1. The use of species is approved:

Species	Approved
Poultry - White Leghorn Chickens	158
Samples	Approved
Gallus gallus - Blood	1588
Gallus gallus - Cloacal and Tracheal	3024

2. Ethics Approval is valid for 1 year and needs to be renewed annually by 2023-09-13.
3. Please remember to use your protocol number (REC105-20) on any documents or correspondence with the AEC regarding your research.
4. Please note that the AEC may ask further questions, seek additional information, require further modification, monitor the conduct of your research, or suspend or withdraw ethics approval.
5. **All incidents** must be reported by the PI by email to Ms Marleze Rheeder (AEC Coordinator) within 3 days, and must be subsequently submitted electronically on the application system within 14 days.
6. The committee also requests that you record major procedures undertaken during your study for own-archiving, using any available digital recording system that captures in adequate quality, as it may be required if the committee needs to evaluate a complaint. However, if the committee has monitored the procedure previously or if it is generally can be considered routine, such recording will not be required.

Ethics approval is subject to the following:

- The ethics approval is conditional on the research being conducted as stipulated by the details of all documents submitted to the Committee. In the event that a further need arises to change who the investigators are, the methods or any other aspect, such changes must be submitted as an Amendment for approval by the Committee.

We wish you the best with your research.

Yours sincerely



Prof. Y. Naidoo
CHAIRPERSON: UP-Animal Ethics Committee

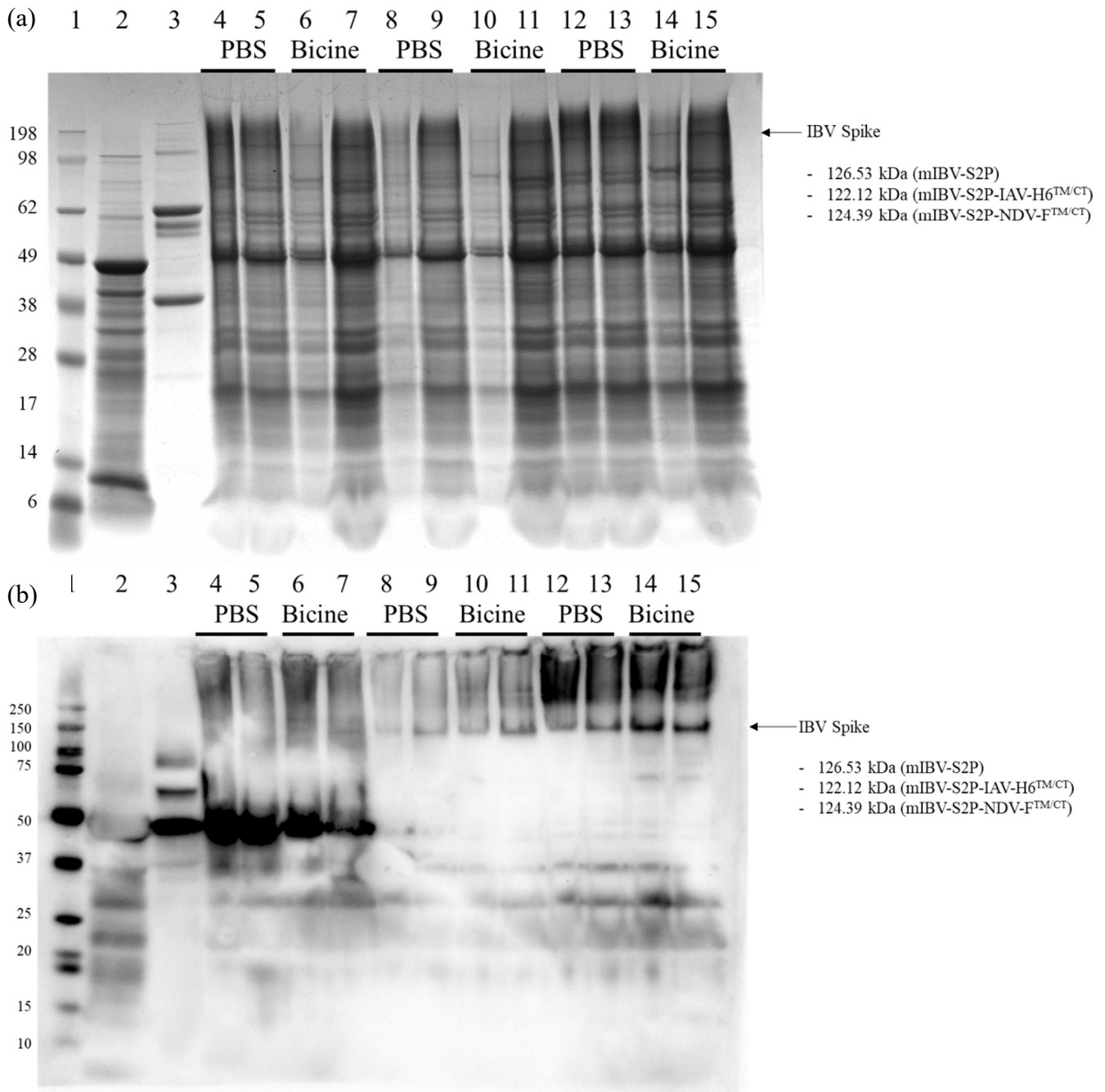


Figure S1. SDS-PAGE (a) and Western blot (b) of plant-produced IBV S protein (mIBV-S2P, mIBV-S2P-IAV-H6^{TM/CT}, and mIBV-S2P-NDV-F^{TM/CT}) purified in PBS or bicine buffer. Lane 1: molecular weight marker; Lane 2: plant-expressed empty pEAQ-HT vector; Lane 3: purified live QX-like IBV strain ck/ZA/3665/11; Lanes 4 and 5: mIBV-S2P:M:E:N Fractions 2 and 3; Lanes 6 and 7: mIBV-S2P:M:E:N Fractions 2 and 3; Lanes 8 and 9: mIBV-S2P-IAV-H6^{TM/CT}:M2 Fractions 2 and 3; Lanes 10 and 11: mIBV-S2P-IAV-H6^{TM/CT}:M2 Fractions 2 and 3; Lanes 12 and 13: mIBV-S2P-NDV-F^{TM/CT}:NDV matrix Fractions 2 and 3; Lanes 14 and 15: mIBV-S2P-NDV-F^{TM/CT}:NDV matrix Fractions 2 and 3.

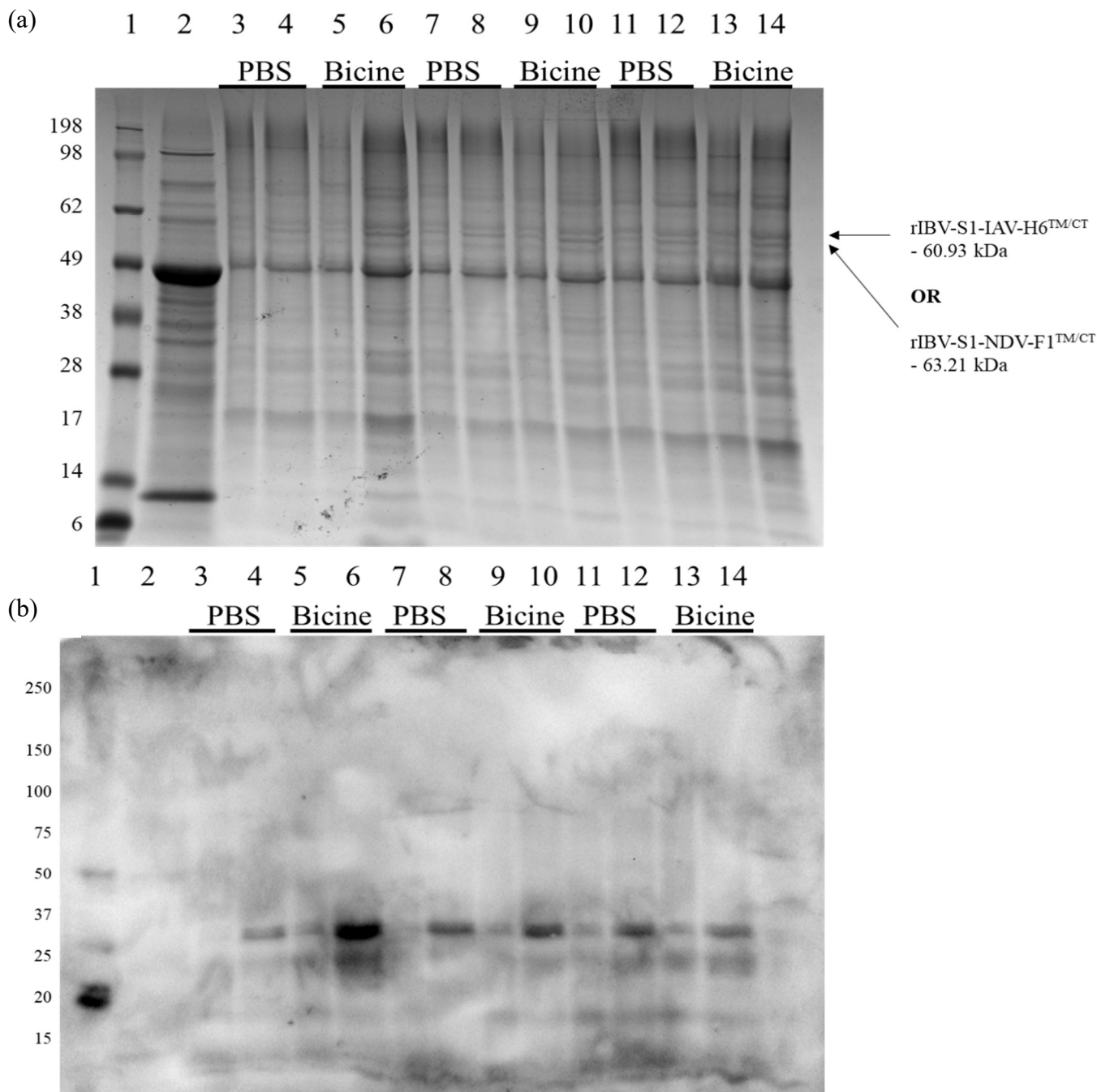


Figure S2. SDS-PAGE (a) and Western blot (b) of plant-produced rIBV-S1-IAV-H6^{TM/CT} and rIBV-S1-NDV-F^{TM/CT} proteins purified in PBS or bicine buffer. Lane 1: molecular weight marker; Lane 2: plant-expressed empty pEAQ-HT vector; Lanes 3 and 4: rIBV-S1-IAV-H6^{TM/CT} :M1 :M2 Fractions 2 and 3; Lanes 5 and 6: rIBV-S1-IAV-H6^{TM/CT} :M1 :M2 Fractions 2 and 3; Lanes 7 and 8: rIBV-S1-IAV-H6^{TM/CT} :M2 Fractions 2 and 3; Lanes 9 and 10: rIBV-S1-IAV-H6^{TM/CT} :M2 Fractions 2 and 3; Lanes 11 and 12: rIBV-S1-NDV-F^{TM/CT} :matrix Fractions 2 and 3; Lanes 13 and 14: rIBV-S1-NDV-F^{TM/CT} :matrix Fractions 2 and 3.

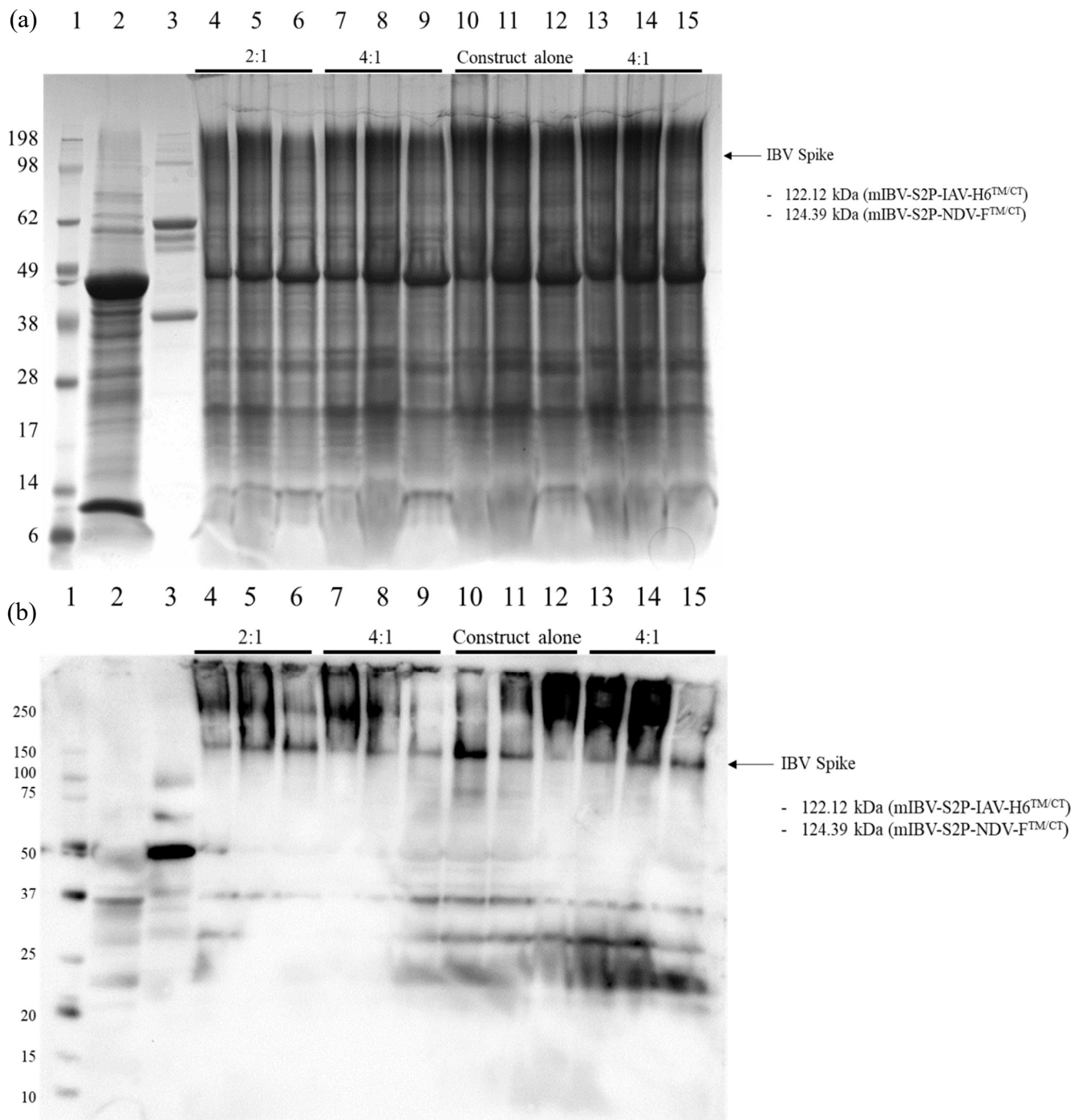
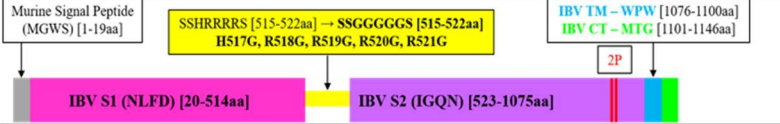

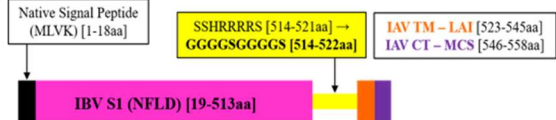
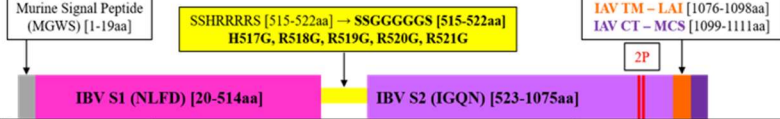
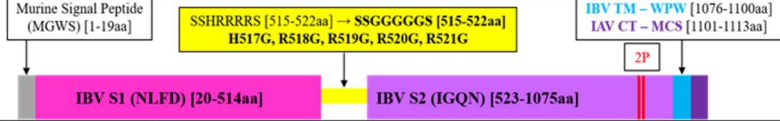
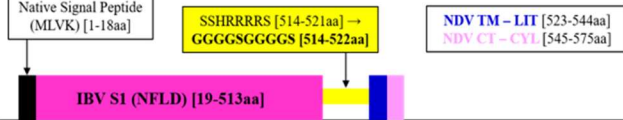
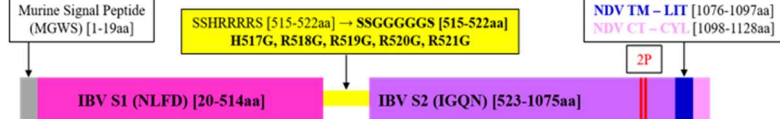
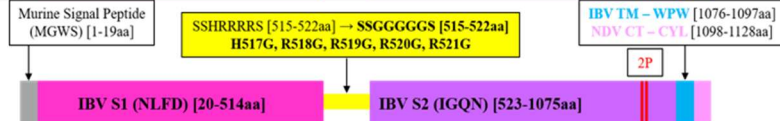
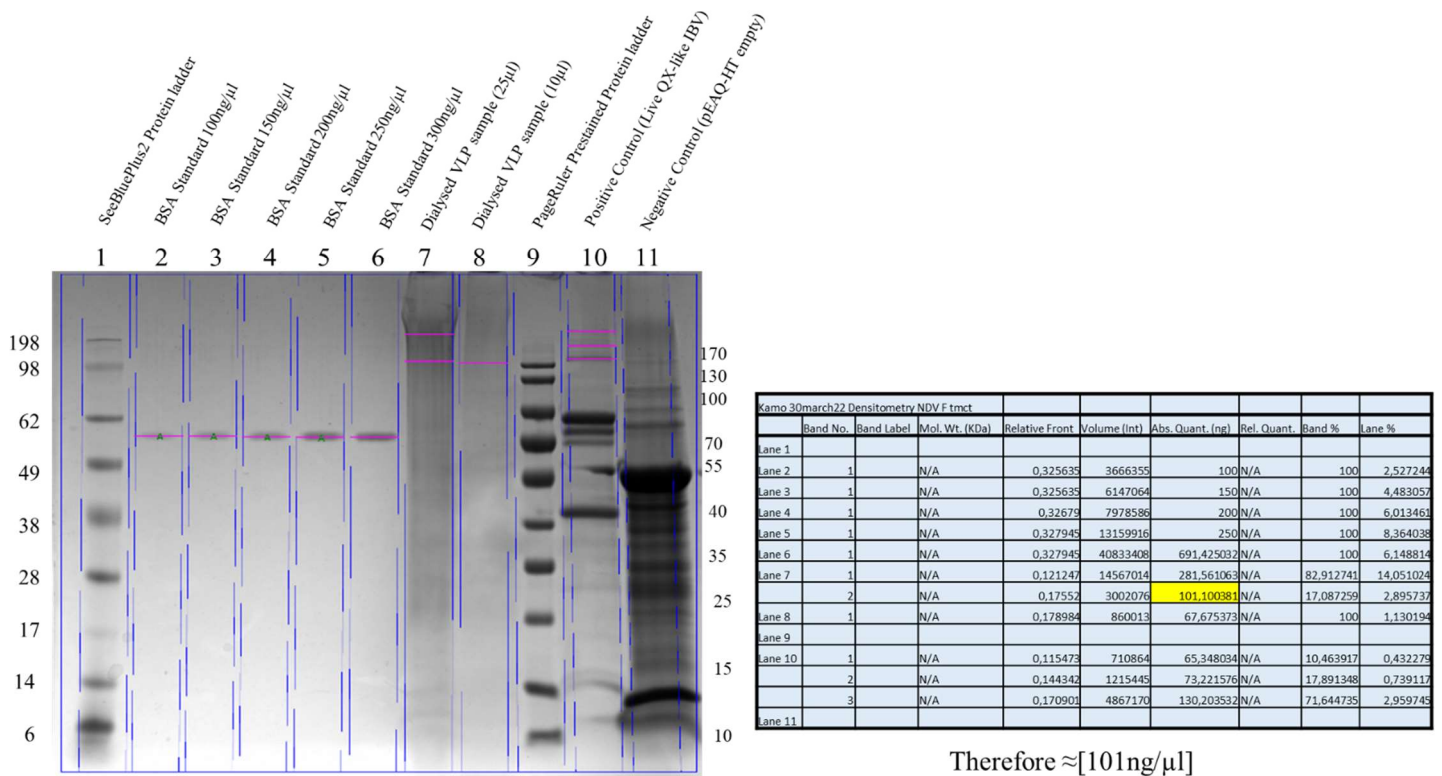


Figure S3. SDS-PAGE (a) and Western blot (b) of plant-produced IBV S protein (mIBV-S2P-IAV-H6^{TM/CT} and mIBV-S2P-NDV-F^{TM/CT}) co-infiltrated at different ratios with their complementary proteins. Lane 1: molecular weight marker; Lane 2: plant-expressed empty pEAQ-HT vector; Lane 3: purified live QX-like IBV strain ck/ZA/3665/11; Lanes 4 - 6: mIBV-S2P-IAV-H6^{TM/CT}:M2 Fractions 2 - 4; Lanes 7 - 9: mIBV-S2P-IAV-H6^{TM/CT}:M2 Fractions 2 - 4; Lanes 10 - 12: mIBV-S2P-NDV-F^{TM/CT} alone Fractions 2 - 4; Lanes 13 - 15: mIBV-S2P-NDV-F^{TM/CT}:matrix Fractions 2 - 4.

Table S1: Schematic diagrams of all designed modified constructs and expression levels

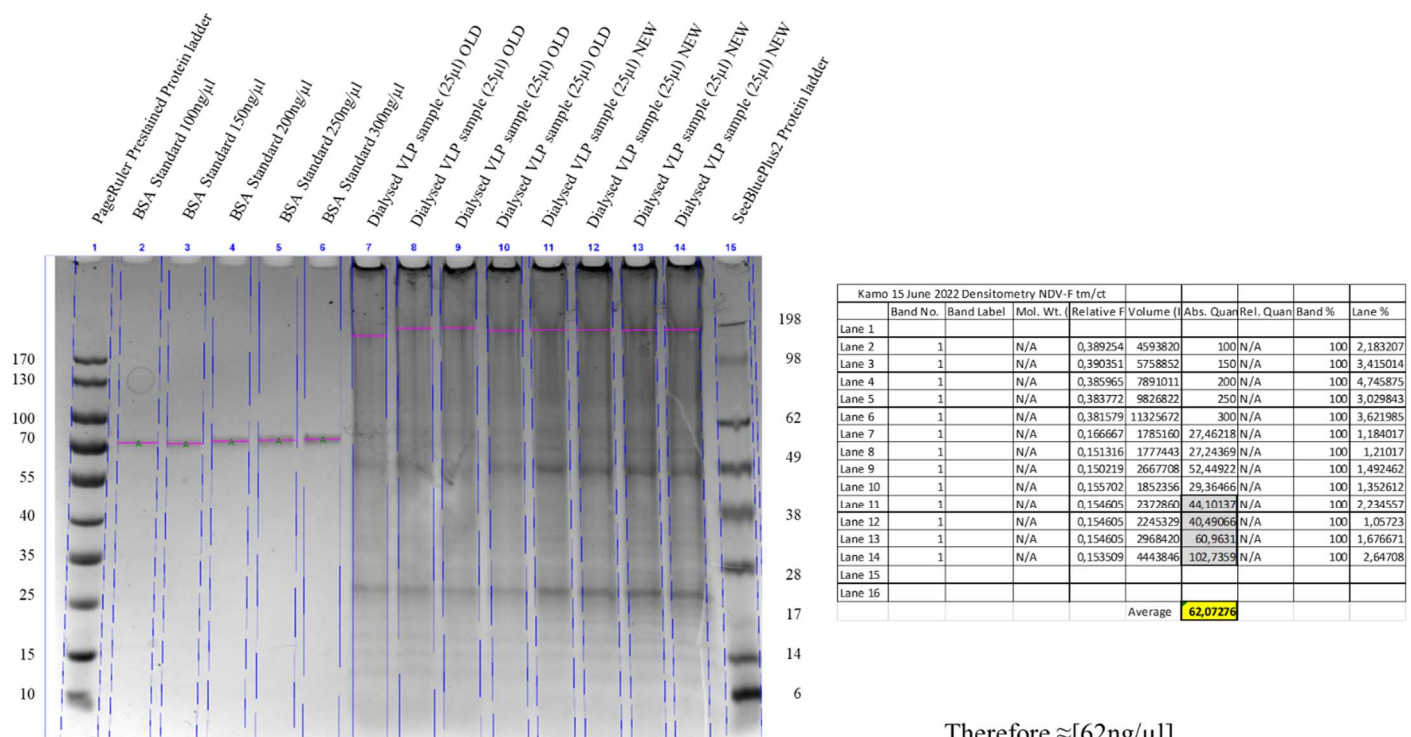
Construct	Schematic Diagrams	Accessory Protein	SDS-PAGE	ImmunoBlot	LC-MS/MS	TEM
mIBV-S2P		M+E	+++	+++	NT	++
		M+E+N	+++	+++	+++	++
rIBV-S1-IAV-H6		M1	-	-	NT	+
		M2	-	-	NT	+
		M1+M2	-	-	NT	+
rIBV-S1-IAV-H6^{TM/CT}		M2	+	-	NT	+
		M1+M2	+	-	NT	+
mIBV-S2P-IAV-H6^{TM/CT}		M2	+++	+++	+++	++
mIBV-S2P-IAV-H6^{CTonly}		M2	+++	++	++++	++++
rIBV-S1-NDV-F^{TM/CT}		Matrix	+	-	NT	+
mIBV-S2P-NDV-F^{TM/CT}		Alone	+++	++++	NT	++
		Matrix	+++	++++	++++	+++
mIBV-S2P-NDV-F^{CTonly}		Alone	+++	++++	++++	+++
		Matrix	+++	+++	+++	++++

* Expression Scoring levels: - No expression; + Low expression, ++ Moderate expression, +++ High Expression; ++++ Very high expression; NT Not tested.



Therefore $\approx [101\text{ng}/\mu\text{l}]$

Figure S4. Densitometric analysis by SDS-PAGE of partially-purified mIBV-S2P-NDV-F^{TM/CT} VLPs. Lane 1: SeeBluePlus2 protein ladder; Lane 2: BSA Standard 100 ng/ μl ; Lane 3: BSA Standard 150 ng/ μl ; Lane 4: BSA Standard 200 ng/ μl ; Lane 5: BSA Standard 250 ng/ μl ; Lane 6: BSA Standard 300 ng/ μl ; Lane 7: Dialysed VLP sample (25 μl); Lane 8: Dialysed VLP sample (10 μl); Lane 9: PageRuler Prestained protein ladder; Lane 10: Positive control (Live QX-like IBV); Lane 11: Negative control (pEAQ-HT-empty). (Chapter 4 – Immunogenicity Study Results).



Therefore $\approx [62\text{ng}/\mu\text{l}]$

Figure S5. Densitometric analysis by SDS-PAGE of partially-purified mIBV-S2P-NDV-F^{TM/CT} VLPs. Lane 1: PageRuler Prestained protein ladder; Lane 2: BSA Standard 100 ng/ μl ; Lane 3: BSA Standard 150 ng/ μl ; Lane 4: BSA Standard 200 ng/ μl ; Lane 5: BSA Standard 250 ng/ μl ; Lane 6: BSA Standard 300 ng/ μl ; Lane 7: Dialysed VLP sample (25 μl) (old sample); Lane 8: Dialysed VLP sample (25 μl) (old sample); Lane 9: Dialysed VLP sample (25 μl) (old sample); Lane 10: Dialysed VLP sample (25 μl) (old sample); Lane 11: Dialysed VLP sample (25 μl) (sample of interest); Lane 12: Dialysed VLP sample (25 μl) (sample of interest); Lane 13: Dialysed VLP sample (25 μl) (sample of interest); Lane 14: Dialysed VLP sample (25 μl) (sample of interest); Lane 15: SeeBluePlus2 protein ladder. (Chapter 5 – Efficacy Trial Results).